GOETHE UNIVERSITÄT FRANKFURT AM MAIN

GEORG SPEYER HAUS
INSTITUT FÜR TUMORBIOLOGIE
UND EXPERIMENTELLE THERAPIE

The role of calcium ions in the leukemic bone marrow microenvironment

Dissertation

zur Erlangung des Doktorgrades

der Naturwissenschaften

vorgelegt beim Fachbereich Biochemie, Chemie und Pharmazie der Goethe-Universität Frankfurt am Main

von

Raquel Soares Pereira

aus Ilha (Pombal, Portugal)

Frankfurt am Main, Februar 2022

vom Fachbereich Biochemie, Chemie und Pharmazie (FB 14) der Goethe-Universität Frankfurt am Main als Dissertation angenommen.

Dekan: Prof. Dr. Clemens Glaubitz

Gutachter: Prof. Dr. Rolf Marchalek

Prof. Dr. Daniela S. Krause

Datum der Disputation: ……..

Declaration

I herewith declare that I have not previously participated in any doctoral examination procedure in a mathematics or natural science discipline.

Frankfurt am Main, ...
(Date) (Signature)

Author's Declaration

I herewith declare that I have produced my doctoral dissertation on the topic of "The role of calcium ions in the leukemic bone marrow microenvironment" independently using only the tools indicated therein. In particular, all the literature and external sources which I employed when producing this academic work are clearly acknowledged and identified.

I confirm that I have respected the principles of good scientific practice and have not made use of the services of any commercial agency in respect of my doctorate.

Frankfurt am Main, ...
(Date) (Signature)

Zusammenfassung

Leukämie, ein Krebs, der aus dem Blut und dem Knochenmark hervorgeht, ist typischerweise durch eine unkontrollierte Proliferation und Akkumulation abnormaler weißer Blutkörperchen gekennzeichnet. Leukämie wird anhand des Krankheitsverlaufs (akut oder chronisch) und des betroffenen Blutzelltyps (myeloid oder lymphoid) klassifiziert, was dementsprechend zu den vier Haupttypen führt: Akute Lymphoblastische Leukämie (ALL), Akute Myeloische Leukämie (AML), Chronische Lymphoblastische Leukämie (CLL) und Chronische Myeloische Leukämie (CML). Leukämie ist für 2,5 % aller Krebsneudiagnosen jährlich verantwortlich und die durchschnittlichen Überlebensraten bei manchen Leukämien verbleiben bei relativ geringen 40 %. Da bisherige Therapien nicht in der Lage sind, Leukämiestammzellen (LSZ) zu eliminieren, kommt es bei vielen Patienten zu Krankheitsrückfällen.

Das Knochenmark-Mikromilieu (KMM) ist ein komplexes System im Knochen, das aus zellulären und nicht-zellulären Komponenten besteht, die alle an der Blutbildung beteiligt sind. Damit bildet das KMM die physische Umgebung, in der Hämatopoetische Stammzellen (HSZ) lokalisiert sind. Das KMM interagiert mit diesen HSZ und beeinflusst diese in einer bestimmten Art und Weise, sodass das KMM eine besondere Nische für diese Zellen darstellt. Von Leukämien ist beispielsweise bekannt, dass das KMM, durch die aktive Unterstützung der Funktion von LSZ, eine besondere Rolle bei der Leukämieaufrechterhaltung und -progression spielt. Abgesehen von der Annahme, dass LSZ die Ursache von Leukämie sind, geht man davon aus, dass diese Zellen für die Krankheitsrückfalle verantwortlich sind. Da sich LSZ meist in einem nicht-aktiven „Ruhezustand“ befinden, können diese durch derzeitige chemotherapeutische Behandlungen, die hauptsächlich auf die Eliminierung sich stark teilender Zellen ausgerichtet sind, nicht ausgelöscht werden. Daher können LSZ auch nach Krebstherapien die Leukämieprogression aufrechterhalten. Derzeitige Studien fokussieren ihre Forschung darauf, die Interaktionen des KMM mit den LSZ zu unterbinden, um diese Zellen wieder für cytotoxische Therapien zu sensitivieren.

Das KMM wir formell in zwei Nischen unterteilt: die endostale und die vaskuläre Nische, welche beide wichtige Funktionen bei der Regulation des Stammzell-Ruhezustands, deren Regenerationsfähigkeit, Einnistung, Mobilisierung und Differenzierung einnehmen. Murine Transplantationsexperimente konnten zeigen, dass HSZ präferentiell zu der endostalen Nische hin migrieren.

Eines der vielen Komponenten des KMM sind Calciumionen. Calcium ist das am häufigsten im Körper vorkommende Mineral und Hauptbestandteil der Knochen. Calciumionen werden dementsprechend hauptsächlich über den Parathyroid-Hormon (PTH)-induzierten Knochen-

Remodellierungsprozess freigesetzt. Es ist bekannt, dass extrazelluläres Calcium an einer Vielzahl von biologischen Prozessen beteiligt ist, wie beispielsweise an der Reizweiterleitung in Nervenzellen, der Blutgerinnung, Hormonsynthese und -sekretion, sowie der Muskelkontraktion, Knochen- und Zahnbildung. Da Calcium an der Regulation vieler essentieller Prozesse beteiligt ist, werden die frei zirkulierenden Mengen an Calcium selber durch ein hoch-komplexes System reguliert.

Einer der Hauptregulatoren der Calcium-Homöostase im Körper ist der Calcium-messende Rezeptor (CaSR). Dieser ist ein G-Protein gekoppelter Rezeptor, der, durch Calciumionen aktiviert, die extrazelluläre Calciumkonzentration misst. Entsprechend seiner Rolle im KMM, ist CaSR unter anderem für die Ansiedelung von HSZ an das Endosteum verantwortlich, in dem er die Anheftung dieser Zellen an Extrazelluläre Matrix (EZM)-Proteine wie Collagen-1 reguliert. Zudem fand man heraus, dass CaSR an der Entstehung weiterer Krebstypen beteiligt ist. Abhängig vom Krebs-Typ, zeigte sich, dass CaSR sowohl als Tumorsuppressor als auch als Onkogen fungieren kann. Nichtdestotrotz ist noch unbekannt, welche Rolle CaSR bei der Leukämieentstehung spielt.

Wir vermuten, dass Calciumionen, die vom Knochen freigesetzt werden, und der feinen Balance zwischen Osteoblasten und Osteoklasten unterworfen sind, und/oder CaSR zur Entstehung, Progression und dem Therapie-Ansprechen von Leukämie beitragen. Um den Effekt des aus dem KMM-stammenden Calciums auf Leukämiezellen zu verstehen, haben wir zuerst die Calciumverteilung innerhalb des Knochens untersucht. Durch *in vivo* Bildgebung und einem genetisch-codierten Calcium-Indikator (GCaMP6s) konnten wir zeigen, dass innerhalb des Knochenmarks ein Calciumgradient existiert, bei dem die Calciumkonzentration in der Nähe des Endosteums, wo auch die Knochenmark-Remodellierung stattfindet, am höchsten ist und graduell zur Mitte des Knochenmarks hin abnimmt.

Um die potentielle Rolle von Calcium und den unterschiedlichen Calciumkonzentrationen im Knochenmark zu untersuchen, haben wir die Calciumkonzentration im Knochenmark von Leukämiepatienten und von Mäusen mit induzierter Leukämie gemessen. Unsere Resultate offenbarten Unterschiede in der Calciumkonzentration im Knochenmark zwischen den verschiedenen Leukämietypen, wobei die Calciumkonzentration in AML-Patienten und in AML-erkrankten Mäusen wesentlich höher als in anderen Leukämien war. Entsprechend konnten wir zeigen, dass die CaSR-Expression in AML-Zellen deutlich höher ist als bei anderen Leukämietypen, insbesondere als in CML-Zellen.

Nachdem wir die höhere Calciumkonzentration bei AML, sowohl bei Patienten als auch im Mausmodell belegen konnten, evaluierten wir die Funktion von Calcium in humanen Ziellinien differenzierter. Wir haben herausgefunden, dass AML- und CML-Zellen unterschiedlich auf

Calciumexposition reagieren, wobei in AML-Zellen Prozesse wie Adhäsion zu der EZM-Komponente Fibronectin und Migration zu CXC-Motiv-Chemokin 12 (CXCL-12) signifikant durch Calcium beeinflusst werden, während CML-Zellen meist unbeeinflusst bleiben. Da LSZ vorzugsweise am Endost-Bereich des Knochenmarks lokalisiert sind, wo die Calciumkonzentrationen besonders hoch sind, vermuten wir, dass Calciumionen die Lokalisation von AML-Zellen im KMM beeinflussen.

Basierend auf den unterschiedlichen Reaktionen von AML- und CML-Zellen auf extrazelluläres Calcium und der verschiedenen CaSR-Expression in diesen Zellen, spekulieren wir, dass CaSR zu der Entstehung und Aufrechterhaltung von Leukämie beiträgt. Um die Beteiligung von CaSR an der Leukämie-Pathogenese *in vivo* zu untersuchen, induzierten wir CML, MLL-AF9-induzierte AML sowie BCR-ABL1-induzierte B-ALL über das retrovirale Transduktions/Transplantations-Modell in Mäusen. Bei CML führte die Abwesenheit von CaSR in Leukämie-initiierenden Zellen (LIZ) zu einem signifikant kürzeren Überleben der Rezipienten-Mäuse im Vergleich zu denjenigen, die die Wildtyp (WT) LIZ erhalten haben. Dementsprechend führte Überexpression von CaSR in CML LIZ zu einem signifikant verlängerten Überleben der Rezipienten-Mäuse. Ähnlich wie bei CML, führte die verringerte CaSR-Expression in LIZ auch zu einem schnelleren B-ALL-Verlauf. Im Gegensatz hierzu resultierte die Transplantation von MLL-AF9^{+} LIZ in WT Mäuse in einem signifikant langsameren AML-Verlauf. Komplementär dazu konnten wir zeigen, dass Überexpression von CaSR in LIZ zu einem signifikant beschleunigten AML-Verlauf führt.

Um zu identifizieren, ob die Rolle von CaSR in AML spezifisch für das MLL-AF9 Onkogen ist oder ob dies auch auf andere AML-induzierende Onkogene übertragen werden kann, haben wir den obengenannten Ansatz auch an einem MN1-induzierten AML-Modell getestet. Vergleichbar zu MLL-AF9, führte CaSR-Defizienz in LIZ auch in der MN1-induzierten AML zu einem signifikant verlängerten Überleben der transplantierten Mäuse.

Fokussierend auf AML, untersuchten wir den Mechanismus, der der Rolle von CaSR bei der AML-Pathogenese und damit auch einer möglichen Regulation von LSZ zu Grunde liegt. Unsere Ergebnisse zeigen, dass CaSR-Defizienz zu einer reduzierten Anzahl und Funktion der myeloiden Progenitorzellen führt, welche die LSZ-Fraktion in diesem Mausmodell miteinschließt. Zudem haben sekundäre Transplantationen und limitierende Verdünnungs-Transplantationsmodelle gezeigt, dass CaSR an der Aufrechterhaltung des LSZ-Pools beteiligt ist, in dem er die Frequenz funktioneller LSZ reguliert. Diese Hypothese wird weiterhin dadurch gestützt, dass Gene, die mit AML-Stammzelleigenschaften und Selbst-Erneuerungskapazität assoziiert sind, hochreguliert werden, sobald CaSR überexprimiert ist und folglich herunterreguliert werden, wenn CaSR ausgeschaltet ist.

Berücksichtigt man, dass LSZ für die hohe Rückfallrate bei AML verantwortlich sind, da sich diese meist in einem Ruhezustand befinden und damit ihr hohes Selbsterneuerungspotential erhalten, weisen unsere Ergebnisse darauf hin, dass das ‚Targeten' von CaSR die LSZ-Aktivität stört und damit möglicherweise relevant für das Verhindern eines AML-Rückfalls sein könnte.

Auf zellulärem Level wurde der Effekt von CaSR in weiteren MLL-AF9^{+} AML-*in vivo*- als auch -*in vitro*-Modellen untersucht. Unsere Daten zeigen, dass CaSR-Defizienz in LIZ *in vivo* zu gesteigerter Apoptose und verringerter Zellzyklusaktivität, Reaktive-Sauerstoff-Spezies (ROS)-Produktion und DNA-Schädigung führt. Dies könnte das verlängerte Überleben der transplantierten Mäuse erklären. Komplementär hierzu konnten *in vitro* Experimente zeigen, dass CaSR-überexprimierende Zellen, im Vergleich zu WT Zellen, einen bestimmten Krebs-fördernden Phänotyp aufweisen. Überexpression von CaSR führte in diesem Falle zu gesteigerter Proliferation, Zellzyklusaktivität, ROS-Produktion, DNA-Schädigung und reduzierter Apoptose.

Um den Beitrag von CaSR an der AML Zellphysiologie und der damit assoziierten molekularen Mechanismen zu charakterisieren, wurde die intrinsische zelluläre Signaltransduktion genauer untersucht. Basierend auf proteomischen Daten und Immunblotting-Analyseverfahren konnten wir zeigen, dass CaSR den MAPK/ERK-Signalweg in AML-Zellen aktiviert. Diese Hypothese wird weiterhin dadurch gestützt, dass nachgeschaltete Target-Moleküle des Transkriptionsfaktor pERK1/2 in CaSR-überexprimierenden Zellen ebenfalls hochreguliert sind. Des Weiteren haben wir herausgefunden, dass CaSR auch den Wnt-β-Catenin-Signalweg in AML-Zellen reguliert. Zellen, die CaSR überexprimieren, weisen hochregulierte Proteinlevel von β-Catenin, c-Myc und Cyclin-D1 sowie höhere T-Zell-Faktor-4 (TCF-4) Transkriptionslevel, des molekularen Interaktionspartners von β-Catenin, auf.

Außerdem deuten die Ergebnisse dieser Arbeit auf eine neuartige Rolle von Filamin A (FLNA), eines mit CaSR-interagierenden Proteins, bei AML hin. Wir konnten zeigen, dass eine erhöhte FLNA-Expression in Verbindung mit einer schlechteren Prognose und einer verringerten Überlebensrate in AML-Patienten steht. Zudem interagiert FLNA mit CaSR in AML-Zellen und, indem wir ein FLNA-KO *in vitro* Modell etablierten, haben wir herausgefunden, dass FLNA die Zell-Proliferation steigert und den Zellzyklus reguliert. Darüber hinaus untersuchten wir die Rolle von FLNA in der AML-Entwicklung in Xenograft-Transplantationen im Mausmodell. Dabei verbesserte die FLNA-Defizienz in Leukämiezellen signifikant die Überlebensrate der Mäuse. Demensprechend erweist sich FLNA, vergleichbar mit CaSR, als ein potentielles Zielprotein für die AML-Therapie.

Um zu testen, ob die Inhibition des CaSR-Signalwegs die Entwicklung von AML unterbinden oder verlangsamen kann, haben wir den potentiellen therapeutischen Effekt des CaSR-spezifischen Antagonisten NPS-2143 evaluiert. Unsere Ergebnisse dazu zeigen, dass die Inhibition von CaSR durch NPS-2143 signifikant die Entwicklung und Progression von AML *in vitro* als auch *in vivo* beeinträchtigt. Mit Hilfe des retroviralen Transduktions-/Transplantations-Modells der MLL-AF9-induzierten AML konnten wir zeigen, dass CaSR-Defizienz in LIZ die Überlebensrate der Mäuse, im Vergleich zu den Vehikel-behandelten, signifikant verbessert hat. Interessanterweise konnte die Kombinationsbehandlung mit NPS-2143 und dem AML-Standard-Therapeutikum Ara-C das Überleben der Mäuse nicht nur im Vergleich zu den Vehikel-behandelten, sondern auch zu den nur mit Ara-C behandelten Mäusen signifikant verbessern. Dies könnte darauf hindeuten, dass zusätzliche Behandlung mit NPS-2143 bereits existierende Therapien verbessern kann. Basierend auf diesen Ergebnissen schlussfolgern wir, dass bei AML nicht nur Leukämiezellen, sondern auch LIZ durch CaSR-Inhibition über NPS-2143 beeinflusst werden können. Demensprechend könnte die Behandlung von Patienten mit einem CaSR-Antagonisten in Kombination mit einer konventionellen Chemotherapie möglicherweise einen besseren Therapieansatz liefern und damit das Rückfallrisiko verringern.

Um zu testen, ob unsere im Mausmodell generierten Ergebnisse auf einen humanen Versuchsansatz übertragen werden können, haben wir den Effekt von CaSR-Inhibition in einem Xeno-Transplantationsexperiment evaluiert, indem wir Primärproben von AML-Patienten transplantierten. Ähnlich wie auch in den zuvor getesteten syngenen Mausmodellen, weist die Kombinations-Therapie mit NPS-2143 und Ara-C auch hier einen Trend gegenüber einem verlängerten Überleben, im Vergleich zu den mit Ara-C behandelten Mäusen hin.

Basierend auf der Annahme, dass CaSR bei CML möglicherweise als Tumorsuppressor fungiert, haben wir den Effekt eines CaSR-Agonisten, Cinacalcet, *in vivo* in Kombination mit dem CML Standard-Therapeutikum Imatinib, getestet. Entsprechend lebten Mäuse, die eine Behandlung von Cinacalcet zusammen mit Imatinib erhielten, signifikant länger als Vehikel-behandelte Mäuse.

Zusammenfassend weisen unsere Ergebnisse darauf hin, dass Calciumionen, die aus dem Calcium-reichen KMM stammen, und/oder CaSR stark und differenziert die Leukämie-Progression beeinflussen. Als Ergänzung zu existierenden Behandlungsmöglichkeiten, könnte das ‚Targeten' von CaSR über spezifische pharmakologische Antagonisten die Überlebensrate von AML-Patienten verbessern, während CaSR-Agonisten unter Umständen vorteilhaft für die CML- und B-ALL-Therapie sein könnten.

Schlüsselwörter: Calcium, Calcium-messende Rezeptor (CaSR), Akute Myeloische Leukämie (AML), Chronische Myeloische Leukämie (CML), Leukämiestammzellen (LSZ), Filamin A (FLNA), NPS-2143.

Summary

Leukemia is a cancer of the blood and bone marrow characterized by an uncontrolled proliferation and accumulation of abnormal white blood cells. Leukemia can be classified based on the course of the disease (acute or chronic) and the blood cell type involved (myeloid or lymphocytic), leading to four main subtypes: acute lymphoblastic leukemia (ALL), acute myeloid leukemia (AML), chronic lymphocytic leukemia (CLL) and chronic myeloid leukemia (CML). Leukemia represents 2.5% of all new cancer cases *per* year, and survival rates in some leukemias remain low at 40%.

The bone marrow microenvironment (BMM) is a system within the bone marrow comprising cellular and acellular components, all of which play a major role in hematopoiesis, providing the physical space where hematopoietic stem cells (HSCs) reside. The BMM interacts with HSCs, offering a “niche” for those cells and in case of leukemia, the BMM has a supportive role in disease maintenance and progression by supporting Leukemia stem cells (LSCs). One of the components of the BMM are calcium ions. Calcium is the most abundant mineral in the body, a key component of bones and is released by parathyroid hormone (PTH)-induced bone remodeling. Calcium ions play a role in the localization, engraftment and adhesion of normal HSC to extracellular matrix (ECM) proteins in the BMM *via* the calcium sensing receptor (CaSR), thereby maintaining normal hematopoiesis. In addition of a major regulator of calcium homeostasis, CaSR contribute to the development of different cancers, functioning as either tumor suppressor or oncogene, depending on the involved tissue. However, the role of CaSR and its associated pathways in the local BMM for the development of leukemia is poorly understood. We hypothesized that calcium ions released from bone, subject to a fine balance between osteoblasts and osteoclasts, and/or CaSR, contribute to development, progression and response to therapy.

We have shown that the local calcium concentration forms a gradient in the bone marrow niche and in mice with CML is similarly low as in control mice, but significantly higher in mice suffering from BCR-ABL1-driven B-ALL or MLL-AF9-driven AML. Similarly, the calcium concentration in the human BMM was found to be higher in AML than in other leukemias. Regarding the function of calcium in leukemia cells, we found that AML and CML cells respond differently to calcium exposure, with AML cells exhibiting regulation of cellular processes such as adhesion to the ECM protein fibronectin and migration toward CXCL-12, whereas CML cells remained mostly unaltered. Using genetic deletion or overexpression of *CaSR* in murine models of leukemia, we observed that CaSR acts as tumor suppressor in BCR-ABL1-driven CML and B-ALL and as oncogene in AML.

Focusing on AML, our data shows that deficiency of CaSR on LICs leads, on one hand to increased apoptosis, and on the other hand to reduced cell cycle, reactive oxygen species (ROS) production and DNA damage *in vivo*, which may explain the observed prolongation of survival of mice. Complementary, *in vitro* experiments demonstrated that cells overexpressing CaSR have a distinct, cancer-promoting phenotype compared to wildtype cells. Overexpression of CaSR led to an increase in proliferation, cell cycle, ROS production, DNA damage and reduced apoptosis. We have identified CaSR-mediated pathways in AML and shown that CaSR enhances leukemia progression by activating MAPK/ERK and Wnt-β-catenin signaling. In addition, the CaSR-interacting protein filamin A (FLNA) was shown to contribute to aggressive disease *in vitro* and *in vivo*. Furthermore, the mechanism underlying the role of CaSR in AML pathogenesis and possible regulation of LSCs was studied. Our findings demonstrated that *CaSR* ablation reduces myeloid progenitor function and proved that CaSR is required for maintenance of LSC pool by regulating its frequency and function. Further supporting the role of CaSR in LSC maintenance, genes associated with AML stemness and self-renewal capacity were upregulated when CaSR was overexpressed and downregulated when CaSR was depleted. Given the role of CaSR in AML, the CaSR antagonist NPS-2143 was tested *in vivo*. The combination treatment of NPS-2143 with the standard of care, ara-C, significantly reduced the tumor burden and prolonged the survival of mice with AML in syngeneic and xenotransplantation experiments. Based on the finding that CaSR functions as a tumor suppressor in CML, treatment of mice with the CaSR agonist cinacalcet in combination with imatinib prolonged survival of mice with CML compared to treatment with the mice given vehicle.

Our results suggest that calcium ions stemming from the calcium-rich BMM *via* CaSR strongly and differentially influence leukemia progression. As an adjunct to existing treatment therapies, targeting of CaSR with specific pharmacologic antagonists may prolong survival of patients with AML, while CaSR agonists may be beneficial in CML and B-ALL.

Keywords: Calcium, Calcium sensing receptor (CaSR), Acute myeloid leukemia (AML), Chronic myeloid leukemia (CML), Leukemia stem cells (LSCs), Filamin A (FLNA), NPS-2143.

Table of Contents

Abbreviations

Abreviation	Definition
5-FU	5-fluorouracil
$1,25(OH)_2D_3$	1,25-dihydroxyvitamin D_3
A-MuLV	Abelson murine leukemia virus
ABC	Animal blood counter
ABL	Ableson leukemia virus
AC	Adenylate cyclase
ACK	Ammonium-chloride-potassium
AD	Alzheimer's disease
ADHH	Autosomal dominant hypocalcemia with hypercalciuria
AlexaFluor	Alexa fluorophore
ALL	Acute lymphoblastic leukemia
ALOX5	Arachidonate 5-lipoxygenase
AML	Acute myelogenous leukemia
Amp	Ampicillin
APC	Allophycocyanin
Ara-C	Cytarabine
As	Anti-sense
ASXL1	Addition of sex combs like 1
ATP	Adenosine triphosphate
AUC	Area under the curve
BAD	BCL2 associated agonist of cell death
BCL	B-cell lymphoma
Bcl-xL	B-cell lymphoma-extra large
BCR	Breakpoint cluster region
BM	Bone marrow
BMM	Bone marrow microenvironment
BMP	Bone morphogenetic proteins
BP1	Beta protein 1
BSA	Bovine serum albumin
BTK	Bruton tyrosine kinase
Ca^{2+}	Calcium
$CaCl_2$	Calcium chloride
CamKII	Calcium/calmodulin-dependent protein kinase II

cAMP	Cyclic adenosine monophosphate
$CaPO_4$	Calcium phosphate
CAR	CXCL-12 abundant reticular cells
Cas9	CRISPR associated protein 9
CaSR	Calcium sensing receptor
CBC	Complete blood cell count
CBF	Core-binding factor
CCL3	C-C motif chemokine ligand
CD	Cluster of differentiation
CDKN1A	CDK inhibitor 1A
CEBPα	CCAAT enhancer binding protein alpha
CFSE	Carboxyfluorescein succinimidyl ester
CLL	Chronic lymphoblastic leukemia
CLP	Common lymphoid progenitors
CML	Chronic myeloid leukemia
CMP	Common myeloid progenitors
cMyc	c-Myelocytomatosis oncogene product
CO_2	Carbon dioxide
CREB	cAMP response element-binding protein
CRKL	Crk like protein
CSC	Cancer stem cells
CSLM	Confocal laser scanning microscope
C_T	Cycle threshold
CXCL-12	C-X-C motif chemokine ligand 12
CXCR4	C-X-C chemokine receptor type 4
Cy7	Cyanine dye 7
DAG	Diacylglycerol
DAPI	4′,6-Diamidin-2-phenylindol
dH_2O	Distilled water
DMEM	Dulbecco’s modified eagle medium
DMSO	Dimethyl sulfoxide
DNA	Deoxyribonucleic acid
DNMT3A	DNA nucleotide methyltransferase 3A
DPBS	Dulbecco’s phosphate-buffered saline
DR3	Death receptor 3
DSB	Double strand break

ECM	Extracellular matrix
ECR	Extracellular domain
EDTA	Ethylene diamine tetraacetic acid
ELK-1	ETS like-1
EPO	Erythropoietin
ER	Endoplasmic reticulum
ERK1/2	Extracellular signal-regulated kinase 1/2
EVI1	Ecotropic viral integration site 1
EZH2	Enhancer of zeste 2 polycomb repressive complex 2 Subunit
FACS	Fluorescence activated cell sorting
FBH/FBHH	Familial hypocalciuric hypercalcemia
FBS	Fetal bovine serum
FILIP	Filamin A-interacting protein
FITC	Fluorescein isothicyanate
FLNA	Filamin A / Filamin-1
FLT3	Fms-like tyrosine kinase 3
FN	Fibronectin
FW	Forward
G-CSF	Granulocyte colony forming factor
GAPDH	Glyceraldehyde 3-phosphate dehydrogenase
GAS6	Growth specific arrest 6
GATA1	GATA binding protein 1
GEF	Guanine nucleotide exchange factors
GFP	Green fluorescence protein
GMP	Granulocyte macrophages progenitors
GPCR	G-protein-coupled receptors
HBS	HEPES buffered saline
HBSS	Hank’s balanced salt solution
HEPES	4-(2-hydroxyethyl)-1-piperazineethanesulfonic acid
HF	High fidelity
HOX	Homebox
HRP	Horseradish peroxidase
HSC	Hematopoietic stem cell
HSCT	Hematopoietic stem cell transplantation
HSPC	Hematopoietic stem and progenitor cells
i.v.	Intravenous

IDH	Isocitrate dehydrogenase
IF	Immunofluorescence
IL	Interleukin
IL2RG	Interleukin 2 receptor gamma
ILK	Integrin-linked kinase
IP3	Inositol-trisphosphate
ITD	Internal tandem duplications
Itgβ3	Integrin β 3
IVM	Intravital microscope
JAK	Janus kinase
KMT2	Histone-lysine N-methyltransferase
KO	Knock out
L-Glu	L-glutamine
LDA	Limiting dilution assay
LDI-PCR	Long-distance inverse PCR
LIC	Leukemia initiating cell
LSC	Leukemic stem cell
LSK	Lin^{-} $Sca1^{+}$ $cKit^{+}$
LT-HSC	Long-term hematopoietic stem cell
MAPK	Mitogen-activated protein kinase
MDS	Myelodysplastic syndrome
MET	Mesenchymal epithelial transition
MFI	Mean fluorescence intensity
MLL	Mixed lineage leukemia
MN1	Meningioma 1
MPO	Myeloperoxidase
MPP	Multipotent progenitor cells
mRNA	Messenger RNA
MSC	Mesenchymal stromal cells
MSCV	Murine stem cell virus
NG2	Neural-glial antigen
NK	Natural killer
NPM1	Nucleophosmin 1
NSG	NOD-scid $IL2r\gamma^{null}$
NSHPT	Neonatal severe primary hyperparathyroidism
NTC	Non-target control

OE	Overexpression
P/S	Penicillin/streptomycin
PB	Pacific blue
PBS	Phosphate buffered saline
PCR	Polymerase chain reaction
PE	Phycoerythrin
PE-Cy7	Phycoerythrin-cyanine 7
PFA	Paraformaldehyde
Ph	Philadelphia chromosome
PI3K/AKT	Phosphoinositide 3-kinase
PKA	Protein kinase A
PKC	Protein kinase C
PLC	Phospholipase C
PTH	Parathyroid hormone
PTHR	Parathyroid hormone receptor
PTHrP	Parathyroid hormone-related peptide
PVDF	Polyvinylidene fluoride
qRT-PCR	Quantitative real-time polymerase chain reaction
RAG2	Recombinant activating gene 2
RANKL	Receptor activator of nuclear factor kappa B ligand
RAR g	Retinoic acid receptor gamma
RBC	Red blood cells
RCC	Renal cell carcinoma
RFP	Red fluorescence protein
RhoA	Ras homolog family member A
RIPA	Radioimmunoprecipitation assay
RNA	Ribonucleic acid
RNase A	Ribonuclease A
ROS	Reactive oxygen species
RPMI	Roswell park memorial institute medium
RT	Room temperature
RUNX	Runt-related transcription factor
RV	Reverse
Sca-1	Stem cell antigen 1
SCF	Stem cell factor
SDF1	Stromal cell-derived factor 1

SDS	Sodium dodecyl sulfate
sgRNA	Single guide RNA
ST-HSC	Short-term hematopoietic stem cell
STAT	Signal transducer and activation of transcription
T-ALL	T-cell acute lymphoblastic leukemia
TBST	Tris-buffered saline containing 0.1 % Tween20
TCF4	T-cell factor 4
TET2	Ten-eleven translocation oncogene family member 2
TF	Transcription factors
TGF	Transforming growth factor
TKI	Tyrosine kinase inhibitor
TNFa	Tumor necrosis factor
TP53	Tumor protein 53
TRP	Transient receptor potential channel
VCAM	Vascular cell adhesion molecule
VDR	Vitamin D receptor
VEGF	Vascular endothelial growth factor
VFT	Venus flytrap
WBC	White blood cell count
Wnt	Wingless-related integration site
WT	Wild type
αKG	Alpha-ketoglutarate
γH2A.X	γH2A histone family member X

List of Figures

List of Tables

1 Importance

Leukemia can be defined as a group of cancers of the blood and bone marrow. Similar to other cancers, there is an uncontrolled growth and accumulation of abnormal cells while the production of healthy blood cells is defective. As a consequence, there is a physiologic disbalance that will, if left untreated, lead to patients' death. Leukemia is still one of the top ten deadliest diseases across the world and it affects both children and adults (The Global Cancer Observatory, 2020).

Conventional therapies are often not curative and the goal is to achieve molecular remission, the moment when leukemia cells are no longer detected in the body. Among the treatment options, leukemia patients can be subjected to chemotherapy, interferon or radiation therapy. If possible, hematopoietic stem cell transplantation (HSCT) provides a chance to increase the overall survival. However, therapies such as intensive chemotherapy and HSCT are generally only suitable for a small subset of patients (Khaddour et al., 2021).

One of the major reasons for the failure of conventional therapies is the difficulty in eradicating leukemia stem cells (LSCs), the cells that are believed to be responsible for the initiation, drug resistance, and relapse of leukemia (Bonnet and Dick, 1997). New and better forms of therapy, especially those with a novel mode of attack to be used in conjunction with existing therapies, are urgently needed in leukemia treatment. Despite an increasing number of studies using so called 'targeted therapies', which target intracellular and often leukemia-specific mechanisms, such treatment is only possible for a very limited number of leukemia types. Acute myeloid leukemia (AML) largely remains without effective therapies with a subset of patients eventually relapsing and dying of the disease. An approach considering a better characterization and targeting of LSCs might lead to deeper clinical remission, longer-lasting responses and substantially improve AML patient outcomes (Chiu et al., 2010; Lapidot et al., 1994; Uckun et al., 1995).

In the last decade, several studies have converged to suggest the microenvironment of LSCs, the bone marrow microenvironment (BMM), as a suitable therapeutic target in leukemia. It has been shown that LSCs are highly dependent on the BMM as they are regulated by its cellular and molecular components (Jin et al., 2006; Krause et al., 2013; Krause et al., 2006). Furthermore, the interaction of leukemia cells with the different cellular and acellular components of the BMM has been shown to mediate pro-survival mechanisms and protect LSCs from conventional and targeted therapy.

As yet, relatively little attention has been directed toward the role of chemical factors in leukemia, such as calcium ions, which are widely present in the BMM. The characterization of

all BMM components, and the identification of the interactions and dependencies between leukemia cells and the environment is necessary for a possible targeting strategy. Modulation of the BMM to make it inhospitable for malignant cells and ultimately eradicate leukemia stem cells is a novel and promising therapeutic strategy to augment existing therapies in leukemia (Krause and Scadden, 2015).

2 Theoretical Background

2.1 Hematopoiesis

Hematopoiesis is the process of producing all of the cellular components of blood, ensuring that an organism's blood supply is never depleted. The formation of blood cells is closely regulated and structured in a hierarchical manner based on the cells' functional capacity. The blood consists of distinct mature cell types, including white blood cells (leukocytes), red blood cells (erythrocytes), megakaryocytes/platelets, mast cells, T- and B- lymphocytes, myeloid cells (monocyte/macrophage and granulocytes), natural killer (NK) cells and dendritic cells (DCs) originating from hematopoietic stem cells (HSCs) (Jagannathan-Bogdan and Zon, 2013).

The HSCs are at the top of the hierarchy and are distinguished by their ability to self-renew and generate progenitor cells that can proliferate, differentiate, and give rise to all cellular components of the blood (Purton and Scadden, 2008). HSC can be categorized into multipotent long-term HSC (LT-HSC) or short-term HSC (ST-HSC) based on their potential to reconstitute lethally irradiated mice for short or long term upon transplantation. Through asymmetric cell division LT-HSC can self-renew to sustain the stem cell pool or differentiate into ST-HSCs and into multipotent progenitors (MPPs), which lose self-renewal potential and differentiate into cells of the various lineages (Rieger and Schroeder, 2012). Further downstream, MPPs advance to oligopotent progenitors as common lymphoid progenitors (CLPs) or common myeloid progenitors (CMPs), which have restricted lineage commitment. CLPs give rise to lymphoid cells as B-lymphocytes (B-cells), T-lymphocytes (T-cells) and natural killer (NK) cells. CMPs can give rise to megakaryocytic/erythroid-progenitors (MEPs), from which erythrocytes, megakaryocytes and platelets develop; granulocyte-macrophage progenitors (GMP), which give rise to granulocytes, monocytes and macrophages (Iwasaki et al., 2006; Manz et al., 2002; Passegué et al., 2003) (Figure 1). This hierarchical structure has recently been challenged, and the concept of hematopoiesis being a continuous and flexible system has been proposed (Zhang et al., 2018).

The primary site of hematopoiesis is the bone marrow (BM), where HSCs reside, are maintained, and differentiate into multiple blood lineages. (Chen et al., 2012; Kiel and Morrison, 2006; Krause and Scadden, 2015; Morrison and Scadden, 2014).

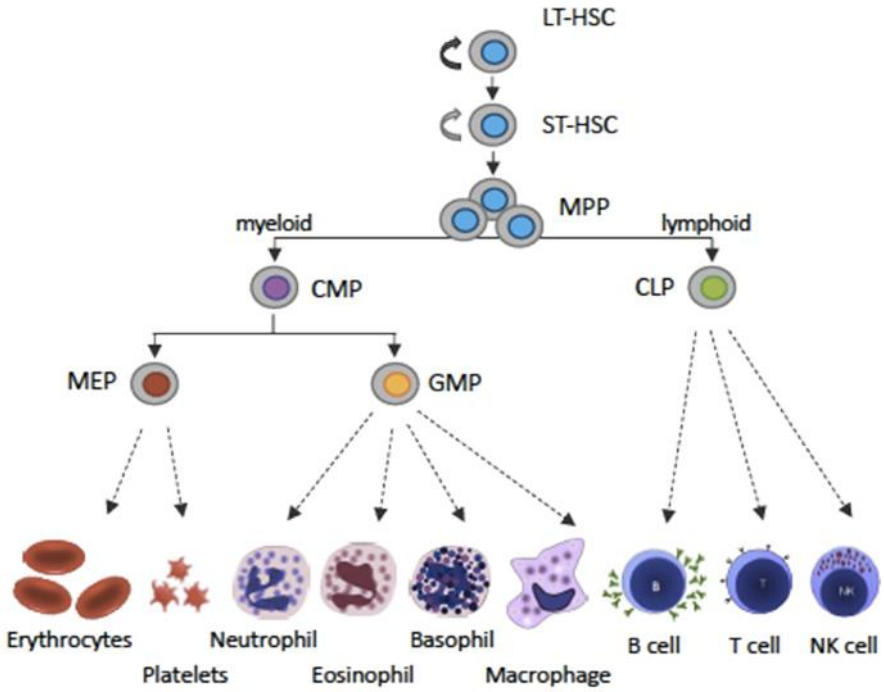

Figure 1. Simplified model of the hematopoietic hierarchy. Adapted from Soverini et al. (2021).

2.2 Hematologic malignancies

The balance between differentiation and self-renewal is strictly regulated by transcriptional and epigenetic regulators, metabolic pathways and cell-intrinsic factors to ensure hematopoietic homeostasis**.** However, mutations can arise in different populations, and if they occur at the top or near the top of the hierarchy, they can damage the entire hematopoietic system, resulting in hematologic malignancies. Hematologic malignancies are tumors of the blood and lymphoid tissue that are classified as leukemia, lymphoma, or myeloma depending on the type of blood cell involved (Jurlander, 2011).

2.3 Leukemia

The leukemia term comes from the Greek words leukos (white) and haima (blood), so leukemia literally means “white blood”. The disease is characterized by the uncontrolled proliferation of abnormal white blood cells (leukocytes) in the bloodstream and bone marrow. Due to their rapid growth, these aberrant cells frequently crowd out normal blood cells.

Leukocytes are important members of the immune system because they recognize pathogens such as bacteria and viruses, promote their phagocytosis, and produce antibodies to protect the body against future infections (Raskin et al., 2004). Leukemia causes imbalances between blood cells, making it harder to fight infections, coagulate blood (by impacting thrombocytes),

and transport oxygen efficiently (by impacting erythrocytes), resulting in symptoms such as fatigue, bone pain, fever, bleeding, infections, and swollen lymph nodes (Löwenberg et al., 1999)**.** The onset of leukemia can be acute or chronic, based on how quickly the disease progresses. In acute leukemia, cancer cells multiply quickly and a large number of leukemia cells accumulate very quickly. In contrast, a chronic leukemia progresses slowly, and early symptoms may be very mild. Leukemia is further classified as myeloid or lymphoid, depending on the type of white blood cell involved. Consequently, the four main types of leukemia are acute lymphoblastic leukemia (ALL), acute myeloid leukemia (AML), chronic lymphocytic leukemia (CLL) and chronic myeloid leukemia (CML) (Arber et al., 2016; Swerdlow et al., 2016).

2.4 Acute myeloid leukemia (AML)

Acute myeloid leukemia (AML) is a very heterogeneous, complex and dynamic malignancy. Pathogenically, AML represents a multistep process which involves multiple somatically acquired driver mutations, epigenetic dysregulation and formation of copy number aberrations. Primarily, AML is caused by genetic abnormalities in hematopoietic stem and progenitor cells, giving rise to preleukemic/leukemic stem cells, which lead to a blockade in the normal maturation process (Arber, 2019; Döhner et al., 2015). As a consequence, there is a clonal expansion and accumulation of abnormal immature blast cells in the bone marrow and peripheral blood (and possibly other organs), which impair normal hematopoietic function by alteration of self-renewal, proliferation and differentiation, eventually leading to bone marrow failure. Some non-random genetic alterations, such as deletions and translocations, have been identified in more than 50 % of AML patients, and they have been associated with the cause and progression of the disease (Pourrajab et al., 2020).

AML is the most predominant acute leukemia diagnosed in adults. It is commonly a rapidly progressive disease, and it accounts for the most leukemia deaths among all types of leukemia with a 5-year survival rate of 25 % (https://www.cancer.net). Targeted therapies for AML are rare and the patients are predominately treated with chemotherapy. As post-remission therapy, an allogeneic hematopoietic cell transplant (HCT) can be performed, but the percentage of patients fitting the eligibility criteria for this treatment is very low (Khaddour et al., 2021).

2.4.1 Morphology and phenotype of blasts

Phenotypically, AML blasts are characterized by large prominent nuclei with finely dispersed chromatin, monocyte-sized and commonly containing several nucleoli. In addition, the presence of myeloperoxidase (MPO) activity is characteristic of these cells (Ahuja et al., 2018).

Immunophenotypically, AML blasts frequently express common differentiation (CD) markers CD33, CD13 and the precursor cell marker CD34, antigens also found on healthy immature myeloid cells. Depending on the stage of differentiation and morphologic subtype of AML, monocytic differentiation markers (CD11b, CD14), megakaryocyte (CD41a, CD61) and erythroid (CD71, CD36) markers are expressed. Occasionally, AML blasts might co-express T- or B-cell specific antigens (e. g., CD7, CD19) (Gorczyca et al., 2011).

The karyotype and other genetic alterations of acute myeloid leukemia (AML) have long been recognized as the most valuable prognostic factor in AML**.** However, karyotypic abnormalities have been only detected in half of all AML cases and approximately 45 % of AML patients are cytogenetically normal (Gaidzik and Döhner, 2008). Normal-karyotype AML patients are part of the intermediate-risk group with a 5-year survival of approximately 35 % following post-remission chemotherapy (Byrd et al., 2002; Copelan et al., 2015; Grimwade, 2007; Grimwade et al., 2010; Koreth et al., 2009)**.** By the employment of high-throughput next-generation sequencing technologies, it is possible to molecularly characterize AML cells and identify multiple genetic alterations, and particular combinations of mutations which contribute to AML pathogenesis and are biologically and prognostically significant (White and DiPersio, 2014).

2.4.2 Genetic abnormalities

In AML, blasts result from clonal transformation of hematopoietic stem and precursor cells (HSPCs) through the acquisition of gene mutations or chromosomal rearrangements which impair cell differentiation and confer proliferation and survival advantages to the transformed cells (Walter et al., 2012). Besides this initial event, AML cells acquire additional genetic mutations, leading to the co-existence of distinct clones. This clonal diversity is used by the malignant cells as survival mechanism in face of chemotherapy or attacks by the immune system, by having distinct resistant subclones survive and propagate the disease (Ishikawa et al., 2007).

In 2001, Gilliland proposed the two-hit model in AML, which postulates that the disease results from the cooperation between two classes of driver mutations, Class I and Class II, which work synergistically during AML development (Figure 2). Class I oncogenes confer proliferative and/or survival advantages or generally activate kinase signaling. Class II oncogenes commonly impair myeloid differentiation and apoptosis and tend to affect transcriptional regulation of genes (Dash and Gilliland, 2001). The coexistence of Class I and II oncogenes is critical to AML development, whereby leukemogenesis is promoted by enhanced proliferation and blockade of differentiation. However, there are exceptions, and some oncogenes can

mediate functions of both classes, which is the case for FLT3-ITD, which in addition to promoting proliferation and viability, is able to regulate the differentiation genes C/EBPα and PU.1 and consequently mediate a differentiation block (Kiyoi and Naoe, 2006). Recently, a new oncogene group has been identified which comprises mutations in epigenetic modifiers which overlap with both Class I and Class II mutations (Lagunas-Rangel et al., 2017).

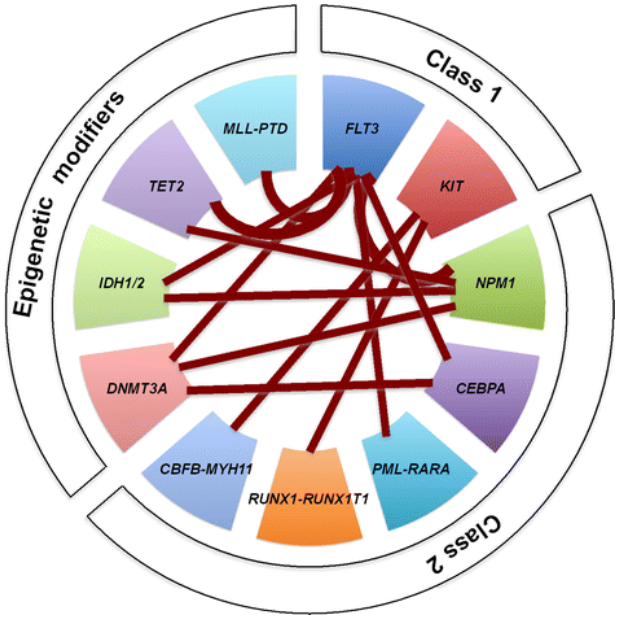

Figure 2. Interaction of genetic mutations in AML. Adapted from Naoe and Kiyoi (2013).

2.4.3 Molecular abnormalities

Several studies published in the previous decade have demonstrated that molecular abnormalities such as particular gene mutations and/or changes in gene expression are prognostically significant and can be utilized to risk stratify patients and predict their outcome, thereby benefitting patients during treatment for AML.

Nucleophosmin 1 (NPM1) mutations are the most frequent mutations in AML, being found in about 30 % of all AML patients (Falini et al., 2005). NPM1 is a phosphoprotein that functions as a molecular chaperone of proteins, and it plays a role in protein transport between the nucleus and the cytoplasm, which is important for critical cell functions such as blockade of ribosome biogenesis, cell proliferation and apoptosis. NPM1 mutations lead to loss of a nucleolar localization signal and consequently abnormal cytoplasmic location. In the cytoplasm, NPM1 cannot perform its normal functions, leading to impairment of nuclear protein transport. This is believed to stimulate myeloid proliferation and leukemia development through a gain versus loss of function in different cellular processes (Falini et al., 2009).

2.4.4 Signaling and kinase pathway mutations

In addition to *NPM1* mutations, around 65 % of AML cases have mutations in cellular signaling pathways such as *FLT3* and *c-KIT*.

Fms-Like Tyrosine Kinase 3 (FLT3) is a transmembrane tyrosine-kinase receptor highly expressed in hematopoietic stem cells, and it is commonly mutated in AML. Approximately 25 % of the AML cases present *FLT3* somatic alterations and it is commonly found in AML with normal karyotype (Kelly et al., 2002). Tyrosine kinase inhibitors (TKIs) have been tested in FLT3 mutated AML patients, though only a transient reduction of blasts was observed. In addition, it was observed that TKI treatment gave rise to the acquisition of secondary mutations, which can lead to drug resistance over time (Daver et al., 2015).

The KIT tyrosine receptor is a highly conserved transmembrane protein, member of the type III tyrosine kinase family. *Kit* mutations are present in less than 5 % of AML cases. However, they are frequently associated with high relapse risk and poor outcome of core-binding factor AML (CBF-AML) (Ayatollahi et al., 2017; Tarlock et al., 2019)**.** As a tyrosine kinase, some studies have been performed in order to pharmacologically target c-KIT by combining standard therapy with the tyrosine kinase inhibitor dasatinib (phase II clinical trial), however the results were inconclusive and more studies are needed (Paschka et al., 2018; Shah et al., 2006a).

2.4.5 Mutations in transcription factors

In the bone marrow, transcription factors, such as the runt-related transcription factor (RUNX1) and the differentiation-inducing transcription factor CCAAT enhancer binding protein α (C/EBPα) establish and maintain genetic networks to maintain the normal hematopoietic system. Mutations in these genes lead to expression of aberrant proteins which can be found in AML patients.

RUNX1, also known as AML1 or core-binding factor subunit α-2 (CBFA2), is a member of the core-binding factor family of transcription factors. Several studies have demonstrated that RUNX1 is a key regulator of hematopoietic genes (Ichikawa et al., 2004). In analogy to normal hematopoiesis, RUNX1 is important in AML pathogenesis and its mutations are found in 5-10 % of AML patients. These mutations are associated with acquired resistance to standard therapy and poorer prognosis (Gaidzik et al., 2016).

C/EBPα belongs to the basic leucin zipper family, and it is known to control gene expression during hematopoiesis. This transcription factor is critical for myeloid cell development and is found mutated in 6-10 % of all AML cases (Ho et al., 2009). *CEBPA* mutations are used to stratify patients with AML and are associated with high response rate. However, they are also

associated with a high relapse rate, which still remains the major cause of treatment failure in AML.

2.4.6 Mutations in epigenetic modifiers

A series of recurrent genetic abnormalities in genes encoding proteins that normally function in the epigenetic regulation of gene transcription have been identified in patients with AML. This involves frequent mutations in the genes *IDH1/2* (isocitrate dehydrogenase 1/2), *TET2* (ten-eleven translocation 2), *DNMT3A* (DNA nucleotide methyltransferase 3A), and *ASXL1* (the addition of sex combs like 1).

IDH mutations are observed in 15-20 % of all AML patients and are associated with advanced age and with patients exhibiting NPM1 mutations (ElNahass et al., 2020)**.** The IDH family includes three homodimeric enzymes that catalyze the conversion of isocitrate to alpha-ketoglutarate (αKG): IDH1, expressed in the cytoplasm; IDH2, a critical component of the Krebs cycle and IDH3, present in the mitochondrial matrix. Several studies have shown that IDH mutations itself are insufficient to induce leukemic transformation in mice; it implies the presence of leukemogenic myeloid progenitor cells, though the prognosis of relapsed/refractory IDH mutated AML patients is particularly poor (Kats et al., 2014).

TET2 is an epigenetic modifier commonly found mutated in myeloid malignancies. It is frequently observed in apparently hematological normal individuals with clonal hematopoiesis and in 7-10 % of adult and 1.5-4 % of pediatric AML patients, and its frequency increases with age (Chou et al., 2011; Wang et al., 2019). Variable TET2 mutations cause loss of function and decreased hydroxymethylation of DNA which leads to aberrant hematopoietic stem and progenitor cell self-renewal, differentiation and cell death (Moran-Crusio et al., 2011). Recent experiments have demonstrated that restoration of TET2 catalytic activity by potent activators (e. g. Vitamin C) are able to reverse the transforming ability of TET2, which can be a promising strategy of treatment for patients harboring this mutation (Cimmino et al., 2017).

DNMT3A mutations are observed in approximately 20 % of AML patients (Ley et al., 2010). DNMT3 is a DNA methyltransferase involved in epigenetic regulation through maintenance of DNA methylation patterns during development, which prevents genomic instability by regulating the expression of tumor suppressors and oncogenes (Sandoval et al., 2019). In addition to aberrant DNA methylation patterning, specific mutations in DNMT3A disturb interactions with regulatory components and are associated with aberrant transcriptional regulation and cellular differentiation. DNMT3A mutations are considered an early event in AML evolution, persisting during remission (Challen et al., 2011).

ASXL 1 is recurrently mutated (deleted or truncated) in all forms of myeloid malignancies, especially in AML. ASXL1 and ASXL2 mutations are mutually exclusive and affect 5-11 % of AML cases. They are associated with poor prognosis in AML, and their frequencies increase with age (Gelsi-Boyer et al., 2012).

2.4.7 Mutations in tumor suppressor genes

Mutations in tumor protein 53 (TP53), a key tumor suppressor gene, are prevalent in solid cancers and can be found in 8-14 % of patients with AML, where they are associated with an unfavorable prognosis (Short et al., 2020). In the hematopoietic compartment of AML, TP53 inactivation was shown to have a very adverse prognosis with increased leukemia-initiating potential, chemoresistance and high relapse rates (Sill et al., 2020; Zhu et al., 1999).

2.4.8 MLL-rearrangements

The mixed lineage leukemia gene (MLL), also known as lysine methyltransferase 2A (KMT2) or ALL-1, is located on chromosome 11q23 and encodes for a 500 kDa protein which has histone methylation activity. This protein is part of a complex that regulates histone methylation and regulates gene transcription and chromatin by binding to target gene promoters, generating a chromatin environment which enables active gene transcription (Muntean and Hess, 2012). MLL rearrangements (MLL-r), results of deletions, duplications, inversions or reciprocal translocations at 11q23, are well-known to cause ALL, AML or mixed phenotype acute leukemia. Acute leukemia with somatic MLL rearrangements involves a chromosomal translocation that fuses the MLL gene with one of the fusion partner genes. More than 80 distinct partner genes for MLL-r have been identified (Winters and Bernt, 2017). MLL rearrangements are found in both myeloid and lymphoid acute leukemia. Frequently these chromosomal translocations lead to dysregulated histone modification and chromatin accessibility. However, the fusion partner gene of MLL is the major determinant of the leukemia phenotype. The majority of the MLL-r ALL (90 %) and around half of the AML cases involve fusions of the 5‘-end of MLL with the 3’ portion of its partner gene. The four most common partner genes are *AF4* t(4,11); *AF9* t(9,11); *ENL* t(11,19) (q23,p13.3) and *AF10* t(10,11) (Harper and Aplan, 2008; Winters and Bernt, 2017).

The MLL fusion genes and their protein function are still poorly understood. However, they are able to transform hematopoietic cells into leukemia cells at different developmental stages by conferring stem-cell like properties. MLL-r ALL cases are believed to result from the activation of “stem cell-like” genetic programs, whereby most MLL-r AML patients present a genetic

program caused by overexpression of HOXA/MEIS1 proteins. Normal hematopoietic stem and early progenitor cells express high levels of HOX and MEIS1 proteins, whose expression levels are downregulated during differentiation (Harper and Aplan, 2008). HOX genes and their cofactor MEIS1 are capable of disrupting crucial transcriptional machinery and maintain cell self-renewal capacity, driving the development and maintenance of MLL-r AML and promoting their oncogenic potential (Alharbi et al., 2013). In contrast to MLL-AF4 which often results in lymphoid malignancies, MLL-AF9 is mostly associated with myeloid leukemias (Chen et al., 2019). This fusion protein promotes the methylation at H3K79 which mediates the overexpression of *HOX* genes and blockade of differentiation, thereby transforming myeloid progenitor cells into GMP. Based on murine transplantation experiments, some studies indicate that MLL-AF9 AML is not only driven by LSCs, but also by CMP and GMP progenitor cells (Chen et al., 2008; Chen et al., 2019; Krivtsov et al., 2013).

As part of this process, meningioma-1 (MN1) is an essential cofactor in MLL-rearranged leukemic transformation. This protein is a transcriptional regulator that forms a complex with a conserved region of MLL, and it is known to induce AML dependent on HOX and MEIS1 genes. MN1 is frequently overexpressed in AML patients and associated with a poor prognosis (Sharma et al., 2020).

2.4.9 Splicing factor gene mutations

The spliceosome is a ribonucleoprotein complex that recognizes and catalyzes the excision of introns (noncoding sequences) and ligation of exons (coding sequences) of nuclear precursor messenger RNA (pre-mRNA) in a sequential manner (Chen and Moore, 2015). This complex and essential step of gene expression is crucial for hematopoietic function. However, mutations in splicing machinery genes are often found in AML and pre-leukemic conditions such as myelodysplastic syndrome (MDS). Approximately 10 % of AML patients present mutations in the splicing factors *SF3B1*, *U2AF1*, *SRSF2* and *ZRSR2* (Dolnik et al., 2012), though whether these mutations mediate or sustain malignant transformation is still unclear. In addition to the presence of mutated splicing factors, the gene regulation can be changed driving an alteration in the stability of the transcripts and an incorrect gene translation and abnormal protein function (Taylor and Lee, 2019).

2.4.10 Mutations in cohesion complex members

Cohesin is a protein complex that encircles the sister chromatids and mediates cohesion during cell division, which is an essential step for chromosome segregation. In addition to its role in mitosis and meiosis, cohesin has also been shown to be required for DNA damage repair and regulation of gene expression through its localization in enhancers and core promoter regions (Brooker and Berkowitz, 2014). The cohesin complex is comprised of four subunits *SMC3*, *SMC1A*, *RAD21*, and *STAG1/2* , and somatic mutations in these genes were identified in approximately 10 % of AML cases (Han et al., 2021). Evidence suggests that, as a pre-leukemic event, cohesin mutations lead to a modulation in the chromatin accessibility in HSPC enforcing the expression and activity of ERG, RUNX1 and GATA2, master hematopoietic transcription factors known to favor self-renewal and impaired differentiation status of the cells (Fisher et al., 2017; Mazumdar et al., 2015) (Figure 3).

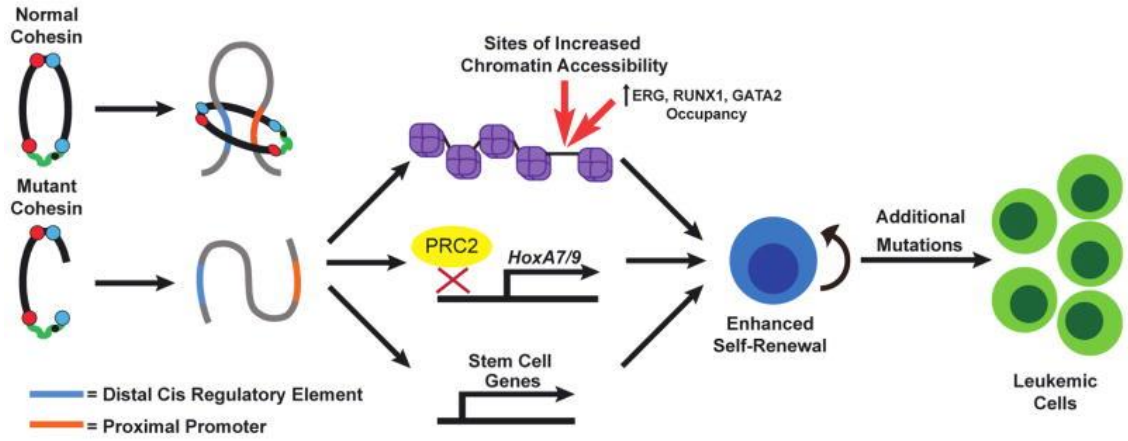

Figure 3. Acute myeloid leukemia is associated with mutations in cohesin (Fisher et al., 2017).

2.5 Chronic myeloid leukemia (CML)

Chronic myeloid leukemia (CML) is a form of leukemia that belongs to the myeloproliferative neoplasms (MPNs). It is one of the most well-studied leukemias, and it is defined by the presence of increased number of myeloid cells in the bloodstream and bone marrow. The myeloid cells are of all stages of maturation (Arber et al., 2016).

CML accounts for 15 % of all types of leukemia, and it is most commonly diagnosed in adults over the age of 64 (https://www.cancer.net). CML can progress into acute leukemia if not treated. Molecularly, CML is caused by a translocation between BCR from chromosome 9 and ABL1 from chromosome 22 (t(9,22)), resulting in the creation of the “Philadelphia chromosome (Ph)” (BCR-ABL1), which is found in nearly all CML patients (Barbui et al., 2018).

This fusion gene functions as a tyrosine kinase oncoprotein that can auto-phosphorylate and is constitutively active. As a result, Abl1 signaling pathways are activated, augmenting cellular activities like proliferation, loss of stromal adhesion, and survival (Laneuville, 1995). BCR-ABL1 activates the Ras-mitogen-activated protein kinase (MAPK), the Janus-activated kinase (JAK)-signal transducers and activators of transcription (STAT) pathway, and the phosphoinositide 3-kinase (PI3K/AKT) pathway, resulting in uncontrolled proliferation and suppression of apoptosis (Cilloni and Saglio, 2012; Skorski et al., 1995).

When evaluating the patient's blood, there are three phases of CML, each of which is distinguished by various illness patterns. The first is chronic phase, which can persist for several years. The blood and bone marrow contain less than 5% blasts, yet are characterized by myeloid cells of various differentiation stages. The chronic phase might proceed to an accelerated phase, in which more blasts (5-19 %) form in the bone marrow and reach the bloodstream. Lastly, patients may experience blast crisis which is marked by >20 % of blasts in the bone marrow and peripheral blood, and the patients might experience fever, fatigue, night sweats, weight loss and splenomegaly (Arber et al., 2016). Blast crisis resembles AML or, less frequently, B-ALL and is fatal in a short period of time, if untreated (Sawyers, 1999).

Fortunately, imatinib mesylate (Gleevec, Novartis), a BCR-ABL1 tyrosine kinase inhibitor, has been available since 2001. By the inhibition of the enzyme's ATP-binding site and the reduction of BCR-ABL1 activity, the CML patients' 5-year survival rates increased to 90 % (Druker et al., 2006). Despite this therapeutic breakthrough, some individuals acquire mutations in the *BCR-ABL1* gene which confer imatinib resistance, resulting in disease recurrence. Furthermore, imatinib therapy does not eliminate leukemic stem cells (LSCs), and when imatinib is stopped, a large percentage of patient’s relapse (Corbin et al., 2011; Hochhaus et al., 2020).

2.6 B-cell acute lymphoblastic leukemia (B-ALL)

Acute lymphoblastic leukemia (ALL) is the result of malignant transformation and a clonal proliferation of lymphoid stem or progenitor cells in the bloodstream, bone marrow and extramedullary sites (Pui, 2010). B-ALL is more frequent than T-ALL. B-ALL is the most frequent type of cancer in children. It is the leading cause of death in children and young adults, even though it has a fair chance of being cured (85%). Adults can develop acute lymphoblastic leukemia. The chances of cure are slim, leading to a five-year overall survival rate lower than 45 % (Bassan and Hoelzer, 2011; Jabbour et al., 2015; Tang et al., 2021). The pathophysiology of B-ALL has been linked to recurrent cytogenetic and molecular abnormalities, and several genetic and transcriptional aberrations have been identified.

Essential functions such as stem cell self-renewal and differentiation, cell cycle regulation, epigenetic modification, and transcriptional regulation are typically affected by these anomalies (Roberts et al., 2012).

B-ALL is a very heterogeneous disease that can manifest itself as numerous genetically diverse clones within a single person. As a contributing factor of this heterogeneity, hyperploidy is a characteristic chromosomal pattern in B-ALL patients, and it is present in 25 % of pediatric and 7 % of adult patients (Harrison et al., 2004; Pui et al., 2004)**.** B-ALL patients usually present mutations in genes important for normal B-cell development such as *PAX5* and *IKZF1*, however a large percentage of mutations occur in *RAS* signaling genes (Paulsson et al., 2008). Additionally, also chromosomal rearrangements of *BCR-ABL, MLL, TEL* and *TCF3* are frequent in B-ALL patients (Mullighan, 2012). In addition to genetic alterations, epigenetic changes have been shown to be able to regulate major mechanisms that promote leukemogenesis in B-ALL (Kuang et al., 2013).

2.7 Leukemia stem cells (LSC)

Stem cells are defined as slowly dividing cells with the capacity to differentiate into a variety of mature cells, generating progeny, while also being able to self-renew, sustaining the stem cell pool (Chagastelles and Nardi, 2011; Passegué et al., 2003). One of the hallmarks of cancer stem cells is the ability to continuously self-renew (Hanahan and Weinberg, 2000), and, similar to normal hematopoiesis, a population of cells with self-renewal capacity, defined as cancer stem cells (CSC), is assumed to be the cause of and sustain cancer development (Lapidot et al., 1994). In the case of leukemia, these cells are designated as leukemia stem cells (LSCs) and despite a certain resemblance to normal HSC, LSCs are able to outcompete normal HSC. Given these similarities, the characterization, identification and targeting of LSCs, which are believed to be the major cause of disease relapse, are challenging. These cells are mostly quiescent (Arai et al., 2004; Essers and Trumpp, 2010; Saito et al., 2010) and due to the fact that the current chemotherapeutic regimens predominantly target dividing cells, LSCs can evade chemotherapy and enhance leukemia progression.

2.8 Bone marrow microenvironment (BMM)

Hematopoiesis and leukemogenesis are processes that occur mainly in the bone, specifically in the spongy tissue of the bone marrow (BM). Normal hematopoietic stem cells and their malignant counterparts reside in the bone marrow microenvironment (BMM) which is a

complex arrangement of various cell types, extracellular matrix proteins (ECM) and cytokines that is responsible for the maintenance of the blood system (Schofield, 1978).

The BMM consists of various cell types such as adipocytes, osteoblasts, osteoclasts, mesenchymal stem cells (MSCs), macrophages, megakaryocytes, fibroblasts, sinusoidal and arteriolar endothelial cells, non-myelinating Schwann cells, sympathetic neurons, perivascular reticular cells and other hematopoietic cells. Collectively, these cells have a functional role in the regulation of hematopoiesis through production of cytokines, chemokines and growth factors, the production and deposition of different ECM proteins. The BMM is also characterized by a defined pH and oxygen tension.

The bone marrow can be formally divided into two major niches: an endosteal or osteoblastic and the vascular niche, which are known to have important and distinct functions on stem cell quiescence, self-renewal, homing, mobilization or lineage commitment (Morrison and Scadden, 2014). However, this terminology has become somewhat outdated. Under homeostatic conditions, HSCs are found close to the endosteal area of the bone (Arai et al., 2004; Gong, 1978; Lord et al., 1975; Zhang et al., 2003). Murine transplantation experiments demonstrated that stem cells preferentially migrate to the endosteal region (Lo Celso and Scadden, 2011; Nilsson et al., 2001; Xie et al., 2009). In addition, some studies demonstrate that osteoblasts are important for maintenance and survival of HSCs (Arai et al., 2004; Calvi et al., 2003; Visnjic et al., 2004; Zhang et al., 2003) and that stem cells isolated from the endosteum have a better proliferative potential, as well as greater long-term hematopoietic restoration capacity (Grassinger et al., 2010; Haylock and Nilsson, 2005). Similar to the osteoblastic niche, also the vascular niche has been shown to function as HSC-supporting niche. HSCs located in close proximity to blood vessels benefit from nutrient delivery and gas exchange promoting their maintenance and expansion (Kiel and Morrison, 2006). The higher oxygen levels in the vascular niche compared to the hypoxic osteoblastic niche is one of the major physiological differences between the two niches (Parmar et al., 2007), however, despite this blood supply, direct measurements of oxygen levels have showed that overall the BM is hypoxic (1-2 % O_2) (Spencer et al., 2014). Some studies indicate that quiescent HSCs preferentially locate in association with sinusoids, immediately adjacent to the endosteal surface rather than to sinusoids in the vascular niche (Acar et al., 2015; Chen et al., 2016; Koechlein et al., 2016). In response to various stimuli, stem cells may migrate to the vascular niche, where increasing oxygen levels support their differentiation potential (Kunisaki et al., 2013)

In addition to cellular elements, non-cellular structures such as ECM proteins play a crucial supporting role for HSCs in the BMM. The main ECM proteins in the BMM include fibronectin

(FN), collagen (types I and IV), hyaluronan and laminin. These proteins are secreted by certain cells into the extracellular space and dynamically interact with the BMM cells, providing a structural scaffold and regulating cell homeostasis through the control of processes such as cell viability, growth, mobilization and differentiation. Furthermore, the structural arrangement of the ECM facilitates the access of cells to growth factors, cytokines and other enzymes (Marastoni et al., 2008).

Recent research has highlighted that hematopoietic cells benefit from cytokines in the BMM (Fidyk et al., 2018). These cytokines are secreted by specific cells in the bone marrow and can regulate and support hematopoiesis by triggering the immune system and inflammation. Processes such as apoptosis, quiescence, self-renewal, differentiation and the mobility of HSCs rely on the presence of multiple cytokines and their signaling. Some of these cytokines include stem cell factor (SCF) (Hassan and Zander, 1996; Ikuta and Weissman, 1992), bone morphogenic proteins (BMPs), transforming growth factor (TGF)-β (Blank et al., 2008; Pimanda et al., 2007), angiopoietin-like proteins (Zhang et al., 2006), thrombopoietin (TPO) (Buza-Vidas et al., 2006; Petit-Cocault et al., 2007), notch ligands (Calvi *et al.*, 2003; Duncan et al., 2005) and fibroblast growth factors (Crcareva et al., 2005).

2.9 The supportive role of the BMM in leukemia

The BM microenvironment, which is composed of a complex and diverse network of different cell types supports and sustains hematopoiesis as mentioned in the previous section. However, its role in development, maintenance and outcome of hematological malignancies has also been described.

Osteoblasts, specialized cells responsible for bone formation, are considered to play a role in leukemia development. Raaijmakers et al. (2010) provided one of the first indications that alterations of osteoblasts might lead to hematopoietic dysregulation by showing that inactivation of Dicer1, an RNA-specific endonuclease, in osteoprogenitors caused myelodysplasia (MDS) in mice. Krause et al. (2013) demonstrated that LSCs could be targeted in CML by osteoblastic cell-specific activation of the parathyroid hormone (PTH) receptor and increased bone remodeling. In support of the significance of osteoblasts in leukemia, ablation of osteoblastic cells accelerated leukemia development in numerous animal models of AML and ALL (Dong et al., 2016; Frisch et al., 2012; Haddy et al., 2001; Sala and Barr, 2007).

Similar to osteoblasts, Mesenchymal stromal cells (MSCs) also support leukemia progression. Many patients with hematologic disorders have MSCs with structural chromosomal

abnormalities, (Blau et al., 2007) and malignant cells were shown to be able to genetically and epigenetically reprogram MSCs in order to promote its proliferation (Medyouf et al., 2014).

Several adhesion molecules have been identified to mediate niche interaction with leukemia cells, driving disease progression. E-selectin, which is expressed on endothelial cells, is known to facilitate LIC engraftment in CML. The interaction with the cell-surface glycoprotein CD44 is necessary for effective homing and engraftment of LSCs (Godavarthy et al., 2020; Krause et al., 2006). Another important cell membrane protein which interacts with several BMM components is the C-X-C chemokine receptor type 4 (CXCR4) that binds C-X-C ligand type 12 (CXCL-12), also known as stromal cell derived factor-1 (SDF-1). The CXCR4-CXCL-12 pathway has been linked to regulation of HSC quiescence regulation (Zhang et al., 2016b), and its overexpression is associated with poor AML survival, most likely due to enhanced migratory capacity (Tavor et al., 2008).

In addition to the supportive role in leukemia maintenance and progression, the BMM has also been shown to provide some protection from chemotherapy. Current research is focused on disrupting the interactions of LSCs with the BM niche in order to sensitize the cells to cytotoxic chemotherapies and eradicate them. One of the mechanisms underlying the resistance of LSCs to therapy is quiescence. Quiescent LSCs have restricted their proliferation and metabolism to the lowest necessary for survival. But as most chemotherapy agents have cell cycle-dependent cytotoxic effects, this results in poor targeting of quiescent LSC. Leukemia stem cells preferentially home and engraft within the endosteal area of the BM, which confers protection from chemotherapy-induced apoptosis (Duan et al., 2014; Ishikawa et al., 2007; Lane et al., 2011).

2.10 Calcium in the BMM

2.10.1 Calcium homeostasis

Calcium (Ca^{2+}) is the most abundant mineral in the human body, and it plays a role in a variety of biological processes. Depending on its specific location, the calcium concentration varies being low in the cytoplasm (cCa^{2+}), nucleus (nCa^{2+}), and mitochondria ($mtCa^{2+}$) *versus* high in the extracellular space (eCa^{2+}) (Bagur and Hajnóczky, 2017). Most of the calcium is stored in the skeleton and teeth, and only a small fraction is detected in circulation and in soft tissues where it has vital functions (Piste et al., 2012). Extracellular calcium is well known to be crucial for the regulation of a wide range of biological processes including transmission of nerve impulses, blood coagulation, hormone synthesis and secretion, muscle contraction and bone and tooth formation (Brown, 1991). Due to all these vital functions, circulating calcium is tightly regulated by a complex system. In this way, circulating plasma calcium is maintained within a

narrow range of 2.5 mM of total calcium containing 1.2 mM of ionic calcium (Bronner, 1997). The homeostatic mechanism balancing extracellular calcium consists of four major components: (1) the parathyroid glands which sense the calcium concentration, (2) the hormones parathyroid hormone (PTH), calcitonin, and 1,25-dihydroxyvitamin D [$1,25(OH)_2D_3$]; (3) the skeleton which is the biggest calcium source and (4) the gut and kidneys, which support calcium transport between the extracellular fluid and the external environment. A decrease in the serum Ca^{2+} concentration is detected by the extracellular calcium-sensing receptor (CaSR) expressed on the parathyroid glands (and other tissues), which induces PTH secretion. The secreted PTH acts on the PTH1 receptor (PTH1R) in the kidneys and in bone. In the bone, PTH1R activation leads to the release of cytokines, which stimulate osteoclastic bone-resorbing activity, thereby releasing calcium from the skeleton into the extracellular fluid. In the kidneys, PTH1R activation increases tubular calcium reabsorption and stimulates the production of the proximal renal tubular 1-α-hydroxylase (CYP27B1) enzyme. This enzyme promotes the conversion of the 1,25-dihydroxyvitamin D3 (1,25D3) metabolite to its active form, also named calcitriol, which is the most common form of vitamin D in circulation. The elevated calcitriol levels lead to an increased absorption of dietary calcium in the intestine *via* activation of vitamin D receptor (VDR). Collectively these processes mediate an increase in circulating Ca^{2+} which will inhibit PTH secretion through a feedback mechanism (Hofer and Brown, 2003; Loupy et al., 2012; Riccardi and Valenti, 2016) (Figure 4).

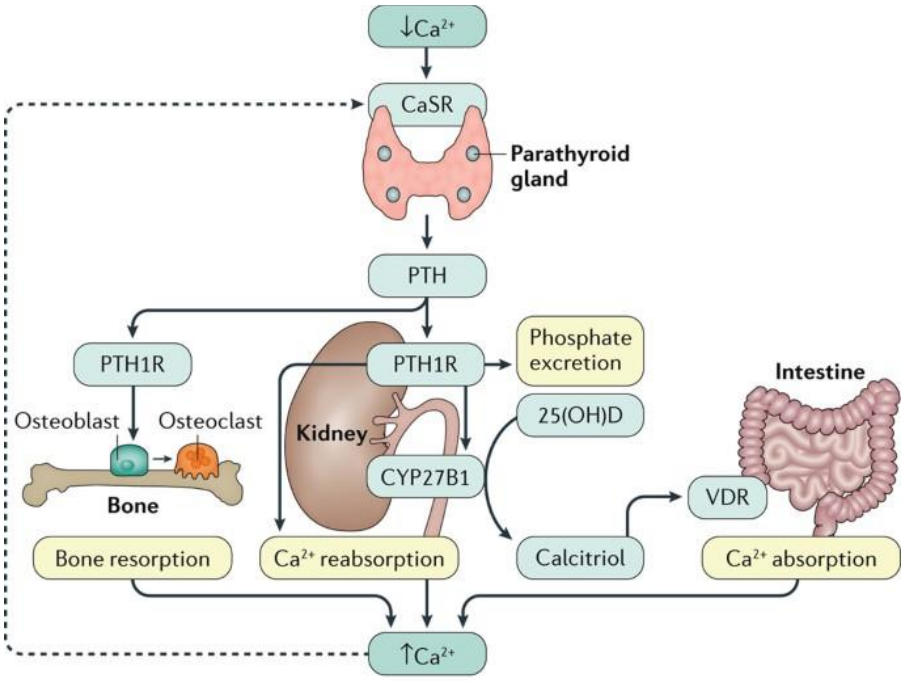

Figure 4. Calcium homeostasis (Mannstadt et al., 2017).

2.10.2 Calcium sensing receptor (CaSR)

The extracellular calcium-sensing receptor (CaSR) is a ubiquitously expressed dimeric class-C G protein-coupled receptor (GPCR). CaSR is an integral membrane protein and highly expressed in the parathyroid glands and kidneys (Regard et al., 2008). The human *CaSR* gene has seven exons, is found on the long arm of chromosome 3 and codes for a 1,078 amino acid protein. Structurally, this transmembrane protein consists of three major domains: an extracellular domain (ECD) at the N-terminal, a seven-pass transmembrane (TM) domain, a common feature of all GPCRs, and an intracellular C-terminal domain (Garrett et al., 1995). The large extracellular domain, which comprises the majority of the CaSR's ligand binding sites, has two globular lobes that adopt a Venus flytrap (VFT) conformation (Zhang et al., 2016a) (Figure 5). In response to agonist activation, the VFT changes its conformation and initiates signal transduction *via* interactions with the transmembrane and intracellular domains (Bai et al., 1998b; Chakravarti et al., 2012; Ray et al., 2007). As a result, CaSR integrates fluctuations in extracellular calcium levels with intracellular signaling. Extracellular calcium ions are the primary ligands for CaSR; however, CaSR can also be activated by other cations, polyamines and polypeptides (Brown et al., 1991a; Brown et al., 1991b; Quinn et al., 1997). These molecules are CaSR agonists, also named type I calcimimetics, and they induce receptor activation if calcium ions are not available. Allosteric modulators, a different type of CaSR agonists, can be observed. *Via* binding in the transmembrane region these modulators might affect the affinity of the receptor to calcium favorably (calcimimetics) or unfavorably (calcilytics) and, thereby, affect signaling (Jensen and Bräuner-Osborne, 2007). While the CaSR is generally found at the cell surface as a homodimer, it may form heterodimeric complexes with other members of family C of the GPCR superfamily (Bai et al., 1998a; Gama et al., 2001). Additionally, it was shown that CaSR can also bind and interact with several other proteins such as filamin, arrestins and dorfin (Hjälm et al., 2001; Pi et al., 2002; Sampson et al., 2003; Zhang and Breitwieser, 2005).

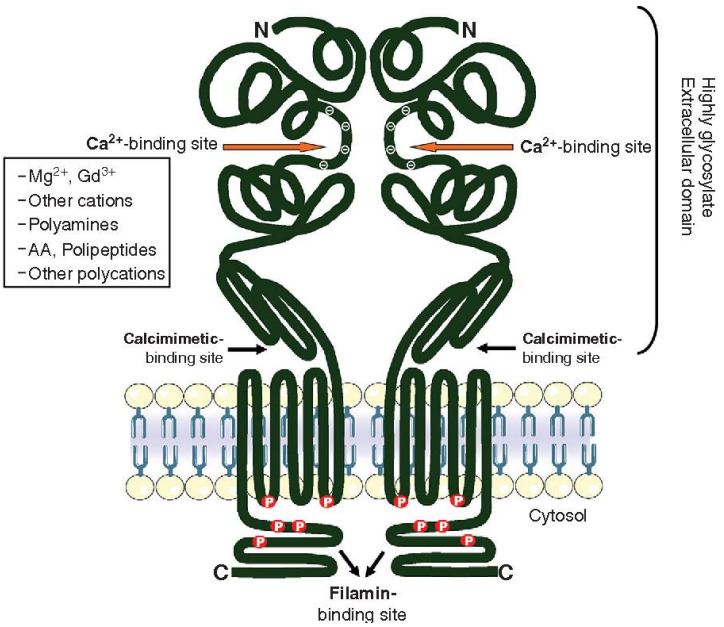

Figure 5. The extracellular calcium sensing receptor structure (Díaz-Soto et al., 2016).

In humans, abnormal CaSR expression is usually linked to calciotropic diseases. Gain of function mutations have been shown to cause autosomal dominant hypocalcemia with hypercalciuria (ADHH) and Bartter's syndrome type V. These disorders can also be acquired if anti-CaSR-blocking or -stimulating antibodies are present, respectively. Loss of function mutations, in turn, have been associated with hypocalciuric hypercalcemia syndromes leading to familial benign hypercalcemia (FHH, FBH or FBHH) or neonatal hyperparathyroidism (NSHPT) if the mutations are heterozygous or homozygous, respectively (Figure 6) (Hannan et al., 2016; Hendy et al., 2000; Pollak et al., 1993; Pollak et al., 1994; Thakker, 2015).

CaSR Abnormality and Disease	CaSR Genotype
Loss-of-function CaSR mutation	
Familial benign hypercalcaemia (FBHH)	Heterozygous
Neonatal severe primary hyperparathyroidism (NSHPT)	Heterozygous or Homozygous (mutant)
Adult primary hyperparathyroidism (AHPT)	Heterozygous or Homozygous (mutant)
Gain-of-function CaSR mutation	
Autosomal dominant hypocalcaemic hypercalciuria (ADHH)	Heterozygous
Bartter syndrome type V	Heterozygous
CaSR Auto-antibodies	
Autoimmune hypocalciuric hypercalcaemia (AHH)	Homozygous (normal)
Acquired hypoparathyroidism (AH)	Homozygous (normal)

Figure 6. Diseases associated with the extracellular calcium-sensing receptor (Thakker, 2012).

CaSR is a chemosensor involved in transducing extracellular metabolic signals. At the cellular level it can regulate gene expression, cell proliferation, differentiation and cell death through regulation of different pathways. Signaling through the CaSR is multifaceted, and CaSR is known to influence MAPK, phospholipase and Rho signaling and to be responsible for cAMP inhibition (Figure 7). Ligand binding to the CaSR results in stimulation of Gq/11 (heterotrimeric G protein alpha subunit), one of its major downstream signaling partners, and activation of the phospholipase C (PLC) pathway (Brown et al., 1987; Brown et al., 1993). The phospholipase Cβ (PLCβ) pathway facilitates the hydrolysis of phosphatidylinositol 4,5-bisphosphate (PIP2) to produce diacylglycerol (DAG) and inositol-trisphosphate (IP3) which will stimulate the release of calcium ions from the endoplasmic reticulum (ER) to the cytoplasm. As a consequence, in addition to an increase of intracellular calcium levels, protein kinase C (PKC) can be phosphorylated, leading to MAPK signaling pathway activation, resulting in ERK1/2 phosphorylation (Handlogten et al., 2001; Kifor et al., 2001; Thomsen et al., 2012). In addition to activation of MAPK signaling, CaSR can inhibit adenylate cyclase (AC), thereby reducing cyclic adenosine monophosphate (cAMP) levels in a Gi/o-dependent manner. Studies involving stimulation of CaSR have shown that its activation leads to a drastic decrease in cAMP levels in the cells which results in a reduction of protein kinase A (PKA) activity (Chang et al., 1998; De Jesus Ferreira and Bailly, 1998). Lastly, CaSR can signal through G12/13 and activate RhoA. It was shown that CaSR stimulation recruits Rho guanine exchange factor (RhoGEF) which subsequently activates RhoA and propagates its signal (Figure 7) (Huang et al., 2004; Pi et al., 2002; Rey et al., 2005).

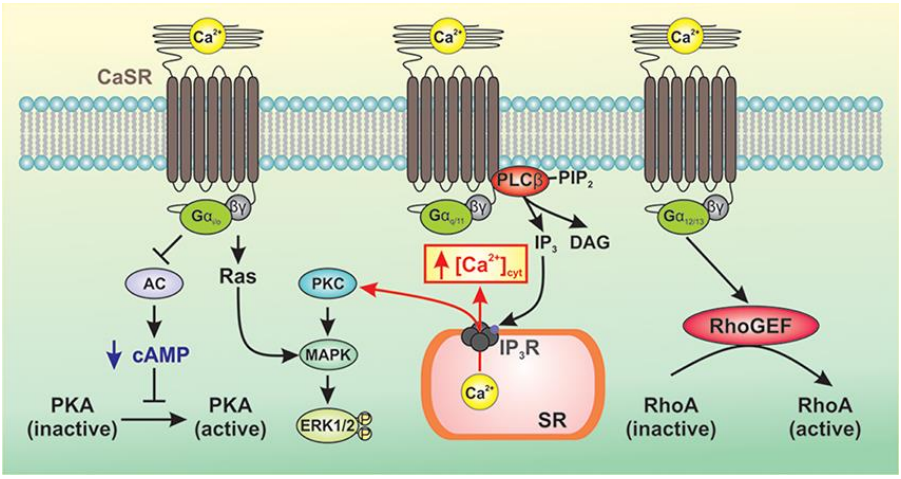

Figure 7. Calcium sensing receptor-mediated signaling pathways (Smith et al., 2016).

2.10.3 CaSR in hematopoiesis

Bone, the primary site of hematopoiesis, is a dynamic organ. In order to maintain skeletal integrity over a life time, the bone matrix is constantly subjected to a physiological process called bone remodeling that involves bone resorption by osteoclasts and bone-formation by osteoblasts (Parfitt, 1994). During bone remodeling, which occurs at the endosteal area of the bone where osteoblasts and osteoclasts are localized, calcium ions may be released. *In vitro* studies show that there is a high extracellular calcium concentration of approximately 40 mM near resorbing osteoclasts (Silver et al., 1988). High calcium levels may be characteristic of the endosteal bone marrow niche, which is the place where HSCs reside during hematopoiesis (mentioned in section 2.8). In 2006, Adams *et al.* showed that in contrast to T-cells, HSCs and stem cell-enriched LSK (lineage$^-$ Sca-1$^+$c-Kit$^+$) cells express CaSR. By using antenatal CaSR KO mice, Adams demonstrated that CaSR is required for the localization of HSC at the endosteum *via* regulation of HSC engraftment and adhesion to the ECM protein collagen 1 (Adams et al., 2006). A putative gradient created by release of calcium ions from the bone matrix within the BM which can be sensed by CaSR expressed on the surface of HSCs was hypothesized to mediate this effect. A few years later, Lam et al. showed that pharmacologic stimulation of CaSR (using the CaSR agonist cinacalcet) was responsible for an increase in homing, lodgment and engraftment of HSCs in the BM. Furthermore, increased CaSR activity enhanced the capacity of HSCs to adhere to the ECM proteins collagen I and fibronectin, and activated CXCR4-mediated signaling (Lam et al., 2011) (Figure 8). Interestingly, the enhanced migration towards SDF-1α (stromal cell-derived factor) was not preceded by an increase of CXCR4 mRNA or protein levels, which was shown to be the case in 2009 in the work by Wu et al. (2009). In this publication CaSR was proven to be a positive regulator of CXCR4 expression and to enhance stem cell mobilization and homing in the presence of high extracellular calcium levels. Moreover, Aguirre et al. (2010) established a model that mimics the high calcium concentration present in the BMM, confirming that extracellular calcium modulates cellular chemotaxis *via* CaSR activation. This demonstrated a CaSR-dependent boost in HSC mobilization, angiogenesis and differentiation (Aguirre et al., 2012).

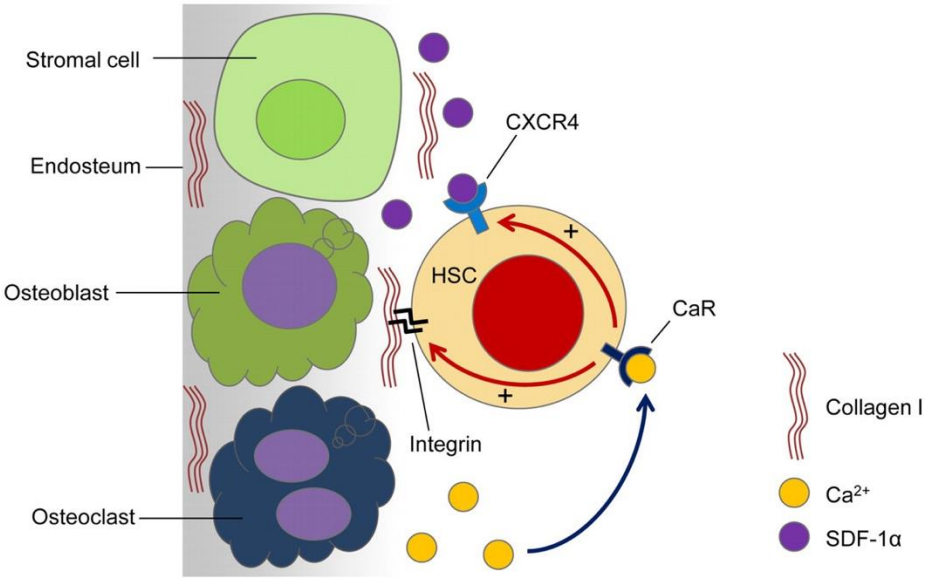

Figure 8. Role of CaSR in the BM localization of HSCs (Lam et al., 2011).

2.10.4 Calcium sensing receptor (CaSR) in cancer

Since important signaling pathways of the cells can be regulated by CaSR, it has a significant impact on cell functions and contribute to different diseases (Hendy and Canaff, 2016; Zhang et al., 2015). When CaSR is abnormally expressed, it has been shown to contribute to Alzheimer's disease (AD) (Armato et al., 2013; Conley et al., 2009), cardiovascular diseases (Alam et al., 2009; März et al., 2007; Schepelmann et al., 2016; Sun et al., 2006), asthma and pulmonary arterial hypertension (Yamamura et al., 2012; Yarova et al., 2015a), inflammatory digestive diseases (Cheng et al., 2014; Kelly et al., 2011), impairment of glucose tolerance (Babinsky et al., 2017) and tumorigenesis (Brennan et al., 2013). The role of CaSR in cancer follows a yin-yang fashion. During cancer development, depending on the tissue where CaSR is expressed, its expression might increase, and the receptor functions as an oncogene contributing to tumor progression and aggressiveness. If CaSR expression decreases, it acts as a tumor suppressor (Brennan et al., 2013) (Figure 9).

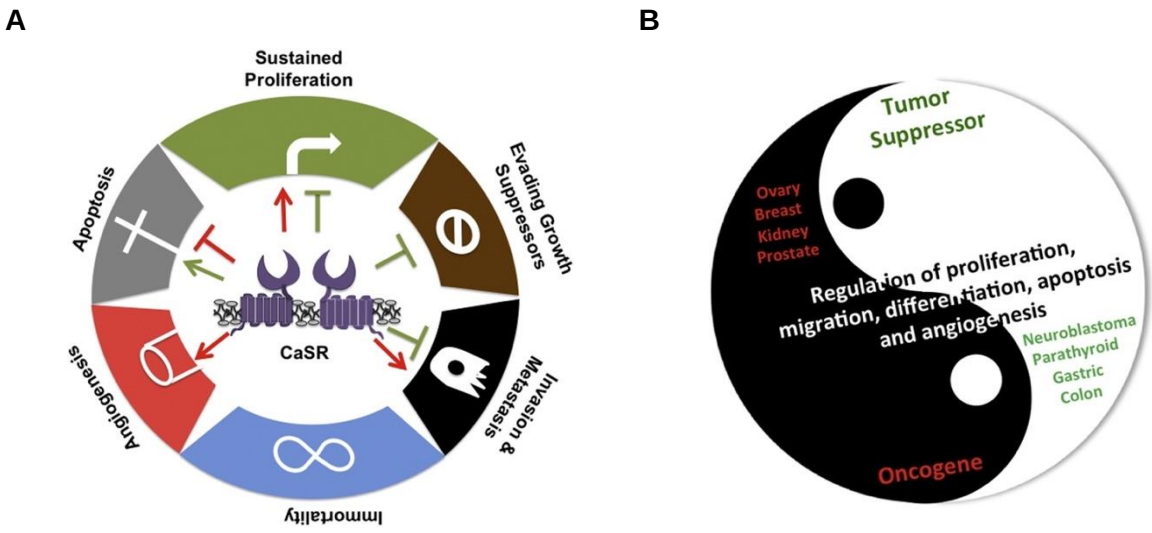

Figure 9. The role of CaSR in cancer. In cancer CaSR can regulate processes such as proliferation, cell death, differentiation, migration and angiogenesis (A). Depending on the cancer type these processes can be differently regulated, and CaSR can promote tumor growth and metastasis acting as an oncogene (shown in red), or it can function as a tumor suppressor (shown in green) (B) (Tennakoon et al., 2016).

Several studies suggest that calcium supplementation lowers the risk of some cancers (Baron et al., 2005; McCullough et al., 2008; Terry et al., 2002; Yang et al., 1999). Due to its calcium regulating function CaSR is believed to mediate this anti-tumorigenic effect (Brennan et al., 2015). In malignancies such as neuroblastomas, colorectal cancer and parathyroid cancer the expression of CaSR in the tumor tissue is very low or negligible (Casalà et al., 2013; Fetahu et al., 2014; Haven et al., 2004). In gastric tumors, a negative correlation between CaSR expression and invasiveness of the tumor was identified. It was demonstrated that CaSR loss triggers stem cell-like molecular mechanisms that support cancer cells and drug-resistant phenotypes (Singh and Chakrabarty, 2013).

In contrast, in cancers such as ovarian, prostate, and testicular cancers, CaSR mediates cancer progression (Feng et al., 2014; Hobson et al., 2003; Tfelt-Hansen et al., 2003). By gene-expression analysis it was found that CaSR expression was correlated with the metastatic behavior of prostate cancer (Dhanasekaran et al., 2001), and complementary studies support the role of CaSR in prostate cancer pathophysiology (Liao et al., 2006). In renal cell carcinoma (RCC), CaSR was also shown to be important for adhesion and migration of cancer cells and a crucial component of metastasis (Frees et al., 2018). Likewise, CaSR expressed on myeloma cells was shown to promote tumor growth in an interleukin-6 (IL-6)-dependent manner, possibly by sensing the high extracellular calcium concentrations within osteolytic bone lesions (Yamaguchi et al., 2002).

2.10.5 Calcium in the bone and bone metastasis

One of the characteristics of cancer that makes it deadly is its ability to spread. The capacity of cancer cells to spread to other regions of the body is known as metastasis. It involves cell migration, angiogenesis, the accessibility to the circulatory system, survival in circulation, escape from immune responses and the adaptability to and the growth capacity in the new organ (Chambers et al., 2001; Luzzi et al., 1998). The bone is the third most common site for metastases after lung and liver (Coleman, 2001). Once cancer spreads to the bone, the likelihood a therapy being successful is very slim. Bone metastasis is commonly observed in thyroid, lung, bladder, renal cell carcinoma and melanoma. However, the majority of bone metastases is observed in prostate and breast cancer patients (Weidle et al., 2016).

The bone matrix has unique characteristics, as growth factors and cytokines, continuously released during bone resorption, which create a chemotactic and growth-promoting environment (Guise, 2010)**.** Additionally, bone has a characteristic pH and serves as a reservoir for extracellular calcium which acts on cancer cells providing homing signals facilitating bone metastasis (Feng and Walsh, 2004; Liao et al., 2006; Saidak et al., 2009) (Figure 10).

Increased CaSR expression in invasive metastatic cancers has been suggested as a new potential prognostic marker for predicting metastasis, particularly to bone tissues, where extracellular calcium concentrations may be sufficient to activate the receptor (Breuksch et al., 2016; Feng et al., 2014; Liu et al., 2020).

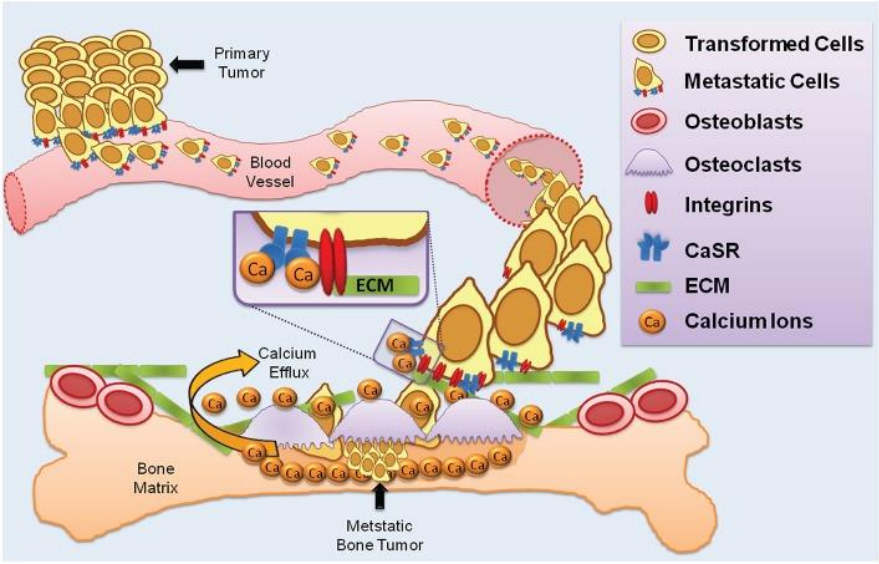

Figure 10. Role of CaSR in cancer metastasis to bone (Tharmalingam and Hampson, 2016).

2.10.6 CaSR interacting partner: Filamin A

Filamins (FLN) are large actin-binding proteins responsible for dynamic modeling and maintenance of the cytoskeleton. The filamin protein family is composed of three isoforms termed A, B and C, products of distinct genes, which are structurally similar but expressed in different cell types (Stossel et al., 2001). Filamin A (FLNA), also known as Filamin-1, is the most abundant and extensively expressed filamin isoform in humans. It is a dimeric scaffold protein of 280 kDa whose major role in the cell is to crosslink actin filaments and maintain cytoskeletal stability (Thelin et al., 2007). In addition to its actin-binding function, several studies have shown that FLNA plays a role in protein signaling with subsequent regulation of diverse cellular processes (Feng and Walsh, 2004; Stossel et al., 2001).

FLNA is composed of an actin-binding N-terminal domain and a C-terminal responsible for its protein dimerization (Travis et al., 2004). FLNA can be cleaved by the calcium-dependent protease calpain, generating fragments of different size (180 or 90 kDa). The 90 kDa fragment can translocate to the nucleus whereas FLNA phosphorylation can prevent proteolytic cleavage and the full-length form localizes in the cytoplasm (Mooso et al., 2012; Planagumà et al., 2012) (Figure 11).

Several studies have identified FLNA as a cancer regulator, being involved in lung (Uramoto et al., 2010)**,** colon (Larriba et al., 2009; Porter et al., 1993) and breast (Alper et al., 2009; Tian et al., 2013) cancers, glioma (McDonough et al., 2005), melanoma (Flanagan et al., 2001), neuroblastoma (Bachmann et al., 2006) and squamous cell carcinoma (Kamochi et al., 2008). In addition, Bedolla *et al.* demonstrated that FLNA also plays a role in prostate cancer and that in contrast to nuclear localization (cleaved FLNA fragment) which has an inhibitory growth effect, the cytoplasmic FLNA promote cancer metastasis (Bedolla et al., 2009)**.** Intracellularly FLNA can regulate MAP kinase-associated proteins, Rho GTPases and Rho kinase, Rho guanine nucleotide exchange factors (GEFs), SMADS and phosphatases (Feng and Walsh, 2004; Stossel et al., 2001). In the cell membrane, FLNA interacts with several membrane proteins (Enz, 2007; Stossel et al., 2001), and the direct binding to G protein-coupled receptors has been shown to induce FLNA phosphorylation (Nakamura et al., 2011; van der Flier and Sonnenberg, 2001). In 2001, two independent studies identified filamin A (FLNA) as a CaSR-interacting protein (Awata et al., 2001; Hjälm et al., 2001). Several studies have demonstrated that FLNA is involved in CaSR signaling and that this interaction prevents CaSR degradation (Zhang and Breitwieser, 2005). The interaction of CaSR with FLNA is required for proper ERK1/2 phosphorylation *via* MAPK (Awata et al., 2001; Hjälm et al., 2001; Huang et al., 2006), for CaSR-mediated Rho signaling (Pi et al., 2002) and for CaSR-mediated intracellular calcium regulation (Rey et al., 2005).

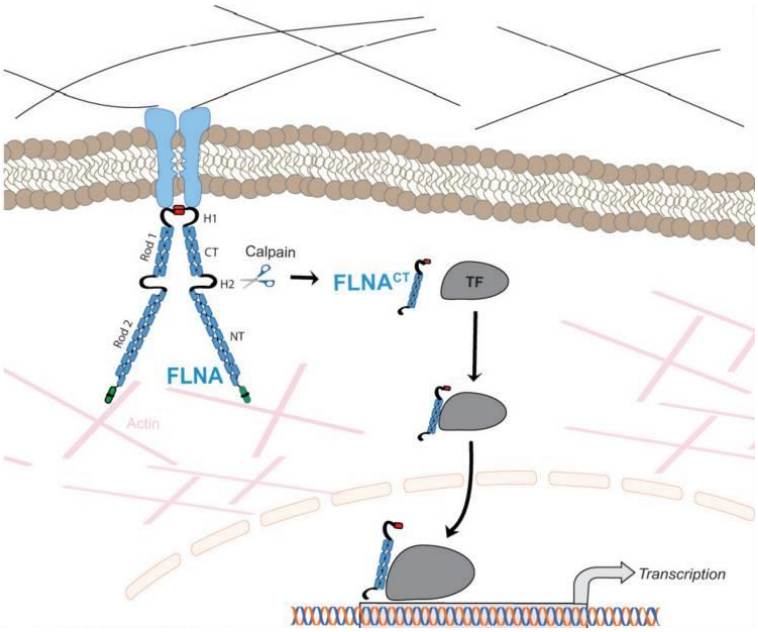

Figure 11. Cellular FLNA localization (Bandaru et al., 2021).

3 Hypothesis

Based on the evidence introduced in the preceding chapter, which described the role of calcium ions in the BMM and in HSCs, as well as the essential role of CaSR in HSCs and in various cancers, the following hypotheses were formulated:

- Calcium ions are not homogenously distributed in the BMM. Instead, a gradient of calcium ions exists, with the highest levels of calcium being close to resorbing osteoclasts in the endosteal niche and gradually declining towards the center of bone.
- The exposure of leukemia cells to a high calcium concentration influences their physiology and associated signal transduction pathways.
- Calcium sensing receptor (CaSR) plays an important role during maintenance and progression of leukemia, and targeting of CaSR might offer a possible novel strategy for treatment of leukemia.

4 Material and Methods

4.1 Plasmid cloning

4.1.1 Generation of overexpression (OE) constructs

The human *CaSR* gene, a 3234 bp fragment, was cloned into the retroviral MSCV-IRES-GFP vector (addgene, 20672) *via* XhoI and ApaI restriction sites. CaSR cDNA was kindly provided by Dr. Bryan K. Ward (University of Western Australia Centre for Medical Research), and the gene amplification was performed using the primers hCaSR.XhoI.F and hCaSR.ApaI.R. hCaSR.seq primers were used for sequencing. Table 1 shows the primer sequences.

In order to overexpress CaSR in human cells, CaSR was cloned into a sleeping beauty (SB) construct *via* SfiI restriction sites. The SB constructs containing the reporter genes were kindly provided by Prof. Dr. Rolf Marschalek (Kowarz et al., 2015) and the cloning strategy design by Erik Kowarz (Goethe University Frankfurt). Due to an internal SfiI site in the CaSR sequence, this was deleted by addition of a silent point mutation with a 2-step PCR approach (overlap extension PCR). Two initial PCRs with the primer combinations hCaSR.Sfi.F / hCaSR.int.R and hCaSR.Sfi.R / hCaSR.int.F were performed, whereby the internal primers covered the internal Sfi-site and introduced the silent point mutation to disrupt it. Subsequently, the two PCR reactions were pooled and used as template for a third PCR with the outer primers hCaSR.Sfi.F / hCaSR.Sfi.R. The amplimer was then gel purified and cloned into a PCR-cloning vector (TopoTA-PCR2.1 Invitrogen) for sequencing. Primers with SF1 to SF5 were used for the sequencing. Error-free clones were digested with SfiI restriction enzyme and ligated in the Sleeping Beauty vectors. Primer sequences are shown in Table 1.

The cloning of GCaMP6s sensor gene into a sleeping beauty construct was performed *via* SfiI restriction sites. The gene sequence was amplified from pGP-CMV-GCaMP6s (addgene, 40753) using the primer combination GCaMP6s.Sfi.F / GCaMP6s.Sfi.R. The amplimers were gel purified and cloned for sequencing into a PCR-cloning vector (TopoTA-PCR2.1 Invitrogen), using the SF1 and SF2 primers (Table 1).

Table 1. Primers used in the generation of overexpression constructs

Primer name	Primer sequence (3' → 5')
hCaSR.XhoI.F	CAGATCTTCCGGATGGCTCGAGT
hCaSR.ApaI.R	ATATATGGGCCCACATCGATTTTCCATGGCAGCTG
hCaSR.seq.1	CTAAGCCTCCGCCTCCTCTTC
hCaSR.seq.2	TGTGCCAGGTGAGTGCCAAG
hCaSR.seq.3	CTTGATCTTTAGCTGCTACTCC
hCaSR.seq.4	CTCACTGAGCTTTGATGAGCT
hCaSR.seq.5	CAGGAGCTGGAGGATGAGAT
hCaSR.Sfi.F	GGCCTCTGAGGCCACCATGGCATTTTATAGCTGCTGCTGGGTCCTCTT
hCaSR.Sfi.R	GGCCTGACAGGCCTTATGAATTCACTACGTTTTCTGTAACAGTGCTGCCT
hCaSR.int.F	CAAGATCTGGCTGGCtAGCGAGGCCT
hCaSR.int.R	AGGCCTCGCTaGCCAGCCAGATCTT
hCaSR.SF1	GTGGGAGCAACTGGCTCA
hCaSR.SF2	TACCTGCTTACCTGGGAGAG
hCaSR.SF3	GGGACCAGGAAAGGGATCAT
hCaSR.SF4	CCTTTGGCATCAGCTTCGT
hCaSR.SF5	GGAAGCTGCCGGAGAACTTC
GCaMP6s.Sfi.F	GGCCTCTGAGGCCACCATGGGTTCTCATCATCATCATCATCATGGT
GCaMP6s.Sfi.R	GGCCTGACAGGCCTCACTTCGCTGTCATCATTTGTACAAACTCT
GCaMP6s.SF1	CCCAACGAGAAGCGCGATCA
GCaMP6s.SF2	GCAGCACGACTTCTTCAAGTC

4.1.2 Generation of CRISPR/Cas9 KO constructs

The sgRNAs were designed to target the sequence of *FLNA* and *CaSR*. All targets were chosen using the benchling design tool (https://benchling.com/crispr). The complementary DNA oligonucleotides containing selected CRISPR/Cas9 target sequences were generated by the annealing of two primers (Table 2) and subsequently cloned into pLentiCRISPR.v2-GFP

or pLentiCRISPR.v2-RFP (Addgene #52961) using BsmBI sites. sgRNA targeting CaSR were cloned into a backbone vector containing GFP as a reporter gene and sgRNA targeting FLNA into a backbone vector expressing RFP. A non-targeting (NTC) sgRNA was used as control and cloned into both vectors. The integration was confirmed by sequencing analysis using the LKO.1 primer shown in Table 2.

Table 2. Primers used in the cloning of sgRNA constructs

Primer name	Primer sequence (3' → 5')
hCaSR 1 s	CACCGCTGTAACCAGCGAAACCCA
hCaSR 1 as	AAACTGGGTTTCGCTGGTTACAGC
hFLNA ex2 s	CACCGCCTGGCGGAGGACGCGCCG
hFLNA ex2 as	AAACCGGCGCGTCCTCCGCCAGGC
NTC s	CACCGTTCCGGGCTAACAAGTCCT
NTC as	AAACAGGACTTGTTAGCCCGGAAC
LKO.1	GACTATCATATGCTTACCGT

4.2 Strains and cell lines

THP1 and K562 cell lines were cultured in RPMI 1640 medium (Thermo Fisher Scientific, Darmstadt), supplemented with 10 % fetal bovine serum (FBS), 2 % L-glutamine and 1 % penicillin/streptomycin. The human cell lines 293T and HS-5 and the mouse cell line NIH/3T3 were cultured in DMEM medium supplemented with 10 % FBS, 2 % L-glutamine and 1 % penicillin/streptomycin. The media for 293T and HS5 cells was further supplemented with 1% non-essential amino acids. The murine pro-B cell line BA/F3 was grown in RPMI containing 10 % FBS, 1 % penicillin/streptomycin and 1 % L-glutamine supplemented with 5 % (v/v) WEHI media as a source of interleukin 3 (IL-3). All cell lines were maintained in a 37 °C, 5 % CO_2 incubator.

4.3 Generation of overexpression (OE) and knockout (KO) cell lines

THP1, K562 and BA/F3 overexpressing cell lines were generated by stable transfection of sleeping beauty constructs. Plasmid transfections were performed using Metafectene Pro transfection reagent (Biontex Laboratories GmbH, Germany) according to the manufacturer’s

instructions. Forty-eight hours after transfection, transformed cells were selected by puromycin (GIBCO, A11138) treatment (1 µg/ml).

The CRISPR/Cas9 KO cells were generated in 2 steps. First, THP1 and K562 cells were transduced with lentivirus containing Cas9 (lentiCas9-Blast, addgene, #52962), produced as shown in the methods section 4.1.2. Upon transduction, cells integrating Cas9 in their genome were selected using blasticidin (Invivogen, San Diego, California) (15 µg/ml). Subsequently, selected cells were transduced with lentivirus containing the sgRNA. The efficiency of transduction was checked by flow cytometry (*BD* Fortessa, Heidelberg, Germany), and cell populations were isolated by sorting of GFP^+ or RFP^+ cells (BD FACSAria Fusion Cell Sorter) (Franklin Lakes, NJ, USA). The KO efficiency was tested by qPCR and Western blot analysis.

4.4 Drug treatments

In order to test the effect of extracellular calcium on THP1 and K562 cells, calcium chloride was added in different concentrations (0.5, 1, 2.5, 5, 7.5 mM), and cells were incubated at 37 °C for 4 h.

To test the effect of the specific CaSR-antagonist NPS-2143 on THP1 cells, $1x10^6$ cells were treated with either vehicle (DMSO) or 5,10 and 20 µM of NPS-2143 (Sigma, Darmstadt, Germany) for 4 h at 37 °C. In intravital microscopy (IVM) studies, THP1 cells were treated with 10 µM of NPS-2143 for 30 min before transplantation.

4.5 Quantitative polymerase chain reaction (qPCR)

The RNA isolation was performed by applying an optimized protocol from the laboratory. In brief, cells were lysed using TRIzol (Life Technologies/Thermo Fisher Scientific, Schwerte, Germany), and chloroform was added (20 % (v/v) of Trizol) followed by phase separation through centrifugation. Next, the aqueous phase was collected and mixed with 70 % ice-cold ethanol for dissolution and washing of salts from the sample. This mixture was transferred into the columns provided by the RNAeasy Mini Kit from Qiagen (Cat. No 74104, Qiagen, Hilden, Germany), and the remaining isolation steps (from step 4 onwards) were performed according to the manufacturer's instructions. Complementary DNA (cDNA) synthesis was performed by reverse transcription (RT) of 250 ng-1 µg of isolated RNA using the ProtoScript First Strand cDNA Synthesis Kit (Cat. No. SE6300S, New England BioLabs, Frankfurt am Main, Germany), following the manufacturer's instructions. The quantitative PCR (qPCR) was performed in triplicates by using Power SyBR Green (A25742, Thermo Fisher Scientific, Darmstadt) containing 10 µM forward and reverse primers using the StepOnePlus Real-Time PCR System

and the StepOne Software v2.3. Primers are listed in Table 7**.** The relative gene expression was assessed using the delta-delta Ct (threshold cycle)-value measurement using glyceraldehyde 3- phosphate dehydrogenase (GAPDH) as housekeeping gene.

4.6 Virus production

The generation of retroviruses to use in transplantation experiments was performed using the calcium phosphate transfection method as described previously (Gavrilescu and Van Etten, 2008). In a 6 cm tissue culture dish, $3.5x10^6$ human HEK 293T cells in medium containing 25 µM chloroquine, seeded the previous day, were co-transfected with the respective retroviral plasmid and the packaging-plasmid EcoPak as shown in Table 3**.**

48 hours after transfection, the conditioned medium containing the viral particles was harvested, and the viral titer was tested *via* transduction of NIH/3T3 cells. For that, $2×10^5$ cells seeded 18 h before were transduced with the virus using different dilutions (1:3 and 1:30). After 72 h, cells were collected and analyzed by flow cytometry.

Table 3. Composition of the transfection solution for retrovirus production

Component	Concentration
DNA of interest	20 µg
EcoPak	10 µg
$CaCl_2$	124 µl
DEPC water	to 1000 µl
2x HBS	1000 µl

The generation of lentiviruses containing the different sgRNA was performed following the protocol as previously described (Tiscornia et al., 2006), based on the calcium phosphate transfection method. On the day prior to transfection, $2×10^6$ HEK 293T cells were seeded in a 10 cm dish and after addition of 25 µM chloroquine to the cells they were transfected with a solution as shown in Table 4 The conditioned medium, containing the lentiviruses was harvested 48 h after transfection and immediately used to transduce cells.

Table 4. Composition of the transfection solution for CRISPR/Cas9 virus production

Component	Concentration
Plasmid (sgRNA)	4.1 µg
VSV-g	1.75 µg
psPAX2	3.25 µg
$CaCl_2$	62 µl
DEPC water	to 1000 µl
2x HBS	500 µl

4.7 Proliferation assay

Cell proliferation was assessed by staining of the cells with *CellTrace™ Far Red Cell Stain* (Carboxyfluorescein succinimidyl ester, CFSE, Invitrogen, Darmstadt, Germany). 8×10^4 cells were plated in 1 ml of medium and incubated at 37 °C for 45 min. The stained cells were analyzed by flow cytometry on a BD Fortessa using the FACSDiva Software, to create a baseline required for the analysis. After 72 h, the cells were run by flow cytometry and the analyses were performed in FlowJo using the 'FlowJo Proliferation Tool'.

4.8 Cell cycle assay

The cell cycle status on primary cells was performed using total BM or spleen cells collected from mice with AML, sacrificed on day 40 after transplantation. The cell cycle status of the different cell lines was analyzed using 5×10^5 serum-starved cells for 16 h. Cells were fixed and permeabilized with BD Cytofix/Cytoperm™, washed with Perm/Wash™ solution (Cat. no.: 554722, 554723; BD Biosciences, San José, CA) and stained overnight at 4 °C with an antibody to Ki-67 (BioLegend, San Diego, CA, USA). On the following day, DAPI (0.2 µg/ml) (Merck, Darmstadt, Germany) was added to each sample, and after 30 minutes of incubation cells were analyzed by flow cytometry (BD Fortessa, Heidelberg, Germany).

4.9 Apoptosis assay

The extent of cell apoptosis of primary BM or spleen cells or the different cell lines was tested by staining of 5×10^5 cells with conjugated-annexin V protein in annexin-binding buffer (V13246, Thermo Fisher Scientific, Schwerte, Germany). After 1 h at 4 °C, cells were

resuspended in DAPI solution (0.2 µg/ml) (Merck, Darmstadt, Germany) and immediately analyzed using a flow cytometer (BD Fortessa, Heidelberg, Germany).

4.10 Reactive oxygen species (ROS) assay

Intracellular ROS levels of either primary cells or cell lines were detected using the ROS assay kit (ThermoFisher, Darmstadt, Germany). 5×10^5 cells were incubated with the CellROX Deep Red oxidative stress reagent for 40 min at 37 °C and analyzed by flow cytometry (BD Fortessa, Heidelberg, Germany).

4.11 DNA damage assay (γH2A.X)

DNA damage was tested in 5×10^5 primary total BM or spleen cells collected from mice with AML, or in cell lines, which had been serum-starved for 16 h. Fixed and permeabilized cells (BD Cytofix/Cytoperm™, Cat. no.: 554722, BD Biosciences, San José, CA) were stained overnight with an antibody to γ H2A.X (Cell Signaling, Frankfurt am Main, Germany), followed by incubation with the secondary antibody Alexa Fluor 647 (Invitrogen, Darmstadt, Germany) for 2 h, at 4 °C.

4.12 BioParticle phagocytosis assay

Phagocytosis was determined by incorporation of bioparticles, as previously reported (Kumar et al., 2020). For this, $2x10^5$ cells were incubated with 1 µg of pHrodo Red E. coli BioParticles Conjugate (ThermoFisher, Darmstadt, Germany) for 90 min at 37 °C, and phagocytosis was assessed by flow cytometry (BD Fortessa, Heidelberg, Germany).

4.13 Adhesion assay

Adhesion experiments were performed by testing the capacity of the cells to adhere to the ECM component fibronectin (FN). Coating of plates was performed in a 48-well plate using 2.5 µg/well of FN (ThermoFisher, Darmstadt, Germany) at 4 °C for 16 h in 20 mM TBS (pH 7.6), containing 1 mM $CaCl_2$, as previously described (Kuzelová et al., 2010). 2 % bovine serum albumin (BSA) was used as control. Unbound fibronectin was removed, carefully washed with PBS and blocked with 2 % BSA in IMDM (Iscove modified Dulbecco medium) for 30 min at room temperature. The wells were carefully washed and $7x10^4$ cells were added to the BSA- or FN-coated well and incubated for 6 h at 37° C. The non-adherent cells were

removed by gently washing the wells, and the number of adherent cells in each condition was counted.

4.14 Chemotaxis assay

The cell migration capacity of the different cell lines was tested by performing a transwell assay (Sarstedt, Nümbrecht, Germany) towards human stromal HS-5 cells (Jo et al., 2000) or CXCL-12 (Cheng et al., 2017) as previously reported. $1.5x10^5$ cells, serum-starved for 16 h, were added to the upper chamber of the transwell assay in full medium and allowed to migrate through a porous membrane (8 µm pore size inserts) for 2, 4 and 6 h towards the lower chamber. When it came to migration towards HS-5 cells, $3x10^4$ cells were seeded in the bottom chamber of a 24-well plate 18 h prior to the start of the experiment. In order to determine migration by flow cytometry, cells were stained with CFSE for 30 min at 37 °C. In the case of migration towards CXCL-12, 100 ng/ml of the chemoattractant protein was added to the bottom chamber, and the migrated cells were counted using a light microscope.

4.15 Calcium flux assay

Mobilization of intracellular calcium was measured by using a flow cytometric assay (Bajnok et al., 2013). Briefly, $1x10^6$ cells were resuspended in 1 ml of cell loading medium (CLM, RPMI containing 2 % FBS and 25 mM HEPES (pH 7.4)). The cells were stained with eBioscience™ Indo-1 AM (1 µM) (ThermoFisher, 65-0856-39, Darmstadt, Germany), at 37 °C for 45 min. For analysis, cells were acquired by using the time parameter in BD Fortessa (Heidelberg, Germany) and analyzed for indo-violet (405 nm) and indo-blue (485 nm). A baseline calcium flux analysis was performed for 90 sec followed by addition of 20 mM $CaCl_2$ and acquisition for 90 sec. Ionomycin (1 µg/ml, I24222, ThermoFisher, Darmstadt, Germany) was added at the end and acquired for 90 sec. The analyses were performed in FlowJo using the 'Kinetics' tool and the area under the curve (AUC) of the ratio 405/485 nm over time, corresponding to the ratio of bound/unbound Indo-1 to calcium.

4.16 Calcium measurement

The calcium quantification in bone marrow of human samples was performed by direct measurement of plasma derived from patients' bone marrow aspirates. In murine experiments, bone marrow plasma was obtained by flushing a femur in 100 µl of PBS and collection of the

supernatant after centrifugation. Total calcium content was measured using a calorimetric calcium assay kit (ab102505, Abcam) following the manufacturer's instruction.

4.17 Long distance inverse (LDI) PCR

LDI-PCR to determine disease clonality was performed, as previously described (Meyer et al., 2005). Briefly, genomic DNA was isolated from spleen of moribund mice using a DNeasy Blood & Tissue Kit (Cat. No 69506, Qiagen, Hilden, Germany)), and 0.5 µg was digested using NcoI-high fidelity (HF) (New England BioLabs, Frankfurt am Main, Germany) and re-ligated. Afterwards, LDI-PCR was performed using GFP or RFP-specific primers.

4.18 Immunoblotting

Cultured cells and primary BM, spleen and lymph node cells were lysed using RIPA buffer (50 mM Tris HCl pH 7.4, 150 mM NaCl, 1 % Triton X-100, 1 % Na DOC, 0.1 % SDS, 1 mM EDTA), freshly supplemented with protease and phosphatase inhibitor cocktails (Sigma-Aldrich, Darmstadt, Germany). The lysates were incubated on ice for 1 h, ultra-centrifuged for 30 min at 14000 rpm, and the supernatant containing the proteins was collected. The protein concentrations were assessed using Protein Assay Dye Reagent Concentrate (Bradford, Bio-Rad, Hercules, CA, USA) and Pre-Diluted Protein Assay Standards: Bovine Serum Albumin (BSA) Set **(**Sigma, A2153**,** Darmstadt, Germany). Equal amounts of protein were mixed with Roti®-Load 1 dye and denatured and run on NuPAGE^{TM} 4 -– 12 % bis-Tris gels (ThermoFisher Scientific, Darmstadt, Germany). Proteins were blotted on methanol-activated PVDF Transfer Membranes (ThermoFisher Scientific, Darmstadt, Germany) using the wet transfer method in presence of 20 % methanol. Subsequently, the membranes were blocked with 5 % milk in 0.1 % TBS-T for 1 h at room temperature and incubated with primary antibodies overnight at 4 °C. After incubation with secondary horseradish-peroxidase (HRP)-conjugated antibodies for 2 h, membranes were washed with 0.1 % TBS-T and developed using X-ray films (Fujifilm, Dusseldorf, Germany). Band intensities were quantified using FIJI ImageJ software. A list of all antibodies can be found in the Table 9**.**

4.19 Protein co-immunoprecipitation (Co-IP)

For the coimmunoprecipitation experiments, K562 and THP1 cells were lysed in lysis buffer (50 mM Tris HCl pH 7.4, 150 mM NaCl, 10 % glycerol, 0.5 % NP-40), and protein was extracted. Equal amounts of protein *per* sample (500 µg) were incubated with 2 µg of antibody

against FLNA (sc-17749, Santa Cruz, Heidelberg, Germany) for 4 h, at 4 °C, followed by overnight incubation with magnetic beads (Dynabeads Protein G, Sigma-Aldrich, Munich, Germany) at 4 °C. The protein-bead complex was washed several times with ice cold RIPA buffer and eluted in 5 x Laemmli buffer, heated to 95 °C for 5 minutes. The eluted proteins were separated by SDS page, as described in the methods section 4.18.

4.20 Immunofluorescence (IF)

Immunofluorescence studies in primitive AML cells were performed by using sorted GFP $(MLL\text{-}AF9)^+$ Lin^- cells (BD FACSAria Fusion Cell Sorter) (Franklin Lakes, NJ, USA), isolated from the BM of AML mice sacrificed on day 40 after transplantation. 7 $x10^4$ primary AML cells or 2 $x10^5$ THP1 and K562 cells were transferred onto glass slides by cytospin (300 rpm for 3 minutes), fixed with 4 % paraformaldehyde (PFA) (Morphisto, Frankfurt, Germany) for 10 minutes and permeabilized with 0.2 % Triton X-100 (Sigma, Darmstadt, Germany) for 5 minutes. The cells were then blocked with 2 % BSA in PBS for 30 minutes at room temperature. To test protein co-localization, cells were stained overnight at 4 °C with FLNA and CaSR antibodies (Table 10) in a humid chamber. Thereafter, cells were stained with fluorophore-labelled secondary antibodies (Table 10) for 2 h. The nuclei were counterstained with 5 µg/ml 4′,6-diamidin-2-phenylindol (DAPI), and cells were mounted using the mounting medium with DAPI-aqueous fluoroshield (Abcam, Cambridge, UK) mounting medium (Merck, Darmstadt, Germany). Images were acquired using a confocal laser scanning microscope (CSLM) (Leica SP5, Wetzlar, Germany), and analyzed with Image J software. In the case of γ H2A.X staining, foci were manually counted from the maximum projection view.

4.21 Giemsa staining

1$x10^5$ BM sorted $MLL\text{-}AF9^+$ $Gr1^{low}$ and $MLL\text{-}AF9^+$ $Gr1^{high}$ cells were collected from mice with AML (sacrificed on day 40 after disease induction) and cytospun (300 rpm for 3 minutes) onto slides. Cells were then fixed with methanol and stained with Giemsa according to standard protocols. The frequency of the leukemia blasts and differentiated cells were determined based on the typical morphologies.

4.22 Data set analysis

The mRNA expression data (log_2) for CaSR and FLNA in the bone marrow cells of AML patients, as well as normal hematopoietic stem cells, was obtained from the BloodSpot database. The data was obtained from the datasets 210577_at and 214752_x_at for CaSR and FLNA, respectively. ANOVA analysis was used to determine statistical differences among the different groups.

The Kaplan-Meier-style survival curves of patients with AML with high or low expression of filamin A were generated using the publicly available dataset TARGET, accessed through the cBioPortal portal (Log-rank test) (https://www.cbioportal.org).

4.23 Mice

Conditional mice lacking CaSR in the hematopoietic system were generated by crossing Mx-Cre mice with mice expressing conditional, mutant CaSR containing loxP sites flanking exon 5 (Toka et al., 2012)**.** Mice homozygous for floxed *CaSR* alleles were crossed to animals heterozygous for the Mx-*Cre* transgene to generate Mx-Cre $^{-/+}$ CaSR $^{flox/-}$. These mice were then crossed with CaSR$^{flox/flox}$ mice to generate litters that are homozygous for flox alleles (Mx-Cre $^{-/+}$ CaSR $^{flox/flox}$). CaSR $^{flox/flox}$ mice (C57/BL6 background) were a kind gift from Prof. Martin Pollack and backcrossed in the animal facility of the Georg-Speyer-Haus, Institute for Tumor Biology and Experimental Therapy. Col1-caPPR mice (FVB background) (Calvi et al., 2001), which contain constitutively active receptor for PTH and PTH-related peptide (PPR) under control of collagen type I α1 promotor on osteoblasts were used to measure the BM calcium concentration. For xenotransplantation experiments, NOD/SCID/IL2Rγ$^{-/-}$ (NSG) mice were obtained from The Jackson Laboratory, housed and bred in specific pathogen-free (SPF) conditions. Animals of different sexes were randomly assigned to experimental groups. All animal studies were performed in compliance with the guiding principles of the 'Guide for the Care and Use of Laboratory Animals' (National Research Council Committee for the Update of the Guide for the and Use of Laboratory, 2011) and approved by the local government (Regierungspräsidium Darmstadt, Germany).

4.24 Genotype analysis

For genotyping, DNA was extracted from ear biopsies by using MyTaq™ Extract-PCR Kit following the manufacturer's instructions. The genomic DNA was subjected to PCR amplification to identify the mutations.

The presence of CasR flox allele was performed by PCR amplification (2 min at 94 °C; 30 sec at 94 °C followed by 30 sec at 60 °C for 34 cycles and 1 min at 68 °C) using Casr-F and Casr-E3-R primers (Table 5). Zygosity was tested by digestion of the PCR product with SalI enzyme (NEB Biolabs) for 3 h at 37 °C, and run on a 1 % agarose gel. Homozygous mice generate 2 bands (400 bp and 250 bp), and heterozygous mice generate 3 bands (650 bp, 400 bp and 250 bp). The *Cre* transgene was detected by PCR using Cre FW and Cre RV primers (Table 5).

The Col1-caPPR mutant mice were identified by PCR using the PPR-Col.I and PPR-G2 primers (Table 5).

Table 5. Sequence of the primers used for genotyping of mutant mice

Primer name	Primer sequence (3' → 5')
CaSR-F	5'-GACTTGCTATGTAGCCCAGAACTG-3'
CaSR-E3-R	5'-AAGGGATGTGCTCGGAGCA-3'
Cre Fw	5'-AAATTGCCAGGATCAGGGTTAAAG-3'
Cre Rv	5'-AGAGTCATCCTTAGCGCCGTAAAT-3'
PPR-Col.I	5'-GAGTCTACATGTCTAGGGTCTA-3'
PPR-G2	5'-TAGTTGGCCCACGTCCTGT-3'

4.25 Human samples

BM samples used in xenotransplantation experiments were collected from patients suffering from AML and approved by the local ethics committee. Samples of subjects of both sexes were included in the study (Table 13).

Bone marrow plasma from patients with different hematological malignancies were provided by the UCT biobank (Frankfurt am Main), and all the experiments were approved by the Ethics Committee of the University Clinic of the Goethe University Frankfurt (Approval number 274/18 and SHN-5-2020).

4.26 Bone marrow transduction/transplantation

4.26.1 Primary transplantation

The transplantation experiments were performed as previously described by Gavrilescu and van Etten (Gavrilescu and Van Etten, 2008). In brief, to induce chronic myeloid leukemia (CML)-like myeloproliferative neoplasia (MPN) or acute myeloid leukemia (AML), donor BM cells from 5-fluorouacil (5-FU)-pre-treated mice (200 mg/kg) were pre-stimulated overnight with medium containing stem cell factor (SCF) (50 ng/ml), IL-6 (10 ng/ml) and IL-3 (6 ng/ml) and transduced on two consecutive days with retrovirus. Subsequently, transduced cells were intravenously transplanted into sublethally irradiated (900 cGy for C57/BL6 and 750 cGy for BALB/c) WT recipient mice.

Depending on the transplantation experiment, the BM cells used as donor and the virus combination differed. The CaSR overexpression (OE) on leukemia initiating cells (LIC) in CML and AML diseases was performed by transduction of BM cells from WT (BALB/c) mice BCR-ABL1 (RFP) or MLL-AF9 (RFP)-expressing virus, respectively, co-transduced with empty vector (GFP) or CaSR OE (GFP)-expressing virus. In order to test the effect of the CaSR depletion on CML LIC, BM cells from WT (Mx-Cre $^{-/-}$ CaSR $^{flox/flox}$) or inducible CaSR KO (Mx-Cre $^{-/+}$ CaSR $^{flox/flox}$) were transduced with BCR-ABL1 (RFP)-expressing virus. In AML, the effect of both CaSR depletion and overexpression was tested simultaneously. For this, BM cells from WT (Mx-Cre $^{-/-}$ CaSR $^{flox/flox}$) and inducible CaSR KO (Mx-Cre $^{-/+}$ CaSR $^{flox/flox}$) were transduced with MLL-AF9 (RFP)-expressing virus, co-transduced with empty vector (GFP) or CaSR OE (GFP)-expressing virus. CaSR depletion on MN1-driven AML LIC was performed by transduction of BM cells from WT (Mx-Cre $^{-/-}$ CaSR $^{flox/flox}$) or inducible CaSR KO (Mx-Cre $^{-/+}$ CaSR $^{flox/flox}$) with MN1 (GFP)-expressing virus (Table 6).

In BALB/c transplantation experiments, a dose of $2.5x10^5$ or $5x10^5$ cells to induce CML or AML, respectively, was used. In the case of CaSR KO (knockout) experiments, Mx-Cre $^{-/-}$ CaSR $^{flox/flox}$ littermates were used as WT mice and $4x10^5$ or $7.5x10^5$ cells were transplanted to induce CML or AML, respectively.

Table 6. Virus combinations used in BM transplantation experiments

Disease	Condition	BM donor cells	Virus combination
CML (BCR-ABL1)	Wildtype	BALB/c	BCR-ABL1 (RFP) Empty vector (GFP)
	CaSR OE	BALB/c	BCR-ABL1 (RFP) CaSR-OE (GFP)
AML (MLL-AF9)	Wildtype	BALB/c	MLL-AF9 (RFP) Empty vector (GFP)
	CaSR OE	BALB/c	MLL-AF9 (RFP) CaSR-OE (GFP)
CML (BCR-ABL1)	Wildtype	Mx-Cre $^{-/-}$ CaSR $^{flox/flox}$	BCR-ABL1 (GFP)
	CaSR KO	Mx-Cre $^{-/+}$ CaSR $^{flox/flox}$	BCR-ABL1 (GFP)
AML (MLL-AF9)	Wildtype	Mx-Cre $^{-/-}$ CaSR $^{flox/flox}$	MLL-AF9 (RFP) Empty vector (GFP)
	CaSR KO	Mx-Cre $^{-/+}$ CaSR $^{flox/flox}$	MLL-AF9 (RFP) Empty vector (GFP)
	CaSR OE	Mx-Cre $^{-/-}$ CaSR $^{flox/flox}$	MLL-AF9 (RFP) CaSR-OE (GFP)
	CaSR KO + CaSR OE	Mx-Cre $^{-/+}$ CaSR $^{flox/flox}$	MLL-AF9 (RFP) CaSR-OE (GFP)
AML (MN1)	Wildtype	Mx-Cre $^{-/-}$ CaSR $^{flox/flox}$	MN1 (GFP)
	CaSR KO	Mx-Cre $^{-/+}$ CaSR $^{flox/flox}$	MN1 (GFP)

B-ALL was induced by retroviral transduction of non-5-FU pre-treated BM cells, either WT or CaSR KO, transduced once with MSCV-IRES GFP BCR-ABL1 and transplanted ($1x10^6$ cells/mouse) into sublethally irradiated (900 cGy) WT mice.

To induce deletion of CaSR, transplanted mice with either WT or inducible KO BM were intraperitoneally treated with 10 mg/kg of poly (I:C) (PHR1787, Sigma, Darmstadt, Germany). Poly (I:C) was administrated 72 h after transplantation for four consecutive days. For the

transplantation experiment with “late KO induction”, poly (I:C) was given in four consecutive days starting on day 12 after transplantation, when short-term engraftment is thought to be completed. The gene depletion efficiency was determined by flow cytometry analysis on leukocytes by using an anti-CaSR antibody (NOVUS biologicals, Wiesbaden, Germany).

4.26.2 Secondary and limiting dilution transplantation

For the secondary transplantation, BM from primary mice with established AML (sacrificed on day 40 after transplantation) was harvested. BM RFP^+ (MLL-AF9) GFP^+ (empty vector or CaSR OE)$^+$ Lin^- cells were sorted on a BD FACSAria Fusion Cell Sorter (Franklin Lakes, NJ, USA). The Lin^- antibody cocktail includes CD11b, Ter119, CD5, B220 and F4/80 antibodies. $1.5x10^4$ sorted cells combined with $2x10^6$ supportive BM cells from healthy mice were intravenously injected into sublethally irradiated (900 cGy) WT recipient mice.

For the limiting dilution transplantation, $2x10^6$ supportive BM cells were transplanted with either $2.5x10^3$, $5x10^3$, $1x10^4$ or $1.5x10^4$ sorted cells into sublethally irradiated (900 cGy) WT mice. The frequency of stem cells was determined by uploading the data into the web-based ELDA (Extreme Limiting Dilution Analysis) statistical software (Hu and Smyth, 2009). Transplanted mice with WBC < 8,000/ µl and MLL-$AF9^+$ $Gr1^+$ cells < 20 % in PB at day 24 after transplantation were considered non-engrafted.

4.26.3 Xenotransplantation

For xenotransplantation of patient samples, bulk BM cells from five different AML patients were intravenously transplanted into sublethally irradiated (125 cGy) NSG mice. Mice from each group were randomly assigned to the different treatment cohorts: vehicle, cytarabine (ara-C, PHR1787, Sigma, Darmstadt, Germany) or the combination of ara-C and NPS-2143 (Santa Cruz Biotechnology, sc-361280, Heidelberg, Germany) as explained in methods section 4.27.

For xenotransplantation of human AML cells THP1, $2x10^6$ cells were transplanted into non-irradiated recipient mice.

4.27 *In vivo* drug treatment

In the AML experiments using a syngeneic mouse model, mice were treated with intraperitoneal (i.p.) injection of vehicle (saline solution), 50 mg/kg of ara-C (Sigma, Darmstadt, Germany), 2 mg/kg of NPS-2143 (Santa Cruz Biotechnology, Heidelberg, Germany) or a

combination of ara-C with NPS-2143, upon establishment of the disease as determined by flow cytometry and complete blood count (CBC). Mice were randomly assigned to the different groups and NPS-2143 and vehicle were administered from day 12 to day 50 after transplantation, as a daily regimen. Ara-C was administered on five consecutive days *per* cycle for three cycles every two weeks, starting on day 18 after transplantation.

In the xenotransplantation experiments, NSG mice were i.p. treated with vehicle (saline solution), ara-C (50 mg/kg) or simultaneously treated with ara-C and NPS-2143 (2 mg/kg). Treatment was performed from day 17, once human $CD45^+$ cells were detected in PB, until day 47 after transplantation. NPS-2143 and vehicle were administrated as a daily regimen and ara-C on three consecutive days *per* cycle, for three cycles every two weeks.

In the CML treatment experiment, mice were randomly assigned to four cohorts: vehicle (water containing 0.01 % DMSO), imatinib (100 mg/kg) (Enzo Life Sciences, ALX-270-492, Farmingdale, NY), cinacalcet (30 mg/kg) (Santa Cruz Biotechnology, sc-207438, Heidelberg, Germany) or a combination of imatinib and cinacalcet. Mice were treated by oral gavage on a daily basis from day 10 to day 26 after transplantation.

4.28 Analysis of diseased mice and tumor burden

The leukemia burden in the peripheral blood of diseased animals was assessed by analysis of peripheral blood using a Scil Vet animal blood counter (Scil Animal Care Company, Viernheim, Germany) and by flow cytometry analysis (BD Fortessa, Heidelberg, Germany). The tumor burden was represented by the percentage of oncogene (GFP or RFP) positive leukocytes stained for CD11b (clone M1/70) antibody in the case of CML-like MPN, BP-1 (clone 6C3) for B-ALL and Gr1 (clone 1A8) for AML. Human CD45 was used to assess the tumor burden in xenotransplanted NSG mice, and in the case of transplantation of patient samples, CD13 was additionally used. CaSR expression was followed in the different transplantation experiments by co-staining of leukocytes with an anti-CaSR antibody (clone 5C10). All used antibodies are listed in Table 8**.**

4.29 Leukemia stem cells and myeloid progenitor analysis

Stem cells and myeloid progenitors present in BM, spleen and PB of healthy mice or mice suffering from AML were analysed by flow cytometry (BD Fortessa, Heidelberg, Germany). Cells were stained for the lineage markers (CD11b, Ter119, CD5, B220 and F4/80), c-Kit, Sca1, CD34 and FcγR (Table 8). Lin^- $c\text{-}Kit^+$ $Sca1^+$ (LKS) cells identified stem cells, Lin^- $Fc\gamma R^+$ $CD34^+$ $c\text{-}Kit^+$ identified granulocyte-monocyte progenitors (GMP), Lin^- $IL7R^-$ $Fc\gamma R^-$ $CD34^-$ $c\text{-}Kit^+$

identified megakaryocyte erythroid progenitors (MEP) and Lin^- $IL7R^-$ $Fc\gamma R^-$ $CD34^+$ $c\text{-}Kit^+$ identified common myeloid progenitors (CMP).

4.30 Colony-formation assay

Colony forming ability of MLL-AF9-transformed mouse cells was examined using Methocult medium (MethoCult GF M3434, StemCell Technologies) according to the manufacturer's information. $1x10^4$ total BM or spleen cells from individual AML mice (sacrificed on day 40 after transplantation) were plated in triplicate in methylcellulose medium containing cytokines. Plates were kept at 37 ºC, and the number of colonies was determined 7 and 10 days after plating.

In serial replating experiments, $1x10^3$ sorted GFP^+ (MLL-AF9) Lin^- cells from the BM of individual AML mice (sacrificed on day 40 after transplantation) were plated in Methocult medium (MethoCult GF M3434, StemCell Technologies). After 7 days, cells were collected from methylcellulose, counted and replated in fresh methylcellulose medium. The same number of cells from primary plating were subjected to secondary plating and the replating was repeated for 6 more times.

4.31 Mass spectrometry

Quantitative mass spectrometry was performed on sorted (BD FACSAria Fusion Cell Sorter) $MLL\text{-}AF9^+$ Lin^- cells from the BM of WT or CaSR KO AML mice, sacrificed on day 40 after transplantation. The experiment was performed in collaboration with Georg Tascher, Institut für Biochemie II, Goethe-Universität Frankfurt am Main.

Sample preparation for mass spectrometry

Cell pellets were dissolved in lysis buffer (2 %SDS, 10 mM TCEP, 40 mM CAA, 50 mM Tris pH 8.5), boiled for 10 minutes at 95 °C followed by 2 minutes of sonication and another 5 minutes of boiling at 95 °C. Proteins were precipitated by methanol-chloroform-precipitation and protein pellets were resuspended in 8 M Urea, 50 mM Tris pH 8.2 and protein concentration determined using BCA assay (Thermo Fisher Scientific, 23225). 40 µg of protein from each sample were diluted to 0.8 M urea using digestion buffer (50 mM Tris pH 8.2) and incubated with LysC (Wako Chemicals) at 1:50 (w/w) ratio and Trypsin (Promega, V5113) at 1:100 (w/w) ratio overnight at 37 °C. Digests were acidified using trifluoroaceticacid (TFA) to 0.5 % and peptides purified using SepPak tC18 columns (Waters, WAT054955). Eluted

peptides were dried, resuspended in TMT labelling buffer (0.1 M EPPS pH 8.2, 20 % Acetonitrile) and peptide concentration determined by micro BCA (Thermo Fisher Scientific, 23235). 10 µg of peptides *per* sample were mixed with TMT10 reagents (ThermoFisher Scientific, 90111, A37724, 90061) in a 1:2 (w/w) ratio (2 µg TMT reagent *per* 1 µg peptide). Reactions were incubated for one hour at RT and subsequently quenched by addition of hydroxylamine to a final concentration of 0.5 % and incubation at RT for 15 min. After verification of labelling efficiency (> 99%) and mixing ratios by LC-MS analysis of a test pool comprising 1/20th of each sample, all samples were pooled accordingly, desalted by SepPak as stated above and dried again.

High pH micro-flow fractionation

Peptides were fractionated using high-pH liquid-chromatography on a micro-flow HPLC (Dionex U3000 RSLC, Thermo Scientific). 30 µg of pooled and purified TMT labelled peptides resuspended in Solvent A (5 mM ammonium-bicarbonate, 5 % ACN) were separated on a C18 column (XSelect CSH, 1 mm x 150 mm, 3.5 µm particle size; Waters) using a multistep gradient from 3-60 % Solvent B (100 % ACN) over 65 minutes at a flow rate of 30 µl/min. Eluting peptides were collected every 43 seconds from minute 2 for 69 minutes into a total of 96 fractions, which were cross-concatenated into 16 fractions. Pooled fractions were evaporated to dryness and stored at -20 °C until mass spectrometry analysis, for which they were resuspended in LC-MS grade water containing 2 % ACN and 0.1 % TFA.

LC-MS Analysis

Tryptic peptides were analyzed on an Orbitrap Lumos coupled to an easy nLC 1200 (ThermoFisher Scientific) using a 35 cm long, 75 µm ID fused-silica column packed in house with 1.9 µm C18 particles (Reprosil pur, Dr. Maisch), and kept at 50 °C using an integrated column oven (Sonation). A synchronous precursor selection (SPS) multi-notch MS3 method was used in order to minimize ratio compression as previously described (McAlister et al., 2014). Assuming equal amounts in each fraction, 750 ng of peptides were eluted by a non-linear gradient from 4 to 32 % ACN over 90 minutes followed by a step-wise increase to 75 % ACN in 6 minutes which was held for another 9 minutes. Full scan MS spectra (350-1400 m/z) were acquired with a resolution of 120,000 at m/z 200, maximum injection time of 100 ms and AGC target value of 4×10^5. The most intense precursors with a charge state between 2 and 6 *per* full scan were selected for fragmentation ("Top Speed" with a cycle time of 1.5 seconds) and isolated with a quadrupole isolation window of 0.7 Th. MS2 scans were

performed in the Ion trap (Turbo) using a maximum injection time of 50 ms, AGC target value of 1.5×10^4 and fragmented using CID with a normalized collision energy (NCE) of 35 %. SPS-MS3 scans for quantification were performed on the 10 most intense MS2 fragment ions with an isolation window of 0.7 Th (MS) and 2 m/z (MS2). Ions were fragmented using HCD with an NCE of 65 % and analyzed in the Orbitrap with a resolution of 50,000 at m/z 200, scan range of 110-500 m/z, AGC target value of 1.5×10^5 and a maximum injection time of 86 ms. Repeated sequencing of already acquired precursors was limited by setting a dynamic exclusion of 45 seconds and 7 ppm and advanced peak determination was deactivated.

Mass Spectrometry data processing

Raw data was analyzed with Proteome Discoverer 2.4 (ThermoFisher Scientific). Acquired MS2-spectra were searched against the mouse reference proteome (Taxonomy ID 10090) downloaded from UniProt (12-March-2020; "One Sequence Per Gene", 21959 sequences) and a collection of common contaminants (244 entries from MaxQuant`s "contaminants.fasta") using SequestHT, allowing a precursor mass tolerance of 7 ppm and a fragment mass tolerance of 0.5 Da after recalibration of mass errors using the Spectra RC-node applying default settings. In addition to standard dynamic (Oxidation on methionines and acetylation/Met-loss or Met-loss+acetylation of protein N-termini) and static (Carbamidomethylation on cysteins) modifications, TMT-labelling of N-termini and lysines were set as static modifications. False discovery rates were controlled on the PSM and protein level using Percolator (< 1 % FDR). Only PSMs with a signal-to-noise above 10 and a co-isolation below 50 % derived from unique peptides we`re used for protein quantification after total intensity normalization.

Mass spectrometry data statistical analysis

Filtering and statistical analysis of the Proteome Discoverer output ("Proteins" table) was performed in Perseus (v 1.6.15.0). Only proteins quantified in all replicates in both experimental groups (WT and KO) were used for statistical analysis. Significant proteins were defined after a Student's t-test applying a p-value cut-off (< 0.01) and fold-change threshold (log2ratio ≥ 1).

4.32 Intravital microscopy (IVM)

Intravital microscopy experiments were performed as previously described (Kumar et al., 2020; Lo Celso et al., 2009). To determine the *in vivo* localization of human THP1 cells, NOD/SCID/IL2Rγ$^{-/-}$ (NSG) mice were intravenously transplanted with 5x10^5 cells, which had treated ex vivo with either vehicle solution or 10 µM of NPS-2143 (Santa Cruz Biotechnology, Heidelberg, Germany) for 4 h at 37 ºC. Cells were subsequently labelled with 1 µM CMTMR dye (C2927, Invitrogen, Germany) and injected into the mice. In order to visualize the vessels, Dextran FITC (1 mg/mouse) (46945, Sigma, Taufkirchen, Germany) was intravenously injected to the mice and imaging was performed 2h after injection.

For indirect measurement of the concentration of calcium ions in the BM, unirradiated immunocompromised triple knockout (Rag-2$^{-/-}$ IL2R $\gamma^{-/-}$ CD47$^{-/-}$) mice were intravenously injected with 5x10^5 BaF3 cells expressing GCamP6s construct followed by visualization by 2-photon microscopy and quantification of the GFP signal in relation to the cells' distance to the bone.

For all IVM experiments, mice were anesthetized with xylazine/ketamine, the scalp removed and the calvarium was visualized under a custom-built confocal two-photon hybrid intravital microscope (LaVision Biotech, Bielefeld) using a 40x objective. The images were analyzed using the ImageJ software.

4.33 Statistical analysis

Statistical analysis was performed using GraphPad software (Prism 9.0). Each experiment was conducted independently at least three times. Data are represented as mean ± SD (standard deviation), and the significance level was set at $P < 0.05$. Statistical significance between two groups were assessed by a Student's t-test, and differences among more than two groups were analyzed using one-way or two-way ANOVA tests followed by post-hoc tests (Dunnet's, Tukey's or Sidak's multiple comparison tests). Differences in survival were assessed by the Kaplan-Meier nonparametric Log-rank test. For the limiting dilution transplantation assay, Poisson statistics were used.

5 Results

5.1 A calcium ion gradient exists inside the BMM

The process of bone remodeling, which is mediated by osteoblasts, that synthesize and mineralize bone, and osteoclasts, that resorb bone, enables a continuous and balanced bone turnover. As a result of bone remodeling, calcium ions are probably released into the bone marrow microenvironment. We hypothesized that this turnover creates a calcium gradient and a higher calcium concentration close to the endosteum where bone remodeling is actively happening, in comparison with areas in the central BM cavity

In order to confirm our hypothesis and indirectly measure the dynamic changes of the calcium concentration inside the bone marrow, we used the genetically encoded fluorescent sensor called GCaMP6s in order to test the extracellular calcium concentration. GCaMP6s is a calcium indicator, which increases its GFP intensity in response to conformational changes upon binding to calcium ions. Through cloning of GCaMP6s into an RFP-expressing vector, whose intensity does not alter with exposure to calcium, we generated a ratiometric calcium sensor (material and methods section 4.1.1).

In order to test whether this construct can be efficiently used to sensitively measure extracellular calcium levels in our system, we stably transfected Ba/F3 cells with the expression construct and exposed these cells to different calcium concentrations and consequently examined the changes in intensity of GFP and RFP fluorescence. As it can be seen in Figure 12A by fluorescence microscopy and in Figure 12B by flow cytometry analysis, there is a clear dose-dependent increase in GFP fluorescence when cells are exposed to calcium, whereas there is no change in RFP fluorescence, proving that small alterations in extracellular calcium concentration can be sensed by the engineered construct.

To determine the distribution of calcium in the BMM, we transplanted Ba/F3 cells expressing GCaMP6s into mice and, using intravital microscopy, visualized the transplanted cells in the calvarium of live mice. The difference in GFP intensity was then investigated in relation to the distance to bone. Our results demonstrate that cells residing closer to bone had higher GFP intensity, indicative of a higher calcium concentration in the surrounding area, which decreases with increasing distance from bone (Figure 12C). The results indicate that calcium levels have distinct distribution patterns inside the BMM, and a calcium gradient exists.

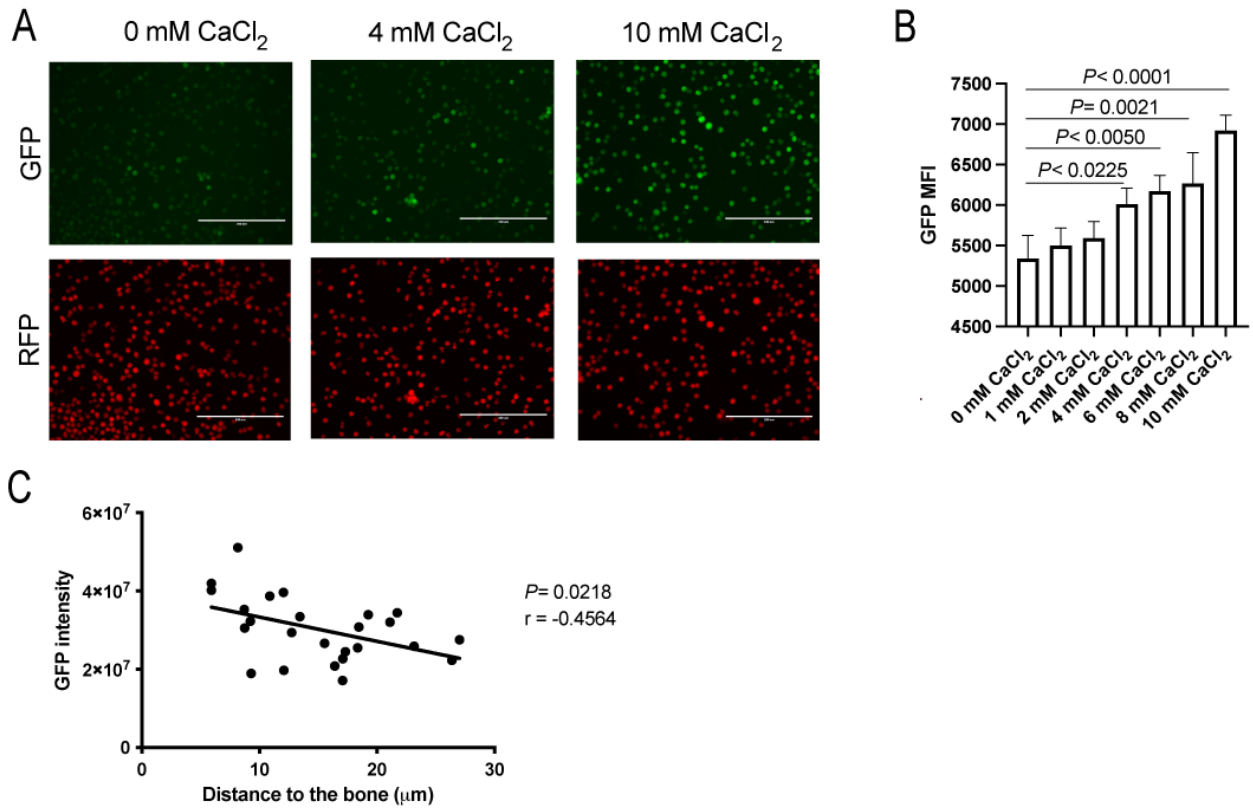

Figure 12. Calcium ions are differentially distributed inside the BM. A) Fluorescence microscopy image of Ba/F3-GCaMP6s cells expressing GFP and RFP. Images were taken 5 minutes post-treatment with 0, 4 or 10 mM of CaCl2. The scale bar represents 400 µm. B) Median fluorescence intensity (MFI) of GFP+ Ba/F3-GCamP6s cells after treatment with 0-10 mM of CaCl2 (n=3, two-way ANOVA, Sidak test). C) Correlation analysis of GFP intensity of Ba/F3-GCaMP6s cells and shortest distance to the bone obtained by intravital microscopy. 2 photon images of cells in the calvarium of mice were taken 2 hours after transplantation, and the GFP intensity was obtained by quantification of the middle stack. The bone is visualized in blue due to second harmonic generation (SHG). The imaging analysis was performed by ImageJ. Pearson's correlation coefficient (r) and p-value are shown (n=25).

To explore the possible role of calcium and differing calcium concentrations in the BMM, we measured the calcium concentration in the BM of control mice (mice transplanted with BM transduced with empty vector) and of leukemic mice suffering from CML, MLL-AF9-driven AML and BCR-ABL1-driven B-ALL. We could see that the calcium concentration in the BMM differs between different leukemia types (Figure 13A), with the calcium concentration being significantly higher in the BM of AML mice, followed by B-ALL and then CML.

In order assess if this finding may be translated to human patients' samples, we measured the calcium concentration in the bone marrow plasma of patients. As our murine data suggested higher calcium levels in AML patients, we based our human sample analysis on AML and non-AML sample sets. We observed that similar to the murine system, patients suffering from

AML also have a higher calcium concentration inside the BM compared to non-AML counterparts (Figure 13B).

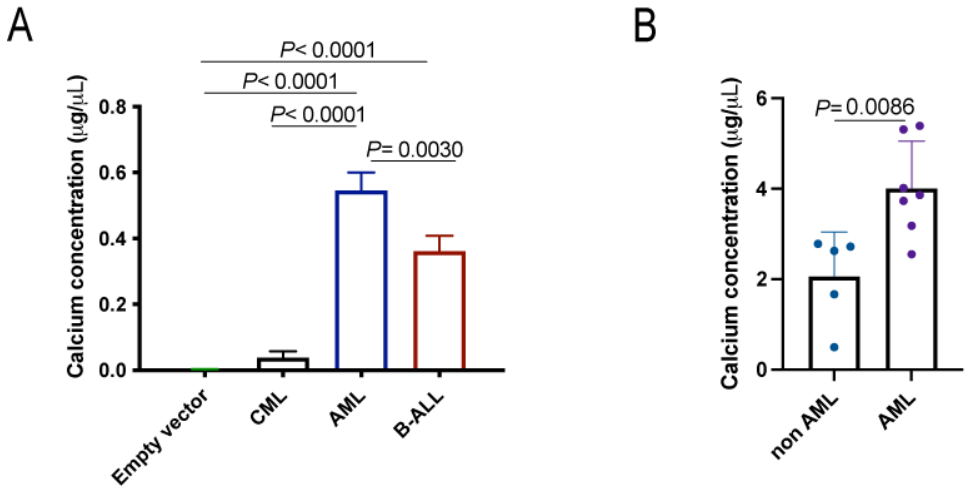

Figure 13. The BM calcium concentration differs between different leukemias. A) Quantification of the calcium (Ca^{2+}) concentration present in the BM of mice transplanted with control BM (empty vector-transduced BM) or moribund mice suffering from CML, AML or B-ALL. The BM of one femur *per* mouse was collected in 100 µl of PBS, and the calcium concentration present in the noncellular fraction was determined (n=3, two-way ANOVA, Tukey test). E) Concentration of calcium present in the BM plasma of patients (AML (n=7); non-AML: CML (n=1), MDS (n=1), ALL (n=2), diffuse large B-cell lymphoma (DLBCL) (n=1), *t*-test).

5.2 Extracellular calcium differentially impacts various leukemias

Once we had confirmed a higher concentration of calcium in both, the murine system and patients, we evaluated the function of calcium in cell line models, particularly, human leukemia cells. We examined the expression levels of calcium sensing receptor (CaSR), the membrane receptor responsible for regulation of cellular responses to extracellular calcium, in several human cell lines by flow cytometry. We observed that the expression of CaSR differed in the respective cell lines and that CaSR is expressed at high levels in the AML cell line THP1 (MLL-AF9$^+$ AML) and expressed at lower levels in the other tested cells, especially K562 cells (BCR-ABL1$^+$ CML) (Figure 14A).

Taking into consideration the observed differences in the calcium concentration in the BM and CaSR expression between CML and AML models, we were interested in understanding, if CaSR expression change in response to differing concentrations of extracellular calcium in these leukemias. Interestingly, when cells were exposed to an increasing calcium concentration, we observed a dose-dependent increase in CaSR expression for the AML cell line THP1 (Figure 14B, Figure S1A) but no changes were observed for the CML cell line K562 (Figure 14C, Figure S1B).

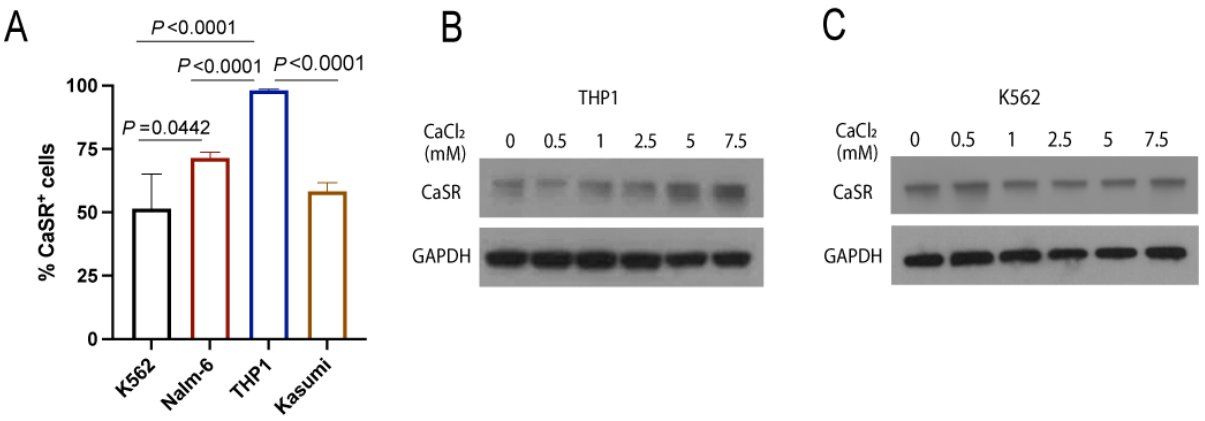

Figure 14. Calcium sensing receptor (CaSR) is expressed differently in various leukemia cell lines. A) Percentage of $CaSR^+$ cells in different human leukemia cell lines (n=3, two-way ANOVA, Tukey test). B-C) Representative immunoblot for CaSR (121 kDa) and GAPDH (37 kDa) expression in lysates of THP1 or K562 treated with 0-7.5 mM of $CaCl_2$ for 4 h.

Next, we tested the effect of extracellular calcium on the adhesion and migration capacity of CML and AML cells. These are two important processes that leukemia cells use for mobilization to and retention in the BMM which have been associated with aggressivity of the disease and worse prognosis (Godavarthy et al., 2020; Kumar et al., 2020). When exposed to extracellular calcium, THP1 cells show a dose-dependent increase in both adhesion to the extracellular matrix protein fibronectin (Figure 15A) and migration towards CXCL-12 (Figure 15B). When we assessed the expression of CXCR4, the membrane receptor on leukemia cells for CXCL-12 and a major regulator of cell migration, we found that exposure of THP1 cells to extracellular calcium increases its membrane expression (Figure 15C), consistent with the increase in migration towards a CXCL-12 gradient.

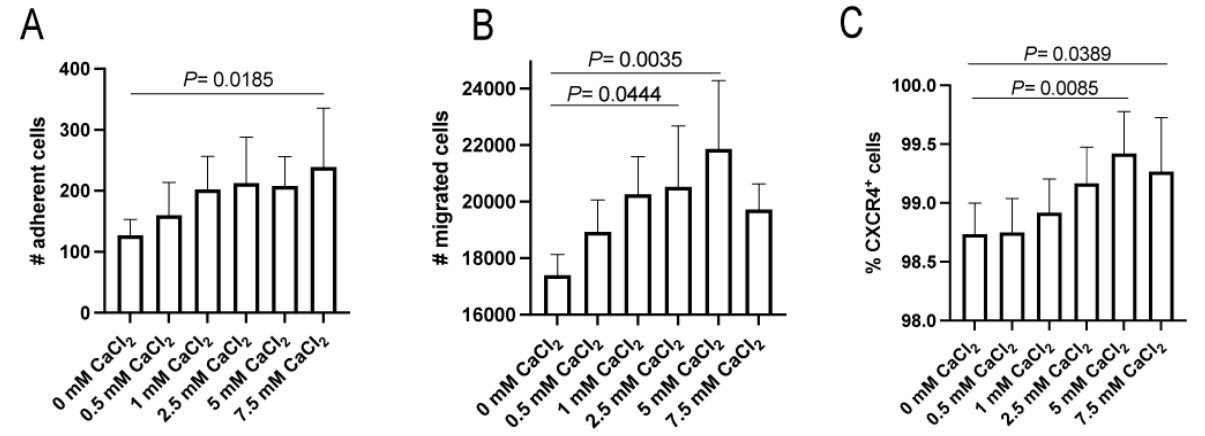

Figure 15. Adhesion, migration and CXCR4 expression of THP1 cells increase with extracellular calcium exposure in a dose dependent manner. A) Number of adherent cells to fibronectin (FN) after 6 h of THP1

cells pre-treated with different calcium concentrations (0-7.5 mM) for 4 h (n=3, two-way ANOVA, Tukey test). B) Number of migrated cells towards CXCL-12 after 2 h of THP1 cells pre-treated with different calcium concentrations (0-7.5 mM) for 4 h (n=3, two-way ANOVA, Tukey test). C) Percentage of $CXCR4^+$ THP1 cells after treatment with different calcium concentrations (0-7.5 mM) for 4 h (n=3, two-way ANOVA, Tukey test).

When adhesion, migration and CXCR4 expression were investigated in K562 cells, the findings were notably different. In contrast to THP1, extracellular calcium had no effect on the adhesion of K562 cells to fibronectin (Figure 16A), on their migratory capacity (Figure 16B) or their CXCR4 expression (Figure 16C). This confirmed a leukemia cell type-specific dependency on calcium ions.

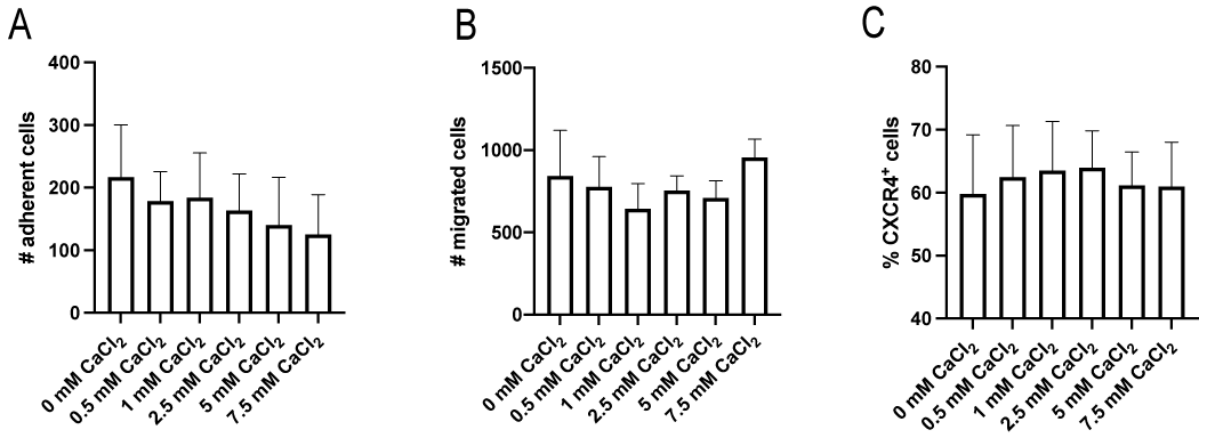

Figure 16. Adhesion, migration and CXCR4 expression of K562 cells are not altered when cells are exposed to varying concentrations of extracellular calcium. A) Number of adherent cells to fibronectin (FN) after 6 h of K562 cells pre-treated with different calcium concentrations (0-7.5 mM) for 4 h (n=3, two-way ANOVA, Tukey test). B) Number of migrated cells towards CXCL-12 after 2 h of K562 cells pre-treated with different calcium concentrations (0-7.5 mM) for 4 h (n=3, two-way ANOVA, Tukey test). C) Percentage of $CXCR4^+$ K562 cells after treatment with different calcium concentrations (0-7.5 mM) for 4 h (n=3, two-way ANOVA, Tukey test).

In addition to the differences in response to calcium treatment, the migratory capacity (Figure S1C) and CXCR4 expression (Figure S1D) were shown to be significantly higher in THP1 than in K562 cells.

Next, we hypothesized that the changes in adhesion and migration may also be accompanied by alterations in cellular features such as cell cycle or cell death stimulated by calcium. To answer this question, we performed apoptosis and cell cycle analysis on THP1 and K562 cells exposed to different calcium concentrations. We observed that the exposure of both cell lines to extracellular calcium (up to 7.5 mM) did not alter cell cycle status or induce apoptosis of the cells (Figure S2).

5.3 *CaSR* acts as a tumor suppressor in CML and B-ALL and as an oncogene in AML

To identify the contribution of CaSR to leukemia pathogenesis we transplanted wildtype (Mx-*Cre* $^{-/-}$ CaSR $^{flox/flox}$) or inducible *CaSR* KO (Mx-*Cre* $^{-/+}$ CaSR $^{flox/flox}$) murine donor BM into wildtype mice (Mx-*Cre* $^{-/-}$ CaSR $^{flox/flox}$) using the retroviral transduction/transplantation models of BCR-ABL1-induced CML-like myeloproliferative neoplasia (MPN) (Krause et al., 2013) or B-ALL (Krause et al., 2006) or MLL-AF9 -driven AML (Krause et al., 2013) (Methods section 4.26).

Gene depletion was performed by treatment of recipient mice with poly I:C on days 3-6 after transplantation to not interfere with homing of the transplanted cells. Homing of transplanted hematopoietic and progenitor cells or leukemia-initiating cells (LICs) is considered to be completed 18 hours after transplantation, suggesting that any observed effects on leukemia induction should not be due to altered homing.

As a complementary experiment, *CaSR* overexpression experiments were performed by co-transduction of BM cells with empty vector or *CaSR*-expressing retrovirus.

In CML, deficiency of *CaSR* on leukemia initiating cells (LICs) did not result in a significant increase in leukocytes (Figure 17A) and BCR-ABL1$^+$ CD11b$^+$ leukocytes (Figure 17B) in the peripheral blood, but a significant shortening of survival of the recipient mice was observed (Figure 17C). In converse, overexpression of *CaSR* in CML LICs (Figure S3A) led to a significant decrease of the leukocyte count (Figure 17D) and a trend towards a lower percentage of BCR-ABL1$^+$ CD11b$^+$ leukocytes (Figure 17E) in the peripheral blood, as well as a significant prolongation of survival of the mice (Figure 17F).

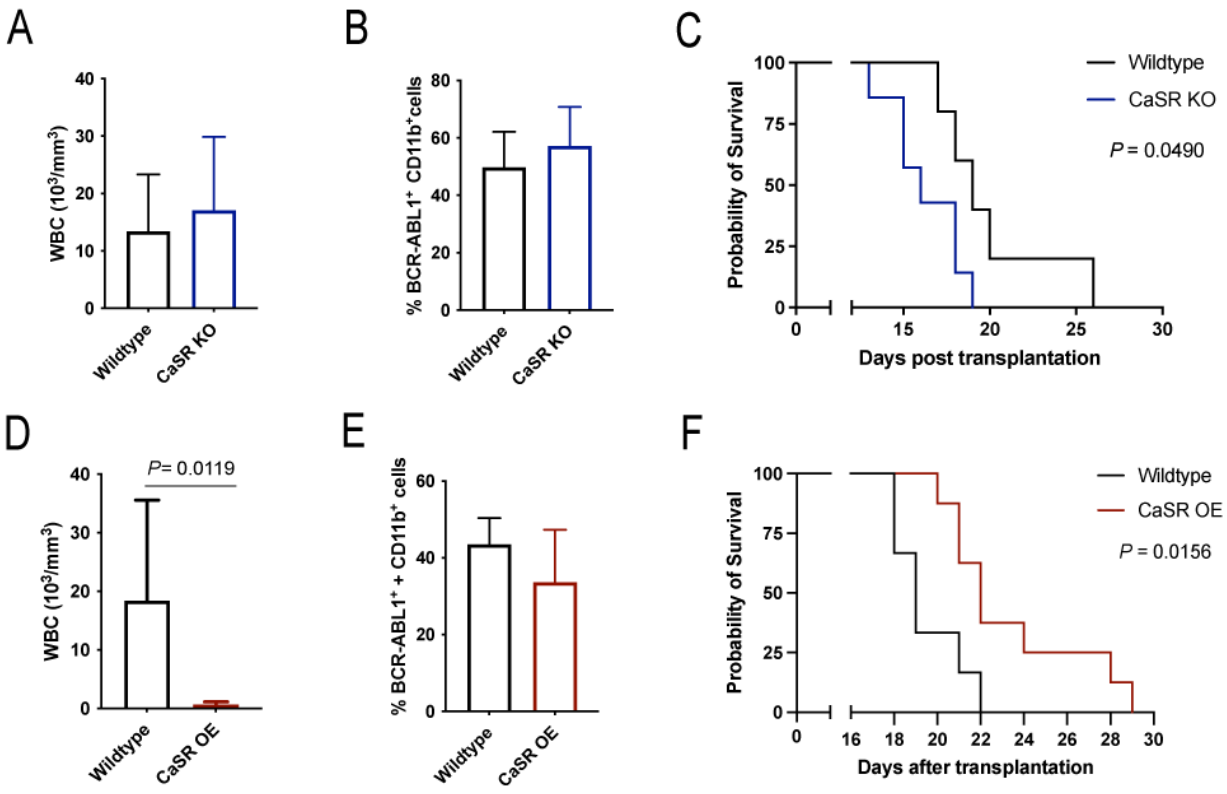

Figure 17. Calcium sensing receptor (CaSR) knockout (KO) in LIC leads to more aggressive CML, while CaSR overexpression (OE) prolongs the survival of mice with CML. A-B) Leukocyte counts (WBC) (A) and the percentage of BCR-ABL1$^+$ CD11b$^+$ cells (B) of wildtype (black) or CaSR KO (blue) cells (n=5-7) in peripheral blood of mice, thirteen days post transplantation. C) Kaplan-Meier-style survival curve of mice transplanted with wildtype (black) or CaSR KO (blue) BM, transduced with BCR-ABL1-expressing retrovirus (n=5-7, Log-rank test). All recipient mice were injected with 10 mg/kg poly I:C on days 3 to 6 after transplantation. D-E) Leukocyte counts (WBC) (D) and percentage of BCR-ABL1$^+$ CD11b$^+$ cells (E) of wildtype (black) or CaSR OE (red) cells (n=6-8) in peripheral blood of mice, fifteen days post transplantation. C) Kaplan-Meier-style survival curve of mice transplanted with wildtype BM transduced with BCR-ABL1 -expressing retrovirus, co-transduced with empty vector- (black) or CaSR-overexpressing retrovirus (red) (n=6-8, Log-rank test).

Similar to CML, reduced expression of *CaSR* on leukemia-initiating cells resulted in a significant rise of leukocyte counts (Figure 18A), an increased percentage of BCR-ABL1$^+$ BP1$^+$ B precursor cells (Figure 18B) and accelerated disease course in BCR-ABL1$^+$ B-ALL (Figure 18C).

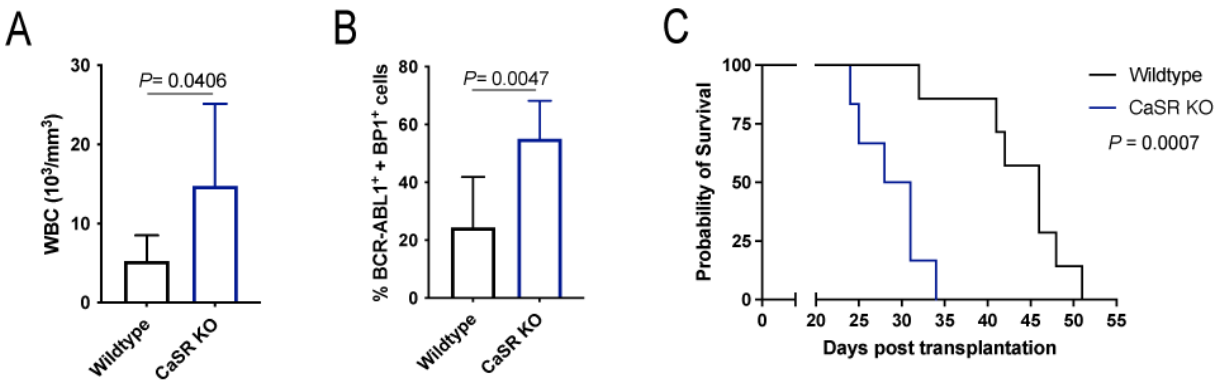

Figure 18. Depletion of CaSR leads to more aggressive B ALL. A-B) Leukocyte counts (WBC) (A) and percentage of BCR-ABL1$^+$ BP1$^+$ cells (B) in peripheral blood of recipients of wildtype (black) or CaSR KO (blue) BM, transduced with BCR-ABL1 in the B-ALL model (n=6-7, *t*-test), eighteen days post transplantation. C) Kaplan-Meier-style survival curve of mice transplanted with wildtype (black) or CaSR KO (blue) BM, transduced with BCR-ABL1 (n=6-7, Log-rank test). All recipient mice were injected with 10 mg/kg poly I:C on days 3-6 after transplantation.

In stark contrast, transplantation of MLL-AF9$^+$ CaSR KO BM cells (Figure S3B) into wildtype mice led to a significant reduction in the number of leukocytes (Figure 19A), a reduction in the percentage of MLL-AF9$^+$ Gr1$^+$ myeloid cells (Figure 19B) in peripheral blood of recipient mice and a significant delay in the course of AML (Figure 19C). Complementarily, we showed that overexpression of CaSR (Figure S3C) in wildtype MLL-AF9$^+$ bone marrow cells significantly increased the leukocyte count (Figure 19D) and the percentage of MLL-AF9$^+$ Gr1$^+$ cells (Figure 19E), which resulted in a significant acceleration of the disease course (Figure 19F).

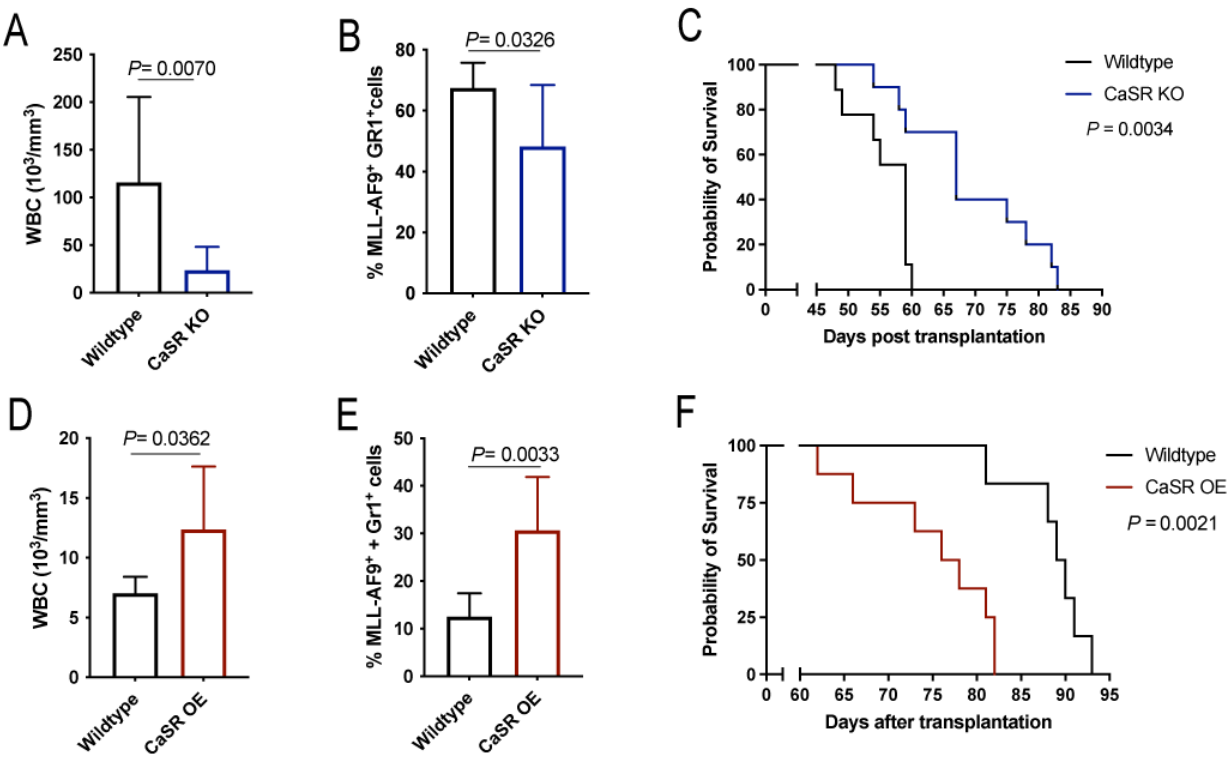

Figure 19. Depletion of CaSR in AML initiating cells prolongs survival of recipient mice, while CaSR overexpression makes the disease more aggressive. A-B) Leukocyte counts (WBC) (A) and percentage of MLL-AF9$^+$ Gr1$^+$ cells (B) in peripheral blood of recipients of wildtype (black) or CaSR KO (blue) cells (n=9-10, *t*-test), transduced with MLL-AF9, fifty-three days post transplantation. C) Kaplan-Meier-style survival curve of mice transplanted with wildtype (black) or CaSR KO (blue) BM, transduced with MLL-AF9 -expressing retrovirus (n=9-10, Log-rank test). All recipient mice were injected with 10 mg/kg poly I:C on days 3-6 after transplantation. D-E) Leukocyte counts (WBC) (D) and percentage of MLL-AF9$^+$ Gr1$^+$ cells (E) in peripheral blood of recipients of wildtype (black) or CaSR OE (red) cells (n=9-10, *t*-test), transduced with MLL-AF9, fifty-four days post transplantation. C) Kaplan-Meier-style survival curve of mice transplanted with wildtype BM transduced with MLL-AF9, co-transduced with empty vector (black) or CaSR -overexpressing retrovirus (red) (n=9-10, Log-rank test).

To confirm and further illustrate the function of CaSR in AML development, we performed a rescue transplantation experiment in which CaSR was overexpressed in CaSR KO MLL-AF9$^+$ BM cells. As can be seen in Figure 20, the prolongation of survival was reversed and the disease 'rescued', when CaSR levels were increased in CaSR KO LIC.

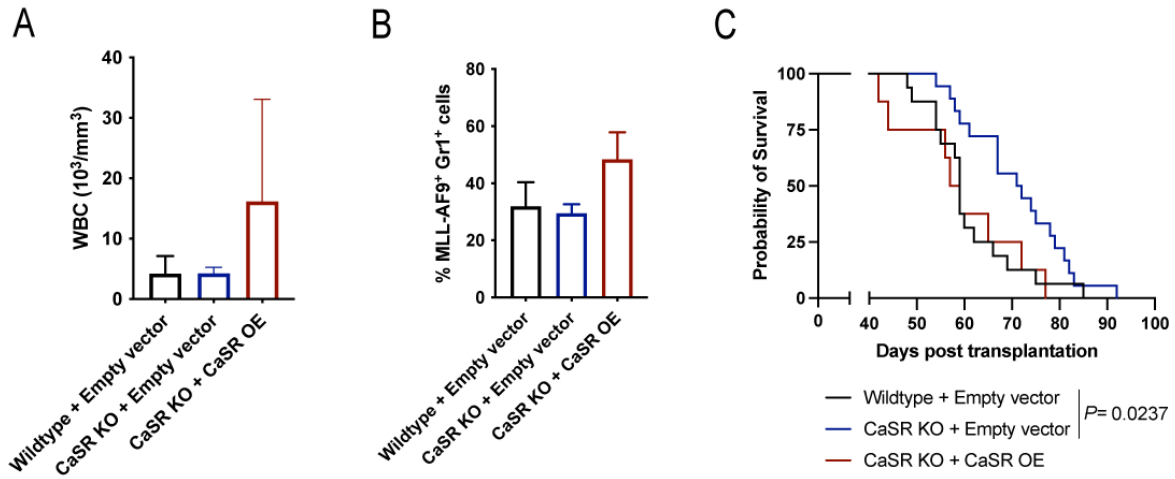

Figure 20. Overexpression of CaSR on MLL AF9⁺ leukemia-initiating cells lacking CaSR restores the disease similar to the phenotype using WT donor BM. A-B) Leukocyte counts (WBC) (A) and percentage of MLL-AF9⁺ Gr1⁺ cells (B) in peripheral blood of recipients of wildtype (black), CaSR KO (blue) or CaSR KO + CaSR OE (red) cells (n=8, two-way ANOVA, Tukey test) transduced with MLL-AF9-expressing retrovirus, twenty-six days post transplantation. C) Kaplan-Meier-style survival curve of mice transplanted with wildtype BM transduced with MLL-AF9 -expressing retrovirus and co-transduced with empty vector (black), or CaSR KO BM transduced with MLL-AF9-expressing retrovirus and co-transduced with empty vector (blue) or CaSR OE -expressing virus (red) (n=8-18, Log-rank test).

In summary, these results indicate that CaSR plays a highly oncogene-specific, differential and essential role in CML, B-ALL and AML development. Our experiments suggests that in AML CaSR functions as oncogene and in B-ALL as a tumor suppressor. Consistent with these observations, there was a significant negative correlation between CaSR expression on leukocytes in the PB of mice with AML and day of death (Figure 21A) and a positive correlation in the case of CML (Figure 21B), suggestive of a differential role of CaSR in the two diseases.

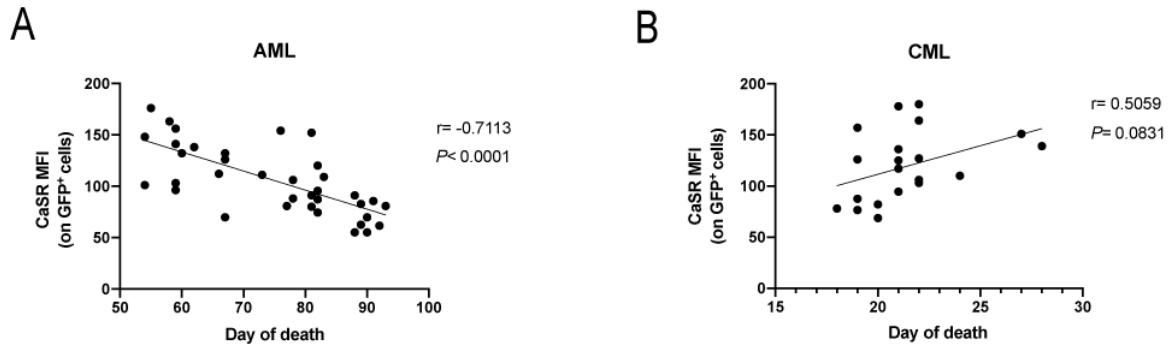

Figure 21. CaSR expression negatively correlates with survival of mice in AML and positively correlates in CML. A) Correlation between CaSR expression on leukocytes from peripheral blood of mice on days 53/54 after transplantation and survival of mice suffering from AML (n=21). B) Correlation between CaSR expression on leukocytes from peripheral blood of mice on day fifteen post transplantation and day of death of mice with CML (n=19). Pearson's correlation (r) and p-values are indicated next to each graph.

5.4 CaSR deficiency prolongs survival of mice with AML, independent of homing

In order to test whether engraftment of CaSR-deficient cells may be contributing to the observed prolongation of survival in AML (Krause et al., 2013; Krause et al., 2006), we performed a BM transplantation experiment and deleted CaSR (Figure S4A) on leukocytes by injecting poly I:C 12 days after transplantation, when the disease was established (Figure 22A). Similar to our results for CaSR depletion 72 h after transplantation, mice receiving CaSR-deficient AML cells showed a significant reduction of the leukocyte count (Figure 22B), a reduction in the percentage of MLL-AF9$^+$ GR1$^+$ cells (Figure 22C) in peripheral blood and a significant prolongation of the survival (Figure 22D).

As supportive data we determined the percentage of MLL-AF9$^+$ Gr1$^+$ myeloid cells and the percentage of granulocyte-monocyte progenitor (GMP) cells, which harbors the LSC fraction in this model (Chen et al., 2019), in the BM of mice transplanted with MLL-AF9$^+$ wildtype or CaSR KO LIC, 12 days after transplantation, whereby the knockout of CaSR was induced on day 3 after transplantation (Figure S4B and C, respectively). This revealed no differences in between the two cell types.

Taken together, these results indicate that prolongation of survival seen throughout our murine KO experiments is not dependent on the alteration of homing or engraftment in absence of CaSR.

In order to test, whether disease clonality (Krause et al., 2013; Krause et al., 2006) may differ between WT and KO LIC, we performed long-distance reverse polymerase chain reaction (LDI-PCR) on splenocytes of AML mice (Meyer and Marschalek, 2009) (Figure 22E). This analysis revealed a trend towards a reduction of the number of proviral integration sites (Figure 22F) represented by individual bands. This revealed a trend towards reduced disease clonality in mice transplanted with CaSR KO compared to wildtype LIC, indicative of less aggressive disease upon CaSR depletion.

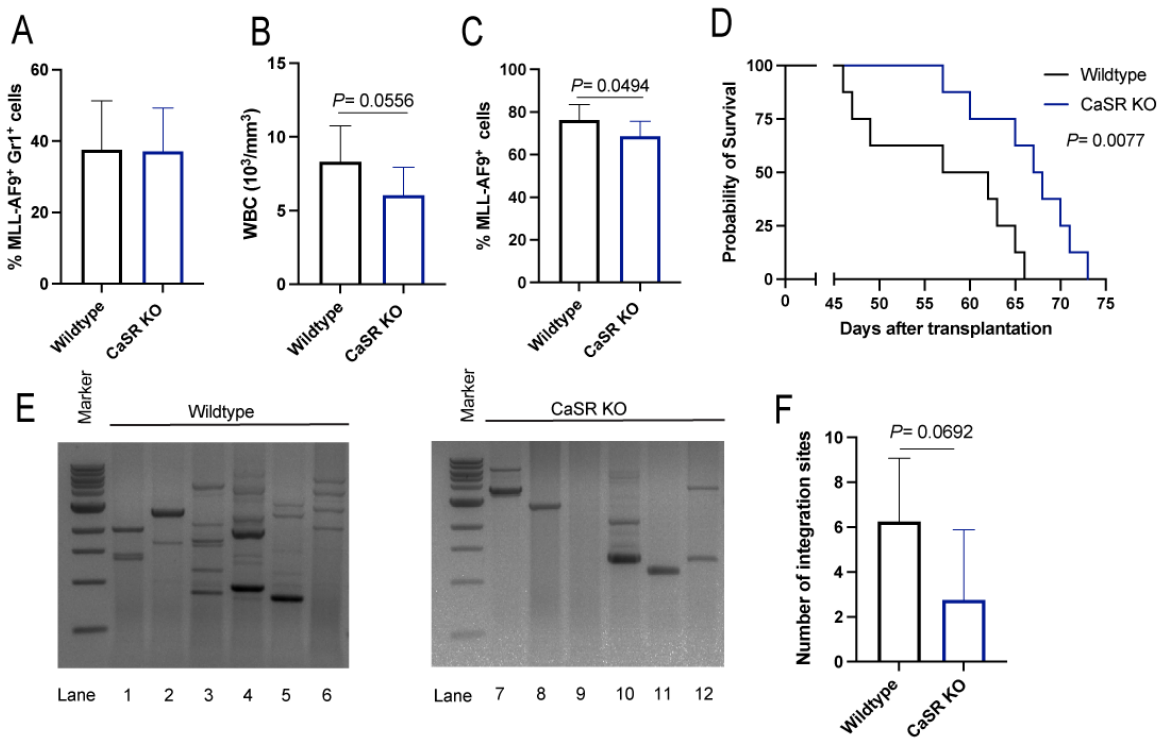

Figure 22. CaSR KO prolongs survival of mice with AML, independent of homing. A) Percentage of MLL-AF9$^+$ Gr1$^+$ wildtype (black) or CaSR KO (blue) cells in peripheral blood of mice transplanted with MLL-AF9$^+$ LIC twelve days post transplantation, before CaSR depletion by poly I:C treatment (n=8, *t*-test). B-C) Leukocyte counts (WBC) (B) and percentage of MLL-AF9$^+$ Gr1$^+$ cells (C) in peripheral blood of mice transplanted with wildtype (black) or CaSR KO (blue) MLL-AF9$^+$ LIC (n=8, *t*-test), 25 and 26 days post transplantation, respectively B and C. D) Kaplan-Meier-style survival curve of mice transplanted with wildtype (black) or CaSR KO (blue) BM, transduced with MLL-AF9 -expressing retrovirus and with gene deletion initiated on day twelve after transplantation (n=8, Log-rank test). E-F) Representative image of agarose gel electrophoresis (E) and quantification (F) of the DNA products amplified by long-distance inverse (LDI) PCR, derived from splenic tissue of wildtype mice which had been transplanted with wildtype (black) or CaSR KO (blue) MLL-AF9 -transduced bone marrow in the AML model.

5.5 CaSR is required for maintenance of stemness and self-renewal abilities of AML leukemia stem cells (LSCs)

Next, to investigate a possible role of CaSR during AML pathogenesis, we hypothesized that CaSR may contribute to LSC stemness and self-renewal in AML. MLL-AF9 -transformed cells derived from the BM of recipient mice, transplanted with MLL-AF9$^+$ wildtype or CaSR KO BM were plated in methylcellulose, and colonies were counted. BM-AML cells deficient for CaSR gave rise to a significantly lower number of colonies in serial replating (Figure 23A) assays, suggesting that CaSR supports progenitor expansion and, in absence of CaSR, the self-renewal ability of stem cells was lost. Complementarily, the percentage of myeloid progenitor cells, including granulocyte-macrophage progenitor (GMP) cells, which comprises the LSC fraction in the MLL-AF9 -induced AML model (Krivtsov et al., 2006), were significantly reduced after CaSR depletion (Figure 23B).

To further complement our data, we next investigated whether CaSR can induce stem cell-associated gene expression in AML. To test this, we performed a targeted gene expression profile for the expression of genes that are known to play a role in the maintenance of leukemic stem cells in AML, by qPCR. The experiment was performed on MLL-AF9 -expressing wildtype, CaSR KO and CaSR OE BM cells from mice. The data indicate that CaSR can regulate the expression of genes associated with stemness, as lower expression of stem cell-related genes was detected when CaSR is depleted and high expression in the cells overexpressing CaSR (Figure 23C).

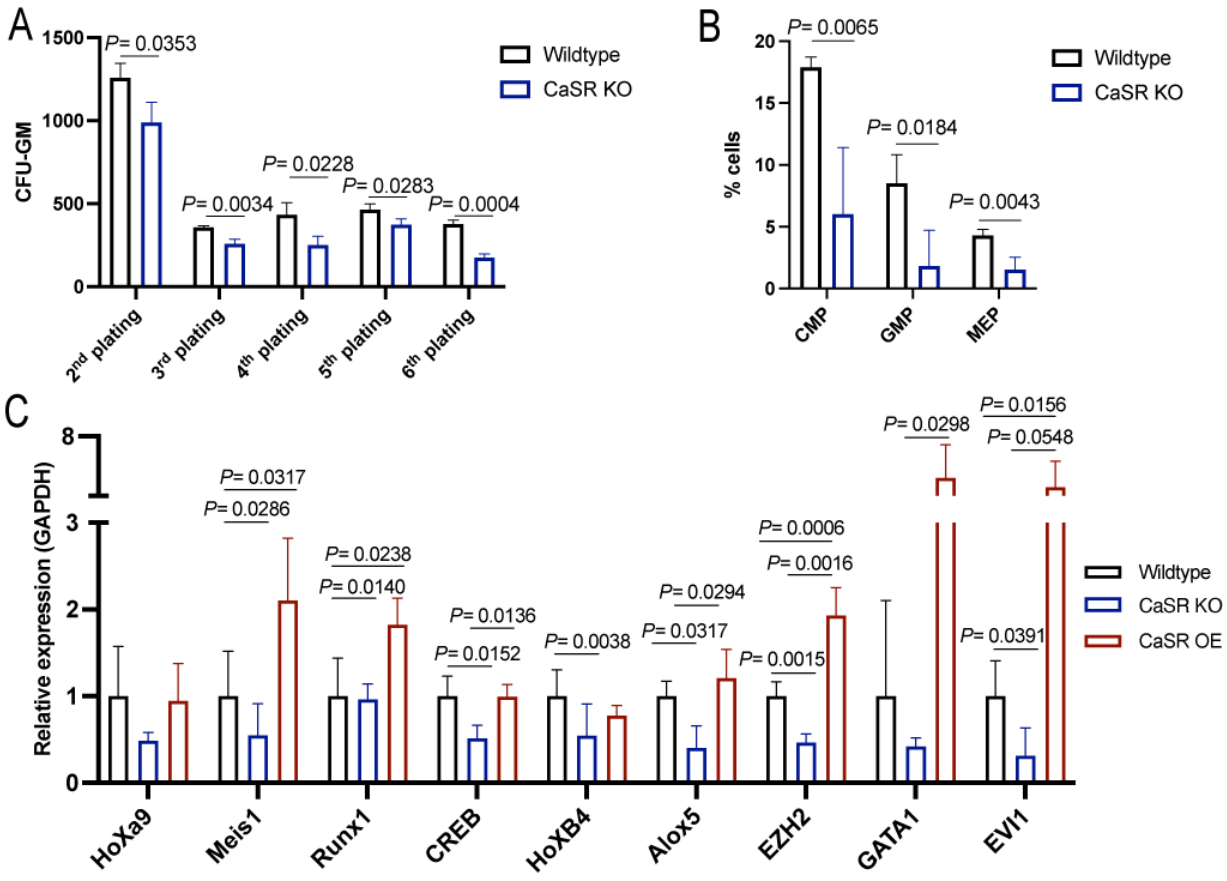

Figure 23. CaSR regulates colony forming ability, frequency of leukemic myeloid precursors and expression of stemness- and self-renewal-associated genes in AML. A) Number of colonies *per* plate derived from serial replating of BM-derived cells from wildtype mice which had been transplanted with wildtype (black) or CaSR KO (blue) MLL-AF9 -transduced bone marrow in the AML model, on day 40 after transplantation (n=3, *t*-test). B) Percentage of common myeloid progenitors (CMP: Lin^- $Sca1^-$ $CD117^+$ $CD34^+$ $CD16/32^-$), granulocyte-monocyte progenitors (GMP: Lin^- $Sca1^-$ $CD117^+$ $CD34^+$ $CD16/32^+$) and megakaryocyte-erythroid progenitors (MEP: Lin^- $Sca1^-$ $CD117^+$ $CD34^-$ $CD16/32^-$) cells in wildtype or CaSR KO BM cells of mice with MLL-AF9-induced AML, on day 40 after transplantation (n=3-4, *t*-test). C) Relative expression levels of some AML stemness- and self-renewal -related genes, determined by RT-qPCR. The mRNA levels were assessed in unsorted wildtype, CaSR KO and CaSR BM cells from mice with MLL-AF9 -induced AML (n=3, two-way ANOVA, Tukey test).

In order to test the impact of CaSR on AML LSC stemness and self-renewal potential *in vivo*, a secondary transplantation was performed using cells derived from primary mice with established disease. The overall survival of the leukemic mice transplanted with MLL-AF9-transformed BM derived from CaSR KO primary mice was markedly extended compared with that of the control mice upon secondary transplantation. This further supported the hypothesis that CaSR may be required for LSC function in AML (Figure 24A) and that in absence of CaSR the stemness and hence the ability to cause malignancy in secondary recipients was reduced.

To confirm and quantify the LSC defect in CaSR KO mice, we assessed the frequency of functional LSC *in vivo* in a limiting dilution assay (LDA) by transplanting wildtype or CaSR KO BM from mice with MLL-AF9-driven AML into wildtype recipients in different doses. Reproducing the secondary transplant results, leukemia development was much slower in the mice transplanted with CaSR KO-derived AML cells than in the control mice, as evidenced by the decreased number of leukocytes (Figure S5A) and frequency of MLL-AF9$^+$ Gr1$^+$ myeloid cells (Figure S5B) in the peripheral blood, which was associated with prolonged overall survival of the mice (Figure 24C). To quantify the extent of a potential LSC defect caused by *CaSR* depletion in these mice, donor cell engraftment was defined as the number of mice having more than 8,000 leukocytes/µl and more than 20 % of MLL-AF9$^+$ GR1$^+$ cells in the peripheral blood on day 24 (Figure 24B and D). The LSC number was calculated using an LDA software analysis (ELDA) (Hu and Smyth, 2009). The results show that the stem cell frequency was reduced 6.5-fold in CaSR KO BM AML cells compared with wildtype mice (1 in 65,937 *versus* 1 in 10,121) (Figure 24B).

These results suggest that CaSR -mediated pathways enhance leukemogenesis and may be a good target for the eradication of leukemia stem cells.

A

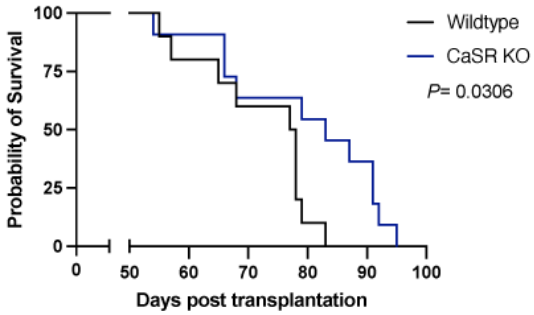

B

Cell dose	Tested	Response	Group
2500	5	1	Wildtype
5000	5	2	Wildtype
10000	5	3	Wildtype
15000	5	4	Wildtype
2500	5	0	CaSR KO
5000	4	0	CaSR KO
10000	4	0	CaSR KO
15000	5	2	CaSR KO
Engraftment: > 20% MLL-AF9⁺ Gr1⁺ > 8,000 WBC//µL in PB on day 24			

C

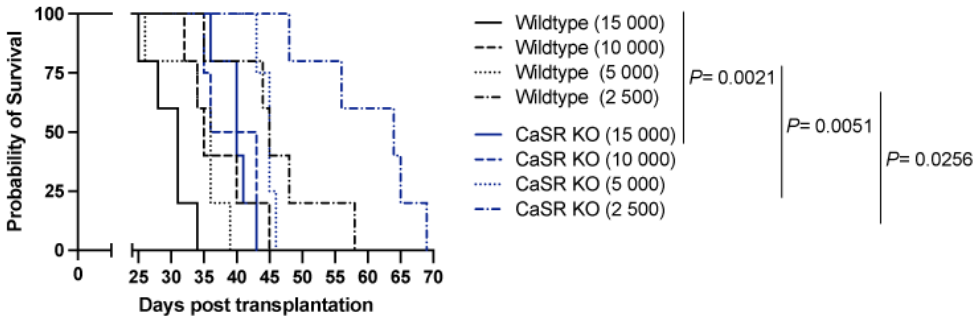

D

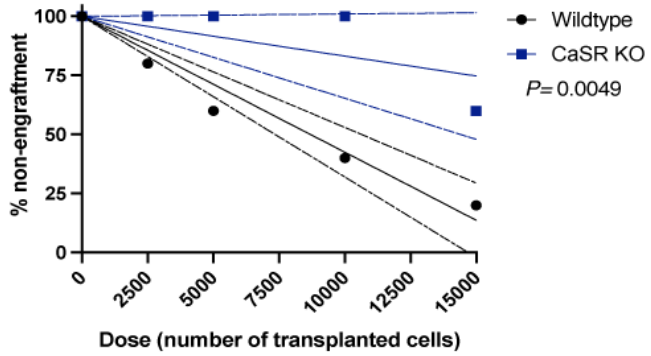

Figure 24. CaSR regulates leukemia stem cell number and function in AML. A) Kaplan-Meier-style survival curve of wildtype secondary mice transplanted with sorted MLL-AF9$^+$ Lin$^-$ BM cells from wildtype or CaSR KO primary mice with established MLL-AF9 -driven AML (n=10-11, Log-rank test). B) Leukemia stem cell (LSC) frequency determined by ELDA (Extreme Limiting Dilution Analysis, Hu & Smyth 2009). C) Kaplan-Meier-style survival curve of wildtype secondary recipient mice transplanted with different doses of sorted MLL-AF9$^+$ Lin$^-$ BM cells (2,500-15,000 cells *per* mouse) (n=4-5, Log-rank test). D) Limiting dilution transplantation analysis for secondary recipient mice transplanted with wildtype or CaSR KO AML cells. Specifically, percent non-engraftment is plotted on the y-axis and transplanted cell number is plotted on the x-axis. Linear regression analysis was performed, and dashed lines indicate 95 % confidence intervals.

5.6 CaSR-deficiency in LIC prolongs survival in an MN1-driven AML model

Seeking to comprehend if the CaSR role in AML was specific to MLL-AF9 -transformed AML or if that could be applied to AML driven by different oncogenes, leukemia progression was tested *in vivo* by transplantation of wildtype or CaSR KO BM cells, transduced with MN1-expressing virus, into wildtype recipients. In MN1-induced AML, deficiency of *CaSR* (Figure S5C) on LICs resulted in a trend towards a decrease in leukocyte count (Figure 25A) and MN1$^+$ leukocytes (Figure 25B) in the peripheral blood of recipient mice. Furthermore, and similar to MLL-AF9, transplantation of MN1- transduced CaSR- deficient LIC led to a significant prolongation of overall survival compared to the wildtype control (Figure 25C).

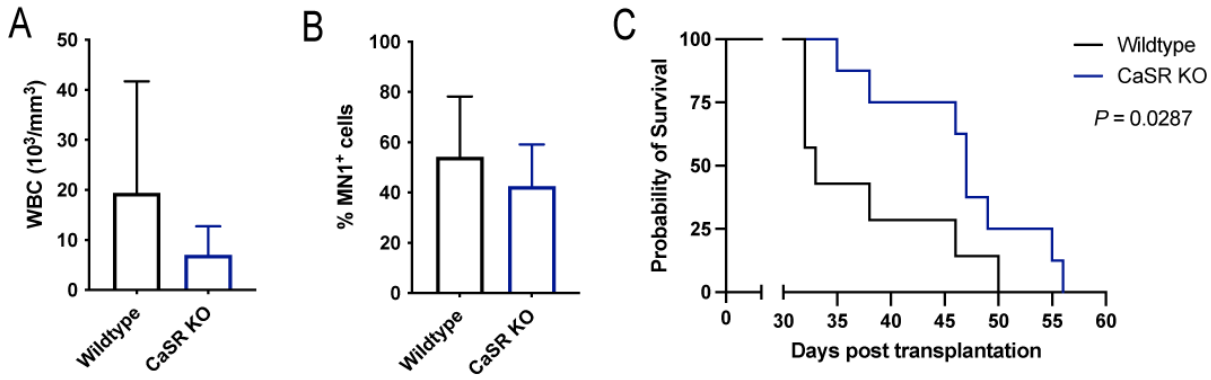

Figure 25. Depletion of CaSR in MN1-driven AML prolonged survival of recipient mice. A-B) Leukocyte counts (WBC) (A) and percentage of MN1$^+$ cells (B) in peripheral blood of mice transplanted with MN1$^+$ wildtype (black) or CaSR KO (blue) BM (n=7-8, *t*-test) on day thirty-two after transplantation. C) Kaplan-Meier-style survival curve of mice transplanted with wildtype (black) or CaSR KO (blue) BM cells, transduced with MN1 -expressing retrovirus (n=7-8, Log-rank test).

5.7 Characterization of CaSR-deficient AML cells

Aiming to characterize the CaSR KO and CaSR OE MLL-AF9-driven AML cells, we performed immunophenotyping of cells derived from leukemic mice during disease progression. Gr1 is a marker that is associated with immature myeloid cells (Bronte et al., 2016). The MLL-AF9$^+$ myeloid cells showed different degrees of expression of the surface protein Gr1 at different stages of disease progression. Populations of Gr1 high and Gr1 low could be observed amongst the leukocytes of mice with AML (Figure 26A). The proportions of these cells varied over the course of the disease (Figure 26A and B), with the percentage of Gr1 high leukocytes decreasing and the Gr1 low population increasing (Figure 26B). As the disease severity in AML is associated with the percentage of undifferentiated cells (Ferrara and Schiffer, 2013), i.e. blasts, and the Gr1 low fraction may be enriched in blasts, we sorted BM-derived MLL-AF9$^+$ cells with high and low Gr1 expression and characterized them morphologically. Indeed, as

shown in Figure 26C by the ratio between BM blasts and neutrophils (differentiated myeloid cells), the proportion of blasts is significantly higher in the Gr1 low population. Consistent with the fact that a higher percentage of blasts in the peripheral blood may reflect a more aggressive disease, MLL-AF9 -induced CaSR KO leukemia cells, which lead to a less aggressive phenotype *in vivo,* show a reduced percentage of Gr1 low cells (Figure 26D). Complementary, CaSR OE on LIC, which mediates an acceleration of the disease, revealed a higher percentage of this blast-enriched population (Figure 26E).

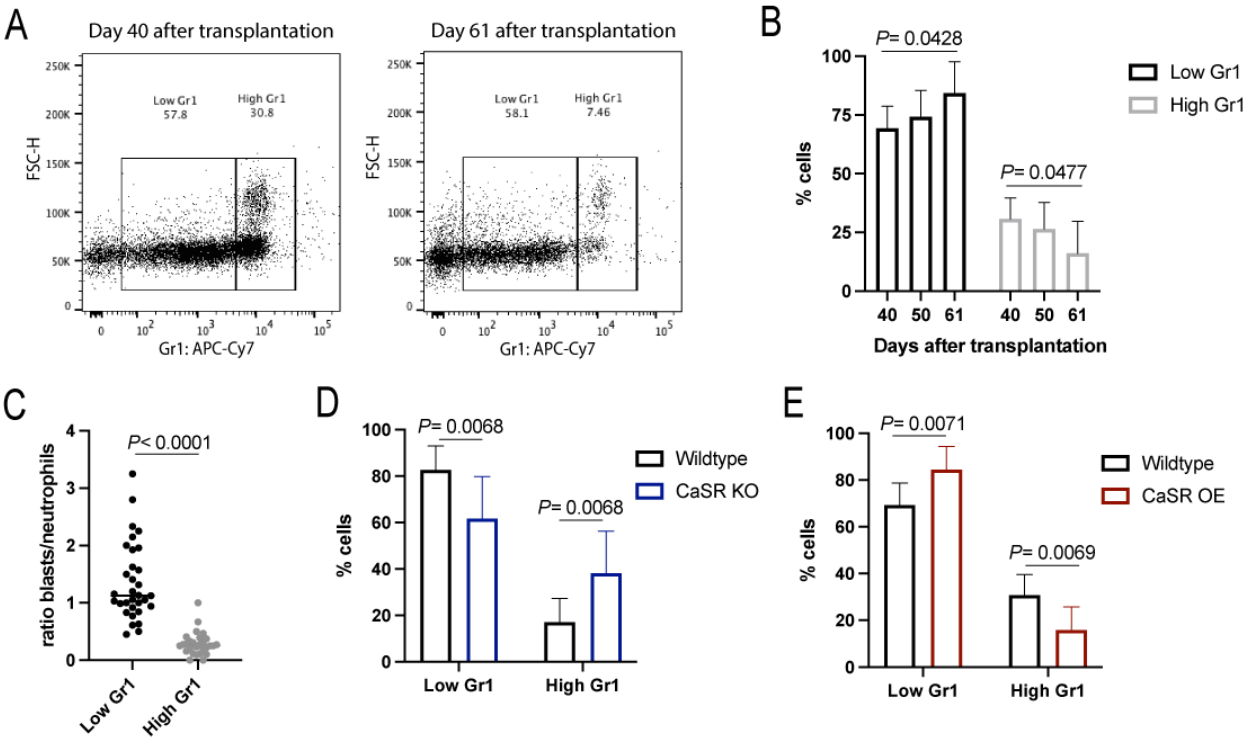

Figure 26. CaSR WT or KO MLL-AF9⁺ AML blasts express differing levels of Gr1. A-B) Representative FACS plots (A) and quantification (B) of the percentage of low and high Gr1 surface expression on CaSR WT or KO MLL-AF9⁺ cells in the PB of wildtype mice over time (days 40, 50 and 61 after transplantation) (n=8, two-way ANOVA, Tukey test). C) Quantification of Giemsa-stained cytospins of MLL-AF9⁺ cells with low or high Gr1 surface expression, isolated from the BM of wildtype mice with AML, on day 40 after transplantation. The graph represents the ratio between blasts and neutrophils based on their morphology (n=28-32, *t*-test). D-E) Percentage of low and high Gr1 surface expression in the PB of wildtype mice which had been transplanted with wildtype (black) or CaSR KO (blue) on day 36 after transplantation (n=9-10, *t*-test) (D), and wildtype mice transplanted with wildtype BM transduced with MLL-AF9, co-transduced with empty vector (black) or CaSR -overexpressing retrovirus (red) on day 40 after transplantation (n=8, *t*-test) (E).

Next, we hypothesized that the survival prolongation of recipients of CaSR-deficient leukemia-initiating cells may be attributed to changes in cellular characteristics, such as apoptosis and cell cycle, in addition to reduced self-renewal of the LSC fraction. Indeed, the percentages of MLL-AF9$^+$ apoptotic cells were significantly increased when CaSR was depleted (Figure 27A). Further, CaSR-deficiency in LIC resulted in a significant increase of cells in the G1 phase and a reduction of cells in the S phase of the cell cycle (Figure 27B). Furthermore, analysis of CaSR KO BM cells from mice with MLL-AF9 -induced AML showed significantly decreased levels of reactive oxygen species (ROS) (Figure 27C) and decreased DNA damage, as measured by staining for γH2A.X (Figure 27D), when compared to the wildtype counterpart. Both of these are factors that may be associated with increased mutations and hence tumor aggressivity in many different cancer types.

Collectively, our data suggest that deficiency of CaSR on LICs leads to increased apoptosis, and reduced cell cycle, ROS production and DNA damage *in vivo*.

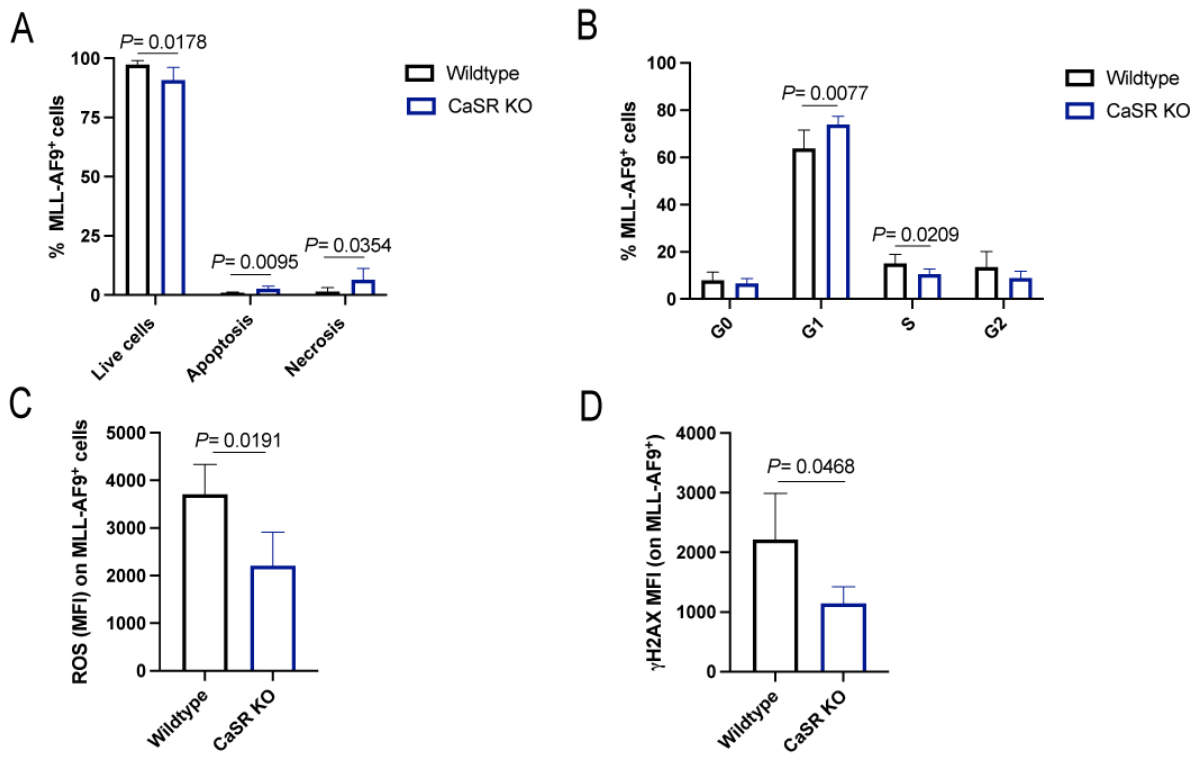

Figure 27. CaSR regulates apoptosis, cell cycle, ROS levels and DNA damage in AML cells. A) Percentage of MLL-AF9$^+$ apoptotic cells in the bone marrow of mice transplanted with wildtype (black) or CaSR KO (blue) LIC, detected by annexin V staining (n=5-6, two-way ANOVA, Tukey test). B) Cell cycle analysis of wildtype (black) or CaSR KO (blue) MLL-AF9$^+$ BM cells using Ki67 staining (n=7, two-way ANOVA, Tukey test). C) Mean fluorescence intensity of ROS in BM cells of mice transplanted with MLL-AF9$^+$ wildtype (black) or CaSR KO (blue) BM (n=5, *t*-test). D) Median fluorescence intensity of γH2A.X in MLL-AF9$^+$ cells in the BM of recipients of wildtype (black) or CaSR KO (blue) LIC, 40 days after transplantation (n=3-4, *t*-test).

5.8 CaSR regulates proliferation, cell cycle, apoptosis, ROS production, differentiation and DNA damage in THP1 cells

In order to study the molecular mechanism of CaSR in AML cells, a gain of function approach, in which CaSR was overexpressed, was used. Using the sleeping beauty system (collaboration with Eric Kowarz, Goethe University Frankfurt), CaSR was successfully (Figure 28) overexpressed in the human MLL-AF9^{+} THP1 cell line, a model for AML.

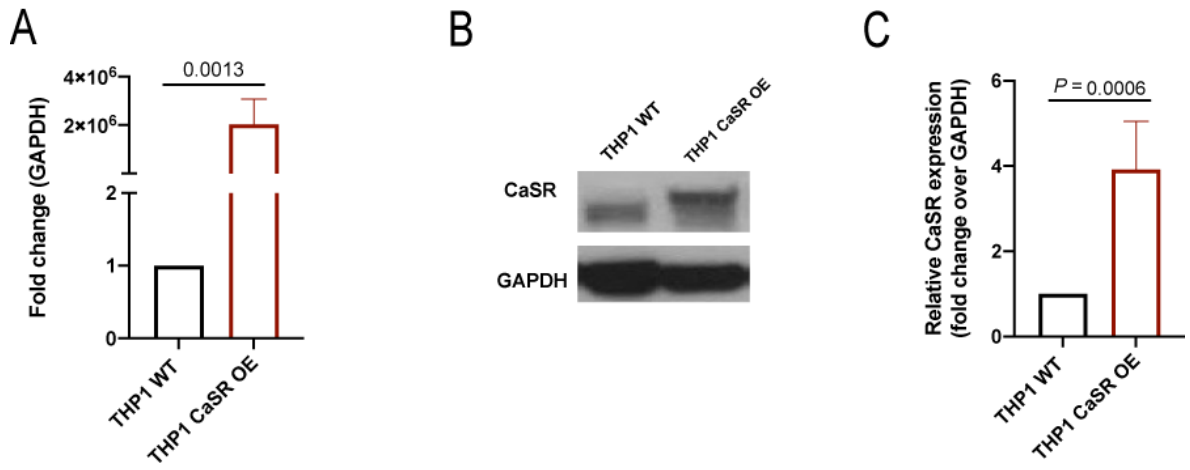

Figure 28. CaSR overexpression in THP1 cells. A) Relative expression of *CaSR* by qRT-PCR analysis of THP1 cells (WT, black) and THP1 cells, overexpressing CaSR (THP1 CaSR OE, n=3, *t*-test). B-C) Representative immunoblot analysis (B) and quantification (C) of CaSR (121 kDa) expression relative to GAPDH (37kDa) in total cell extracts of THP1 WT and THP1 CaSR OE cells (n=4, *t*-test).

In order to evaluate the impact of CaSR overexpression on the cellular physiology of THP1 cells, we performed a set of experiments. Initially, in a proliferation assay, THP1 cells overexpressing CaSR showed a higher proliferation capacity when compared to their wildtype counterparts (Figure 29A). Complementarily, CaSR overexpression also led to an increase in cell cycle with a significant reduction of cells in G0 and G1 phases and increases of cells in the S and G2 phases of the cell cycle (Figure 29B). Additionally, CaSR overexpression also led to an effect on the viability of THP1 cells, as a significant increase in viable cells and a decrease in the apoptotic and necrotic fractions (Figure 29C) were observed. These findings were confirmed by the upregulation of the anti-apoptotic protein BCL-XL (Figure S8A) in THP1 cells overexpressing CaSR. Further studies demonstrated that the production of reactive oxygen species (ROS) was affected by CaSR, and it was higher in the CaSR-overexpressing cells than in the wildtype counterparts (Figure 29D). Quantification of DNA damage (Nagelkerke and Span, 2016) by measurement of H2A.X phosphorylation (γH2A.X) using flow cytometry (Figure 29E) and analysis of DNA repair, determined by immunofluorescence (Figure 29F),

showed that in comparison with the wildtype THP1, overexpression of CaSR have an increases in their DNA damage. These cellular changes were accompanied by a possible loss of differentiation as previously described (Kumar et al., 2020; Vieira Torquato et al., 2017) and suggested by a significant decrease in the percentage of $CD11b^{+}$ myeloid cells (Figure 29G) and a reduced ability to phagocytose bacterial bioparticles (Figure 29H).

In sum, these results show that THP1 cells overexpressing CaSR have a distinct, cancer -promoting phenotype compared to wildtype cells. This demonstrates a more aggressive phenotype, complementing our *in vivo* studies.

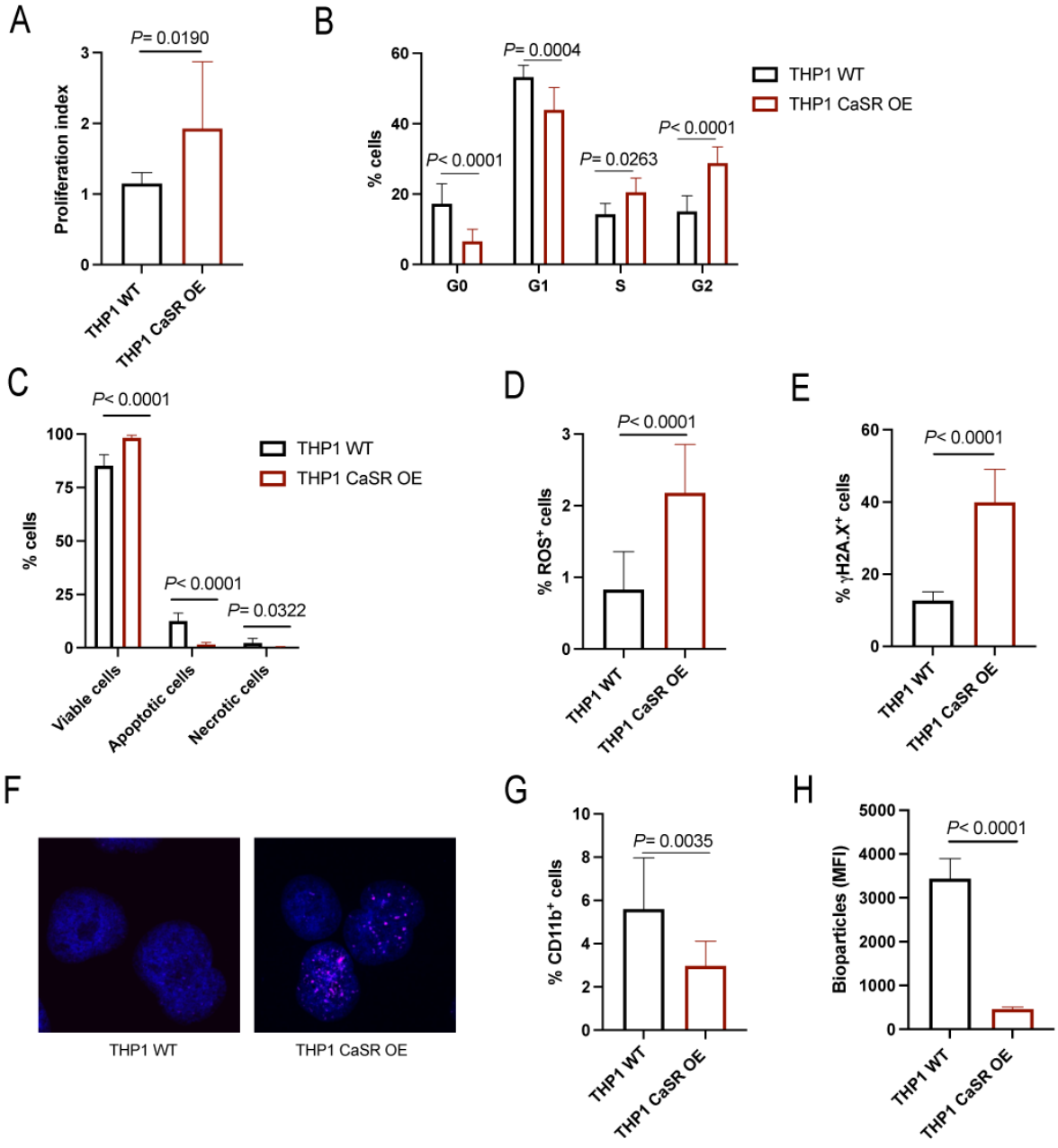

Figure 29. CaSR regulates proliferation, cell cycle, apoptosis, ROS production, differentiation and DNA damage in THP1 cells. A) Proliferation of THP1 WT (black) and THP1 CaSR OE (red) cells after 72 h of

culture, assessed by CFSE staining (n=4, *t*-test). B) Cell cycle analysis of THP1 WT (black) and THP1 CaSR OE (red) cells by Ki67 and DAPI staining (n=4, two-way ANOVA, Sidak test). C) Percentage of apoptotic THP1 WT (black) and THP1 CaSR OE (red) cells detected by annexin V staining (n=4, two-way ANOVA, Sidak test). D) Percentage of ROS^+ cells in THP1 WT (black) versus THP1 CaSR OE (red) cells determined by flow cytometry (n=4, *t*-test). E) Percentage of $\gamma H2A.X^+$ THP1 WT (black) and THP1 CaSR OE (red) cells by flow cytometry (n=3, *t*-test). F) Immunofluorescence (IF) staining of γH2A.X in THP1 WT (left) and THP1 CaSR OE (right) cells. DNA double strand breaks (DSBs) were detected by staining with γH2A.X and AF-647 (foci shown in magenta). Nuclear staining by DAPI is represented in blue. G) Percentage of $CD11b^+$ cells on THP1 WT (black) and THP1 CaSR OE (red) cells (n=5, *t*-test). H) Mean fluorescence intensity (MFI) of THP1 WT (black) and THP1 CaSR OE (red) cells positive for phagocytosed, phycoerythrin (PE)-conjugated pHrodo E.coli bioparticles (n=5, *t*-test).

5.9 CaSR overexpression activates MAPK and Wnt-β-catenin signaling pathways in THP1 cells

In order to characterize the contribution of CaSR to AML cell physiology and associated molecular mechanisms, the intrinsic cellular signal transduction pathways must be understood. CaSR is well known to modulate MAPK/ERK signaling in several cancers (Brennan et al., 2013; Chakravarti et al., 2012; Smith et al., 2016), and, indeed, proteomic analysis performed on Lin^- MLL-$AF9^+$ cells derived from BM of AML mice revealed significantly increased expression of Dusp3 (dual specificity phosphatase 3), a negative regulator of MAPK/ERK signaling, when CaSR was depleted (Figure S6A). Taking these data into consideration, we hypothesized that in AML CaSR signals through this pathway and, consequently, the phosphorylation of ERK1/2, the downstream component of MAPK/ERK, was tested (Figure 30A). The results showed that this pathway is indeed activated by CaSR, and our results demonstrate a significantly higher expression of pERK1/2 (Figure 30B) in THP1 cells overexpressing CaSR in comparison to wildtype cells. Supportive evidence of the activation of this pathway is provided by the upregulation of the expression of downstream targets of the transcription factor pERK1/2 in THP1 cells overexpressing CaSR and wildtype cells (Figure 30C).

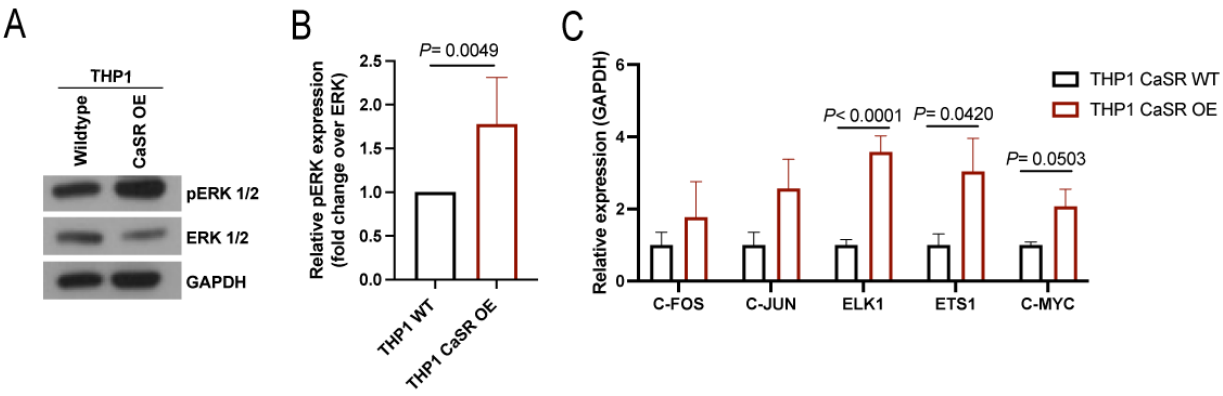

Figure 30. CaSR overexpression activates MAPK signaling in THP1 cells. A-B) Representative immunoblot analysis (A) and quantification (B) of ERK 1/2 (42, 44 kDa) and (pERK 1/2) (phospho ERK 1/2, thr 202/tyr 204) expression in extracts of THP1 WT and THP1 CaSR OE cells (n=6, *t*-test). C) Relative expression levels of some pERK 1/2 downstream targets, determined by RT-qPCR (n=9, *t*-test).

In addition to MAPK/ERK, CaSR has also been implicated in regulating Wnt-β-catenin signaling (Brennan et al., 2013; MacLeod, 2013; Rey et al., 2012). This pathway plays a major role in hematopoiesis and has been observed to be dysregulated in hematological malignancies such as AML (Staal et al., 2016). Hypothesizing that Wnt-β-catenin could be another mechanism underlying the aggressive phenotype mediated by CaSR, this pathway was tested. The results confirmed our hypothesis, and upregulation of β-catenin was indeed observed in cells overexpressing CaSR (Figure 31A). Additionally, CaSR overexpressing cells showed higher transcript levels of T cell factor 4 (TCF4), the nuclear interacting partner of β-catenin (Shin et al., 2017), than the wildtype (Figure 31B).

Considering that vitamin D receptor (VDR), along with CaSR, is also involved in calcium homeostasis and VDR is known to downregulate Wnt-β-catenin signaling (Shah et al., 2006b), we examined the expression of VDR. In addition to an activation of Wnt-β-catenin signaling in THP1 cells overexpressing CaSR, VDR expression was significantly lower (Figure 31C). Western blot studies further showed that expression of c-Myc (Figure 31D) and cyclin D1, (Figure 31E), downstream targets of both MAPK/ERK and Wnt-β-catenin signaling, was higher in THP1 -overexpressing cells compared to wildtype.

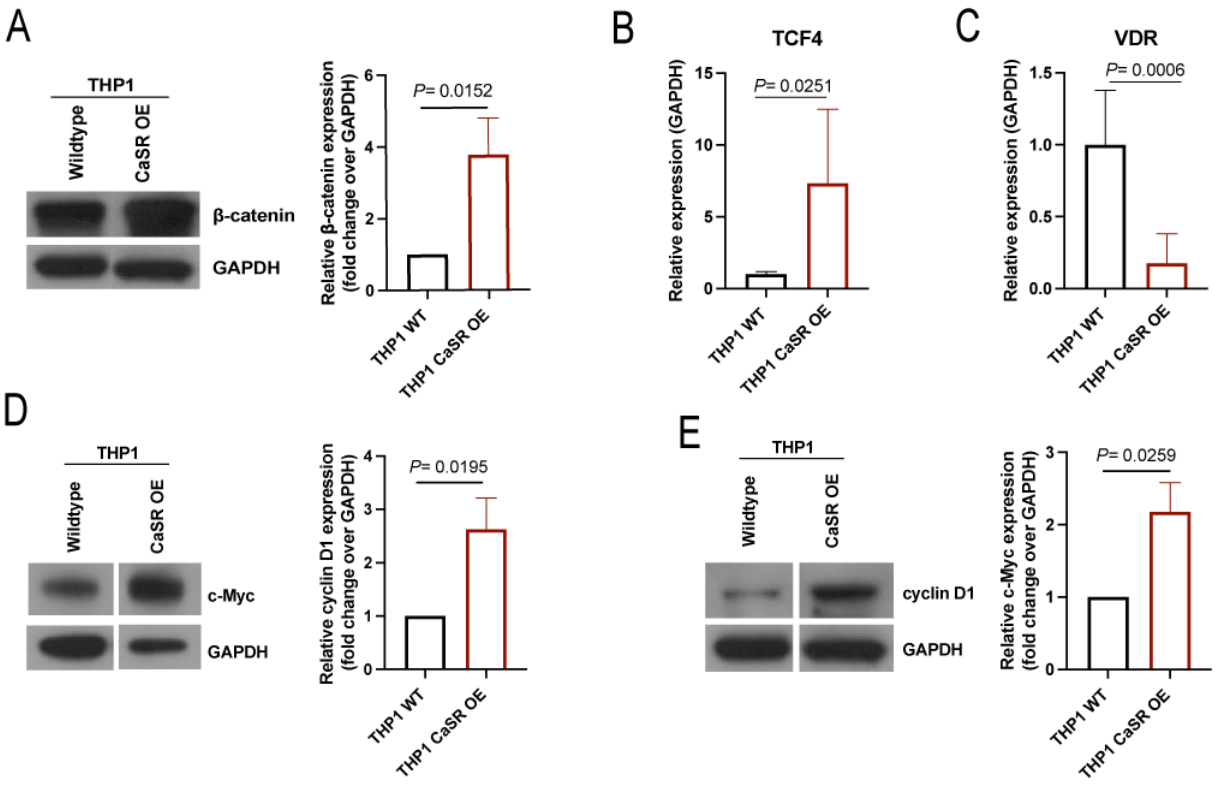

Figure 31. CaSR overexpression activates Wnt-β-catenin signaling in THP1 cells. A) Representative immunoblot analysis (left) and quantification (right) of β-catenin (92 kDa) (n=9, *t*-test) of THP1 WT and THP1 CaSR OE cells. B-C) Relative expression of *TCF4* (n=5, *t*-test) (B) and *VDR* (n=5, *t*-test) (C) by qRT-PCR analysis of non-transduced THP1 cells (WT, black) and THP1 cells overexpressing CaSR (THP1 CaSR OE). D-E) Representative immunoblot analysis (left) and quantification (right) of c-Myc (62 kDa) (n=4, *t*-test) (D) and cyclin D1 (34 kDa) (n=6, *t*-test) (E) using GAPDH (37 kDa) as loading control in extracts of THP1 WT and THP1 CaSR OE cells.

5.10 Intracellular calcium signaling may be reduced in CaSR -overexpressing cells

In addition to being a major regulator of extracellular calcium, CaSR has also been reported to regulate intracellular calcium signaling (Smith et al., 2016). To test that, the expression of a downstream target of active intracellular signaling, MEF2C, was tested, and the results showed that overexpression of CaSR in THP1 cells leads to a downregulation of *MEF2C* (Figure 32A). In order to further explore the intracellular calcium dynamics in THP1 cells, we performed calcium flux analysis as described previously (MacFarlane et al., 2010). Overexpression of CaSR resulted in a reduction of intracellular calcium (Figure 32B) at baseline (Figure 32C) in response to extracellular calcium (Figure 32D) and after addition of ionomycin (Figure 32E), which promotes calcium release from intracellular calcium storages into the cytoplasm, and reflects the maximum intracellular calcium in the cell. In order to further examine the intracellular calcium alterations, proteins related to endoplasmic reticulum (ER) stress, which

is a process that can be induced by alteration of calcium levels and can affect cell physiology, were tested in WT and THP1 CaSR OE cells. However, no CaSR -related differences were observed (Figure 32F to G).

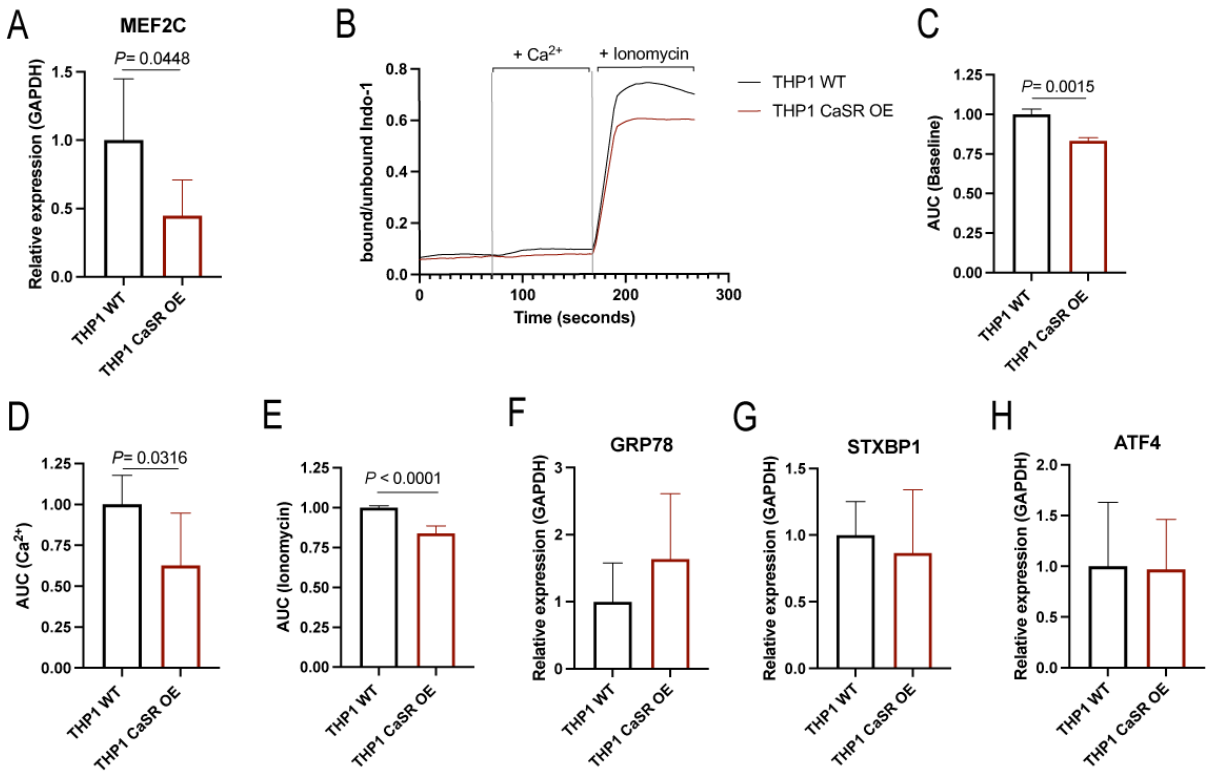

Figure 32. CaSR overexpression inhibits intracellular calcium in THP1 cells. A-B) Relative expression of *VDR* (n=6, *t*-test) (A) and *MEF2C* (n=5, *t*-test) as analyzed by qRT-PCR of wildtype THP1 cells (WT, black) and THP1 cells overexpressing CaSR (THP1 CaSR OE, red). C) Calcium flux analysis of THP1 wildtype (black) and THP1 CaSR -overexpressing cells (red) using Indo-1 dye (n=3). D-F) Calcium flux analysis represented by quantification of the area under the curve (AUC) at baseline (D), after addition of calcium (E) and after addition of ionomycin (F) (n=3, *t*-test). G-I) Relative expression of *GRP78* (n=5, *t*-test) (G), *STXBP1* (n=5, *t*-test) (H) and *ATF4* (n=4, *t*-test) by qRT-PCR analysis of THP1 wildtype (black) and THP1 CaSR OE (red).

5.11 CaSR signaling can be inhibited by the CaSR antagonist NPS-2143

To study the effects of CaSR inhibition in THP1 cells, a calcilytic agent and a specific CaSR antagonist termed NPS-2143 (Hannan et al., 2015; Lo Giudice et al., 2019) was used in our further studies. As a first experiment, the effect of NPS-2143 on cell death was assessed. We found that CaSR antagonism induced apoptosis in THP1 WT (Figure S6B) and THP1 CaSR OE (Figure S6C) cells in a concentration-dependent manner. Additionally, NPS-2143 treatment significantly reduced the protein levels (as assessed by immunoblot) of β-catenin (Figure 33A), cyclin D1 (Figure 33B) and c-myc (Figure 33C) in a dose-dependent manner in THP1 WT (Figure 33D) and THP1 CaSR OE (Figure 33E) cells.

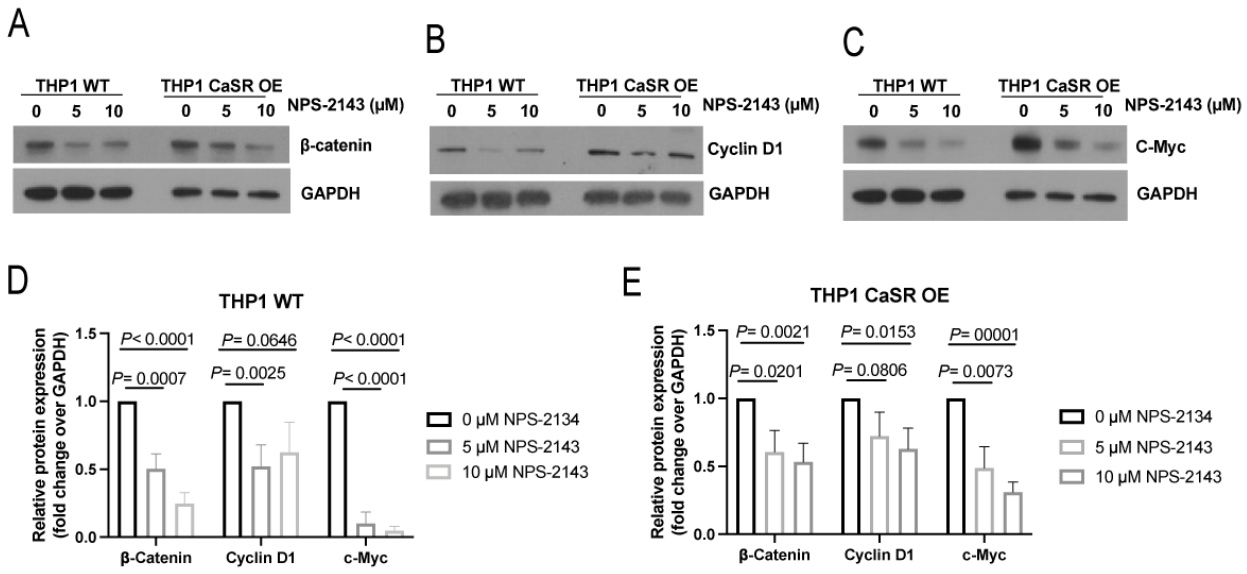

Figure 33. The CaSR antagonist NPS-2143 inhibits the activation of the Wnt-β-catenin signaling pathway in THP1 cells. A-C) Representative immunoblot analysis of the expression of β-catenin (92 kDa) (A), cyclin D1 (34 kDa) (B), c-myc (62 kDa) (C) and GAPDH (37 kDa) as loading control in cell lysates from THP1 WT and THP1 CaSR OE cells after treatment with NPS-2143 (0-10 μM, 4 h). D-E) Quantification of the immunoblot analysis of the indicated proteins in THP1 WT (D) and THP1 CaSR OE cells (E) normalized to GAPDH (n=3-7, two-way ANOVA, Tukey test).

5.12 The CaSR-interacting protein FLNA influences leukemia progression

Several studies have reported the interaction between CaSR and filamin A (FLNA) in a variety of tissues. However, so far, no information regarding a co-involvement of these two proteins in hematological or leukemia cells has been addressed. As we saw a strong indication for the role of CaSR in AML cell physiology and during AML progression, we hypothesized that there could be a possible interaction between CaSR and FLNA, and CaSR might regulate FLNA expression in leukemia. Hence, the expression of FLNA was investigated in THP1 cells. In accordance with the hypothesis, THP1 cells overexpressing CaSR demonstrated higher FLNA levels than THP1 wildtype cells, both on a transcriptional (Figure S8B) and a translational (Figure 34A and B) level.

Evaluating a possible physical interaction between these two proteins, a co-immunoprecipitation (co-IP) assay was performed in the leukemia cells K562 and THP1. Interestingly, the interaction was observed in both cell lines, and in the FLNA pull-down fraction it was possible to detect CaSR (Figure 34C). Furthermore, immunofluorescence (IF) studies revealed a clear colocalization of CaSR and FLNA in AML cells, both in primary AML cells (Figure 34D) and THP1 cells (Figure 34E).

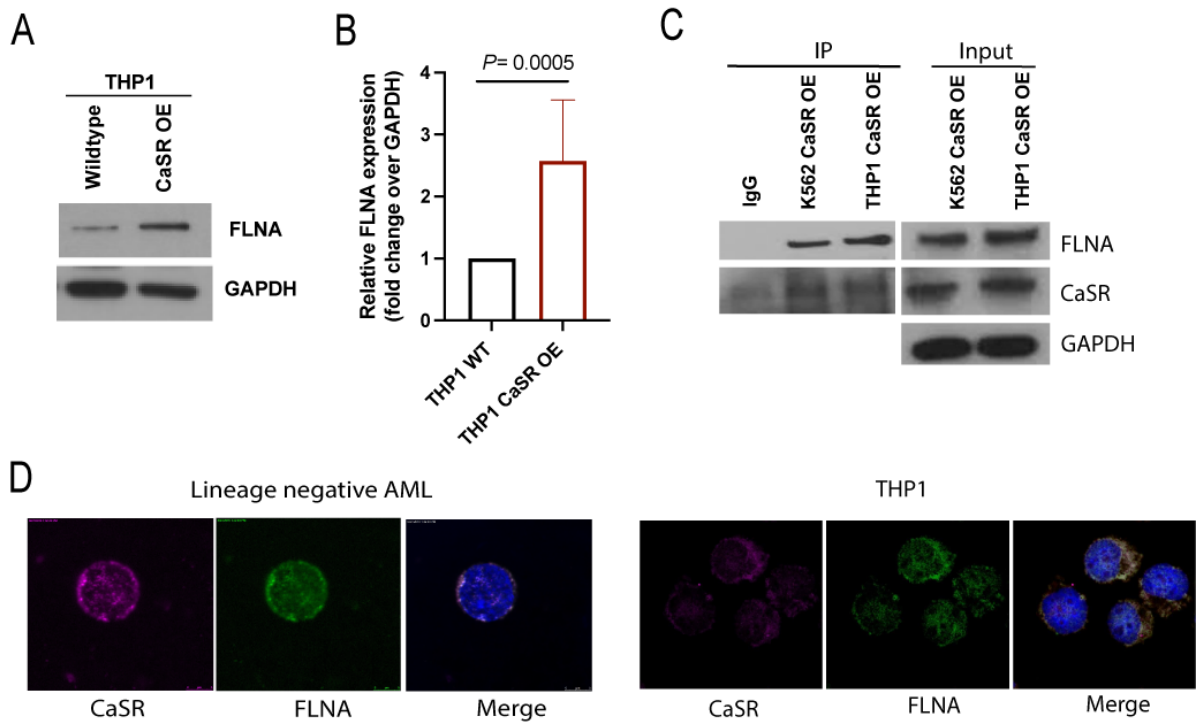

Figure 34. CaSR interacts with filamin A (FLNA). A-B) Representative immunoblot analysis (A) and quantification (B) of the expression of FLNA (280 kDa) and GAPDH (37 kDa) as loading control in extracts of THP1 WT and THP1 CaSR OE cells (n=7, *t*-test). C) Immunoblot for CaSR (121 kDa) and FLNA (280 kDa) in lysates of K562 and THP1 cells overexpressing CaSR, in which an anti-FLNA antibody was used to co-immunoprecipitate CaSR. The input is shown on the right, and GAPDH (37 kDa) was used as loading control. D-E) Immunofluorescence staining for CaSR and FLNA in sorted Lin^- MLL-$AF9^+$ cells from WT AML mice, sacrificed on day 40 after transplantation (left), and in THP1 WT cells (right). The images are representative of three independent experiments.

To test if, similar to CaSR, FLNA may influence AML cell physiology, a FLNA knock-out cell line was generated. By using the CRISPR-Cas9 strategy, *FLNA* was depleted in THP1 cells. A transformed non-targeted guide RNA was used as a control (NTC) (Figure S7A). Strikingly, the THP1 cells had significantly reduced proliferative capacity when FLNA was depleted (Figure 35A) and a consistently reduced percentage of cells in S-phase, as well as arrest in the G1 phase of the cell cycle (Figure 35B) compared to control. However, depletion of FLNA in THP1 cells did not induce apoptosis (Figure S7B).

Considering that filamin has been shown to interact with CXCR4 (Gómez-Moutón et al., 2015), the migration capacity in response to the potent chemoattractant CXCL-12 was assessed using a transwell system. This showed that FLNA is important for migration of THP1 cells (Figure 35C). Assessing a potential physical interaction between FLNA and CXCR4, a co-IP assay was performed in the leukemia cells K562 and THP1 (Figure 35D). This showed that in the tested leukemia cells CXCR4 and FLNA interact.

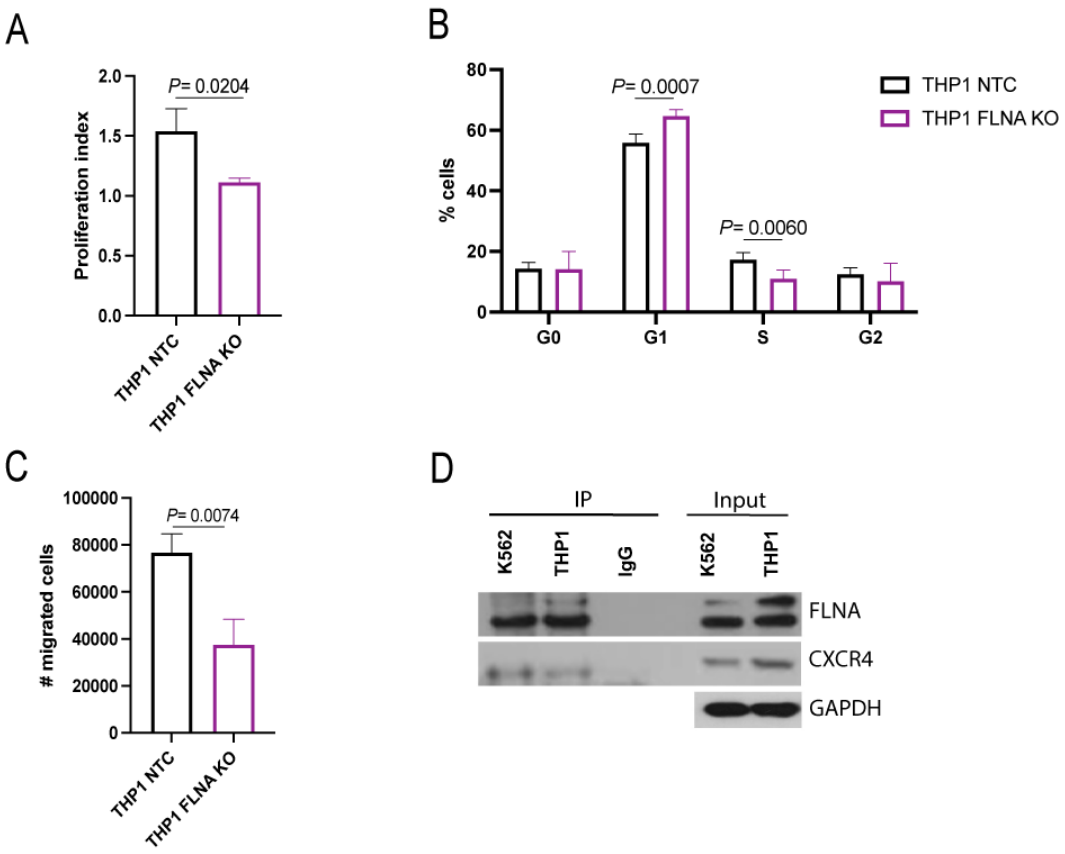

Figure 35. FLNA regulates proliferation, cell cycle and migration of THP1 cells. A) Proliferation of THP1 NTC (black) and THP1 FLNA KO (pink) cells after 72 h of culture, assessed by CFSE staining (n=4, *t*-test). B) Cell cycle analysis by ki-67 and DAPI staining of THP1 NTC (black) and THP1 FLNA KO (pink) cells (n=5, two-way ANOVA, Sidak test). C) Number of migrated THP1 NTC and THP1 FLNA KO cells towards CXCL-12 within 2 h (n=3, *t*-test). D) Immunoblot for CXCR4 (40 kDa) and FLNA (280 kDa) in lysates of K562 and THP1 cells, in which an anti-FLNA antibody was used to co-immunoprecipitate CXCR4. The input is shown on the right, and GAPDH (37 kDa) was used as loading control.

To further examine the role of FLNA in the human setting, we first analyzed the mRNA levels in human AML cells using the bloodspot database. Strikingly, we observed that the mRNA level in AML cells was significantly higher than in normal BM cells (Figure 36A). To investigate the clinical relevance of FLNA expression in AML, we examined its relationship with patient prognosis, as provided by the TCGA database. As our murine experiments predicted, also in humans the FLNA level is negatively correlated with overall survival of AML patients, suggesting that it may play an important role in leukemogenesis (Figure 36B).

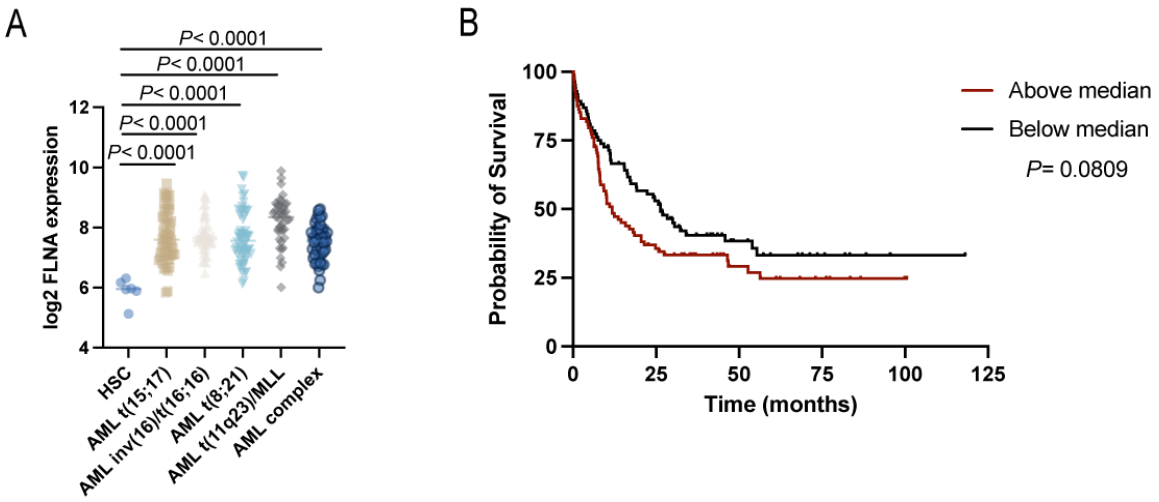

Figure 36. FLNA may influence leukemia progression in human AML patients. A) Log2 expression of *FLNA* in BM cells from healthy individuals (n= 6), patients with AML t(15;17) (n= 54), AML inv(16)/t(16;16) (n= 47), AML t(8;21) (n= 60), AML t(11q23)/MLL (n= 43) or AML with complex karyotype (n= 46) (ANOVA, Tukey test), taken from the Bloodspot database. B) Kaplan-Meier-style survival of patients with AML with high (n= 89) or low (n= 84) expression of *FLNA*. The curves were generated using the publicly available dataset, accessed *via* the *cBioPortal For Cancer Genomics* portal (Log-rank test).

To understand if FLNA may interfere with leukemia progression, THP1 NTC and THP1 FLNA KO cells were transplanted into immunodeficient, NOD SCID interleukin-2 receptor γ knockout (NSG) mice. We observed that the mice receiving THP1 FLNA KO cells showed a reduction in leukemia cell frequency (human $CD45^+$) in the peripheral blood (Figure 37A) and a notable delay in leukemia development, with a significant prolongation of overall survival of mice (Figure 37B) compared to mice receiving control cells. Remarkably, all mice transplanted with the control THP1 cells died of infiltration of different organs by malignant cells, while mice receiving THP1 FLNA KO cells developed enlarged lymph nodes and eventually became paralyzed. As proof of principle, leukemia-infiltrated tissues (kidney and lymph nodes) were analyzed in the transplanted mice at the time of death, and FLNA depletion was proven for the transplanted mice (Figure 37C).

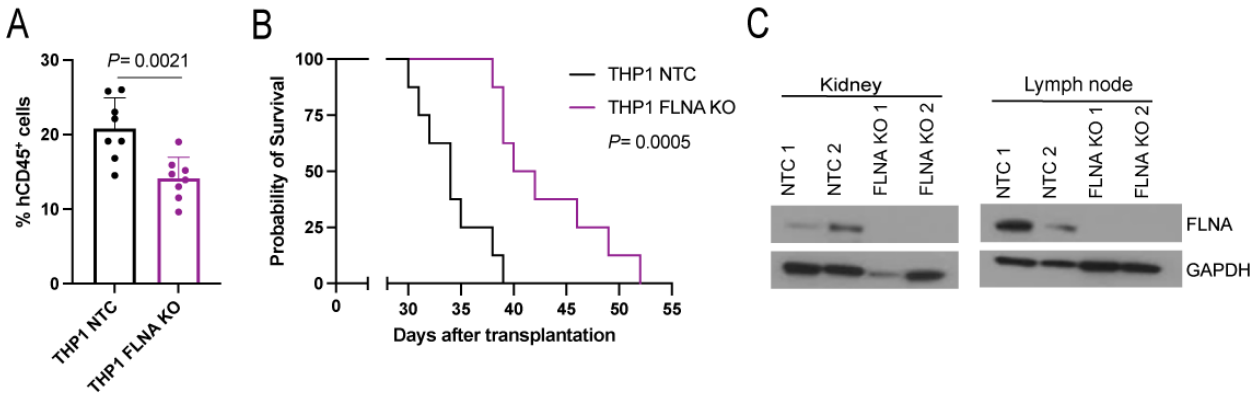

Figure 37. Deletion of FLNA in THP1 cells prolongs AML survival *in vivo*. A) Percentage of human CD45⁺ leukocytes in the peripheral blood of NOD SCID interleukin-2 receptor γ knockout (NSG) mice transplanted with 1x10^6 THP1 NTC (non-target control) or THP1 FLNA KO cells (n=8, *t*-test), 21 days post transplantation. B) Kaplan-Meier-style survival of NSG recipient mice transplanted with THP1 NTC (black) or THP1 FLNA KO (pink) cells (n=8, Log-rank test). C) Immunoblot showing the expression of FLNA (280 kDa) and GAPDH (37 kDa) in lysates of kidney and lymph nodes isolated from moribund mice transplanted with either THP1 NTC or THP1 FLNA KO cells. Each column represents a single mouse.

5.13 The CaSR antagonist NPS-2143 is effective in targeting AML *in vivo*

In order to test, whether the blockade of CaSR signaling can inhibit AML development, we evaluated the potential therapeutic effect of the CaSR-specific antagonist NPS-2143 *in vivo*.

As a first experiment, using the retroviral transduction/ transplantation model of MLL-AF9 driven AML, recipient mice of wildtype BM were randomized into 2 cohorts and treated with either vehicle (saline solution) or NPS-2143 (1 mg/kg), starting on day 19 (Figure 38A) after transplantation, e.g., after establishment of the disease. Treatment with NPS-2143 led to a significant reduction in the number of leukocytes (Figure 38B) and a strong trend towards an extended overall survival of the mice (Figure 38C).

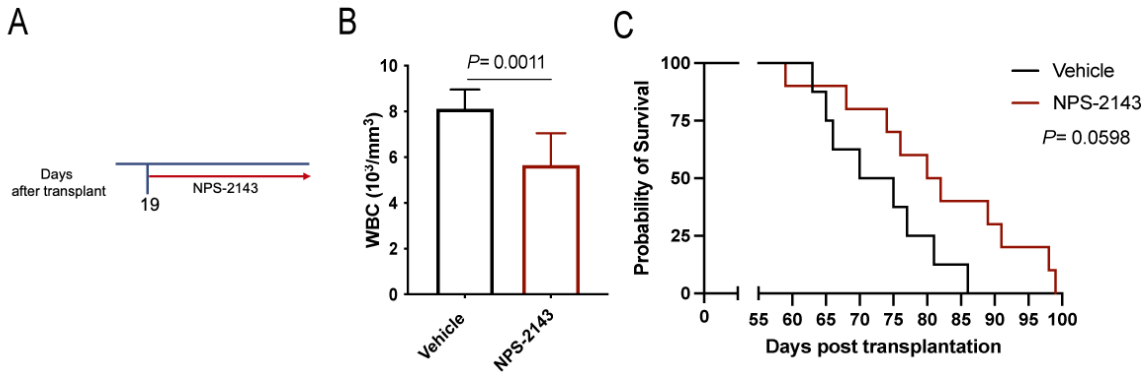

Figure 38. NPS-2143 treatment may lead to a prolongation of survival in mice with AML. A) Treatment scheme for wildtype murine recipients with MLL-AF9 -induced AML treated with vehicle (PBS) or NPS-2143 (1 mg/kg). Treatment was performed every day, starting on day 19 after transplantation. B) Leukocyte count (WBC) x 10^3/µl in peripheral blood of mice with MLL-AF9 -induced AML treated with vehicle or NPS-2143 forty-four days after transplantation (n=8-10, ANOVA, Tukey test). C) Kaplan-Meier-style survival curve of recipient mice with MLL-AF9 -driven AML treated with vehicle (black) or NPS-2143 (red) (n=8-10, Log-rank test).

Hypothesizing that treatment with NPS-2143 may be beneficial in combination with the standard of care, namely cytarabine (ara-C), an AML transplantation experiment was performed, whereby mice were divided into 4 treatment groups: vehicle, NPS-2143, ara-C and the combination of both, NPS-2143 and ara-C, as shown in Figure 39A. Due to the absence of side effects in the mice treated with NPS-2143 in the first treatment experiment (Figure 38) and as we aimed at a stronger effect on disease progression in the treated mice, the NPS-2143 dose was increased to 2 mg/kg. Treatment of mice with ara-C or the combination of ara-C with NPS-2143 showed a significant reduction in the number of leukocytes (Figure 39A) and a reduction in the number of MLL-AF9$^+$ Gr1$^+$ myeloid cells (Figure 39B) in the peripheral blood compared with vehicle-treated mice. Interestingly, the combination treatment of ara-C with NPS-2143 led to a significant reduction in tumor burden compared with mice treated with ara-C alone (Figure 39A and B). Strikingly and resembling the CaSR KO in LIC (Figures 19 and 20), wildtype murine recipients with MLL-AF9 -induced AML treated with NPS-2143 alone had significantly prolonged survival in comparison to the vehicle-treated mice. As expected, also the ara-C -treated mice showed extended overall survival in comparison with the vehicle-treated cohort. However, and most interestingly, the combination treatment of ara-C with NPS-2143 led to significant prolongation of survival compared to vehicle or ara-C alone (Figure 39C) suggesting a possible additive effect of the two therapies.

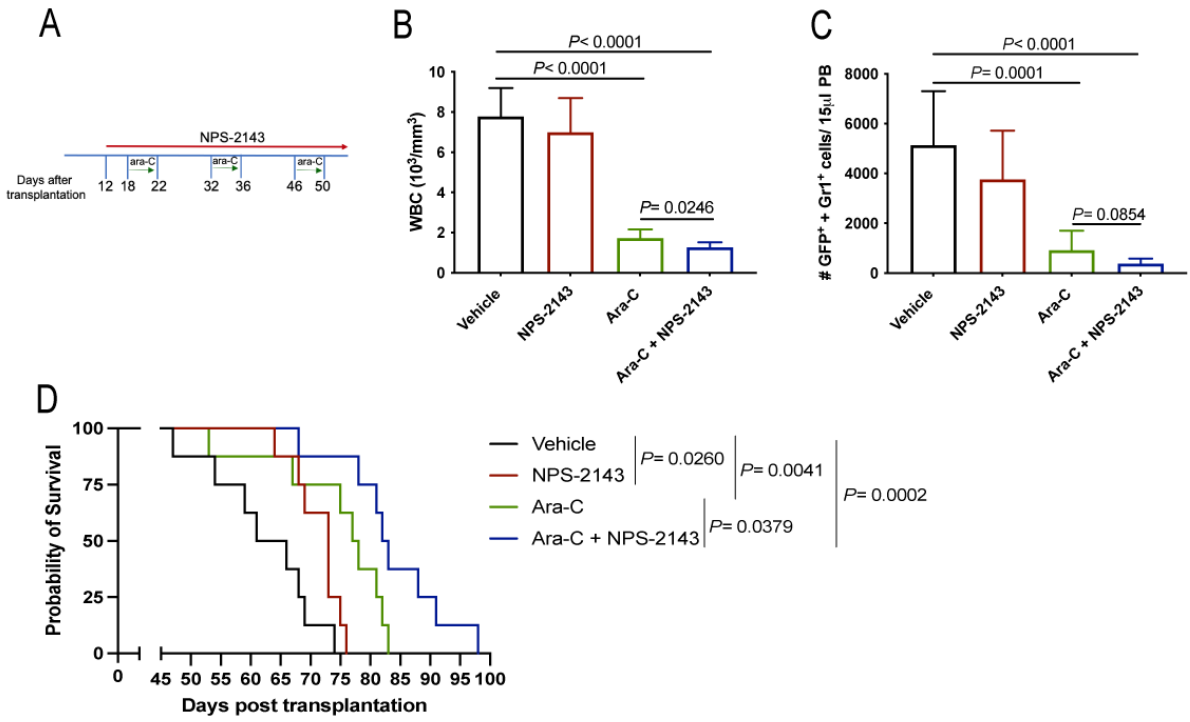

Figure 39. Treatment of syngeneic mice with AML with NPS-2143 leads to a prolongation of survival. A) Schematic representation for wildtype murine recipients with MLL-AF9-induced AML treated with vehicle (PBS), NPS-2143 (2 mg/kg), ara-C (cytarabine, 50 mg/kg) and the combination of both, NPS-2143 and ara-C. Treatment started 12 days after transplantation. B-C) Leukocyte count (WBC) x 10^3/µl (A) and number of GFP$^+$ (MLL-AF9$^+$) Gr1$^+$ cells/15 µl (B) peripheral blood in treated mice with MLL-AF9-induced AML (n=8, ANOVA, Tukey test), twenty-five days post transplantation. D) Kaplan-Meier-style survival curve of recipient mice with MLL-AF9-induced AML treated with vehicle (black), NPS-2143 (red), ara-C (green) and the combination of both NPS-2143 and ara-C (blue) (n=8, Log-rank test).

Considering the role of CaSR for AML stemness and self-renewal capacity (Figures 23 and 24), the possible effects of NPS-2143 for the maintenance and function of leukemia progenitor and leukemia stem cells were assessed in a secondary transplantation experiment. BM cells from mice in the different treatment groups were transplanted into untreated, irradiated secondary recipient mice. Expectedly, secondary mice receiving bone marrow cells from primary mice treated with the combination of ara-C and NPS-2143 showed a significant reduction in the number of leukocytes (Figure 40A) and in the percentage of MLL-AF9$^+$ Gr1$^+$ myeloid cells (Figure 40B) in peripheral blood in comparison with mice receiving BM from mice with AML treated with vehicle or ara-C. Consistent with the reduced tumor burden, secondary recipients of AML cells from primary mice treated with the combination treatment had significantly prolonged survival prolongation compared with mice receiving BM from mice with AML treated with ara-C alone (Figure 40C). Unexpectedly, mice receiving BM from mice with AML treated with NPS-2143 and ara-C alone did not show any survival benefit in comparison

with the secondary mice receiving BM from vehicle -treated primary mice with AML, with a trend towards more aggressive disease.

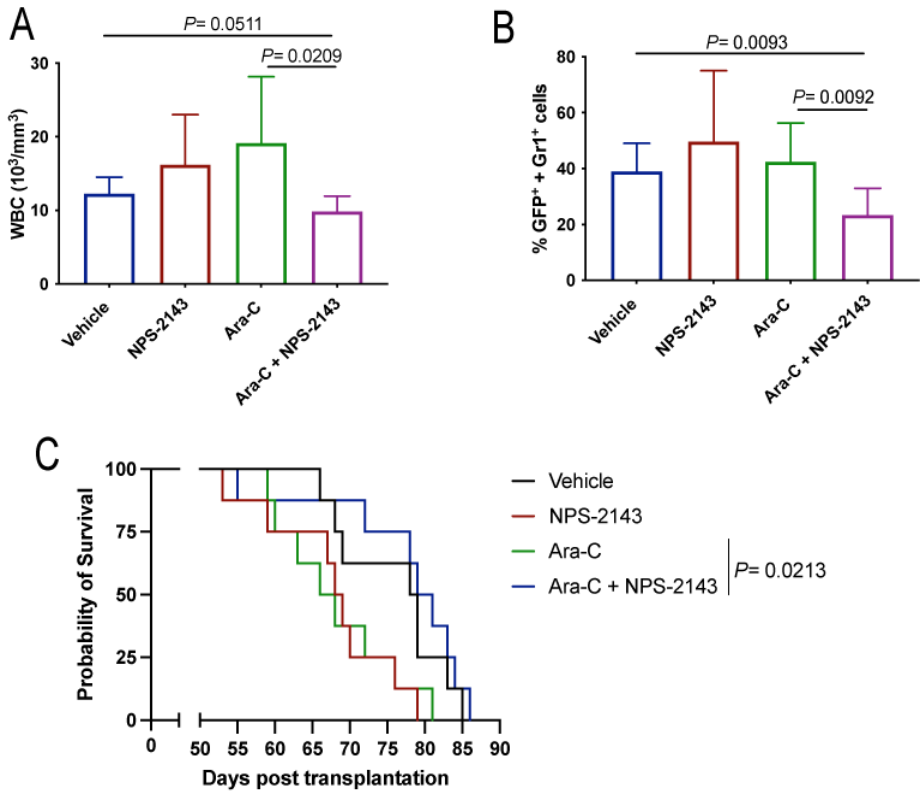

Figure 40. Transplantation of BM cells from mice with AML treated with NPS-2143 in combination with ara-C leads to a survival benefit in secondary recipient mice. A-B) Leukocyte count (WBC) x 10^3/µl (A) and percentage of GFP^+ ($MLL\text{-}AF9^+$) $Gr1^+$ cells (B) in peripheral blood of secondary recipient mice transplanted with BM derived from mice with MLL-AF9+ AML (n=8, ANOVA, Tukey test), fifty-four days after transplantation. C) Kaplan-Meier-style survival curve of untreated secondary recipient mice of BM from mice with AML treated with vehicle (black), NPS-2143 (red), ara-C (green) and the combination of both NPS-2143 and ara-C (blue) (n=8, Log-rank test).

In order to test whether our murine findings may be transferrable to human malignancies, similar to FLNA, we analyzed publicly available datasets. We found that CaSR has a much greater expression in the unsorted BM cells of AML patients than in healthy BM (Figure 41A), complementing our findings.

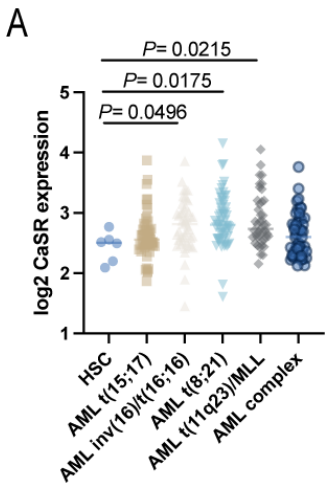

Figure 41. CaSR is highly expressed on whole BM cells of human AML patients. A) Log2 expression of *CaSR* in unsorted BM cells from healthy individuals (n= 6), patients with AML t(15;17) (n= 54), AML inv(16)/t(16;16) (n= 47), AML t(8;21) (n= 60), AML t(11q23)/MLL (n= 43) or AML with complex karyotype (n= 46) (ANOVA, Tukey test), taken from the Bloodspot database.

Considering that CaSR is highly expressed on human AML cells, we observed an impact of NPS-2143 on human THP1 cells (Figure 33) and that NPS-2143 prolonged survival *in vivo* (Figure 39), we tested the effect of inhibition of CaSR in a xenotransplantation experiment using primary human samples from AML patients, which we transplanted into NSG mice. The mice were then treated as shown in the schematic (Figure 40A). Similar to the syngeneic model (Figure 39), the mice were treated with vehicle, ara-C or the combination of ara-C with NPS-2143. The treatment was started 12 days post transplantation (Figure 42A), when human cells were detectable in the peripheral blood of the recipient mice (Figure S9A and B). The disease progression was followed by flow cytometry of leukocytes in the peripheral blood of the transplanted mice using antibodies to human CD45 and CD33, which are expressed on human AML blasts. Indeed, in the cohort of mice treated with the combination of ara-C with NPS-2143 there was a trend towards a reduction of the percentage of human $CD45^+$ (Figure 42B) and $CD33^+$ (Figure 42C) cells, when compared to mice treated with ara-C alone. Consistently, these differences also led to a trend towards survival prolongation of mice treated with the combination of ara-C and NPS-2143 in comparison with ara-C -treated mice. Furthermore, unlike ara-C alone, the double treatment significantly prolonged the survival of mice compared to the vehicle -treated group (Figure 42D).

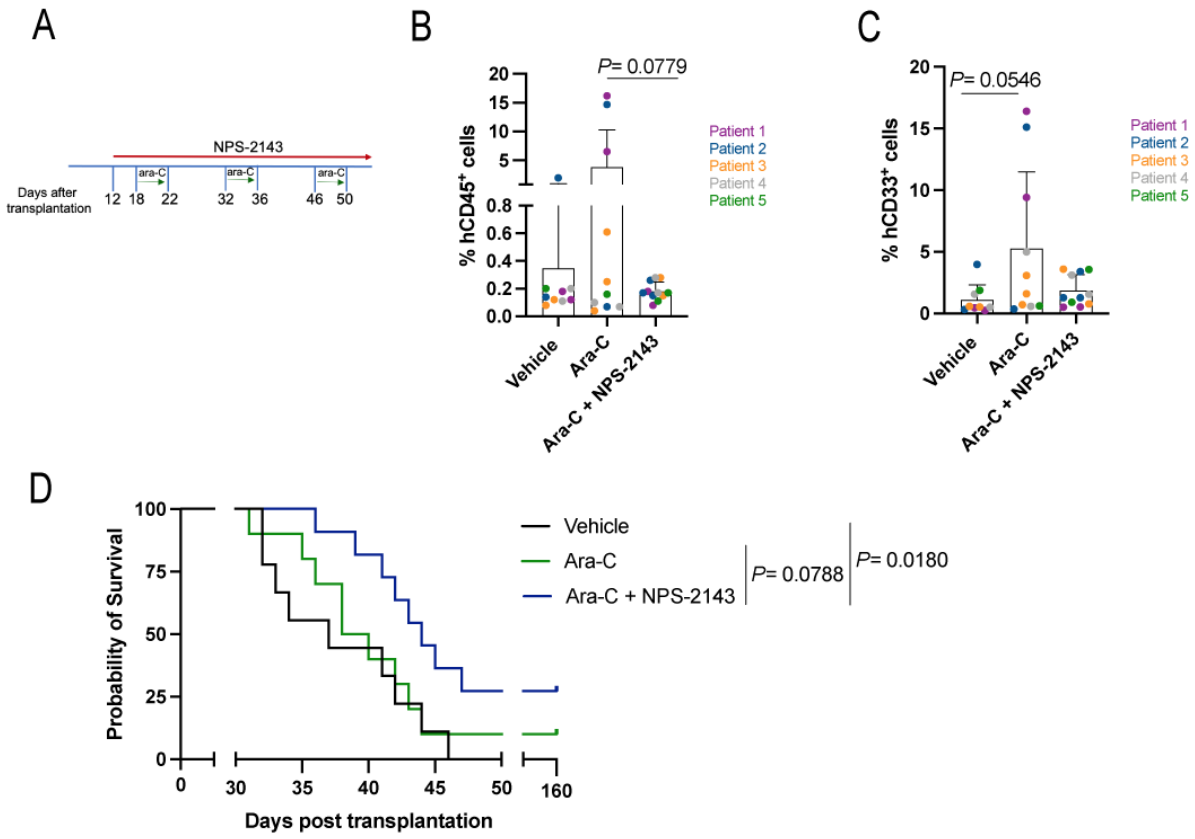

Figure 42. The combination treatment of NPS-2143 with ara-C leads to prolongation of survival in NSG mice transplanted with human AML cells. A) Treatment scheme for NOD SCID interleukin-2 receptor γ knockout (NSG) mice transplanted with 2x10^6 BM cells derived from 5 patients suffering from AML. Each sample was transplanted into 4-7 mice, whereby cohorts of mice were treated with vehicle, ara-c (50 mg/kg) or the combination of ara-C (50 mg/kg) and NPS-2143 (2 mg/kg). Treatment started on day 12 after transplantation. B-C) Percentage of human CD45$^+$ (B) and CD33$^+$ (C) leukocytes in peripheral blood of NSG mice transplanted with human AML cells and treated with vehicle (n=9), ara-C (n=10) or the combination of ara-C and NPS-2143 (n=11), thirty days post transplantation. Recipients of the same human AML sample are indicated by the same color (ANOVA, Tukey test). C) Kaplan-Meier-style survival curve of NSG mice transplanted with human AML cells and treated with vehicle (black), ara-C (green) or the combination of ara-C and NPS-2143 (blue) (n=9-11, Log-rank test).

AML is a heterogenous disease, harboring different types of mutations. Importantly, when the survival of treated mice transplanted with human AML cells, from patients harboring different mutations (Figure S9C) were analyzed separately, it was possible to observe differences in the response to the treatment (Figure 43A to E). In line with the increased CaSR expression in the BM of AML patients compared with healthy controls (Figure 41), a moderate correlation between CaSR expression and percentage of human AML cells (hCD45$^+$) in the peripheral blood of the xenograft mice was observed, which, however, reached significance (Figure 43F).

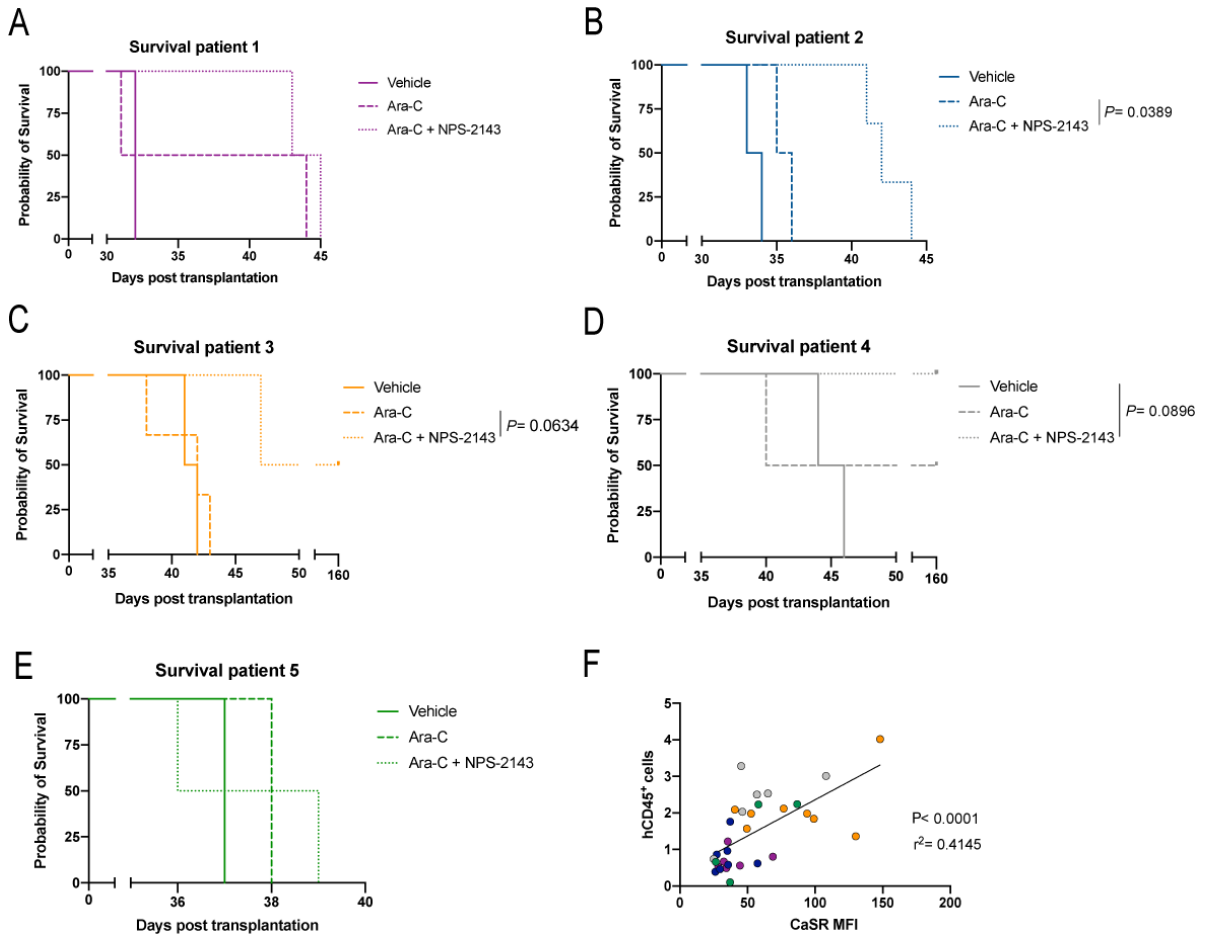

Figure 43. The treatment of NPS-2143 with ara-C leads to prolongation of survival in NSG mice transplanted with AML cells from different patients. A-E) Kaplan-Meier-style survival curve of NSG mice transplanted with human AML cells and treated with vehicle (solid line), ara-C (dashed line) or the combination of ara-C and NPS-2143 (dotted line). Recipients of the same human AML sample are indicated by the same color: patient 1 in pink (A) (n=6), patient 2 in blue (B) (n=7), patient 3 in yellow (C) (n=7), patient 4 in grey (D) (n=6) and patient 5 in green (E) (n=5) (Log-rank test). F) Correlation of human $CD45^+$ cells and median fluorescence intensity (MFI) of CaSR on peripheral blood leukocytes of NSG mice transplanted with human AML cells, 17 days after transplantation. Pearson's correlation coefficient (r) and p-value are shown.

5.14 The CaSR agonist cinacalcet might be effective in the treatment of CML

Based on our data, CaSR seems to work as a tumor suppressor in CML (Figure 17). Therefore, we hypothesized that a CaSR agonist may target CML cells. To test that, a CaSR agonist named cinacalcet (Sensipar, Mimpara) was used in our retroviral transplantation model of CML. Cincalcet is an approved drug used for the treatment of chronic kidney disease, secondary hyperparathyroidism and hypercalcemia in patients with parathyroid cancer (Dillon and Frazee, 2011; Warady et al., 2020). Similar to AML (Figure 39), the CaSR agonist was used in combination with the standard CML therapy, and four treatment cohorts were created: vehicle, cinacalcet, imatinib and the combination of imatinib with cinacalcet, following the scheme shown in Figure 43A. The tyrosine kinase inhibitor imatinib is standard of care for

patients with CML. Treatment of murine recipients with CML with a combination of imatinib and cinacalcet resulted in a trend towards a reduced leukocyte count (Figure 43B), as well as a reduction in the number of BCR-ABL1$^+$ CD11b$^+$ myeloid cells (Figure 43C) compared to vehicle-treated mice. In terms of overall survival, mice given the combination of cinacalcet and imatinib lived significantly longer than mice given vehicle. Surprisingly, treatment of mice with cinacalcet alone did not lead to a survival advantage, and imatinib alone did not significantly prolong the survival of mice in relation to vehicle-treated mice (Figure 43D). All the mice represented in the survival curve developed CML and died of pulmonary infiltration by malignant myeloid cells, as described previously in this retroviral transplantation model (Krause et al., 2014).

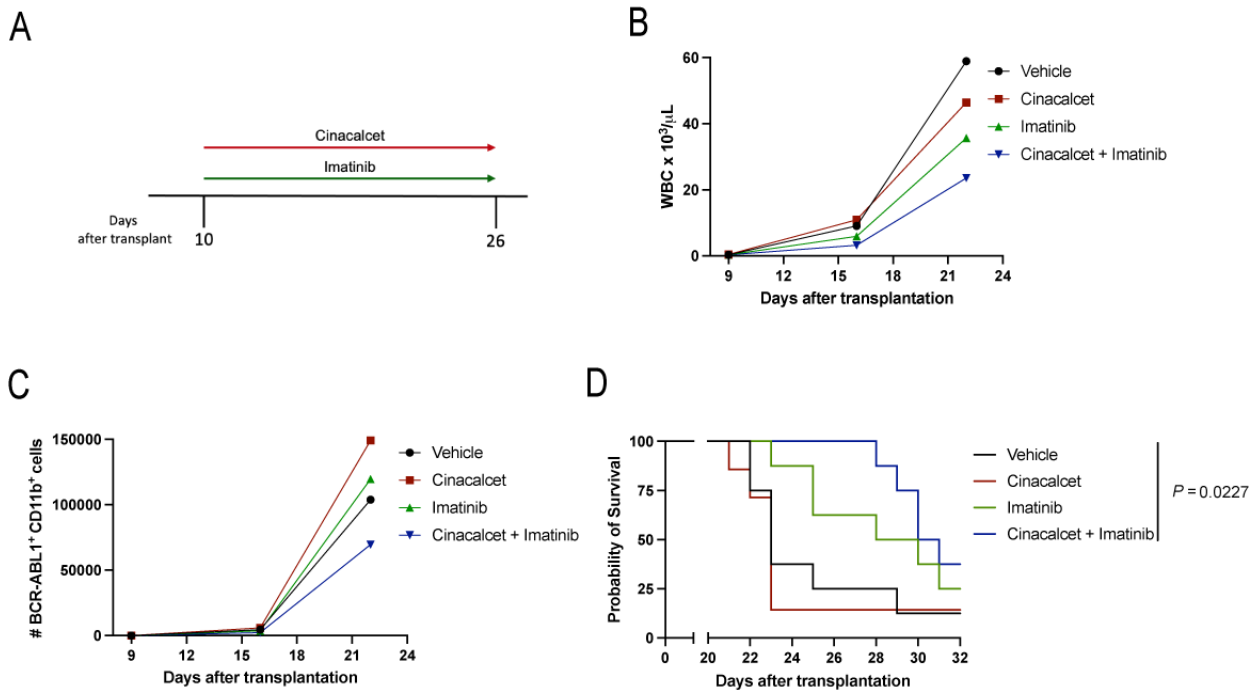

Figure 44. Treatment of syngeneic mice with CML with Cinacalcet in combination with Imatinib leads to a prolongation of survival.A) Treatment scheme for wildtype mice with BCR-ABL1-induced CML. Mice were randomly assigned to 4 cohorts and treated with vehicle (water), cinacalcet (30 mg/kg), imatinib (100 mg/kg) or the combination of both cinacalcet and imatinib. Treatment started 10 days after transplantation. B-C) Leukocytes (WBC) x 10^3/µl (A) and number of BCR-ABL1$^+$ Gr1$^+$ cells/15 µl (B) in peripheral blood of mice with BCR-ABL1-induced CML and treatment as in A) on days 9, 16 and 22 after transplantation (n=7-8). D) Kaplan-Meier-style survival curve of mice with CML treated with vehicle (black), cinacalcet (red), imatinib (green) or the combination of both cinacalcet and imatinib (blue) (n=7-8, Log-rank test).

6 Discussion

Calcium is a mineral that is important for the correct functioning of the human body. It has been identified as a universal signaling molecule that is intimately engaged in a variety of physiological functions, such as brain networks, muscular contraction, cell development, and cell migration (Berridge et al., 2000). Intracellular calcium signaling is also one of the most extensively studied cellular mechanisms. However, extracellular calcium (eCa^{2+}) and its associated signaling as well as its impact on cellular physiology, on the other hand, has received far less attention. The bone serves as a calcium reservoir and a location of continuous calcium turnover, with eCa^{2+} levels beneath a resorbing osteoclast reaching 40 mM, which is 20 times greater than serum calcium concentrations (Silver et al., 1988). During bone remodeling, through the process of bone formation by osteoblasts and bone resorption by osteoclasts, calcium ions are released from the osseous tissue into the bone marrow (Rowe et al., 2020). In this work we revealed that these calcium ions can influence leukemia cell behavior.

Calcium is an important component of the leukemic BMM

First, we demonstrated, using *in vivo* imaging of mice transplanted with cells expressing a genetically encoded calcium indicator (GCaMP6s), that a calcium gradient exists inside the bone marrow, with a higher concentration near the endosteum, where bone remodeling occurs, and a gradual decrease towards the center of the BM (Figure 12). We then showed, that the level of calcium in the BM differed between different leukemias, with the calcium concentration in mice with AML being higher than in other leukemias, particularly CML (Figure 13A). We were able to extend these findings to the human setting as well, where also a greater calcium concentration was revealed in the BM of AML patients compared to patients with other hematological malignancies (Figure 13B). Additional and likewise to the calcium concentration, CaSR, the extracellular calcium sensor and regulator, showed to also be expressed at a greater level on AML cells than CML cells (Figure 14A). These differences in expression of CaSR and the influence of the calcium concentration between AML and CML were further emphasized when we exposed leukemia cells to exogenous calcium. And also when we treated THP1 cells, a model for AML, with calcium, CaSR expression increased in a dose-dependent manner, while there were no differences in K562, a model for CML. Additionally, the calcium-treated THP1 cells showed a dose-dependent increase in adhesion to the ECM protein fibronectin, as well as migration toward CXCL-12 and CXCR4 (Figure 15), while the K562 cells showed no change (Figure 16).

These findings suggest that BM niche and leukemia-niche interactions in AML are substantially different from those in CML, with our data demonstrating a marked difference in calcium ion concentration as well as leukemia cell activity. Besides intrinsic differences in leukemia cells, differential interactions of leukemia cells with components of the BMM might contribute to these disparities. This aligns with recent studies showing that AML and CML may impact osteoblast differentiation in opposite ways: An enrichment of mature osteoblasts was reported in a model of CML (Schepers et al., 2013), whereas a significant reduction was observed in the MLL-AF9^{+} AML model (Battula et al., 2017; Hanoun et al., 2014) and a BCR-ABL1^{+} CML blast crisis model, which resembled acute leukemia (Frisch et al., 2012). Discrepancies between these myeloid leukemias were also demonstrated by Krause *et al.*, proving that increased bone remodeling *via* PTH activation promotes AML leukemic development while inhibiting CML progression (Krause et al., 2013).

Furthermore, our study found that AML and CML cells respond differently to calcium exposure, with AML cells exhibiting a significant regulation of cellular processes and pathways, whereas CML cells remained mostly unaltered. The observed increased calcium levels in the AML niche could be the result of deficient mineralization and lack of terminally differentiated osteoblasts, as recently demonstrated (Battula et al., 2017). An imbalance between osteoblast and osteoclasts may promote bone degradation with a consequent rise on calcium release. This high calcium concentration in the BMM may activate the CaSR on leukemia cells and, similar to its role in breast cancer cells (Saidak et al., 2009), promoting cancer cell adhesion and migration.

Such an involvement of calcium and CaSR in cell adhesion and migration was already observed in several different malignancies. CaSR has been shown to form complexes with integrin molecules, particularly integrin β3 (Itgb3), and CaSR-mediated activation of integrins facilitates cell migration (Tharmalingam and Hampson, 2016). Numerous reports have provided important evidence that integrin-ligand interactions are dependent on divalent ions (Mould et al., 1995), that cell-cell contacts in epithelial cells are formed upon calcium stimulation (Perez-Moreno et al., 2003) and that CaSR is important for E-cadherin mediated cell adhesion in epidermal keratinocytes (Tu et al., 2008). In a MLL-AF9-driven AML model, Miller et al. (2013) demonstrated that Itgb3 is required for AML growth and maintenance. Interestingly, *in vivo* experiments using a imatinib-resistant CML model, which resembled blast crisis, proved that overexpression of Itgb3 on leukemia-initiating cells prolonged the survival of mice, possibly by increasing myeloid maturation (Kumar et al., 2020). Based on our and the preceding reports, it can therefore be hypothesized that the expression and function of adhesion molecules, such as ITGB3, in leukemia cells are differentially regulated by the

different BM calcium concentrations to which they are exposed. The same seems to apply to CaSR expression, which may contribute to leukemia progression.

Our data on CaSR-mediated adhesion and migration in response to calcium ions supports the concept that calcium acts as a facilitator of cancer mobility to the bone *via* CaSR, as detailed in section 2.10.5. Following up on the findings by Adams *et al.* (2006), who demonstrated that CaSR is required for BM localization of HSCs, Lam *et al.* (2011) proved that CaSR stimulation enhances CXCR4 signaling, which is a major pathway implicated in LSC retention in the BM. Similarly, we found that an increase in CaSR expression in AML cells was accompanied by an increase in CXCR4 expression (Figure 15). According to this, it is possible that, similar to HSC, CaSR can regulate BM localization of leukemia cells.

To test this hypothesis, intravital microscopy experiments are ongoing to determine the cells' localization inside the BM of THP1 cells with CaSR depletion or overexpression, as well as cells treated with the CaSR inhibitor NPS-2143. If CaSR affects AML cell localization in the BMM, cells overexpressing CaSR should localize closer to the endosteum, where calcium levels are higher, while cells with depleted or suppressed CaSR should localize more in the central marrow region, where calcium levels are lower. As mentioned in section 2.8 for HSCs and section 2.9 for LSCs, distinct patterns of lodgment of stem cells in the BM cavity with a preferential localization in the endosteal area (Christodoulou et al., 2020; Nombela-Arrieta et al., 2013), have been highlighted, which in turn has a regulatory effect on cells with regards to quiescence or differentiation (Nilsson et al., 2001). In the case of AML, LSC quiescence is closely linked to resistance to ara-C treatment, which targets fast cycling cells, resulting in a high probability of relapse (Duan et al., 2014; Ishikawa et al., 2007; Ninomiya et al., 2007). In line with our findings and hypotheses that CaSR influences AML cell location in the BMM, CaSR depletion, similar to administering the CaSR antagonist NPS-2143, may improve the efficacy of chemotherapy and provide a novel targeting strategy for the eradication of LSC.

CaSR is expressed by a range of cell types in the bone marrow (House et al., 1997), including osteoblasts (Godwin and Soltoff, 1997; Sugimoto et al., 1993), and other stromal cells (Yamaguchi et al., 1998a). It is worth noting that CaSR signaling activation on BMM cells promotes osteoclast activity and stimulates bone resorption (Dvorak et al., 2007), highlighting the importance of extracellular calcium in bone remodeling. Through studies on bone remodeling in AML, in addition to studies on leukemia-induced alterations of osteolytic activity (Frisch et al., 2012) and impaired bone mineralization (Hanoun et al., 2014), Duarte *et al.* proposed that preventing endosteal vasculature degradation could increase the efficacy of chemotherapy and prolong AML survival (Duarte et al., 2018). These findings point to a previously unrecognized and understudied link between bone remodeling and changes in

calcium ion levels, as well as subsequent CaSR signaling activity, which may influence AML progression.

Although we have shown that calcium affects leukemia cells *via* CaSR, the influence of other calcium modulating/interacting molecules cannot be excluded. Another G-protein coupled receptor, GPRC6A (G Protein-Coupled Receptor Class C Group 6 Member A), has been found to be abundantly expressed in bone cells (Pi et al., 2008; Pi et al., 2005), and, like CaSR, it has extracellular calcium/calcimimetic-sensing characteristics (Kuang et al., 2005). Even though this protein has not been completely studied, several reports indicate that it is expressed in BMM cells and can regulate bone remodeling (Pi et al., 2008; Pi et al., 2005), making it a strong candidate for involvement in leukemia development.

In addition to G protein-coupled receptors, calcium channels or transporters, such as transient receptor potential channels (TRP) (Chen et al., 2020; Huang et al., 2015; Semenova et al., 2009; Soh and Park, 2001; Takahashi et al., 2018) and purinergic receptors (ATP-gated cation channel P2X7 receptor) (He et al., 2021; Pegoraro et al., 2020), allow calcium influx across the plasma membrane and have been reported to play a role in leukemia. More research on the impact of these receptors and the effect of calcium channel blockers in leukemia patients would be clinically relevant and might complement our findings on the effect of extracellular calcium on leukemia cells. However, that was not investigated in this study.

It is worth pointing out that, given the widespread role of calcium in cellular mechanisms and the multiple molecules involved in its regulation, we have centered our studies on the influence of CaSR in leukemia using both *in vitro, in vivo,* gain and loss of function data.

CaSR influences leukemia development in a differential manner

Extracellular calcium is known to be critical for several cell types, including B-cell activation and function (Hammond et al., 2007) and T-cell growth (Shirakawa et al., 1986). Furthermore, extracellular calcium has been demonstrated to impact leukemia cells. Early studies demonstrated that calcium contributes to the inhibition of cell proliferation and the differentiation of murine AML cells into macrophages (Miyaura et al., 1984). Soon thereafter, Barnett and Evans demonstrated that calcium promotes the membrane permeability in K562 cells, resulting in the inhibition of cell proliferation (Barnett and Evans, 1990). More recently, it was demonstrated that human chronic lymphocytic leukemia (CLL) cells that are responsive to extracellular calcium have a more aggressive phenotype, which is associated with a worse prognosis (Hammond et al., 2009). However, it remains to be shown if the effect described in these studies is related to the sensing of extracellular calcium *via* CaSR or CaSR expression.

In this work, we demonstrated the influence of CaSR in leukemia. CaSR functions as a tumor suppressor or an oncogene, depending on the cell type affected and the involved oncogene (section 2.10.4). Our *in vivo* experiments showed that CaSR favors tumorigenesis in AML (Figures 19 and 20) and functions as a tumor suppressor in CML (Figure 17) and BCR-ABL1-driven B-ALL (Figure 18). *CaSR* can be termed a "double agent" because of this property, and leukemia is one of the cancer types with an over-representation of these genes (Shen et al., 2018). A similar “double agent” role was described for TGF-β1 in CML versus AML. Using a retroviral mouse model, Krause *et al.* demonstrated that PTH prolongs survival of mice with CML and increases the aggressivity of the disease in MLL-AF9-driven AML. Release of TGF-β1, as a result of PTH-induced bone remodeling, was shown to suppress CML and accelerate AML development (Krause et al., 2013). Our findings on the role of CaSR in these two distinct leukemias are consistent with the findings of this study and may be complementary. It is possible that, in addition to TGF-β1, extracellular calcium released from the bone matrix as a result of PTH-induced bone remodeling promotes CaSR signaling in leukemia cells, hence mediating the observed phenotype. We have also shown that the sensitivity of CaSR to different concentrations of extracellular calcium varies between CML and AML cells and may contribute to disease development in distinct ways.

As CML and B-ALL in our models are induced by the oncogenic tyrosine kinase BCR-ABL1, it is possible that the observed phenotype is oncogene-specific. Normal B-cells, unlike other hematopoietic cells, are not known to express CaSR (Yamaguchi et al., 1998b; Yamaguchi et al., 2002). However, it remains unknown if they can directly respond to extracellular calcium (Hammond et al., 2007). Our findings corroborate the notion that, in contrast to normal B-cells, malignant B-ALL cells express CaSR. However, we did not investigate whether B-ALL cells respond to extracellular calcium through CaSR. Future research may expand current findings on the role of CaSR in B-ALL by investigating the responsiveness of these cells to extracellular calcium and by modulating CaSR expression *in vitro* and *in vivo*.

CaSR is an essential gene required for organismal survival, and a murine model with constitutive gene depletion is not viable. Mouse models with homozygous germline deletion of CaSR show high calcium and PTH levels in the blood, skeletal abnormalities, growth retardation, parathyroid hyperplasia, and they die prematurely (between days 3 and 30 of life) (Ho et al., 1995; Toka et al., 2012). In the present study, we employed an inducible CaSR KO mouse model, which was then used in bone marrow transplantation experiments. The incomplete gene depletion observed in our experiments may be explained by an inefficient recombination rate upon poly I:C treatment and consequently leaky expression of CaSR. Additional genetic analysis on the leukemia cells, such as DNA amplification and/or sequencing, may be conducted to determine the cause of ineffective gene ablation.

In summary, our findings reveal that CaSR has a very strong and opposite impact in AML when compared to CML and B-ALL. Given the role of CaSR as a tumor suppressor in CML and B-ALL, using a CaSR agonist to treat patients with these leukemias may be a new therapeutic option. Preliminary findings indicate that combining imatinib with a specific CaSR agonist, cinacalcet, significantly increases the survival of mice suffering from CML (Figure 44). It is relevant to mention that the mouse model utilized in this experiment is particularly aggressive, which means that once the illness is established, it progresses exponentially and the animals' overall survival is rather short, making small differences difficult to detect. Following research would need to optimize the treatment regimen, test the impact of cinacalcet in human samples through xenotransplantation experiments, and investigate the molecular mechanism(s) resulting from cinacalcet treatment of CML cells. Similarly, studying the efficacy of cinacalcet or another CaSR agonist in a mouse model of B-ALL is relevant.

Given the greater impact of extracellular calcium and CaSR on AML cells, as well as the clinical need for better treatments, the impact of CaSR and its underlying molecular mechanism(s) in AML were the focus of this study.

CaSR maintains stemness and self-renewal ability of AML LSC

We demonstrated that the mechanism underlying the enhanced aggressivity of the leukemia phenotype associated with elevated CaSR expression in AML involves regulation of genes associated with leukemia stemness. We showed that *CaSR* ablation reduced myeloid progenitor function and the number of granulocyte-macrophage progenitor (GMP) cells (Figure 23), which comprise the LSC fraction in this mouse model (Krivtsov et al., 2006). Furthermore, secondary and limiting-dilution transplantation assays (Figure 24) showed that CaSR is required for maintenance of the LSC pool by regulating its function and frequency. Complementary, we found that genes associated with AML stemness and self-renewal capacity were upregulated when *CaSR* was overexpressed and downregulated when *CaSR* was depleted (Figure 23C), which further supports the role of CaSR in LSC maintenance.

For the question of how this regulation occurs, the well-known transcription factors, such as RUNX 1 (Wesely et al., 2020), EVI 1 (Paredes et al., 2020), CREB (He et al., 2021), MEIS 1 and the Homeobox (Hox) proteins HOXA9 and HOXB4 (Abramovich et al., 2005) might contribute for the phenotype. Those showed in our experiments to be up- or downregulated, which may be either a consequence of the aggressiveness of the disease or a result of the complex signal transduction pathways *via* CaSR. Further experiments to differentiate between cause and effect would be required by future research.

Given the contribution of LSCs to the high relapse rate in AML due to the difficulties of targeting quiescent LSCs (section 2.7), our findings imply that targeting of CaSR might impair LSC activity and might be relevant in preventing relapse.

CaSR signaling in AML

Activation of Wnt/β-catenin signaling

To investigate the effect of CaSR on LSCs, we first focused on the Wnt/β-catenin pathway. This pathway is dysregulated in a variety of cancers, including leukemia (Gruszka et al., 2019). Studies in different mouse models of AML demonstrated that canonical Wnt/β-catenin signaling is required for self-renewal of LSCs (Wang et al., 2010; Yeung et al., 2010), and it is considered a good target in this disease.

CaSR can act as modulator of Wnt/β-catenin (MacLeod, 2013), and our findings suggest that CaSR can regulate this pathway in AML cells: CaSR overexpression increased Wnt/β-catenin activation in the human AML cell line THP1 (Figure 31), and inhibition of CaSR with a specific antagonist resulted in its inactivation (Figure 33). Furthermore, we found that the vitamin D receptor (VDR), an important regulator of calcium homeostasis (section 2.10.1) and a Wnt/β-catenin repressor (Muralidhar et al., 2019; Shah et al., 2006b), was downregulated in AML cells overexpressing CaSR (Figure 31). This is important to note, as a recent study using several AML models found that VDR signaling is associated with a better prognosis in AML patients and can control leukemia stem cell function (Paubelle et al., 2020). This suggests that VDR, which is a potential target for the treatment of AML is negatively regulated by CaSR, and this contributes to Wnt/β-catenin activation. However, the mechanism behind this regulation remains elusive. Likewise, it is an open question, how this finding can be conciliated with recent research on parathyroid, thyroid, and kidney cells, where vitamin D response elements have been found in the *CaSR* promoter region (Canaff and Hendy, 2002).

In contrast to the Wnt/β-catenin pathway, we found that the non-canonical Wnt/Ca^{2+} pathway was decreased in CaSR-overexpressing cells. This pathway would be activated by the major ligand Wnt5a, which has in turn been shown to suppress Wnt/β-catenin signaling (Topol et al., 2003). Interestingly, and in line with our findings, analysis of samples isolated from ALL and AML patients revealed a decrease in expression of the *WNT5A* gene and protein expression (Liang et al., 2003). Activation of the Wnt/Ca^{2+} pathway would trigger the mobilization of free intracellular calcium *via* protein kinase C (PKC) and calcium/calmodulin-dependent protein kinase II (CaMKII) activation (Kikuchi et al., 2012; Slusarski et al., 1997). This is important, as a recent study in HSC discovered an inverse relationship between intracellular calcium levels and stem cell characteristics and maintenance of stem cell features. HSCs have lower

intracellular calcium levels than progenitor cells, and culture in low-calcium medium improved their maintenance (Luchsinger et al., 2019).

Collectively, our findings suggest that an inverse relationship between Wnt/β-catenin and Wnt/Ca^{2+} pathways can be found in AML. Furthermore, the role of CaSR for the maintenance of LSC and a malignancy might be mediated by activation of Wnt/β-catenin signaling, with subsequent suppression of Wnt/Ca^{2+} signaling. It is possible that in AML, like in HSCs, lower intracellular calcium levels, caused by suppression of the Wnt/Ca^{2+} pathway, contribute to LSC maintenance.

The molecular mechanism behind intracellular calcium regulation in response to CaSR overexpression (Figure 32) was not addressed in this study. Further research on this will need to be undertaken.

ERK/MAPK signaling activation

Our study has established a critical role of CaSR in prompting proliferation and survival in MLL-AF9-induced AML *in vitro* (Figure 29) and *in vivo* (Figure 27). CaSR has been demonstrated to regulate the cell cycle, promoting S-phase entrance and G1-phase exit (Torii et al., 2006) , which likely supports the observed increase in proliferation. Furthermore, we have shown that CaSR functions as a negative regulator of apoptosis, possibly *via* upregulation of the anti-apoptotic gene BcL-X_L (Figure S8). Proapoptotic and cell survival pathways are often impaired in AML (Ketley et al., 2000), and CaSR-mediated upregulation of these genes may contribute to the observed survival advantage.

The Wnt/β-catenin signaling pathway, in addition to being a primary stem cell regulatory pathway, controls important cell processes, such as proliferation, survival, and cell-fate regulation (Gandillet et al., 2011; Okuhashi et al., 2011; Reya and Clevers, 2005). We have seen in the previous section that CaSR plays a key role in activating this pathway. Similarly, the ERK/MAPK signaling pathway is another key regulator of cell proliferation and survival that drives oncogenic transformation in several cancers (Chang et al., 2003). This signaling pathway is constitutively activated in more than 50% of patients with AML (Milella et al., 2001), and it has been linked to cell growth (Ricciardi et al., 2005). Comparable to the Wnt/β-catenin signaling pathway, CaSR functions as a robust MAPK activator in various cell types, multiple heterologous expression systems, and different mouse models (section 2.10.2) *via* phosphorylation of ERK1/2 (Handlogten et al., 2001; Kifor et al., 2001; Thomsen et al., 2012).

Our findings show that CaSR controls ERK/MAPK signaling in AML cells (Figure 30). However, they do not support the concept that the role of CaSR for the phenotype is exclusively attributed to ERK/MAPK or Wnt/β-catenin signaling. CaSR activates multiple

signal transduction pathways, including MAPK and Wnt/β-catenin signaling, both of which may contribute to leukemogenesis.

The mechanism by which CaSR regulates AML development may include additional signaling pathways that were not investigated in our research. More research is needed to characterize CaSR signaling in AML. Studies employing a high-throughput RNA sequencing technology and *in vitro* loss-of-function experiments are currently being carried out in our laboratory, which may help to elucidate the mechanism.

Filamin A signaling activation

Filamin A (FLNA) is a well-known actin interacting protein that interacts with Rho family GTPases and several of their regulatory cofactors (Duval et al., 2014; Washington and Knecht, 2008). Because of its involvement facilitating cell adhesion and migration (Lamsoul et al., 2020), it is often associated with cancer invasion and metastasis (Ketebo et al., 2021; Zhang et al., 2014). In addition to interacting with Rho GTPases, FLNA has been described as a CaSR-interacting protein that participates in CaSR signaling (Awata et al., 2001; Hjälm et al., 2001; Huang et al., 2006).

The findings of this work point to a novel role of filamin A (FLNA), contributing to AML development: We demonstrated that increased FLNA expression is associated with a worse prognosis and a decrease of overall patient survival (Figure 36). This could in part be explained by our findings, showing that FLNA interacts with CaSR in AML cells (Figure 34) and, similar to CaSR, promotes cell proliferation (Figure 35A) and cell cycle regulation (Figure 35B). More critically, we showed that FLNA depletion in leukemia cells of a human xenograft mouse model improved overall mouse survival (Figure 37B).

The role of FLNA in cell mobility *via* interaction with small GTPases of the Rho family, i.e., RAC, RHO and CDC42, may explain the defective migration (Figure 35C) and reduced *in vivo* organ infiltration of THP1 cells after FLNA deletion, as reported in our xenotransplantation, which subsequently influenced mouse survival. One of the most powerful chemokine receptors implicated in AML cell migration and retention in the BMM is CXCR4 (Cancilla et al., 2020). FLNA may be critical for transduction of CXCR4-mediated signaling pathways in AML, comparable to prior results in HEK 293 cells (Gómez-Moutón et al., 2015). The observed interaction of FLNA with CXCR4 (Figure 35D) may possibly contribute to this phenotype.

As a versatile scaffolding protein, FLNA interacts with several membrane receptors, and the interaction with CaSR is required for activation of MAPK signaling through ERK phosphorylation (Awata et al., 2001; Hjälm et al., 2001). The mechanism(s) by which FLNA is regulated by CaSR, as well as the potential relevance of this interaction for CaSR signaling

however remains unclear. Preliminary findings suggest that FLNA is required for ERK/MAPK signaling in AML cells rather than Wnt/β-catenin signaling (data not shown). Further research is needed to draw a definitive conclusion.

Taken together, our findings support the notion that FLNA may be a potential target for AML. However, since FLNA is a ubiquitous structural protein involved in many essential cellular functions (Nakamura et al., 2007), FLNA inhibition may not be possible therapeutically. Alternatively, overexpression or activation of FILIP (Filamin A interacting protein), which stimulates FLNA degradation (Nagano et al., 2002), might indirectly target FLNA. Based on our findings, disruption of the interacting motif of CaSR with FLNA can be a potential targeting strategy. FLNA has been proven to be necessary for CaSR stability by reducing its degradation (Zhang and Breitwieser, 2005) as well as its signaling (Awata et al., 2001; Hjälm et al., 2001).

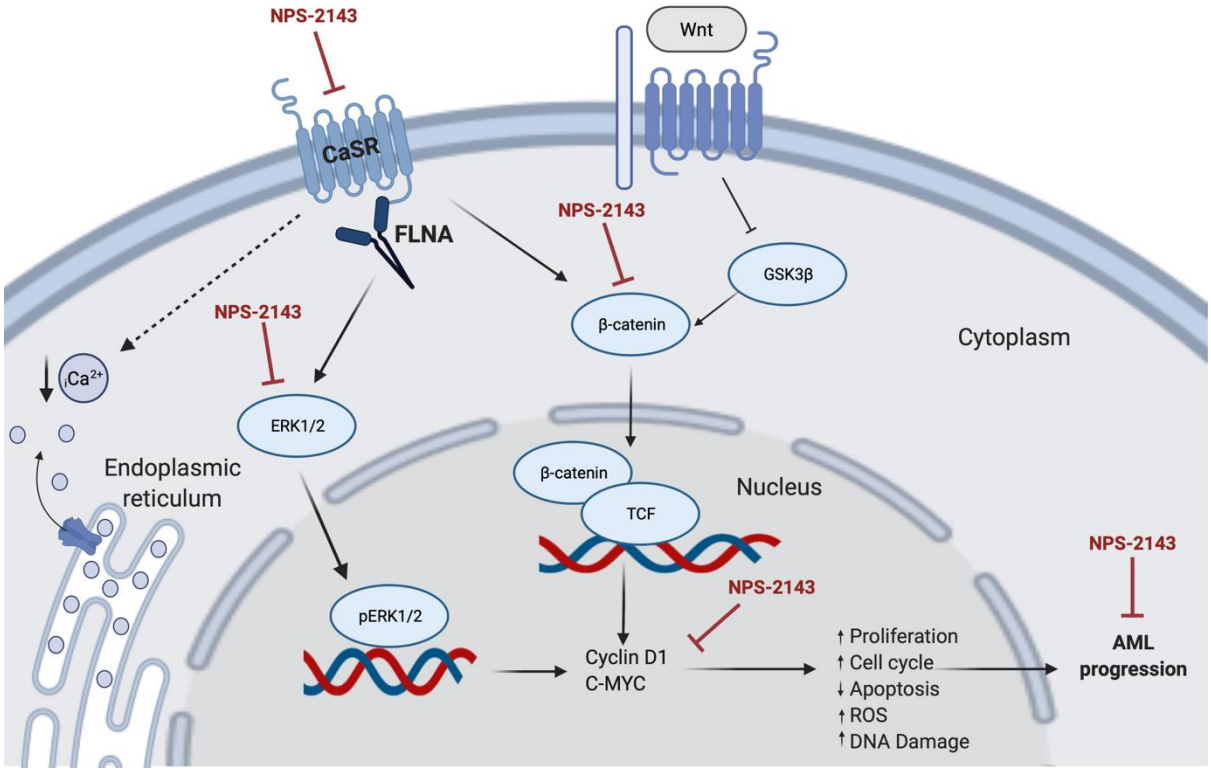

Figure 45. Schematic view of the proposed mechanism for CaSR signaling in AML.CaSR activates MAPK signaling *via* phosphorylation of ERK1/2, which translocates to the nucleus and functions as a transcription factor. CaSR also stimulates Wnt/β-catenin signaling by stabilizing, supporting the accumulation and translocating β-catenin to the nucleus. In the nucleus, β-catenin forms a complex with TCF, which leads to transcriptional regulation. The activation of MAPK and Wnt/β-catenin signaling results in the upregulation of c-Myc and cyclin D1, which leads to enhanced proliferation, cell cycle progression, ROS production and DNA damage accumulation as well as antagonism of apoptosis. As a result, these processes contribute to AML progression. The specific CaSR antagonist NPS-2143, illustrated by the red lines may block CaSR signaling at distinct steps, inhibiting AML progression. Schematic created with BioRender.com.

The CaSR antagonist NPS-2143 is effective in targeting AML

Our findings show that inhibition of CaSR signaling with NPS-2143 effectively impairs leukemia growth and progression *in vitro* (Figure 33) and *in vivo* (Figures 38 and 39). NPS-2143 is a strong CaSR antagonist (Nemeth et al., 2001; Nemeth et al., 2018), and we demonstrated that its usage in combination with conventional chemotherapy reduces tumor burden and prolongs survival of mice with AML, as shown in our xenotransplantation (Figure 42) and syngeneic (Figure 39) models. Furthermore, given the critical role of CaSR in regulation of LSCs shown in our study, NPS-2143 may be able to target LSCs in AML (Figure 40). Based on these findings, we reasoned that in AML, not only leukemia cells, but also LSCs, may be sensitive to CaSR inhibition, and that treating patients with a CaSR inhibitor in combination with conventional chemotherapy may provide a better therapy and prevent the risk of relapse.

It is worth noting that the treatment experiments included systemic delivery of NPS-2143, which possibly blocks CaSR expressed in a variety of cell types other than leukemia cells. As a result, one may not be able to exclude the possibility that this inhibition has an additional influence on mouse survival. CaSR is expressed and required for the function of a variety of BMM cells (section 2.10.2), which contribute to leukemia regulation (section 2.9). The contribution of CaSR from BMM cells should be addressed in the future.

In our murine data, *CaSR* deletion affected the survival of mice with AML induced by different oncogenes in a similar way (Figures 19, 22 and 25). It is therefore likely that our findings are not specific to MLL-AF9-driven AML, but it can be applied to other AML types as well. Furthermore, we observed that CaSR expression differed between AML types (Figure 41) and so did the responses to CaSR inhibition (Figure 43). Monitoring CaSR expression and sensitivity to CaSR inhibition may therefore be clinically relevant in the future and may aid in risk stratification of patients. However, given the ubiquitous role of CaSR in regulating physiological functions, the risks involved in systemic administration of calcilytics such as NPS-2143 (Nemeth and Goodman, 2016) will need to be carefully assessed.

Looking beyond AML, CaSR has been linked to the etiology of a variety of cancers (section 2.10.4). Studies on human cell lines have shown that inhibition of CaSR with NPS-2143 is a promising therapy in melanoma (Wang et al., 2018), gastric (Zhang et al., 2020), prostate (Yamamura et al., 2019) and breast cancer (Alqudah et al., 2021; Orduña-Castillo et al., 2021). In addition to cancer, NPS-2143 has been found to be effective in allergic asthma (Yarova et al., 2015b) and chronic obstructive pulmonary disease (Lee et al., 2017) by reducing the airway hyperresponsiveness and inflammation. Furthermore, CaSR signaling is critical for disease progression in Alzheimer's disease and can be suppressed by NPS-2143 (Chiarini et al., 2017). In line with this, research into the intrinsic molecular mechanisms of CaSR in various

pathologies, as well as the clinical development of effective drugs such as NPS-2143 and future derivatives, may help to improve the current treatments.

7 Conclusion

In this thesis, we showed that the calcium concentration in the BMM significantly impacts leukemia progression and revealed targeting of calcium sensing receptor (CaSR) signaling as a novel leukemia treatment candidate, combinable with conventional treatment methods.

We started by demonstrating that calcium ions, which are abundant in the BMM, are not uniformly distributed within. Instead, there is a calcium ion gradient in the bone marrow that may influence leukemia cell location, proliferation, and survival, ultimately impacting disease progression, response to therapy and relapse. This influence of the calcium ions was furthermore shown to be dependent on the specific type of leukemia. Specifically, the calcium content in the BM is greater in AML than in other leukemias, and we have shown that calcium exposure has a significant influence on AML cells while having no effect on CML cells. We have further shown that CaSR, the receptor responsible for sensing extracellular calcium, is differentially expressed in distinct types of leukemia and that it plays a varied and crucial role in the development of CML, B-ALL, and AML. More concretely, we have shown that CaSR is acting as tumor suppressor in CML and B-ALL, and as oncogene in AML. We have identified CaSR-mediated pathways in AML and shown that CaSR enhances leukemia progression by regulating proliferation, cell cycle, apoptosis, ROS generation, differentiation, and DNA damage. Furthermore, we have demonstrated that CaSR is necessary for stemness and self-renewal capabilities of LSCs in AML.

Novel treatment options for leukemia are in dire need and our study suggests that targeting CaSR with a specific inhibitor efficiently suppresses AML development. Moreover, combination with conventional chemotherapy may significantly improve the outcome of AML patients and prevent or reduce the frequency of relapse after treatment. Going forward with this research, clinical trials would be needed to evaluate the potential therapy’s efficacy. Lastly, we have provided first evidence that combination of a CaSR activator with standard therapy may also provide a novel strategy for treatment of CML. However, research on the effect of CaSR on CML is still in its early stages and thorough future experiments on the function and molecular signaling of CaSR in CML will be necessary before any conclusions can be drawn.

8 Supplementary data

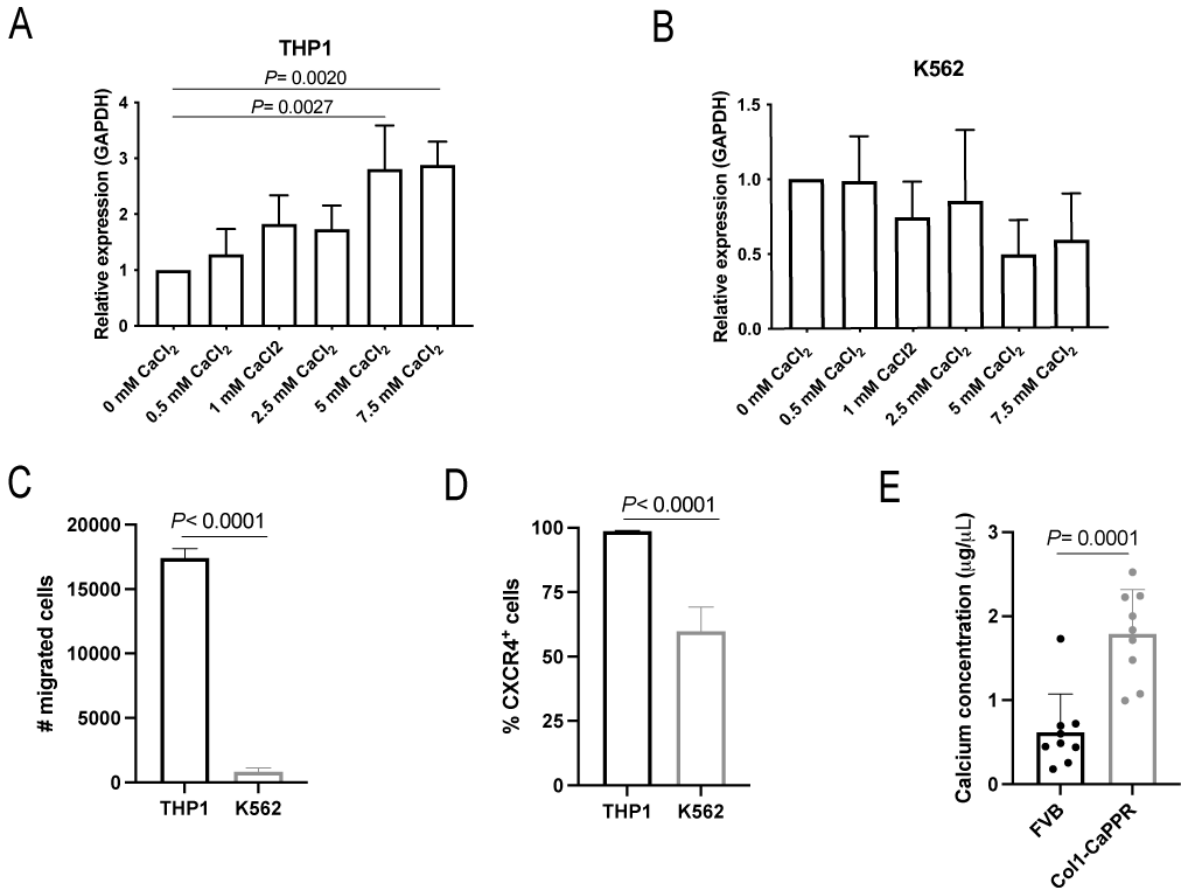

Figure S1. A-B) Quantification of the immunoblot analysis for CaSR expression in lysates of THP1 (A) or K562 (B) cells treated with different calcium concentrations (0-7.5 mM) for 4 h. C) Number of THP1 and K562 cells migrated towards CXCL-12 within 2 h of (n=3, *t*-test). D) Percentage of $CXCR4^+$ cells of total THP1 or K562 cells determined by flow cytometry (n=3, *t*-test). E) Quantification of the calcium (Ca^{2+}) concentration in the BM of healthy control (FVB) mice and Col1-CaPPR mice. The BM of one femur *per* mouse was collected in 100 µl of PBS and the calcium concentration present in the noncellular fraction was determined, after centrifugation of the sample (n=3, *t*-test).

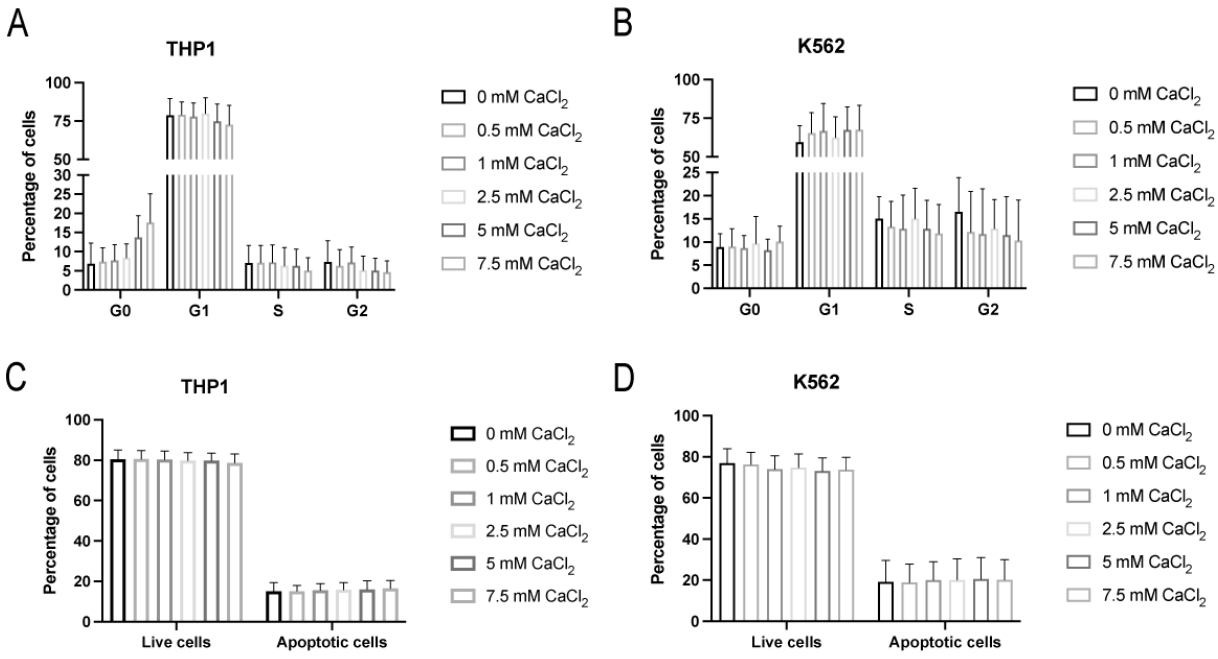

Figure S2. A-B) Cell cycle analysis of THP1 (A) and K562 (B) cells treated with different calcium concentrations (0-7.5 mM) for 4 h (n=3). C-D) Percentage of apoptotic THP1 (C) and K562 (D) cells treated with different calcium concentrations (0-7.5 mM) for 4 h, detected by annexin V staining (n=3).

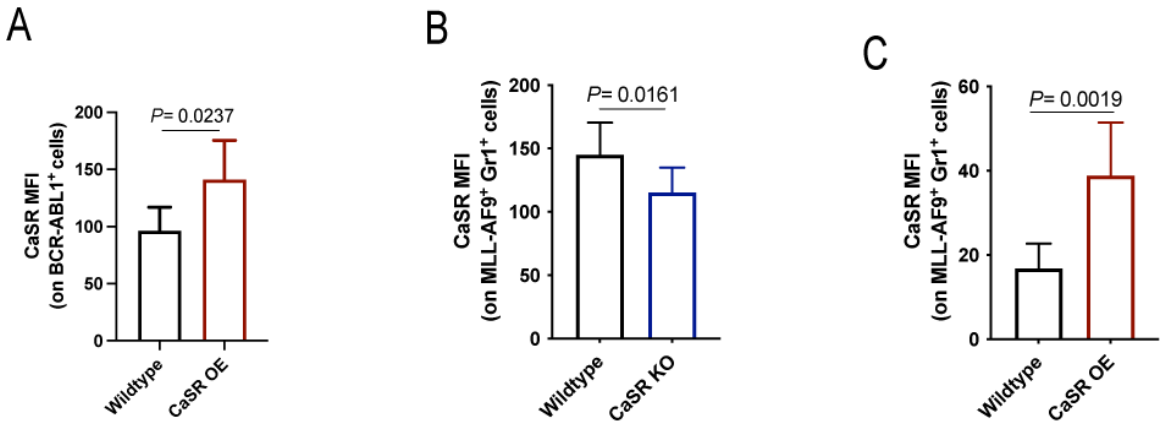

Figure S3. A) Mean fluorescence intensity (MFI) of CaSR on peripheral blood leukocytes of wildtype mice transplanted with BCR-ABL1$^+$ LIC, co-transduced with empty vector (black) or CaSR-overexpressing retrovirus (red) in the CML model (n=6-8, *t*-test) fifteen days after transplantation. B) Mean fluorescence intensity (MFI) of CaSR on peripheral blood leukocytes of wildtype mice transplanted with MLL-AF9$^+$ wildtype (black) or CaSR KO (blue) LIC in the AML model (n=9-10, *t*-test) fifty-three days after transplantation. C) Mean fluorescence intensity (MFI) of CaSR on peripheral blood leukocytes of wildtype mice transplanted with MLL-AF9$^+$ LIC, co-transduced with empty vector (black) or CaSR-overexpressing retrovirus (red) in the CML model (n=9-10, *t*-test) fifty-four days post transplantation.

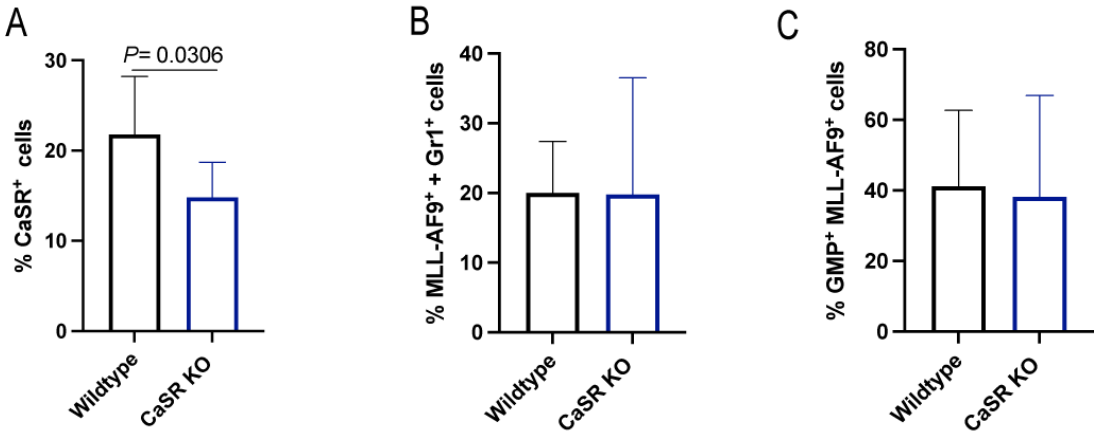

Figure S4. A) Percentage of CaSR$^+$ cells in the peripheral blood of mice transplanted with MLL-AF9$^+$ wildtype (black) or CaSR KO (blue) LIC, determined on day thirty-six after transplantation. CaSR gene depletion was performed on day twelve after transplantation (n=8, *t*-test). B-C) Percentage of MLL-AF9$^+$ Gr1$^+$ (B) and granulocyte-monocyte progenitor (GMP: Lin$^-$ Sca1$^-$ CD117$^+$ CD34$^+$ CD16/32$^+$) (C) cells in BM of mice transplanted with MLL-AF9+ wildtype or CaSR KO LIC, on day 12 after transplantation (n=4, *t*-test).

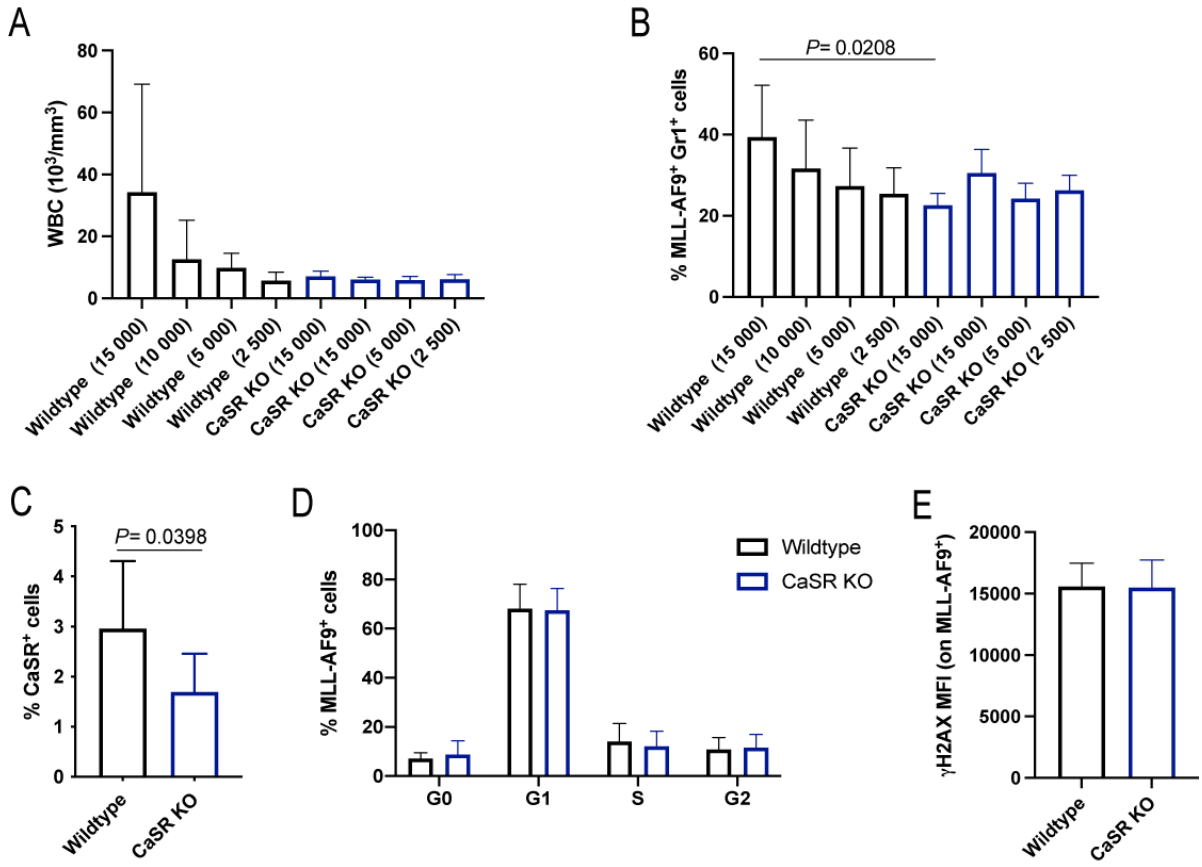

Figure S5. A-B) Leukocyte counts (WBC) (A) and percentage of MLL-AF9$^+$ Gr1$^+$ cells (B) in the peripheral blood of secondary mice, transplanted with sorted wildtype or CaSR KO MLL-AF9$^+$ Lin$^-$ BM cells from primary mice with established MLL-AF9-induced AML, transplanted in different doses (2,500-15,000) (n=4-5, ANOVA, Tukey test). C) Percentage of CaSR$^+$ cells in peripheral blood of mice

transplanted with wildtype (black) or CaSR KO (blue) MN1^{+} LIC, determined on day twenty-five after transplantation (n=7-8, *t*-test). D) Cell cycle analysis of wildtype (black) or CaSR KO (blue) MLL-AF9^{+} cells derived from spleen (n=7, two-way ANOVA, Tukey test), sacrificed on day forty after transplantation. E) Median fluorescence intensity of γH2A.X in spleen-derived wildtype (black) or CaSR KO (blue) MLL-AF9^{+} cells, 40 days after transplantation (n=3-4, *t*-test).

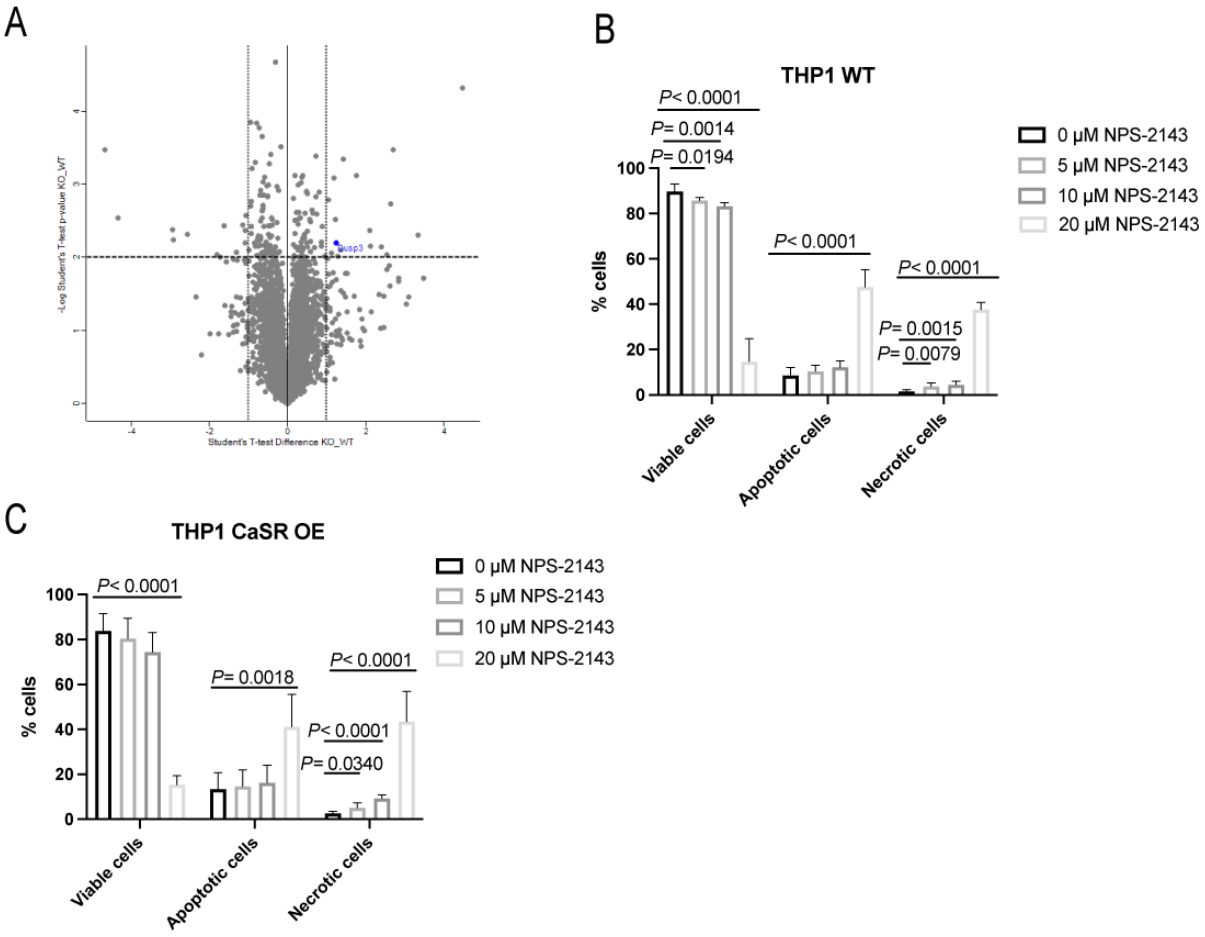

Figure S6. A) Volcano plot of proteomics data in sorted Lin^{-} MLL-AF9^{+} cells derived from BM of wildtype mice transplanted with either wildtype or CaSR KO MLL-AF9^{+} LIC. Each protein is represented by a dot, which is mapped regarding its statistical significance (p-value) versus magnitude of change (fold change). The x-axis indicates the fold change and the y-axis indicates the - log10 p-value. Differentially expressed proteins (P < 0.01 and a fold rate > 1.2) are listed in Tables 11 and 12. B-C) Percentage of apoptotic THP1 WT (B) and THP1 CaSR OE (C) cells treated with different NPS-2143 concentrations (0-20 µM) detected by annexin V staining of (n=3, two-way ANOVA, Sidak test).

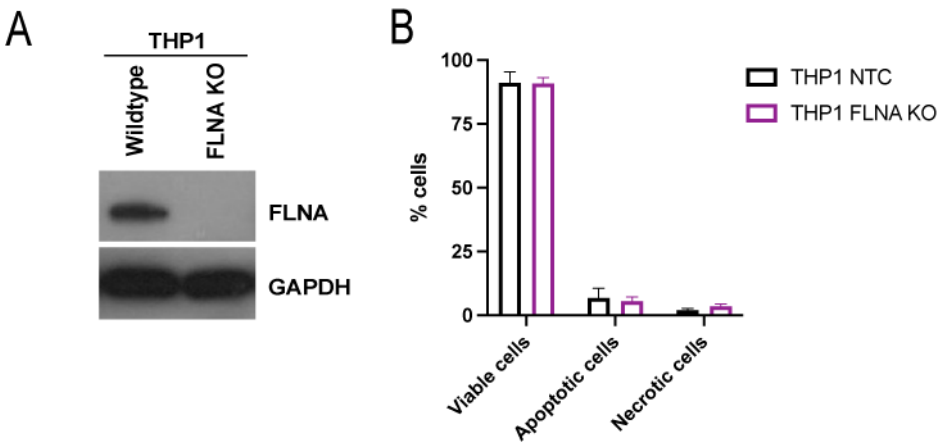

Figure S7. A) Representative immunoblot analysis of the expression of FLNA (180 kDa) and GAPDH (37 kDa) as loading control in extracts of THP1 wildtype and THP1 FLNA KO cells. B) Percentage of apoptosis in THP1 non-target control (NTC, black) and THP1 FLNA KO (pink) cells (n=3).

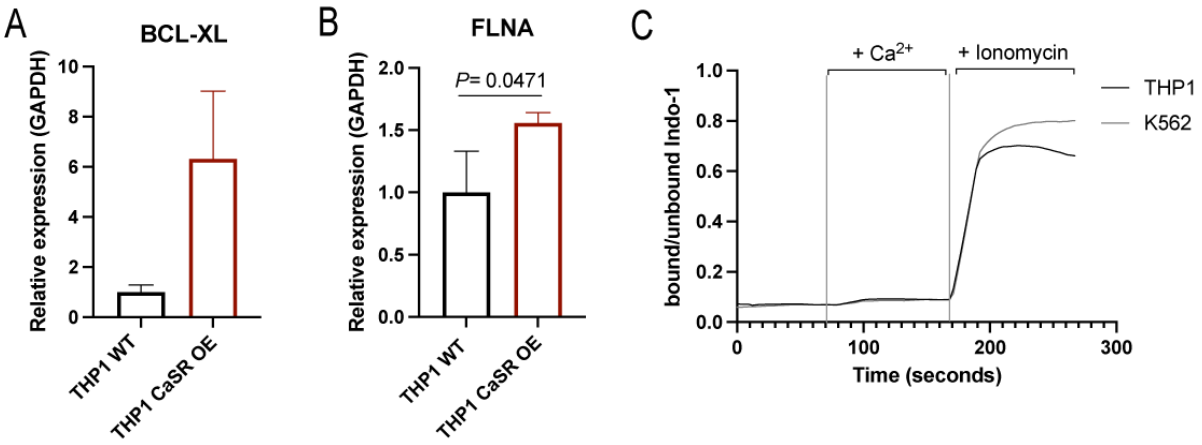

Figure S8. A-B) Relative expression of BCL-XL (A) (n=4, t-test) and FLNA (B) (n=3, t-test) by qRT-PCR analysis of WT THP1 cells (WT, black) and THP1 cells overexpressing CaSR (THP1 CaSR OE, red). C) Calcium flux analysis of THP1 (black) and K562 (grey) cells using Indo-1 (n=4).

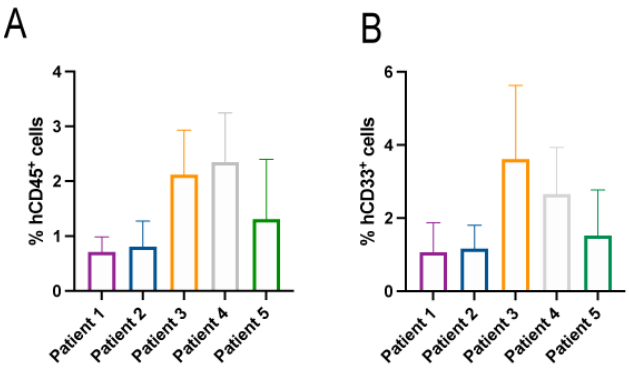

C

	Mutations
Patient 1	NPM-1 Mutation Pos. FLT LM Pos.
Patient 2	NPM1 Mutation Typ A
Patient 3	NPM1
Patient 4	ASXL1, DNMT3A, IDH-2, RUNX1, SRSF2
Patient 5	FLT3-ITD, NPM1

Figure S9. A-B) Percentage of human CD45$^+$ (A) and CD33$^+$ (B) leukocytes in peripheral blood of NSG mice transplanted with human AML cells, seventeen days after transplantation. Recipients of different human AML samples are represented in different colors (n=5-7). C) Mutations present in the BM cells derived from AML patients used in xenotransplantation experiments.

9 Supplementary material

Table 7. List of qPCR primers

Primer name	Primer sequence (3' → 5')	Species
CASR_FW	GCAACCAGGAGCTGGAGGAT	Mouse/human
CASR_RV	CAGGCAGGTGTAGCCGATCA	Mouse/human
FLNA_FW	CATCAAGTACGGTGGTGACG	Mouse/human
FLNA_RV	ACATCCACCTCTGAGCCATC	Mouse/human
VDR_FW	CCAGTTCGTGTGAATGATGG	Mouse/human
VDR_RV	AGATTGGAGAAGCTGGACGA	Mouse/human
HOXA9_FW	GGTTCTCCTCCAGTTGATAGAGA	Mouse
HOXA9_RV	GAGCGAGCATGTAGCCAGTTG	Mouse
MEIS1_FW	ACGGCATCCACTCGTTCA	Mouse
MEIS1_RV	TGGCTGTCCATCAGGGTT	Mouse
RUNX1_FW	GATGGCACTCTGGTCACCG	Mouse
RUNX1_RV	GCCGCTCGGAAAAGGACAA	Mouse
CREB_FW	AGCAGCTCATGCAACATCATC	Mouse
CREB_RV	AGTCCTTACAGGAAGACTGAACT	Mouse
HOXB4_FW	CGTGAGCACGGTAAACCCC	Mouse
HOXB4_RV	GTGTTGGGCAACTTGTGGTC	Mouse
ALOX5_FW	CTACGATGTCACCGTGGATG	Mouse
ALOX5_RV	GTGCTGCTTGAGGATGTGAA	Mouse
EZH2_FW	GTGACCACAGGATAGGCATCT	Mouse
EZH2_RV	CAAGGGATTTCCATTTCTCG	Mouse
GATA-1_FW	CCCACCTCTATCAGG GCCTA	Mouse/human
GATA-1_RV	GAGGTTGTAGGCGAT CCCAG	Mouse/human
EVI1_FW	CTGGCTGCTGCTGATCTTAT	Mouse/human

EVI1_RV	AGTTCGCTTACCTTCCGATTT	Mouse/human
MYC_FW	CCTGGTGCTCCATGAGGAGAC	Human
MYC_RV	CAGACTCTGACCTTTTGCCAGG	Human
C-JUN_FW	ATCAAGGCGGAGAGGAAGCG	Human
C-JUN_RV	TGAGCATGTTGGCCGTGGAC	Human
C-FOS_FW	CTGGCGTTGTGAAGACCAT	Human
C-FOS_RV	TCCCTTCGGATTCTCCTTTT	Human
ETS_FW	GTGCTGTCAGGCGTTCT	Human
ETS_RV	GGGAGAGGAGCAGACGAG	Human
ELK1_FW	CGCAAGAACAAGACCAACATG	Human
ELK1_RV	TCAGGGTAGGACACAAACTTG	Human
BCL-XL_FW	GGAGAACGGCGGCTGGGATA	Human
BCL-XL_RV	GGCCACAGTCATGCCCGTCA	Human
TCF4_FW	GCCTCTTCACAGTAGTGCCAT	Human
TCF4_RV	TCCCTGTTGTAGTCGGCAGT	Human
MEF2C _FW	ATGCCGATGCAGACGATTCAG	Human
MEF2C_RV	AACAGCACACAATCTTTGCCT	Human
GRP78_FW	TTCAGCCAATTATCAGCAAACTCT	Mouse/human
GRP78_RV	TTTTCTGATGTATCCTCTTCACCAGT	Mouse/human
STXBP1_FW	CTGAGTCCGAATCAGGTGCAG	Mouse/human
STXBP1_RV	GTCCATGGGAAGATGTTCTGG	Mouse/human
ATF4_FW	GGGACAGATTGGATGTTGGAGA	Mouse/human
ATF4_RV	ACCCAACAGGGCATCCAAGT	Mouse/human
GAPDH_FW	AGGTCGGTGTGAACGGATTTG	Mouse/human
GAPDH_RV	GGGGTCGTTGATGGCAACA	Mouse/human

Table 8. List of flow cytometry antibodies

Antibody	Fluorochrome	Clone	Company	Catalogue number
CaSR-Biotin		HL-1499	NOVUS biologicals	#NB-1830
CaSR	Alexa Fluor 647	5C10	NOVUS biologicals	#NB-120-19347
CXCR4	PE	2B11	BD Biosciences	#561734
CD11b	PE	M1/70	Biolegend	#101207
CD11b (Mac-1)	APC	M1/70	BD Biosciences	#553312
CD349 (BP1)	PE	2D3/APA	BD Biosciences	#564533
Ter119-Biotin			BD Biosciences	#553672
LY-6G and LY-6C (GR1) Biotin		RB6-8C5	BD Biosciences	#553125
LY-6G and LY-6C (GR1)	PE	RB6-8C5	Invitrogen	#12-5931-83
LY-6G and LY-6C (GR1)	APC-Cy7	RB6-BC5	BD Biosciences	#557661
CD5-Biotin		53-73	BD Biosciences	#553019
B220-Biotin		RA3-6B2	BD Biosciences	#553086
F4/80-Biotin		BM8	eBiosciences	#13-4801-82
CD117 (c-Kit)	APC	2B8	BD Biosciences	#553356
CD117 (c-Kit)	PE	2B8	BD Biosciences	#553355
CD117 (c-Kit)	BV711	2B8	Biolegend	#105835
Ly6A (Sca-1)	PE-Cy7	D7	Biolegend	#108114
Ly6A (Sca-1)	PerCP	D7	Biolegend	#108122
CD34	BV421	RAM34	BD Horizon	#562608
CD34	APC	RAM34	eBiosciences	#50-0341-82
CD34	PE	RAM34	BD Biosciences	#551387
CD16/CD32 (FCγRII)	V450	2.4G2	BD Horizon	#560539
CD127 (IL7R)	BV711	A7R34	Biolegend	#135035

Human CD33	PerCP Cyanine5.5	WM53	BioLegend	#303414
Human CD45	PE	HI30	BD Biosciences	#555483
Annexin V	APC		BioLegend	#640920
KI-67	PE	16A8	BioLegend	#151210
KI-67	APC	16A8	BioLegend	#652406
4′,6-diamidino-2-phenyl-indol-dihydrochlorid (DAPI)			Sigma-Aldrich	#D9542
CELLTrace far red			Invitrogen	#C34564
p-Histone H2A.X rabbit mAb (S139)		20E3	Cell Signaling Technology	#9718S
Goat anti-rabbit IGG (H+L)	Alexa Fluor-647		Invitrogen	#A21244
INDO-1 AM			Invitrogen	#65-0856-39
CELLROX Deep red			Invitrogen	#C10422

Table 9. List of antibodies used in western blot

Antibody		Company	Catalogue number
GAPDH	Mouse monoclonal	Santa Cruz Biotechnology	#Sc-32233
CaSR	Mouse monoclonal	Santa Cruz Biotechnology	#Sc-47741
Filamin-1	Mouse monoclonal	Santa Cruz Biotechnology	#Sc-17749
Filamin A	Rabbit Ab	Cell Signaling Technology	#4762S
ERK1/2	Mouse monoclonal	Santa Cruz Biotechnology	#Sc-514302
p-ERK	Mouse monoclonal	Santa Cruz Biotechnology	#Sc-7383
Cyclin D1	Rabbit Ab	Cell Signaling Technology	#E3P5S
β-catenin	Rabbit polyclonal IgG	EMD Millipore Corp, Merck	#2942488
c-Myc	Rabbit mAb	Cell Signaling Technology	#E5Q6W
CXCR4	Rabbit polyclonal	Invitrogen	#PA3-305
anti-mouse IGG HRP-linked ab		Cell Signaling Technology	#34
anti-rabbit IGG HRP-linked ab		Cell Signaling Technology	#29

Table 10. List of antibodies used in immunofluorescence

Antibody		Company	Catalogue number
CaSR	Mouse Ab	Abcam	#GR3309582-6
Filamin-1	Mouse Ab	Santa Cruz Biotechnology	#Sc-17749
Filamin A	Rabbit Ab	Cell Signaling Technology	#4762S
p-histone H2A.X (S139)	Rabbit Ab	Cell Signaling Technology	#9718S
Alexa fluor 488	Goat anti-mouse IgG (H+L)	Invitrogen	#A11029
Alexa fluor plus 647	Goat anti-mouse IgG (H+L)	Invitrogen	#A32728
Alexa fluor 647	Goat anti-rabbit IgG (H+L)	Invitrogen	#A21244

Table 11. List of proteins identified upregulated (KO/WT) in the proteomics study

Accession	Gene name	Protein name
P16460	Ass1	Argininosuccinate synthase
A8DUK4	Hbb-bs	GLOBIN domain-containing protein
Q922W5	Pycr1	Pyrroline-5-carboxylate reductase 1, mitochondrial
O08529	Capn2	Calpain-2 catalytic subunit
P35173	Stfa3	Stefin-3
Q9JHK5	Plek	Pleckstrin
P01942	Hba	Hemoglobin subunit alpha
Q03145	Epha2	Ephrin type-A receptor 2
Q9D7X3	Dusp3	Dual specificity protein phosphatase 3
Q04447	Ckb	Creatine kinase B-type
Q9DB42	Znf593	Zinc finger protein 593
D3Z2R5	Selenon	Selenoprotein N
P14069	S100a6	Protein S100-A6
P30280	Ccnd2	G1/S-specific cyclin-D2
Q8BTY2	Slc4a7	Sodium bicarbonate cotransporter 3
Q8CB65	Nemp2	Nuclear envelope integral membrane protein 2
O08800	Serpinb8	Serpin B8

Table 12. List of proteins identified downregulated (KO/WT) in the proteomics study

Accession	Gene name	Protein name
Q3UP87	Elane	Neutrophil elastase
Q99N80	Sytl1	Synaptotagmin-like protein 1
Q61096	Prtn3	Myeloblastin
P22437	Ptgs1	Prostaglandin G/H synthase 1
Q9DAV9	Tmem38b	Trimeric intracellular cation channel type B
P02089	Hbb-b2	Hemoglobin subunit beta-2
E9Q4P1	Wdfy1	WD repeat and FYVE domain-containing protein 1
P35505	Fah	Fumarylacetoacetase
Q9D114	Hddc3	Guanosine-3',5'-bis(diphosphate) 3'-pyrophosphohydrolase MESH1
Q9JJ00	Plscr1	Phospholipid scramblase 1
P23475	Xrcc6	X-ray repair cross-complementing protein 6
P27641	Xrcc5	X-ray repair cross-complementing protein 5
Q9D8M3	Slc48a1	Heme transporter HRG1

Table 13. Patient samples used in the study

	Diagnosis	Subtype (FAB)	Gender	Age	First diagnosis	Treatment	Organ
Patient 1	AML	M2	Female	69	Yes	No	BM
Patient 2	AML	M4	Female	57	Yes	No	BM
Patient 3	AML		Female	76	Yes	No	BM
Patient 4	AML	M4	Male	67	Yes	No	BM
Patient 5	AML		Female	60	Yes	No	BM

10 References

Abramovich, C., Pineault, N., Ohta, H., and Humphries, R.K. (2005). Hox genes: from leukemia to hematopoietic stem cell expansion. Ann N Y Acad Sci *1044*, 109-116. 10.1196/annals.1349.014.

Acar, M., Kocherlakota, K.S., Murphy, M.M., Peyer, J.G., Oguro, H., Inra, C.N., Jaiyeola, C., Zhao, Z., Luby-Phelps, K., and Morrison, S.J. (2015). Deep imaging of bone marrow shows non-dividing stem cells are mainly perisinusoidal. Nature *526*, 126-130. 10.1038/nature15250.

Adams, G.B., Chabner, K.T., Alley, I.R., Olson, D.P., Szczepiorkowski, Z.M., Poznansky, M.C., Kos, C.H., Pollak, M.R., Brown, E.M., and Scadden, D.T. (2006). Stem cell engraftment at the endosteal niche is specified by the calcium-sensing receptor. Nature *439*, 599-603. 10.1038/nature04247.

Aguirre, A., González, A., Navarro, M., Castaño, Ó., Planell, J.A., and Engel, E. (2012). Control of microenvironmental cues with a smart biomaterial composite promotes endothelial progenitor cell angiogenesis. Eur Cell Mater *24*, 90-106; discussion 106. 10.22203/ecm.v024a07.

Aguirre, A., González, A., Planell, J.A., and Engel, E. (2010). Extracellular calcium modulates in vitro bone marrow-derived Flk-1+ CD34+ progenitor cell chemotaxis and differentiation through a calcium-sensing receptor. Biochem Biophys Res Commun *393*, 156-161. 10.1016/j.bbrc.2010.01.109.

Ahuja, A., Tyagi, S., Seth, T., Pati, H.P., Gahlot, G., Tripathi, P., Somasundaram, V., and Saxena, R. (2018). Comparison of Immunohistochemistry, Cytochemistry, and Flow Cytometry in AML for Myeloperoxidase Detection. Indian J Hematol Blood Transfus *34*, 233-239. 10.1007/s12288-017-0849-1.

Alam, M.U., Kirton, J.P., Wilkinson, F.L., Towers, E., Sinha, S., Rouhi, M., Vizard, T.N., Sage, A.P., Martin, D., Ward, D.T., et al. (2009). Calcification is associated with loss of functional calcium-sensing receptor in vascular smooth muscle cells. Cardiovasc Res *81*, 260-268. 10.1093/cvr/cvn279.

Alharbi, R.A., Pettengell, R., Pandha, H.S., and Morgan, R. (2013). The role of HOX genes in normal hematopoiesis and acute leukemia. Leukemia *27*, 1000-1008. 10.1038/leu.2012.356.

Alper, O., Stetler-Stevenson, W.G., Harris, L.N., Leitner, W.W., Ozdemirli, M., Hartmann, D., Raffeld, M., Abu-Asab, M., Byers, S., Zhuang, Z., et al. (2009). Novel anti-filamin-A antibody

detects a secreted variant of filamin-A in plasma from patients with breast carcinoma and high-grade astrocytoma. Cancer Sci *100*, 1748-1756. 10.1111/j.1349-7006.2009.01244.x.

Alqudah, M.A., Azaizeh, M., Zayed, A., and Asaad, L. (2021). Calcium-sensing receptor antagonist NPS-2143 inhibits breast cancer cell proliferation, migration and invasion via downregulation of p-ERK1/2, Bcl-2 and Integrin β1 and induces caspase 3/7 activation. Advanced Pharmaceutical Bulletin.

Arai, F., Hirao, A., Ohmura, M., Sato, H., Matsuoka, S., Takubo, K., Ito, K., Koh, G.Y., and Suda, T. (2004). Tie2/angiopoietin-1 signaling regulates hematopoietic stem cell quiescence in the bone marrow niche. Cell *118*, 149-161. 10.1016/j.cell.2004.07.004.

Arber, D.A. (2019). The 2016 WHO classification of acute myeloid leukemia: What the practicing clinician needs to know. Semin Hematol *56*, 90-95. 10.1053/j.seminhematol.2018.08.002.

Arber, D.A., Orazi, A., Hasserjian, R., Thiele, J., Borowitz, M.J., Le Beau, M.M., Bloomfield, C.D., Cazzola, M., and Vardiman, J.W. (2016). The 2016 revision to the World Health Organization classification of myeloid neoplasms and acute leukemia. Blood *127*, 2391-2405. 10.1182/blood-2016-03-643544.

Armato, U., Chiarini, A., Chakravarthy, B., Chioffi, F., Pacchiana, R., Colarusso, E., Whitfield, J.F., and Dal Prà, I. (2013). Calcium-sensing receptor antagonist (calcilytic) NPS 2143 specifically blocks the increased secretion of endogenous Aβ42 prompted by exogenous fibrillary or soluble Aβ25-35 in human cortical astrocytes and neurons-therapeutic relevance to Alzheimer's disease. Biochim Biophys Acta *1832*, 1634-1652. 10.1016/j.bbadis.2013.04.020.

Awata, H., Huang, C., Handlogten, M.E., and Miller, R.T. (2001). Interaction of the calcium-sensing receptor and filamin, a potential scaffolding protein. J Biol Chem *276*, 34871-34879. 10.1074/jbc.M100775200.

Ayatollahi, H., Shajiei, A., Sadeghian, M.H., Sheikhi, M., Yazdandoust, E., Ghazanfarpour, M., Shams, S.F., and Shakeri, S. (2017). Prognostic Importance of C-KIT Mutations in Core Binding Factor Acute Myeloid Leukemia: A Systematic Review. Hematol Oncol Stem Cell Ther *10*, 1-7. 10.1016/j.hemonc.2016.08.005.

Babinsky, V.N., Hannan, F.M., Ramracheya, R.D., Zhang, Q., Nesbit, M.A., Hugill, A., Bentley, L., Hough, T.A., Joynson, E., Stewart, M., et al. (2017). Mutant Mice With Calcium-Sensing

Receptor Activation Have Hyperglycemia That Is Rectified by Calcilytic Therapy. Endocrinology *158*, 2486-2502. 10.1210/en.2017-00111.

Bachmann, A.S., Howard, J.P., and Vogel, C.W. (2006). Actin-binding protein filamin A is displayed on the surface of human neuroblastoma cells. Cancer Sci *97*, 1359-1365. 10.1111/j.1349-7006.2006.00327.x.

Bagur, R., and Hajnóczky, G. (2017). Intracellular Ca(2+) Sensing: Its Role in Calcium Homeostasis and Signaling. Mol Cell *66*, 780-788. 10.1016/j.molcel.2017.05.028.

Bai, M., Trivedi, S., and Brown, E.M. (1998a). Dimerization of the extracellular calcium-sensing receptor (CaR) on the cell surface of CaR-transfected HEK293 cells. J Biol Chem *273*, 23605-23610. 10.1074/jbc.273.36.23605.

Bai, M., Trivedi, S., Lane, C.R., Yang, Y., Quinn, S.J., and Brown, E.M. (1998b). Protein kinase C phosphorylation of threonine at position 888 in Ca2+o-sensing receptor (CaR) inhibits coupling to Ca2+ store release. J Biol Chem *273*, 21267-21275. 10.1074/jbc.273.33.21267.

Bajnok, A., Kaposi, A., Kovács, L., Vásárhelyi, B., Balog, A., and Toldi, G. (2013). Analysis by flow cytometry of calcium influx kinetics in peripheral lymphocytes of patients with rheumatoid arthritis. Cytometry A *83*, 287-293. 10.1002/cyto.a.22256.

Bandaru, S., Ala, C., Zhou, A.X., and Akyürek, L.M. (2021). Filamin A Regulates Cardiovascular Remodeling. Int J Mol Sci *22*. 10.3390/ijms22126555.

Barbui, T., Thiele, J., Gisslinger, H., Kvasnicka, H.M., Vannucchi, A.M., Guglielmelli, P., Orazi, A., and Tefferi, A. (2018). The 2016 WHO classification and diagnostic criteria for myeloproliferative neoplasms: document summary and in-depth discussion. Blood Cancer J *8*, 15. 10.1038/s41408-018-0054-y.

Barnett, S.C., and Evans, C.H. (1990). Influence of extracellular calcium on cell permeabilization and growth regulation by the lymphokine leukoregulin. J Cell Biochem *43*, 89-101. 10.1002/jcb.240430109.

Baron, J.A., Beach, M., Wallace, K., Grau, M.V., Sandler, R.S., Mandel, J.S., Heber, D., and Greenberg, E.R. (2005). Risk of prostate cancer in a randomized clinical trial of calcium supplementation. Cancer Epidemiol Biomarkers Prev *14*, 586-589. 10.1158/1055-9965.Epi-04-0319.

Bassan, R., and Hoelzer, D. (2011). Modern therapy of acute lymphoblastic leukemia. J Clin Oncol *29*, 532-543. 10.1200/jco.2010.30.1382.

Battula, V.L., Le, P.M., Sun, J.C., Nguyen, K., Yuan, B., Zhou, X., Sonnylal, S., McQueen, T., Ruvolo, V., Michel, K.A., et al. (2017). AML-induced osteogenic differentiation in mesenchymal stromal cells supports leukemia growth. JCI Insight *2*. 10.1172/jci.insight.90036.

Bedolla, R.G., Wang, Y., Asuncion, A., Chamie, K., Siddiqui, S., Mudryj, M.M., Prihoda, T.J., Siddiqui, J., Chinnaiyan, A.M., Mehra, R., et al. (2009). Nuclear versus cytoplasmic localization of filamin A in prostate cancer: immunohistochemical correlation with metastases. Clin Cancer Res *15*, 788-796. 10.1158/1078-0432.Ccr-08-1402.

Berridge, M.J., Lipp, P., and Bootman, M.D. (2000). The versatility and universality of calcium signalling. Nat Rev Mol Cell Biol *1*, 11-21. 10.1038/35036035.

Blank, U., Karlsson, G., and Karlsson, S. (2008). Signaling pathways governing stem-cell fate. Blood *111*, 492-503. 10.1182/blood-2007-07-075168.

Blau, O., Hofmann, W.K., Baldus, C.D., Thiel, G., Serbent, V., Schümann, E., Thiel, E., and Blau, I.W. (2007). Chromosomal aberrations in bone marrow mesenchymal stroma cells from patients with myelodysplastic syndrome and acute myeloblastic leukemia. Exp Hematol *35*, 221-229. 10.1016/j.exphem.2006.10.012.

Bonnet, D., and Dick, J.E. (1997). Human acute myeloid leukemia is organized as a hierarchy that originates from a primitive hematopoietic cell. Nat Med *3*, 730-737. 10.1038/nm0797-730.

Brennan, S.C., Mun, H.C., Leach, K., Kuchel, P.W., Christopoulos, A., and Conigrave, A.D. (2015). Receptor expression modulates calcium-sensing receptor mediated intracellular Ca2+ mobilization. Endocrinology *156*, 1330-1342. 10.1210/en.2014-1771.

Brennan, S.C., Thiem, U., Roth, S., Aggarwal, A., Fetahu, I., Tennakoon, S., Gomes, A.R., Brandi, M.L., Bruggeman, F., Mentaverri, R., et al. (2013). Calcium sensing receptor signalling in physiology and cancer. Biochim Biophys Acta *1833*, 1732-1744. 10.1016/j.bbamcr.2012.12.011.

Breuksch, I., Weinert, M., and Brenner, W. (2016). The role of extracellular calcium in bone metastasis. J Bone Oncol *5*, 143-145. 10.1016/j.jbo.2016.06.004.

Bronner, F. (1997). Adaptation and nutritional needs. Am J Clin Nutr *65*, 1570. 10.1093/ajcn/65.5.1570.

Bronte, V., Brandau, S., Chen, S.-H., Colombo, M.P., Frey, A.B., Greten, T.F., Mandruzzato, S., Murray, P.J., Ochoa, A., Ostrand-Rosenberg, S., et al. (2016). Recommendations for myeloid-derived suppressor cell nomenclature and characterization standards. Nature Communications *7*, 12150. 10.1038/ncomms12150.

Brooker, A.S., and Berkowitz, K.M. (2014). The roles of cohesins in mitosis, meiosis, and human health and disease. Methods Mol Biol *1170*, 229-266. 10.1007/978-1-4939-0888-2_11.

Brown, E., Enyedi, P., LeBoff, M., Rotberg, J., Preston, J., and Chen, C. (1987). High extracellular Ca2+ and Mg2+ stimulate accumulation of inositol phosphates in bovine parathyroid cells. FEBS Lett *218*, 113-118. 10.1016/0014-5793(87)81029-3.

Brown, E.M. (1991). Extracellular Ca2+ sensing, regulation of parathyroid cell function, and role of Ca2+ and other ions as extracellular (first) messengers. Physiol Rev *71*, 371-411. 10.1152/physrev.1991.71.2.371.

Brown, E.M., Butters, R., Katz, C., and Kifor, O. (1991a). Neomycin mimics the effects of high extracellular calcium concentrations on parathyroid function in dispersed bovine parathyroid cells. Endocrinology *128*, 3047-3054. 10.1210/endo-128-6-3047.

Brown, E.M., Gamba, G., Riccardi, D., Lombardi, M., Butters, R., Kifor, O., Sun, A., Hediger, M.A., Lytton, J., and Hebert, S.C. (1993). Cloning and characterization of an extracellular Ca(2+)-sensing receptor from bovine parathyroid. Nature *366*, 575-580. 10.1038/366575a0.

Brown, E.M., Katz, C., Butters, R., and Kifor, O. (1991b). Polyarginine, polylysine, and protamine mimic the effects of high extracellular calcium concentrations on dispersed bovine parathyroid cells. J Bone Miner Res *6*, 1217-1225. 10.1002/jbmr.5650061112.

Buza-Vidas, N., Antonchuk, J., Qian, H., Månsson, R., Luc, S., Zandi, S., Anderson, K., Takaki, S., Nygren, J.M., Jensen, C.T., and Jacobsen, S.E. (2006). Cytokines regulate postnatal hematopoietic stem cell expansion: opposing roles of thrombopoietin and LNK. Genes Dev *20*, 2018-2023. 10.1101/gad.385606.

Byrd, J.C., Mrózek, K., Dodge, R.K., Carroll, A.J., Edwards, C.G., Arthur, D.C., Pettenati, M.J., Patil, S.R., Rao, K.W., Watson, M.S., et al. (2002). Pretreatment cytogenetic abnormalities are predictive of induction success, cumulative incidence of relapse, and overall survival in adult patients with de novo acute myeloid leukemia: results from Cancer and Leukemia Group B (CALGB 8461). Blood *100*, 4325-4336. 10.1182/blood-2002-03-0772.

Calvi, L.M., Adams, G.B., Weibrecht, K.W., Weber, J.M., Olson, D.P., Knight, M.C., Martin, R.P., Schipani, E., Divieti, P., Bringhurst, F.R., et al. (2003). Osteoblastic cells regulate the haematopoietic stem cell niche. Nature *425*, 841-846. 10.1038/nature02040.

Calvi, L.M., Sims, N.A., Hunzelman, J.L., Knight, M.C., Giovannetti, A., Saxton, J.M., Kronenberg, H.M., Baron, R., and Schipani, E. (2001). Activated parathyroid hormone/parathyroid hormone-related protein receptor in osteoblastic cells differentially affects cortical and trabecular bone. J Clin Invest *107*, 277-286. 10.1172/jci11296.

Canaff, L., and Hendy, G.N. (2002). Human calcium-sensing receptor gene. Vitamin D response elements in promoters P1 and P2 confer transcriptional responsiveness to 1,25-dihydroxyvitamin D. J Biol Chem *277*, 30337-30350. 10.1074/jbc.M201804200.

Cancilla, D., Rettig, M.P., and DiPersio, J.F. (2020). Targeting CXCR4 in AML and ALL. Front Oncol *10*, 1672. 10.3389/fonc.2020.01672.

Casalà, C., Gil-Guiñón, E., Ordóñez, J.L., Miguel-Queralt, S., Rodríguez, E., Galván, P., Lavarino, C., Munell, F., de Alava, E., Mora, J., and de Torres, C. (2013). The calcium-sensing receptor is silenced by genetic and epigenetic mechanisms in unfavorable neuroblastomas and its reactivation induces ERK1/2-dependent apoptosis. Carcinogenesis *34*, 268-276. 10.1093/carcin/bgs338.

Chagastelles, P.C., and Nardi, N.B. (2011). Biology of stem cells: an overview. Kidney Int Suppl (2011) *1*, 63-67. 10.1038/kisup.2011.15.

Chakravarti, B., Chattopadhyay, N., and Brown, E.M. (2012). Signaling through the extracellular calcium-sensing receptor (CaSR). Adv Exp Med Biol *740*, 103-142. 10.1007/978-94-007-2888-2_5.

Challen, G.A., Sun, D., Jeong, M., Luo, M., Jelinek, J., Berg, J.S., Bock, C., Vasanthakumar, A., Gu, H., Xi, Y., et al. (2011). Dnmt3a is essential for hematopoietic stem cell differentiation. Nature genetics *44*, 23-31. 10.1038/ng.1009.

Chambers, A.F., Naumov, G.N., Varghese, H.J., Nadkarni, K.V., MacDonald, I.C., and Groom, A.C. (2001). Critical steps in hematogenous metastasis: an overview. Surg Oncol Clin N Am *10*, 243-255, vii.

Chang, F., Steelman, L., Lee, J., Shelton, J., Navolanic, P., Blalock, W.L., Franklin, R., and McCubrey, J. (2003). Signal transduction mediated by the Ras/Raf/MEK/ERK pathway from

cytokine receptors to transcription factors: potential targeting for therapeutic intervention. Leukemia (08876924) *17*.

Chang, W., Pratt, S., Chen, T.H., Nemeth, E., Huang, Z., and Shoback, D. (1998). Coupling of calcium receptors to inositol phosphate and cyclic AMP generation in mammalian cells and Xenopus laevis oocytes and immunodetection of receptor protein by region-specific antipeptide antisera. J Bone Miner Res *13*, 570-580. 10.1359/jbmr.1998.13.4.570.

Chen, J.Y., Miyanishi, M., Wang, S.K., Yamazaki, S., Sinha, R., Kao, K.S., Seita, J., Sahoo, D., Nakauchi, H., and Weissman, I.L. (2016). Hoxb5 marks long-term haematopoietic stem cells and reveals a homogenous perivascular niche. Nature *530*, 223-227. 10.1038/nature16943.

Chen, S.J., Bao, L., Keefer, K., Shanmughapriya, S., Chen, L., Lee, J., Wang, J., Zhang, X.Q., Hirschler-Laszkiewicz, I., Merali, S., et al. (2020). Transient receptor potential ion channel TRPM2 promotes AML proliferation and survival through modulation of mitochondrial function, ROS, and autophagy. Cell Death Dis *11*, 247. 10.1038/s41419-020-2454-8.

Chen, W., Kumar, A.R., Hudson, W.A., Li, Q., Wu, B., Staggs, R.A., Lund, E.A., Sam, T.N., and Kersey, J.H. (2008). Malignant transformation initiated by Mll-AF9: gene dosage and critical target cells. Cancer cell *13*, 432-440. 10.1016/j.ccr.2008.03.005.

Chen, W., and Moore, M.J. (2015). Spliceosomes. Curr Biol *25*, R181-183. 10.1016/j.cub.2014.11.059.

Chen, X., Burkhardt, D.B., Hartman, A.A., Hu, X., Eastman, A.E., Sun, C., Wang, X., Zhong, M., Krishnaswamy, S., and Guo, S. (2019). MLL-AF9 initiates transformation from fast-proliferating myeloid progenitors. Nature Communications *10*, 5767. 10.1038/s41467-019-13666-5.

Chen, Y., Jacamo, R., Shi, Y.X., Wang, R.Y., Battula, V.L., Konoplev, S., Strunk, D., Hofmann, N.A., Reinisch, A., Konopleva, M., and Andreeff, M. (2012). Human extramedullary bone marrow in mice: a novel in vivo model of genetically controlled hematopoietic microenvironment. Blood *119*, 4971-4980. 10.1182/blood-2011-11-389957.

Cheng, S.X., Lightfoot, Y.L., Yang, T., Zadeh, M., Tang, L., Sahay, B., Wang, G.P., Owen, J.L., and Mohamadzadeh, M. (2014). Epithelial CaSR deficiency alters intestinal integrity and promotes proinflammatory immune responses. FEBS Lett *588*, 4158-4166. 10.1016/j.febslet.2014.05.007.

Cheng, Y., Qu, J., Che, X., Xu, L., Song, N., Ma, Y., Gong, J., Qu, X., and Liu, Y. (2017). CXCL12/SDF-1α induces migration via SRC-mediated CXCR4-EGFR cross-talk in gastric cancer cells. Oncol Lett *14*, 2103-2110. 10.3892/ol.2017.6389.

Chiarini, A., Armato, U., Liu, D., and Dal Prà, I. (2017). Calcium-Sensing Receptor Antagonist NPS 2143 Restores Amyloid Precursor Protein Physiological Non-Amyloidogenic Processing in Aβ-Exposed Adult Human Astrocytes. Sci Rep *7*, 1277. 10.1038/s41598-017-01215-3.

Chiu, P.P., Jiang, H., and Dick, J.E. (2010). Leukemia-initiating cells in human T-lymphoblastic leukemia exhibit glucocorticoid resistance. Blood *116*, 5268-5279. 10.1182/blood-2010-06-292300.

Chou, W.C., Chou, S.C., Liu, C.Y., Chen, C.Y., Hou, H.A., Kuo, Y.Y., Lee, M.C., Ko, B.S., Tang, J.L., Yao, M., et al. (2011). TET2 mutation is an unfavorable prognostic factor in acute myeloid leukemia patients with intermediate-risk cytogenetics. Blood *118*, 3803-3810. 10.1182/blood-2011-02-339747.

Christodoulou, C., Spencer, J.A., Yeh, S.A., Turcotte, R., Kokkaliaris, K.D., Panero, R., Ramos, A., Guo, G., Seyedhassantehrani, N., Esipova, T.V., et al. (2020). Live-animal imaging of native haematopoietic stem and progenitor cells. Nature *578*, 278-283. 10.1038/s41586-020-1971-z.

Cilloni, D., and Saglio, G. (2012). Molecular pathways: BCR-ABL. Clin Cancer Res *18*, 930-937. 10.1158/1078-0432.Ccr-10-1613.

Cimmino, L., Dolgalev, I., Wang, Y., Yoshimi, A., Martin, G.H., Wang, J., Ng, V., Xia, B., Witkowski, M.T., Mitchell-Flack, M., et al. (2017). Restoration of TET2 Function Blocks Aberrant Self-Renewal and Leukemia Progression. Cell *170*, 1079-1095.e1020. 10.1016/j.cell.2017.07.032.

Coleman, R.E. (2001). Metastatic bone disease: clinical features, pathophysiology and treatment strategies. Cancer Treat Rev *27*, 165-176. 10.1053/ctrv.2000.0210.

Conley, Y.P., Mukherjee, A., Kammerer, C., DeKosky, S.T., Kamboh, M.I., Finegold, D.N., and Ferrell, R.E. (2009). Evidence supporting a role for the calcium-sensing receptor in Alzheimer disease. Am J Med Genet B Neuropsychiatr Genet *150b*, 703-709. 10.1002/ajmg.b.30896.

Copelan, E.A., Grunwald, M.R., Druhan, L.J., and Avalos, B.R. (2015). Use of molecular markers to determine postremission treatment in acute myeloid leukemia with normal cytogenetics. Hematology/Oncology and Stem Cell Therapy *8*, 143-149.

Corbin, A.S., Agarwal, A., Loriaux, M., Cortes, J., Deininger, M.W., and Druker, B.J. (2011). Human chronic myeloid leukemia stem cells are insensitive to imatinib despite inhibition of BCR-ABL activity. J Clin Invest *121*, 396-409. 10.1172/jci35721.

Crcareva, A., Saito, T., Kunisato, A., Kumano, K., Suzuki, T., Sakata-Yanagimoto, M., Kawazu, M., Stojanovic, A., Kurokawa, M., Ogawa, S., et al. (2005). Hematopoietic stem cells expanded by fibroblast growth factor-1 are excellent targets for retrovirus-mediated gene delivery. Exp Hematol *33*, 1459-1469. 10.1016/j.exphem.2005.09.001.

Dash, A., and Gilliland, D.G. (2001). Molecular genetics of acute myeloid leukaemia. Best Pract Res Clin Haematol *14*, 49-64. 10.1053/beha.2000.0115.

Daver, N., Cortes, J., Ravandi, F., Patel, K.P., Burger, J.A., Konopleva, M., and Kantarjian, H. (2015). Secondary mutations as mediators of resistance to targeted therapy in leukemia. Blood *125*, 3236-3245. 10.1182/blood-2014-10-605808.

De Jesus Ferreira, M.C., and Bailly, C. (1998). Extracellular Ca2+ decreases chloride reabsorption in rat CTAL by inhibiting cAMP pathway. Am J Physiol *275*, F198-203. 10.1152/ajprenal.1998.275.2.F198.

Dhanasekaran, S.M., Barrette, T.R., Ghosh, D., Shah, R., Varambally, S., Kurachi, K., Pienta, K.J., Rubin, M.A., and Chinnaiyan, A.M. (2001). Delineation of prognostic biomarkers in prostate cancer. Nature *412*, 822-826. 10.1038/35090585.

Díaz-Soto, G., Rocher, A., García-Rodríguez, C., Núñez, L., and Villalobos, C. (2016). The Calcium-Sensing Receptor in Health and Disease. Int Rev Cell Mol Biol *327*, 321-369. 10.1016/bs.ircmb.2016.05.004.

Dillon, M.L., and Frazee, L.A. (2011). Cinacalcet for the treatment of primary hyperparathyroidism. Am J Ther *18*, 313-322. 10.1097/MJT.0b013e3181bdc3d0.

Döhner, H., Weisdorf, D.J., and Bloomfield, C.D. (2015). Acute Myeloid Leukemia. N Engl J Med *373*, 1136-1152. 10.1056/NEJMra1406184.

Dolnik, A., Engelmann, J.C., Scharfenberger-Schmeer, M., Mauch, J., Kelkenberg-Schade, S., Haldemann, B., Fries, T., Krönke, J., Kühn, M.W., Paschka, P., et al. (2012). Commonly altered genomic regions in acute myeloid leukemia are enriched for somatic mutations involved in chromatin remodeling and splicing. Blood *120*, e83-92. 10.1182/blood-2011-12-401471.

Dong, L., Yu, W.M., Zheng, H., Loh, M.L., Bunting, S.T., Pauly, M., Huang, G., Zhou, M., Broxmeyer, H.E., Scadden, D.T., and Qu, C.K. (2016). Leukaemogenic effects of Ptpn11 activating mutations in the stem cell microenvironment. Nature *539*, 304-308. 10.1038/nature20131.

Druker, B.J., Guilhot, F., O'Brien, S.G., Gathmann, I., Kantarjian, H., Gattermann, N., Deininger, M.W., Silver, R.T., Goldman, J.M., Stone, R.M., et al. (2006). Five-year follow-up of patients receiving imatinib for chronic myeloid leukemia. N Engl J Med *355*, 2408-2417. 10.1056/NEJMoa062867.

Duan, C.W., Shi, J., Chen, J., Wang, B., Yu, Y.H., Qin, X., Zhou, X.C., Cai, Y.J., Li, Z.Q., Zhang, F., et al. (2014). Leukemia propagating cells rebuild an evolving niche in response to therapy. Cancer Cell *25*, 778-793. 10.1016/j.ccr.2014.04.015.

Duarte, D., Hawkins, E.D., Akinduro, O., Ang, H., De Filippo, K., Kong, I.Y., Haltalli, M., Ruivo, N., Straszkowski, L., Vervoort, S.J., et al. (2018). Inhibition of Endosteal Vascular Niche Remodeling Rescues Hematopoietic Stem Cell Loss in AML. Cell Stem Cell *22*, 64-77.e66.

Duncan, A.W., Rattis, F.M., DiMascio, L.N., Congdon, K.L., Pazianos, G., Zhao, C., Yoon, K., Cook, J.M., Willert, K., Gaiano, N., and Reya, T. (2005). Integration of Notch and Wnt signaling in hematopoietic stem cell maintenance. Nat Immunol *6*, 314-322. 10.1038/ni1164.

Duval, D., Lardeux, A., Le Tourneau, T., Norris, R.A., Markwald, R.R., Sauzeau, V., Probst, V., Le Marec, H., Levine, R., Schott, J.J., and Merot, J. (2014). Valvular dystrophy associated filamin A mutations reveal a new role of its first repeats in small-GTPase regulation. Biochimica et Biophysica Acta (BBA) - Molecular Cell Research *1843*, 234-244.

Dvorak, M.M., Chen, T.H., Orwoll, B., Garvey, C., Chang, W., Bikle, D.D., and Shoback, D.M. (2007). Constitutive activity of the osteoblast Ca2+-sensing receptor promotes loss of cancellous bone. Endocrinology *148*, 3156-3163. 10.1210/en.2007-0147.

ElNahass, Y.H., Badawy, R.H., ElRefaey, F.A., Nooh, H.A., Ibrahiem, D., Nader, H.A., Mahmoud, H.K., and ElMetnawy, W.H. (2020). IDH Mutations in AML Patients; A higher Association with Intermediate Risk Cytogenetics. Asian Pac J Cancer Prev *21*, 721-725. 10.31557/APJCP.2020.21.3.721.

Enz, R. (2007). The trick of the tail: protein-protein interactions of metabotropic glutamate receptors. Bioessays *29*, 60-73. 10.1002/bies.20518.

Essers, M.A., and Trumpp, A. (2010). Targeting leukemic stem cells by breaking their dormancy. Mol Oncol *4*, 443-450. 10.1016/j.molonc.2010.06.001.

Falini, B., Bolli, N., Liso, A., Martelli, M.P., Mannucci, R., Pileri, S., and Nicoletti, I. (2009). Altered nucleophosmin transport in acute myeloid leukaemia with mutated NPM1: molecular basis and clinical implications. Leukemia *23*, 1731-1743. 10.1038/leu.2009.124.

Falini, B., Mecucci, C., Tiacci, E., Alcalay, M., Rosati, R., Pasqualucci, L., La Starza, R., Diverio, D., Colombo, E., Santucci, A., et al. (2005). Cytoplasmic nucleophosmin in acute myelogenous leukemia with a normal karyotype. N Engl J Med *352*, 254-266. 10.1056/NEJMoa041974.

Feng, J., Xu, X., Li, B., Brown, E., Farris, A.B., Sun, S.Y., and Yang, J.J. (2014). Prostate cancer metastatic to bone has higher expression of the calcium-sensing receptor (CaSR) than primary prostate cancer. Receptors Clin Investig *1*. 10.14800/rci.270.

Feng, Y., and Walsh, C.A. (2004). The many faces of filamin: a versatile molecular scaffold for cell motility and signalling. Nat Cell Biol *6*, 1034-1038. 10.1038/ncb1104-1034.

Ferrara, F., and Schiffer, C.A. (2013). Acute myeloid leukaemia in adults. The Lancet *381*, 484-495.

Fetahu, I.S., Höbaus, J., Aggarwal, A., Hummel, D.M., Tennakoon, S., Mesteri, I., Baumgartner-Parzer, S., and Kállay, E. (2014). Calcium-sensing receptor silencing in colorectal cancer is associated with promoter hypermethylation and loss of acetylation on histone 3. Int J Cancer *135*, 2014-2023. 10.1002/ijc.28856.

Fidyk, W., Mitrus, I., Ciomber, A., Smagur, A., Chwieduk, A., Głowala-Kosińska, M., and Giebel, S. (2018). Evaluation of proinflammatory and immunosuppressive cytokines in blood and bone marrow of healthy hematopoietic stem cell donors. Cytokine *102*, 181-186. 10.1016/j.cyto.2017.09.001.

Fisher, J.B., McNulty, M., Burke, M.J., Crispino, J.D., and Rao, S. (2017). Cohesin Mutations in Myeloid Malignancies. Trends Cancer *3*, 282-293. 10.1016/j.trecan.2017.02.006.

Flanagan, L.A., Chou, J., Falet, H., Neujahr, R., Hartwig, J.H., and Stossel, T.P. (2001). Filamin A, the Arp2/3 complex, and the morphology and function of cortical actin filaments in human melanoma cells. J Cell Biol *155*, 511-517. 10.1083/jcb.200105148.

Frees, S., Breuksch, I., Haber, T., Bauer, H.K., Chavez-Munoz, C., Raven, P., Moskalev, I., N, D.C., Tan, Z., Daugaard, M., et al. (2018). Calcium-sensing receptor (CaSR) promotes development of bone metastasis in renal cell carcinoma. Oncotarget *9*, 15766-15779. 10.18632/oncotarget.24607.

Frisch, B.J., Ashton, J.M., Xing, L., Becker, M.W., Jordan, C.T., and Calvi, L.M. (2012). Functional inhibition of osteoblastic cells in an in vivo mouse model of myeloid leukemia. Blood *119*, 540-550. 10.1182/blood-2011-04-348151.

Gaidzik, V., and Döhner, K. (2008). Prognostic implications of gene mutations in acute myeloid leukemia with normal cytogenetics. Semin Oncol *35*, 346-355. 10.1053/j.seminoncol.2008.04.005.

Gaidzik, V.I., Teleanu, V., Papaemmanuil, E., Weber, D., Paschka, P., Hahn, J., Wallrabenstein, T., Kolbinger, B., Köhne, C.H., Horst, H.A., et al. (2016). RUNX1 mutations in acute myeloid leukemia are associated with distinct clinico-pathologic and genetic features. Leukemia *30*, 2160-2168. 10.1038/leu.2016.126.

Gama, L., Wilt, S.G., and Breitwieser, G.E. (2001). Heterodimerization of calcium sensing receptors with metabotropic glutamate receptors in neurons. J Biol Chem *276*, 39053-39059. 10.1074/jbc.M105662200.

Gandillet, A., Park, S., Lassailly, F., Griessinger, E., Vargaftig, J., Filby, A., Lister, T.A., and Bonnet, D. (2011). Heterogeneous sensitivity of human acute myeloid leukemia to β-catenin down-modulation. Leukemia *25*, 770-780. 10.1038/leu.2011.17.

Garrett, J.E., Capuano, I.V., Hammerland, L.G., Hung, B.C., Brown, E.M., Hebert, S.C., Nemeth, E.F., and Fuller, F. (1995). Molecular cloning and functional expression of human parathyroid calcium receptor cDNAs. J Biol Chem *270*, 12919-12925. 10.1074/jbc.270.21.12919.

Gavrilescu, L.C., and Van Etten, R.A. (2008). Murine retroviral bone marrow transplantation models for the study of human myeloproliferative disorders. Curr Protoc Pharmacol *Chapter 14*, Unit14.10. 10.1002/0471141755.ph1410s43.

Gelsi-Boyer, V., Brecqueville, M., Devillier, R., Murati, A., Mozziconacci, M.-J., and Birnbaum, D. (2012). Mutations in ASXL1 are associated with poor prognosis across the spectrum of malignant myeloid diseases. Journal of Hematology & Oncology *5*, 12. 10.1186/1756-8722-5-12.

Godavarthy, P.S., Kumar, R., Herkt, S.C., Pereira, R.S., Hayduk, N., Weissenberger, E.S., Aggoune, D., Manavski, Y., Lucas, T., Pan, K.T., et al. (2020). The vascular bone marrow niche influences outcome in chronic myeloid leukemia via the E-selectin - SCL/TAL1 - CD44 axis. Haematologica *105*, 136-147. 10.3324/haematol.2018.212365.

Godwin, S.L., and Soltoff, S.P. (1997). Extracellular calcium and platelet-derived growth factor promote receptor-mediated chemotaxis in osteoblasts through different signaling pathways. J Biol Chem *272*, 11307-11312. 10.1074/jbc.272.17.11307.

Gómez-Moutón, C., Fischer, T., Peregil, R.M., Jiménez-Baranda, S., Stossel, T.P., Nakamura, F., and Mañes, S. (2015). Filamin A interaction with the CXCR4 third intracellular loop regulates endocytosis and signaling of WT and WHIM-like receptors. Blood *125*, 1116-1125. 10.1182/blood-2014-09-601807.

Gong, J.K. (1978). Endosteal marrow: a rich source of hematopoietic stem cells. Science *199*, 1443-1445. 10.1126/science.75570.

Gorczyca, W., Sun, Z.Y., Cronin, W., Li, X., Mau, S., and Tugulea, S. (2011). Immunophenotypic pattern of myeloid populations by flow cytometry analysis. Methods Cell Biol *103*, 221-266. 10.1016/b978-0-12-385493-3.00010-3.

Grassinger, J., Haylock, D.N., Williams, B., Olsen, G.H., and Nilsson, S.K. (2010). Phenotypically identical hemopoietic stem cells isolated from different regions of bone marrow have different biologic potential. Blood *116*, 3185-3196. 10.1182/blood-2009-12-260703.

Grimwade, D. (2007). Impact of Cytogenetics on Clinical Outcome in AML. In Acute Myelogenous Leukemia, J.E. Karp, ed. (Humana Press), pp. 177-192. 10.1007/978-1-59745-322-6_8.

Grimwade, D., Hills, R.K., Moorman, A.V., Walker, H., Chatters, S., Goldstone, A.H., Wheatley, K., Harrison, C.J., and Burnett, A.K. (2010). Refinement of cytogenetic classification in acute myeloid leukemia: determination of prognostic significance of rare recurring chromosomal abnormalities among 5876 younger adult patients treated in the United Kingdom Medical Research Council trials. Blood *116*, 354-365. 10.1182/blood-2009-11-254441.

Gruszka, A.M., Valli, D., and Alcalay, M. (2019). Wnt Signalling in Acute Myeloid Leukaemia. Cells *8*. 10.3390/cells8111403.

Guise, T. (2010). Examining the metastatic niche: targeting the microenvironment. Semin Oncol *37 Suppl 2*, S2-14. 10.1053/j.seminoncol.2010.10.007.

Haddy, T.B., Mosher, R.B., and Reaman, G.H. (2001). Osteoporosis in survivors of acute lymphoblastic leukemia. Oncologist *6*, 278-285. 10.1634/theoncologist.6-3-278.

Hammond, C.M., Shi, Y., White, D., Cervi, D., Tomic, J., and Spaner, D.E. (2009). The B-cell calcium sensor predicts progression of chronic lymphocytic leukemia. Leukemia *23*, 426-429. 10.1038/leu.2008.351.

Hammond, C.M., White, D., Tomic, J., Shi, Y., and Spaner, D.E. (2007). Extracellular calcium sensing promotes human B-cell activation and function. Blood *110*, 3985-3995. 10.1182/blood-2007-05-088468.

Han, C., Gao, X., Li, Y., Zhang, J., Yang, E., Zhang, L., and Yu, L. (2021). Characteristics of Cohesin Mutation in Acute Myeloid Leukemia and Its Clinical Significance. Front Oncol *11*, 579881. 10.3389/fonc.2021.579881.

Hanahan, D., and Weinberg, R.A. (2000). The hallmarks of cancer. Cell *100*, 57-70. 10.1016/s0092-8674(00)81683-9.

Handlogten, M.E., Huang, C., Shiraishi, N., Awata, H., and Miller, R.T. (2001). The Ca2+-sensing receptor activates cytosolic phospholipase A2 via a Gqalpha -dependent ERK-independent pathway. J Biol Chem *276*, 13941-13948. 10.1074/jbc.M007306200.

Hannan, F.M., Babinsky, V.N., and Thakker, R.V. (2016). Disorders of the calcium-sensing receptor and partner proteins: insights into the molecular basis of calcium homeostasis. J Mol Endocrinol *57*, R127-142. 10.1530/jme-16-0124.

Hannan, F.M., Walls, G.V., Babinsky, V.N., Nesbit, M.A., Kallay, E., Hough, T.A., Fraser, W.D., Cox, R.D., Hu, J., Spiegel, A.M., and Thakker, R.V. (2015). The Calcilytic Agent NPS 2143 Rectifies Hypocalcemia in a Mouse Model With an Activating Calcium-Sensing Receptor (CaSR) Mutation: Relevance to Autosomal Dominant Hypocalcemia Type 1 (ADH1). Endocrinology *156*, 3114-3121. 10.1210/en.2015-1269.

Hanoun, M., Zhang, D., Mizoguchi, T., Pinho, S., Pierce, H., Kunisaki, Y., Lacombe, J., Armstrong, Scott A., Dührsen, U., and Frenette, Paul S. (2014). Acute Myelogenous Leukemia-Induced Sympathetic Neuropathy Promotes Malignancy in an Altered Hematopoietic Stem Cell Niche. Cell Stem Cell *15*, 365-375.

Harper, D.P., and Aplan, P.D. (2008). Chromosomal rearrangements leading to MLL gene fusions: clinical and biological aspects. Cancer Res *68*, 10024-10027. 10.1158/0008-5472.Can-08-2208.

Harrison, C.J., Moorman, A.V., Broadfield, Z.J., Cheung, K.L., Harris, R.L., Reza Jalali, G., Robinson, H.M., Barber, K.E., Richards, S.M., Mitchell, C.D., et al. (2004). Three distinct subgroups of hypodiploidy in acute lymphoblastic leukaemia. Br J Haematol *125*, 552-559. 10.1111/j.1365-2141.2004.04948.x.

Hassan, H.T., and Zander, A. (1996). Stem cell factor as a survival and growth factor in human normal and malignant hematopoiesis. Acta Haematol *95*, 257-262. 10.1159/000203893.

Haven, C.J., van Puijenbroek, M., Karperien, M., Fleuren, G.J., and Morreau, H. (2004). Differential expression of the calcium sensing receptor and combined loss of chromosomes 1q and 11q in parathyroid carcinoma. J Pathol *202*, 86-94. 10.1002/path.1489.

Haylock, D., and Nilsson, S. (2005). Stem Cell Regulation by the Haemopoietic Stem Cell Niche. Cell cycle (Georgetown, Tex.) *4*, 1353-1355. 10.4161/cc.4.10.2056.

He, X., Wan, J., Yang, X., Zhang, X., Huang, D., Li, X., Zou, Y., Chen, C., Yu, Z., Xie, L., et al. (2021). Bone marrow niche ATP levels determine leukemia-initiating cell activity via P2X7 in leukemic models. J Clin Invest *131*. 10.1172/jci140242.

Hendy, G.N., and Canaff, L. (2016). Calcium-Sensing Receptor Gene: Regulation of Expression. Front Physiol *7*, 394. 10.3389/fphys.2016.00394.

Hendy, G.N., D'Souza-Li, L., Yang, B., Canaff, L., and Cole, D.E. (2000). Mutations of the calcium-sensing receptor (CASR) in familial hypocalciuric hypercalcemia, neonatal severe hyperparathyroidism, and autosomal dominant hypocalcemia. Hum Mutat *16*, 281-296. 10.1002/1098-1004(200010)16:4<281::Aid-humu1>3.0.Co;2-a.

Hjälm, G., MacLeod, R.J., Kifor, O., Chattopadhyay, N., and Brown, E.M. (2001). Filamin-A binds to the carboxyl-terminal tail of the calcium-sensing receptor, an interaction that participates in CaR-mediated activation of mitogen-activated protein kinase. J Biol Chem *276*, 34880-34887. 10.1074/jbc.M100784200.

Ho, C., Conner, D.A., Pollak, M.R., Ladd, D.J., Kifor, O., Warren, H.B., Brown, E.M., Seidman, J.G., and Seidman, C.E. (1995). A mouse model of human familial hypocalciuric hypercalcemia and neonatal severe hyperparathyroidism. Nature Genetics *11*, 389-394. 10.1038/ng1295-389.

Ho, P.A., Alonzo, T.A., Gerbing, R.B., Pollard, J., Stirewalt, D.L., Hurwitz, C., Heerema, N.A., Hirsch, B., Raimondi, S.C., Lange, B., et al. (2009). Prevalence and prognostic implications of

CEBPA mutations in pediatric acute myeloid leukemia (AML): a report from the Children's Oncology Group. Blood *113*, 6558-6566. 10.1182/blood-2008-10-184747.

Hobson, S.A., Wright, J., Lee, F., McNeil, S.E., Bilderback, T., and Rodland, K.D. (2003). Activation of the MAP kinase cascade by exogenous calcium-sensing receptor. Mol Cell Endocrinol *200*, 189-198. 10.1016/s0303-7207(01)00749-3.

Hochhaus, A., Baccarani, M., Silver, R.T., Schiffer, C., Apperley, J.F., Cervantes, F., Clark, R.E., Cortes, J.E., Deininger, M.W., Guilhot, F., et al. (2020). European LeukemiaNet 2020 recommendations for treating chronic myeloid leukemia. Leukemia *34*, 966-984. 10.1038/s41375-020-0776-2.

Hofer, A.M., and Brown, E.M. (2003). Extracellular calcium sensing and signalling. Nat Rev Mol Cell Biol *4*, 530-538. 10.1038/nrm1154.

House, M.G., Kohlmeier, L., Chattopadhyay, N., Kifor, O., Yamaguchi, T., Leboff, M.S., Glowacki, J., and Brown, E.M. (1997). Expression of an extracellular calcium-sensing receptor in human and mouse bone marrow cells. J Bone Miner Res *12*, 1959-1970. 10.1359/jbmr.1997.12.12.1959.

Hu, Y., and Smyth, G.K. (2009). ELDA: extreme limiting dilution analysis for comparing depleted and enriched populations in stem cell and other assays. J Immunol Methods *347*, 70-78. 10.1016/j.jim.2009.06.008.

Huang, C., Hujer, K.M., Wu, Z., and Miller, R.T. (2004). The Ca2+-sensing receptor couples to Galpha12/13 to activate phospholipase D in Madin-Darby canine kidney cells. Am J Physiol Cell Physiol *286*, C22-30. 10.1152/ajpcell.00229.2003.

Huang, C., Wu, Z., Hujer, K.M., and Miller, R.T. (2006). Silencing of filamin A gene expression inhibits Ca2+ -sensing receptor signaling. FEBS Lett *580*, 1795-1800. 10.1016/j.febslet.2006.02.035.

Huang, W., Lu, C., Wu, Y., Ouyang, S., and Chen, Y. (2015). T-type calcium channel antagonists, mibefradil and NNC-55-0396 inhibit cell proliferation and induce cell apoptosis in leukemia cell lines. J Exp Clin Cancer Res *34*, 54. 10.1186/s13046-015-0171-4.

Ichikawa, M., Asai, T., Chiba, S., Kurokawa, M., and Ogawa, S. (2004). Runx1/AML-1 ranks as a master regulator of adult hematopoiesis. Cell Cycle *3*, 722-724.

Ikuta, K., and Weissman, I.L. (1992). Evidence that hematopoietic stem cells express mouse c-kit but do not depend on steel factor for their generation. Proc Natl Acad Sci U S A *89*, 1502-1506. 10.1073/pnas.89.4.1502.

Ishikawa, F., Yoshida, S., Saito, Y., Hijikata, A., Kitamura, H., Tanaka, S., Nakamura, R., Tanaka, T., Tomiyama, H., Saito, N., et al. (2007). Chemotherapy-resistant human AML stem cells home to and engraft within the bone-marrow endosteal region. Nature Biotechnology *25*, 1315-1321. 10.1038/nbt1350.

Iwasaki, H., Mizuno, S., Arinobu, Y., Ozawa, H., Mori, Y., Shigematsu, H., Takatsu, K., Tenen, D.G., and Akashi, K. (2006). The order of expression of transcription factors directs hierarchical specification of hematopoietic lineages. Genes Dev *20*, 3010-3021. 10.1101/gad.1493506.

Jabbour, E., O'Brien, S., Konopleva, M., and Kantarjian, H. (2015). New insights into the pathophysiology and therapy of adult acute lymphoblastic leukemia. Cancer *121*, 2517-2528. 10.1002/cncr.29383.

Jagannathan-Bogdan, M., and Zon, L.I. (2013). Hematopoiesis. Development *140*, 2463-2467. 10.1242/dev.083147.

Jensen, A.A., and Bräuner-Osborne, H. (2007). Allosteric modulation of the calcium-sensing receptor. Curr Neuropharmacol *5*, 180-186. 10.2174/157015907781695982.

Jin, L., Hope, K.J., Zhai, Q., Smadja-Joffe, F., and Dick, J.E. (2006). Targeting of CD44 eradicates human acute myeloid leukemic stem cells. Nat Med *12*, 1167-1174. 10.1038/nm1483.

Jo, D.Y., Rafii, S., Hamada, T., and Moore, M.A. (2000). Chemotaxis of primitive hematopoietic cells in response to stromal cell-derived factor-1. J Clin Invest *105*, 101-111. 10.1172/jci7954.

Jurlander, J. (2011). Hematological Malignancies, Leukemias and Lymphomas. In Encyclopedia of Cancer, M. Schwab, ed. (Springer Berlin Heidelberg), pp. 1640-1644. 10.1007/978-3-642-16483-5_2615.

Kamochi, N., Nakashima, M., Aoki, S., Uchihashi, K., Sugihara, H., Toda, S., and Kudo, S. (2008). Irradiated fibroblast-induced bystander effects on invasive growth of squamous cell carcinoma under cancer-stromal cell interaction. Cancer Sci *99*, 2417-2427. 10.1111/j.1349-7006.2008.00978.x.

Kats, L.M., Reschke, M., Taulli, R., Pozdnyakova, O., Burgess, K., Bhargava, P., Straley, K., Karnik, R., Meissner, A., Small, D., et al. (2014). Proto-oncogenic role of mutant IDH2 in leukemia initiation and maintenance. Cell stem cell *14*, 329-341. 10.1016/j.stem.2013.12.016.

Kelly, J.C., Lungchukiet, P., and Macleod, R.J. (2011). Extracellular Calcium-Sensing Receptor Inhibition of Intestinal EpithelialTNF Signaling Requires CaSR-Mediated Wnt5a/Ror2 Interaction. Front Physiol *2*, 17. 10.3389/fphys.2011.00017.

Kelly, L.M., Liu, Q., Kutok, J.L., Williams, I.R., Boulton, C.L., and Gilliland, D.G. (2002). FLT3 internal tandem duplication mutations associated with human acute myeloid leukemias induce myeloproliferative disease in a murine bone marrow transplant model. Blood *99*, 310-318. 10.1182/blood.v99.1.310.

Ketebo, A.A., Park, C., Kim, J., Jun, M., and Park, S. (2021). Probing mechanobiological role of filamin A in migration and invasion of human U87 glioblastoma cells using submicron soft pillars. Nano Convergence *8*, 19. 10.1186/s40580-021-00267-6.

Ketley, N.J., Allen, P.D., Kelsey, S.M., and Newland, A.C. (2000). Mechanisms of resistance to apoptosis in human AML blasts: the role of differentiation-induced perturbations of cell-cycle checkpoints. Leukemia *14*, 620-628. 10.1038/sj.leu.2401715.

Khaddour, K., Hana, C.K., and Mewawalla, P. (2021). Hematopoietic Stem Cell Transplantation. In StatPearls, (StatPearls Publishing).

Kiel, M.J., and Morrison, S.J. (2006). Maintaining hematopoietic stem cells in the vascular niche. Immunity *25*, 862-864. 10.1016/j.immuni.2006.11.005.

Kifor, O., MacLeod, R.J., Diaz, R., Bai, M., Yamaguchi, T., Yao, T., Kifor, I., and Brown, E.M. (2001). Regulation of MAP kinase by calcium-sensing receptor in bovine parathyroid and CaR-transfected HEK293 cells. Am J Physiol Renal Physiol *280*, F291-302. 10.1152/ajprenal.2001.280.2.F291.

Kikuchi, A., Yamamoto, H., Sato, A., and Matsumoto, S. (2012). Wnt5a: its signalling, functions and implication in diseases. Acta Physiol (Oxf) *204*, 17-33. 10.1111/j.1748-1716.2011.02294.x.

Kiyoi, H., and Naoe, T. (2006). Biology, clinical relevance, and molecularly targeted therapy in acute leukemia with FLT3 mutation. Int J Hematol *83*, 301-308. 10.1532/ijh97.06071.

Koechlein, C.S., Harris, J.R., Lee, T.K., Weeks, J., Fox, R.G., Zimdahl, B., Ito, T., Blevins, A., Jung, S.H., Chute, J.P., et al. (2016). High-resolution imaging and computational analysis of haematopoietic cell dynamics in vivo. Nat Commun *7*, 12169. 10.1038/ncomms12169.

Koreth, J., Schlenk, R., Kopecky, K.J., Honda, S., Sierra, J., Djulbegovic, B.J., Wadleigh, M., DeAngelo, D.J., Stone, R.M., Sakamaki, H., et al. (2009). Allogeneic stem cell transplantation for acute myeloid leukemia in first complete remission: systematic review and meta-analysis of prospective clinical trials. Jama *301*, 2349-2361. 10.1001/jama.2009.813.

Kowarz, E., Löscher, D., and Marschalek, R. (2015). Optimized Sleeping Beauty transposons rapidly generate stable transgenic cell lines. Biotechnol J *10*, 647-653. 10.1002/biot.201400821.

Krause, D.S., Fulzele, K., Catic, A., Sun, C.C., Dombkowski, D., Hurley, M.P., Lezeau, S., Attar, E., Wu, J.Y., Lin, H.Y., et al. (2013). Differential regulation of myeloid leukemias by the bone marrow microenvironment. Nat Med *19*, 1513-1517. 10.1038/nm.3364.

Krause, D.S., Lazarides, K., Lewis, J.B., von Andrian, U.H., and Van Etten, R.A. (2014). Selectins and their ligands are required for homing and engraftment of BCR-ABL1+ leukemic stem cells in the bone marrow niche. Blood *123*, 1361-1371. 10.1182/blood-2013-11-538694.

Krause, D.S., Lazarides, K., von Andrian, U.H., and Van Etten, R.A. (2006). Requirement for CD44 in homing and engraftment of BCR-ABL-expressing leukemic stem cells. Nat Med *12*, 1175-1180. 10.1038/nm1489.

Krause, D.S., and Scadden, D.T. (2015). A hostel for the hostile: the bone marrow niche in hematologic neoplasms. Haematologica *100*, 1376-1387. 10.3324/haematol.2014.113852.

Krivtsov, A.V., Figueroa, M.E., Sinha, A.U., Stubbs, M.C., Feng, Z., Valk, P.J., Delwel, R., Döhner, K., Bullinger, L., Kung, A.L., et al. (2013). Cell of origin determines clinically relevant subtypes of MLL-rearranged AML. Leukemia *27*, 852-860. 10.1038/leu.2012.363.

Krivtsov, A.V., Twomey, D., Feng, Z., Stubbs, M.C., Wang, Y., Faber, J., Levine, J.E., Wang, J., Hahn, W.C., Gilliland, D.G., et al. (2006). Transformation from committed progenitor to leukaemia stem cell initiated by MLL-AF9. Nature *442*, 818-822. 10.1038/nature04980.

Kuang, D., Yao, Y., Lam, J., Tsushima, R.G., and Hampson, D.R. (2005). Cloning and characterization of a family C orphan G-protein coupled receptor. J Neurochem *93*, 383-391. 10.1111/j.1471-4159.2005.03025.x.

Kuang, S.Q., Fang, Z., Zweidler-McKay, P.A., Yang, H., Wei, Y., Gonzalez-Cervantes, E.A., Boumber, Y., and Garcia-Manero, G. (2013). Epigenetic inactivation of Notch-Hes pathway in human B-cell acute lymphoblastic leukemia. PLoS One *8*, e61807. 10.1371/journal.pone.0061807.

Kumar, R., Pereira, R.S., Zanetti, C., Minciacchi, V.R., Merten, M., Meister, M., Niemann, J., Dietz, M.S., Rüssel, N., Schnütgen, F., et al. (2020). Specific, targetable interactions with the microenvironment influence imatinib-resistant chronic myeloid leukemia. Leukemia *34*, 2087-2101. 10.1038/s41375-020-0866-1.

Kunisaki, Y., Bruns, I., Scheiermann, C., Ahmed, J., Pinho, S., Zhang, D., Mizoguchi, T., Wei, Q., Lucas, D., Ito, K., et al. (2013). Arteriolar niches maintain haematopoietic stem cell quiescence. Nature *502*, 637-643. 10.1038/nature12612.

Kuzelová, K., Pluskalová, M., Brodská, B., Otevrelová, P., Elknerová, K., Grebenová, D., and Hrkal, Z. (2010). Suberoylanilide hydroxamic acid (SAHA) at subtoxic concentrations increases the adhesivity of human leukemic cells to fibronectin. J Cell Biochem *109*, 184-195. 10.1002/jcb.22397.

Lagunas-Rangel, F.A., Chávez-Valencia, V., Gómez-Guijosa, M., and Cortes-Penagos, C. (2017). Acute Myeloid Leukemia-Genetic Alterations and Their Clinical Prognosis. Int J Hematol Oncol Stem Cell Res *11*, 328-339.

Lam, B.S., Cunningham, C., and Adams, G.B. (2011). Pharmacologic modulation of the calcium-sensing receptor enhances hematopoietic stem cell lodgment in the adult bone marrow. Blood *117*, 1167-1175. 10.1182/blood-2010-05-286294.

Lamsoul, I., Dupré, L., and Lutz, P.G. (2020). Molecular Tuning of Filamin A Activities in the Context of Adhesion and Migration. Frontiers in Cell and Developmental Biology *8*. 10.3389/fcell.2020.591323.

Lane, S.W., Wang, Y.J., Lo Celso, C., Ragu, C., Bullinger, L., Sykes, S.M., Ferraro, F., Shterental, S., Lin, C.P., Gilliland, D.G., et al. (2011). Differential niche and Wnt requirements during acute myeloid leukemia progression. Blood *118*, 2849-2856. 10.1182/blood-2011-03-345165.

Laneuville, P. (1995). Abl tyrosine protein kinase. Semin Immunol *7*, 255-266. 10.1006/smim.1995.0030.

Lapidot, T., Sirard, C., Vormoor, J., Murdoch, B., Hoang, T., Caceres-Cortes, J., Minden, M., Paterson, B., Caligiuri, M.A., and Dick, J.E. (1994). A cell initiating human acute myeloid leukaemia after transplantation into SCID mice. Nature *367*, 645-648. 10.1038/367645a0.

Larriba, M.J., Martín-Villar, E., García, J.M., Pereira, F., Peña, C., de Herreros, A.G., Bonilla, F., and Muñoz, A. (2009). Snail2 cooperates with Snail1 in the repression of vitamin D receptor in colon cancer. Carcinogenesis *30*, 1459-1468. 10.1093/carcin/bgp140.

Lee, J.-W., Park, H.A., Kwon, O.-K., Park, J.-W., Lee, G., Lee, H.J., Lee, S.J., Oh, S.-R., and Ahn, K.-S. (2017). NPS 2143, a selective calcium-sensing receptor antagonist inhibits lipopolysaccharide-induced pulmonary inflammation. Molecular Immunology *90*, 150-157.

Ley, T.J., Ding, L., Walter, M.J., McLellan, M.D., Lamprecht, T., Larson, D.E., Kandoth, C., Payton, J.E., Baty, J., Welch, J., et al. (2010). DNMT3A mutations in acute myeloid leukemia. N Engl J Med *363*, 2424-2433. 10.1056/NEJMoa1005143.

Liang, H., Chen, Q., Coles, A.H., Anderson, S.J., Pihan, G., Bradley, A., Gerstein, R., Jurecic, R., and Jones, S.N. (2003). Wnt5a inhibits B cell proliferation and functions as a tumor suppressor in hematopoietic tissue. Cancer Cell *4*, 349-360. 10.1016/s1535-6108(03)00268-x.

Liao, J., Schneider, A., Datta, N.S., and McCauley, L.K. (2006). Extracellular calcium as a candidate mediator of prostate cancer skeletal metastasis. Cancer Res *66*, 9065-9073. 10.1158/0008-5472.Can-06-0317.

Liu, L., Fan, Y., Chen, Z., Zhang, Y., and Yu, J. (2020). CaSR Induces Osteoclast Differentiation and Promotes Bone Metastasis in Lung Adenocarcinoma. Front Oncol *10*, 305. 10.3389/fonc.2020.00305.

Lo Celso, C., Fleming, H.E., Wu, J.W., Zhao, C.X., Miake-Lye, S., Fujisaki, J., Côté, D., Rowe, D.W., Lin, C.P., and Scadden, D.T. (2009). Live-animal tracking of individual haematopoietic stem/progenitor cells in their niche. Nature *457*, 92-96. 10.1038/nature07434.

Lo Celso, C., and Scadden, D.T. (2011). The haematopoietic stem cell niche at a glance. J Cell Sci *124*, 3529-3535. 10.1242/jcs.074112.

Lo Giudice, M., Mihalik, B., Turi, Z., Dinnyés, A., and Kobolák, J. (2019). Calcilytic NPS 2143 Reduces Amyloid Secretion and Increases sAβPPα Release from PSEN1 Mutant iPSC-Derived Neurons. J Alzheimers Dis *72*, 885-899. 10.3233/JAD-190602.

Lord, B.I., Testa, N.G., and Hendry, J.H. (1975). The relative spatial distributions of CFUs and CFUc in the normal mouse femur. Blood *46*, 65-72.

Loupy, A., Ramakrishnan, S.K., Wootla, B., Chambrey, R., de la Faille, R., Bourgeois, S., Bruneval, P., Mandet, C., Christensen, E.I., Faure, H., et al. (2012). PTH-independent regulation of blood calcium concentration by the calcium-sensing receptor. J Clin Invest *122*, 3355-3367. 10.1172/jci57407.

Löwenberg, B., Downing, J.R., and Burnett, A. (1999). Acute myeloid leukemia. N Engl J Med *341*, 1051-1062. 10.1056/nejm199909303411407.

Luchsinger, L.L., Strikoudis, A., Danzl, N.M., Bush, E.C., Finlayson, M.O., Satwani, P., Sykes, M., Yazawa, M., and Snoeck, H.W. (2019). Harnessing Hematopoietic Stem Cell Low Intracellular Calcium Improves Their Maintenance In Vitro. Cell Stem Cell *25*, 225-240.e227. 10.1016/j.stem.2019.05.002.

Luzzi, K.J., MacDonald, I.C., Schmidt, E.E., Kerkvliet, N., Morris, V.L., Chambers, A.F., and Groom, A.C. (1998). Multistep nature of metastatic inefficiency: dormancy of solitary cells after successful extravasation and limited survival of early micrometastases. Am J Pathol *153*, 865-873. 10.1016/s0002-9440(10)65628-3.

MacFarlane, A.W.t., Oesterling, J.F., and Campbell, K.S. (2010). Measuring intracellular calcium signaling in murine NK cells by flow cytometry. Methods Mol Biol *612*, 149-157. 10.1007/978-1-60761-362-6_10.

MacLeod, R.J. (2013). Extracellular calcium-sensing receptor/PTH knockout mice colons have increased Wnt/β-catenin signaling, reduced non-canonical Wnt signaling, and increased susceptibility to azoxymethane-induced aberrant crypt foci. Laboratory Investigation *93*, 520-527. 10.1038/labinvest.2013.51.

Mannstadt, M., Bilezikian, J.P., Thakker, R.V., Hannan, F.M., Clarke, B.L., Rejnmark, L., Mitchell, D.M., Vokes, T.J., Winer, K.K., and Shoback, D.M. (2017). Hypoparathyroidism. Nat Rev Dis Primers *3*, 17055. 10.1038/nrdp.2017.55.

Manz, M.G., Miyamoto, T., Akashi, K., and Weissman, I.L. (2002). Prospective isolation of human clonogenic common myeloid progenitors. Proc Natl Acad Sci U S A *99*, 11872-11877. 10.1073/pnas.172384399.

Marastoni, S., Ligresti, G., Lorenzon, E., Colombatti, A., and Mongiat, M. (2008). Extracellular matrix: a matter of life and death. Connect Tissue Res *49*, 203-206. 10.1080/03008200802143190.

März, W., Seelhorst, U., Wellnitz, B., Tiran, B., Obermayer-Pietsch, B., Renner, W., Boehm, B.O., Ritz, E., and Hoffmann, M.M. (2007). Alanine to serine polymorphism at position 986 of the calcium-sensing receptor associated with coronary heart disease, myocardial infarction, all-cause, and cardiovascular mortality. J Clin Endocrinol Metab *92*, 2363-2369. 10.1210/jc.2006-0071.

Mazumdar, C., Shen, Y., Xavy, S., Zhao, F., Reinisch, A., Li, R., Corces, M.R., Flynn, R.A., Buenrostro, J.D., Chan, S.M., et al. (2015). Leukemia-Associated Cohesin Mutants Dominantly Enforce Stem Cell Programs and Impair Human Hematopoietic Progenitor Differentiation. Cell Stem Cell *17*, 675-688.

McAlister, G.C., Nusinow, D.P., Jedrychowski, M.P., Wühr, M., Huttlin, E.L., Erickson, B.K., Rad, R., Haas, W., and Gygi, S.P. (2014). MultiNotch MS3 enables accurate, sensitive, and multiplexed detection of differential expression across cancer cell line proteomes. Anal Chem *86*, 7150-7158. 10.1021/ac502040v.

McCullough, M.L., Bandera, E.V., Moore, D.F., and Kushi, L.H. (2008). Vitamin D and calcium intake in relation to risk of endometrial cancer: a systematic review of the literature. Prev Med *46*, 298-302. 10.1016/j.ypmed.2007.11.010.

McDonough, W.S., Tran, N.L., and Berens, M.E. (2005). Regulation of glioma cell migration by serine-phosphorylated P311. Neoplasia *7*, 862-872. 10.1593/neo.05190.

Medyouf, H., Mossner, M., Jann, J.C., Nolte, F., Raffel, S., Herrmann, C., Lier, A., Eisen, C., Nowak, V., Zens, B., et al. (2014). Myelodysplastic cells in patients reprogram mesenchymal stromal cells to establish a transplantable stem cell niche disease unit. Cell Stem Cell *14*, 824-837. 10.1016/j.stem.2014.02.014.

Meyer, C., and Marschalek, R. (2009). LDI-PCR: identification of known and unknown gene fusions of the human MLL gene. Methods Mol Biol *538*, 71-83. 10.1007/978-1-59745-418-6_5.

Meyer, C., Schneider, B., Reichel, M., Angermueller, S., Strehl, S., Schnittger, S., Schoch, C., Jansen, M.W., van Dongen, J.J., Pieters, R., et al. (2005). Diagnostic tool for the identification of MLL rearrangements including unknown partner genes. Proc Natl Acad Sci U S A *102*, 449-454. 10.1073/pnas.0406994102.

Milella, M., Kornblau, S.M., Estrov, Z., Carter, B.Z., Lapillonne, H., Harris, D., Konopleva, M., Zhao, S., Estey, E., and Andreeff, M. (2001). Therapeutic targeting of the MEK/MAPK signal transduction module in acute myeloid leukemia. J Clin Invest *108*, 851-859. 10.1172/jci12807.

Miller, Peter G., Al-Shahrour, F., Hartwell, Kimberly A., Chu, Lisa P., Järås, M., Puram, Rishi V., Puissant, A., Callahan, Kevin P., Ashton, J., McConkey, Marie E., et al. (2013). In Vivo RNAi Screening Identifies a Leukemia-Specific Dependence on Integrin Beta 3 Signaling. Cancer Cell *24*, 45-58.

Miyaura, C., Abe, E., and Suda, T. (1984). Extracellular calcium is involved in the mechanism of differentiation of mouse myeloid leukemia cells (M1) induced by 1 alpha, 25-dihydroxyvitamin D3. Endocrinology *115*, 1891-1896. 10.1210/endo-115-5-1891.

Mooso, B.A., Vinall, R.L., Tepper, C.G., Savoy, R.M., Cheung, J.P., Singh, S., Siddiqui, S., Wang, Y., Bedolla, R.G., Martinez, A., et al. (2012). Enhancing the effectiveness of androgen deprivation in prostate cancer by inducing Filamin A nuclear localization. Endocr Relat Cancer *19*, 759-777. 10.1530/erc-12-0171.

Moran-Crusio, K., Reavie, L., Shih, A., Abdel-Wahab, O., Ndiaye-Lobry, D., Lobry, C., Figueroa, M.E., Vasanthakumar, A., Patel, J., Zhao, X., et al. (2011). Tet2 loss leads to increased hematopoietic stem cell self-renewal and myeloid transformation. Cancer cell *20*, 11-24. 10.1016/j.ccr.2011.06.001.

Morrison, S.J., and Scadden, D.T. (2014). The bone marrow niche for haematopoietic stem cells. Nature *505*, 327-334. 10.1038/nature12984.

Mould, A.P., Akiyama, S.K., and Humphries, M.J. (1995). Regulation of integrin alpha 5 beta 1-fibronectin interactions by divalent cations. Evidence for distinct classes of binding sites for Mn2+, Mg2+, and Ca2+. J Biol Chem *270*, 26270-26277. 10.1074/jbc.270.44.26270.

Mullighan, C.G. (2012). Molecular genetics of B-precursor acute lymphoblastic leukemia. The Journal of clinical investigation *122*, 3407-3415. 10.1172/JCI61203.

Muntean, A.G., and Hess, J.L. (2012). The pathogenesis of mixed-lineage leukemia. Annu Rev Pathol *7*, 283-301. 10.1146/annurev-pathol-011811-132434.

Muralidhar, S., Filia, A., Nsengimana, J., Poźniak, J., O'Shea, S.J., Diaz, J.M., Harland, M., Randerson-Moor, J.A., Reichrath, J., Laye, J.P., et al. (2019). Vitamin D-VDR Signaling Inhibits Wnt/β-Catenin-Mediated Melanoma Progression and Promotes Antitumor Immunity. Cancer Res *79*, 5986-5998. 10.1158/0008-5472.Can-18-3927.

Nagano, T., Yoneda, T., Hatanaka, Y., Kubota, C., Murakami, F., and Sato, M. (2002). Filamin A-interacting protein (FILIP) regulates cortical cell migration out of the ventricular zone. Nat Cell Biol *4*, 495-501. 10.1038/ncb808.

Nagelkerke, A., and Span, P.N. (2016). Staining Against Phospho-H2AX (γ-H2AX) as a Marker for DNA Damage and Genomic Instability in Cancer Tissues and Cells. Adv Exp Med Biol *899*, 1-10. 10.1007/978-3-319-26666-4_1.

Nakamura, F., Osborn, T.M., Hartemink, C.A., Hartwig, J.H., and Stossel, T.P. (2007). Structural basis of filamin A functions. J Cell Biol *179*, 1011-1025. 10.1083/jcb.200707073.

Nakamura, F., Stossel, T.P., and Hartwig, J.H. (2011). The filamins: organizers of cell structure and function. Cell Adh Migr *5*, 160-169. 10.4161/cam.5.2.14401.

Naoe, T., and Kiyoi, H. (2013). Gene mutations of acute myeloid leukemia in the genome era. International Journal of Hematology *97*, 165-174. 10.1007/s12185-013-1257-4.

National Research Council Committee for the Update of the Guide for the, C., and Use of Laboratory, A. (2011). The National Academies Collection: Reports funded by National Institutes of Health. In Guide for the Care and Use of Laboratory Animals. 10.17226/12910.

Nemeth, E.F., Delmar, E.G., Heaton, W.L., Miller, M.A., Lambert, L.D., Conklin, R.L., Gowen, M., Gleason, J.G., Bhatnagar, P.K., and Fox, J. (2001). Calcilytic compounds: potent and selective Ca2+ receptor antagonists that stimulate secretion of parathyroid hormone. Journal of Pharmacology and Experimental Therapeutics *299*, 323-331.

Nemeth, E.F., and Goodman, W.G. (2016). Calcimimetic and Calcilytic Drugs: Feats, Flops, and Futures. Calcified Tissue International *98*, 341-358. 10.1007/s00223-015-0052-z.

Nemeth, E.F., Van Wagenen, B.C., and Balandrin, M.F. (2018). Discovery and development of calcimimetic and calcilytic compounds. Progress in medicinal chemistry *57*, 1-86.

Nilsson, S.K., Johnston, H.M., and Coverdale, J.A. (2001). Spatial localization of transplanted hemopoietic stem cells: inferences for the localization of stem cell niches. Blood *97*, 2293-2299. 10.1182/blood.v97.8.2293.

Ninomiya, M., Abe, A., Katsumi, A., Xu, J., Ito, M., Arai, F., Suda, T., Ito, M., Kiyoi, H., Kinoshita, T., and Naoe, T. (2007). Homing, proliferation and survival sites of human leukemia cells in vivo in immunodeficient mice. Leukemia *21*, 136-142. 10.1038/sj.leu.2404432.

Nombela-Arrieta, C., Pivarnik, G., Winkel, B., Canty, K.J., Harley, B., Mahoney, J.E., Park, S.Y., Lu, J., Protopopov, A., and Silberstein, L.E. (2013). Quantitative imaging of haematopoietic stem and progenitor cell localization and hypoxic status in the bone marrow microenvironment. Nat Cell Biol *15*, 533-543. 10.1038/ncb2730.

Okuhashi, Y., Itoh, M., Nara, N., and Tohda, S. (2011). Effects of combination of notch inhibitor plus hedgehog inhibitor or Wnt inhibitor on growth of leukemia cells. Anticancer Res *31*, 893-896.

Orduña-Castillo, L.B., Del-Río-Robles, J.E., García-Jiménez, I., Zavala-Barrera, C., Beltrán-Navarro, Y.M., Hidalgo-Moyle, J.J., Ramírez-Rangel, I., Hernández-Bedolla, M.A., Reyes-Ibarra, A.P., Valadez-Sánchez, M., et al. (2021). Calcium sensing receptor stimulates breast cancer cell migration via the Gβγ-AKT-mTORC2 signaling pathway. J Cell Commun Signal. 10.1007/s12079-021-00662-y.

Paredes, R., Kelly, J.R., Geary, B., Almarzouq, B., Schneider, M., Pearson, S., Narayanan, P., Williamson, A., Lovell, S.C., Wiseman, D.H., et al. (2020). EVI1 phosphorylation at S436 regulates interactions with CtBP1 and DNMT3A and promotes self-renewal. Cell Death & Disease *11*, 878. 10.1038/s41419-020-03099-0.

Parfitt, A.M. (1994). Osteonal and hemi-osteonal remodeling: the spatial and temporal framework for signal traffic in adult human bone. J Cell Biochem *55*, 273-286. 10.1002/jcb.240550303.

Parmar, K., Mauch, P., Vergilio, J.A., Sackstein, R., and Down, J.D. (2007). Distribution of hematopoietic stem cells in the bone marrow according to regional hypoxia. Proc Natl Acad Sci U S A *104*, 5431-5436. 10.1073/pnas.0701152104.

Paschka, P., Schlenk, R.F., Weber, D., Benner, A., Bullinger, L., Heuser, M., Gaidzik, V.I., Thol, F., Agrawal, M., Teleanu, V., et al. (2018). Adding dasatinib to intensive treatment in core-binding factor acute myeloid leukemia—results of the AMLSG 11-08 trial. Leukemia *32*, 1621-1630. 10.1038/s41375-018-0129-6.

Passegué, E., Jamieson, C.H., Ailles, L.E., and Weissman, I.L. (2003). Normal and leukemic hematopoiesis: are leukemias a stem cell disorder or a reacquisition of stem cell characteristics? Proc Natl Acad Sci U S A *100 Suppl 1*, 11842-11849. 10.1073/pnas.2034201100.

Paubelle, E., Zylbersztejn, F., Maciel, T.T., Carvalho, C., Mupo, A., Cheok, M., Lieben, L., Sujobert, P., Decroocq, J., Yokoyama, A., et al. (2020). Vitamin D Receptor Controls Cell

Stemness in Acute Myeloid Leukemia and in Normal Bone Marrow. Cell Reports *30*, 739-754.e734.

Paulsson, K., Horvat, A., Strömbeck, B., Nilsson, F., Heldrup, J., Behrendtz, M., Forestier, E., Andersson, A., Fioretos, T., and Johansson, B. (2008). Mutations of FLT3, NRAS, KRAS, and PTPN11 are frequent and possibly mutually exclusive in high hyperdiploid childhood acute lymphoblastic leukemia. Genes Chromosomes Cancer *47*, 26-33. 10.1002/gcc.20502.

Pegoraro, A., Orioli, E., De Marchi, E., Salvestrini, V., Milani, A., Di Virgilio, F., Curti, A., and Adinolfi, E. (2020). Differential sensitivity of acute myeloid leukemia cells to daunorubicin depends on P2X7A versus P2X7B receptor expression. Cell Death & Disease *11*, 876. 10.1038/s41419-020-03058-9.

Perez-Moreno, M., Jamora, C., and Fuchs, E. (2003). Sticky Business: Orchestrating Cellular Signals at Adherens Junctions. Cell *112*, 535-548.

Petit-Cocault, L., Volle-Challier, C., Fleury, M., Péault, B., and Souyri, M. (2007). Dual role of Mpl receptor during the establishment of definitive hematopoiesis. Development *134*, 3031-3040. 10.1242/dev.001818.

Pi, M., Chen, L., Huang, M.Z., Zhu, W., Ringhofer, B., Luo, J., Christenson, L., Li, B., Zhang, J., Jackson, P.D., et al. (2008). GPRC6A null mice exhibit osteopenia, feminization and metabolic syndrome. PLoS One *3*, e3858. 10.1371/journal.pone.0003858.

Pi, M., Faber, P., Ekema, G., Jackson, P.D., Ting, A., Wang, N., Fontilla-Poole, M., Mays, R.W., Brunden, K.R., Harrington, J.J., and Quarles, L.D. (2005). Identification of a novel extracellular cation-sensing G-protein-coupled receptor. J Biol Chem *280*, 40201-40209. 10.1074/jbc.M505186200.

Pi, M., Spurney, R.F., Tu, Q., Hinson, T., and Quarles, L.D. (2002). Calcium-sensing receptor activation of rho involves filamin and rho-guanine nucleotide exchange factor. Endocrinology *143*, 3830-3838. 10.1210/en.2002-220240.

Pimanda, J.E., Donaldson, I.J., de Bruijn, M.F., Kinston, S., Knezevic, K., Huckle, L., Piltz, S., Landry, J.R., Green, A.R., Tannahill, D., and Göttgens, B. (2007). The SCL transcriptional network and BMP signaling pathway interact to regulate RUNX1 activity. Proc Natl Acad Sci U S A *104*, 840-845. 10.1073/pnas.0607196104.

Piste, P., Sayaji, D., and Avinash, M. (2012). Calcium and its Role in Human Body. Int J Res Pharm Biomed Sci *4*, 2229-3701.

Planagumà, J., Minsaas, L., Pons, M., Myhren, L., Garrido, G., and Aragay, A.M. (2012). Filamin A-hinge region 1-EGFP: a novel tool for tracking the cellular functions of filamin A in real-time. PLoS One *7*, e40864. 10.1371/journal.pone.0040864.

Pollak, M.R., Brown, E.M., Chou, Y.H., Hebert, S.C., Marx, S.J., Steinmann, B., Levi, T., Seidman, C.E., and Seidman, J.G. (1993). Mutations in the human Ca(2+)-sensing receptor gene cause familial hypocalciuric hypercalcemia and neonatal severe hyperparathyroidism. Cell *75*, 1297-1303. 10.1016/0092-8674(93)90617-y.

Pollak, M.R., Brown, E.M., Estep, H.L., McLaine, P.N., Kifor, O., Park, J., Hebert, S.C., Seidman, C.E., and Seidman, J.G. (1994). Autosomal dominant hypocalcaemia caused by a Ca(2+)-sensing receptor gene mutation. Nat Genet *8*, 303-307. 10.1038/ng1194-303.

Porter, R.M., Holme, T.C., Newman, E.L., Hopwood, D., Wilkinson, J.M., and Cuschieri, A. (1993). Monoclonal antibodies to cytoskeletal proteins: an immunohistochemical investigation of human colon cancer. J Pathol *170*, 435-440. 10.1002/path.1711700406.

Pourrajab, F., Zare-Khormizi, M.R., Hashemi, A.S., and Hekmatimoghaddam, S. (2020). Genetic Characterization and Risk Stratification of Acute Myeloid Leukemia. Cancer Manag Res *12*, 2231-2253. 10.2147/cmar.S242479.

Pui, C.H. (2010). Recent research advances in childhood acute lymphoblastic leukemia. J Formos Med Assoc *109*, 777-787. 10.1016/s0929-6646(10)60123-4.

Pui, C.H., Relling, M.V., and Downing, J.R. (2004). Acute lymphoblastic leukemia. N Engl J Med *350*, 1535-1548. 10.1056/NEJMra023001.

Purton, L.E., and Scadden, D.T. (2008). The hematopoietic stem cell niche. In StemBook. 10.3824/stembook.1.28.1.

Quinn, S.J., Ye, C.P., Diaz, R., Kifor, O., Bai, M., Vassilev, P., and Brown, E. (1997). The Ca2+-sensing receptor: a target for polyamines. Am J Physiol *273*, C1315-1323. 10.1152/ajpcell.1997.273.4.C1315.

Raaijmakers, M.H., Mukherjee, S., Guo, S., Zhang, S., Kobayashi, T., Schoonmaker, J.A., Ebert, B.L., Al-Shahrour, F., Hasserjian, R.P., Scadden, E.O., et al. (2010). Bone progenitor dysfunction induces myelodysplasia and secondary leukaemia. Nature *464*, 852-857. 10.1038/nature08851.

Raskin, R.E., Latimer, K.S., and Tvedten, H. (2004). Leukocyte Disorders. Small Animal Clinical Diagnosis by Laboratory Methods, 63-91. 10.1016/B0-72-168903-5/50008-2.

Ray, K., Adipietro, K.A., Chen, C., and Northup, J.K. (2007). Elucidation of the role of peptide linker in calcium-sensing receptor activation process. J Biol Chem *282*, 5310-5317. 10.1074/jbc.M609610200.

Regard, J.B., Sato, I.T., and Coughlin, S.R. (2008). Anatomical profiling of G protein-coupled receptor expression. Cell *135*, 561-571. 10.1016/j.cell.2008.08.040.

Rey, O., Chang, W., Bikle, D., Rozengurt, N., Young, S.H., and Rozengurt, E. (2012). Negative cross-talk between calcium-sensing receptor and β-catenin signaling systems in colonic epithelium. The Journal of biological chemistry *287*, 1158-1167. 10.1074/jbc.M111.274589.

Rey, O., Young, S.H., Yuan, J., Slice, L., and Rozengurt, E. (2005). Amino acid-stimulated Ca2+ oscillations produced by the Ca2+-sensing receptor are mediated by a phospholipase C/inositol 1,4,5-trisphosphate-independent pathway that requires G12, Rho, filamin-A, and the actin cytoskeleton. J Biol Chem *280*, 22875-22882. 10.1074/jbc.M503455200.

Reya, T., and Clevers, H. (2005). Wnt signalling in stem cells and cancer. Nature *434*, 843-850. 10.1038/nature03319.

Riccardi, D., and Valenti, G. (2016). Localization and function of the renal calcium-sensing receptor. Nat Rev Nephrol *12*, 414-425. 10.1038/nrneph.2016.59.

Ricciardi, M.R., McQueen, T., Chism, D., Milella, M., Estey, E., Kaldjian, E., Sebolt-Leopold, J., Konopleva, M., and Andreeff, M. (2005). Quantitative single cell determination of ERK phosphorylation and regulation in relapsed and refractory primary acute myeloid leukemia. Leukemia *19*, 1543-1549. 10.1038/sj.leu.2403859.

Rieger, M.A., and Schroeder, T. (2012). Hematopoiesis. Cold Spring Harb Perspect Biol *4*. 10.1101/cshperspect.a008250.

Roberts, K.G., Morin, R.D., Zhang, J., Hirst, M., Zhao, Y., Su, X., Chen, S.C., Payne-Turner, D., Churchman, M.L., Harvey, R.C., et al. (2012). Genetic alterations activating kinase and cytokine receptor signaling in high-risk acute lymphoblastic leukemia. Cancer Cell *22*, 153-166. 10.1016/j.ccr.2012.06.005.

Rowe, P., Koller, A., and Sharma, S. (2020). Physiology, Bone Remodeling (StatPearls Publishing, Treasure Island (FL)).

Saidak, Z., Boudot, C., Abdoune, R., Petit, L., Brazier, M., Mentaverri, R., and Kamel, S. (2009). Extracellular calcium promotes the migration of breast cancer cells through the activation of the calcium sensing receptor. Exp Cell Res *315*, 2072-2080. 10.1016/j.yexcr.2009.03.003.

Saito, Y., Kitamura, H., Hijikata, A., Tomizawa-Murasawa, M., Tanaka, S., Takagi, S., Uchida, N., Suzuki, N., Sone, A., Najima, Y., et al. (2010). Identification of therapeutic targets for quiescent, chemotherapy-resistant human leukemia stem cells. Sci Transl Med *2*, 17ra19. 10.1126/scitranslmed.3000349.

Sala, A., and Barr, R.D. (2007). Osteopenia and cancer in children and adolescents: the fragility of success. Cancer *109*, 1420-1431. 10.1002/cncr.22546.

Sampson, L.J., Leyland, M.L., and Dart, C. (2003). Direct interaction between the actin-binding protein filamin-A and the inwardly rectifying potassium channel, Kir2.1. J Biol Chem *278*, 41988-41997. 10.1074/jbc.M307479200.

Sandoval, J.E., Huang, Y.H., Muise, A., Goodell, M.A., and Reich, N.O. (2019). Mutations in the DNMT3A DNA methyltransferase in acute myeloid leukemia patients cause both loss and gain of function and differential regulation by protein partners. J Biol Chem *294*, 4898-4910. 10.1074/jbc.RA118.006795.

Sawyers, C.L. (1999). Chronic myeloid leukemia. N Engl J Med *340*, 1330-1340. 10.1056/nejm199904293401706.

Schepelmann, M., Yarova, P.L., Lopez-Fernandez, I., Davies, T.S., Brennan, S.C., Edwards, P.J., Aggarwal, A., Graça, J., Rietdorf, K., Matchkov, V., et al. (2016). The vascular Ca2+-sensing receptor regulates blood vessel tone and blood pressure. Am J Physiol Cell Physiol *310*, C193-204. 10.1152/ajpcell.00248.2015.

Schepers, K., Pietras, Eric M., Reynaud, D., Flach, J., Binnewies, M., Garg, T., Wagers, Amy J., Hsiao, Edward C., and Passegué, E. (2013). Myeloproliferative Neoplasia Remodels the Endosteal Bone Marrow Niche into a Self-Reinforcing Leukemic Niche. Cell Stem Cell *13*, 285-299.

Schofield, R. (1978). The relationship between the spleen colony-forming cell and the haemopoietic stem cell. Blood Cells *4*, 7-25.

Semenova, S.B., Vassilieva, I.O., Fomina, A.F., Runov, A.L., and Negulyaev, Y.A. (2009). Endogenous expression of TRPV5 and TRPV6 calcium channels in human leukemia K562 cells. Am J Physiol Cell Physiol *296*, C1098-1104. 10.1152/ajpcell.00435.2008.

Shah, N.P., Lee, F.Y., Luo, R., Jiang, Y., Donker, M., and Akin, C. (2006a). Dasatinib (BMS-354825) inhibits KITD816V, an imatinib-resistant activating mutation that triggers neoplastic growth in most patients with systemic mastocytosis. Blood *108*, 286-291. 10.1182/blood-2005-10-3969.

Shah, S., Islam, M.N., Dakshanamurthy, S., Rizvi, I., Rao, M., Herrell, R., Zinser, G., Valrance, M., Aranda, A., Moras, D., et al. (2006b). The Molecular Basis of Vitamin D Receptor and β-Catenin Crossregulation. Molecular Cell *21*, 799-809.

Sharma, A., Jyotsana, N., Gabdoulline, R., Heckl, D., Kuchenbauer, F., Slany, R.K., Ganser, A., and Heuser, M. (2020). Meningioma 1 is indispensable for mixed lineage leukemia-rearranged acute myeloid leukemia. Haematologica *105*, 1294-1305. 10.3324/haematol.2018.211201.

Shen, L., Shi, Q., and Wang, W. (2018). Double agents: genes with both oncogenic and tumor-suppressor functions. Oncogenesis *7*, 25. 10.1038/s41389-018-0034-x.

Shin, S.H., Lim, D.Y., Reddy, K., Malakhova, M., Liu, F., Wang, T., Song, M., Chen, H., Bae, K.B., Ryu, J., et al. (2017). A Small Molecule Inhibitor of the β-Catenin-TCF4 Interaction Suppresses Colorectal Cancer Growth In Vitro and In Vivo. EBioMedicine *25*, 22-31. 10.1016/j.ebiom.2017.09.029.

Shirakawa, F., Yamashita, U., Oda, S., Chiba, S., Eto, S., and Suzuki, H. (1986). Calcium dependency in the growth of adult T-cell leukemia cells in vitro. Cancer Res *46*, 658-661.

Short, N.J., Montalban-Bravo, G., Hwang, H., Ning, J., Franquiz, M.J., Kanagal-Shamanna, R., Patel, K.P., DiNardo, C.D., Ravandi, F., Garcia-Manero, G., et al. (2020). Prognostic and therapeutic impacts of mutant TP53 variant allelic frequency in newly diagnosed acute myeloid leukemia. Blood Adv *4*, 5681-5689. 10.1182/bloodadvances.2020003120.

Sill, H., Zebisch, A., and Haase, D. (2020). Acute Myeloid Leukemia and Myelodysplastic Syndromes with TP53 Aberrations - A Distinct Stem Cell Disorder. Clin Cancer Res *26*, 5304-5309. 10.1158/1078-0432.Ccr-20-2272.

Silver, I.A., Murrills, R.J., and Etherington, D.J. (1988). Microelectrode studies on the acid microenvironment beneath adherent macrophages and osteoclasts. Exp Cell Res *175*, 266-276. 10.1016/0014-4827(88)90191-7.

Singh, N., and Chakrabarty, S. (2013). Induction of CaSR expression circumvents the molecular features of malignant CaSR null colon cancer cells. Int J Cancer *133*, 2307-2314. 10.1002/ijc.28270.

Skorski, T., Kanakaraj, P., Nieborowska-Skorska, M., Ratajczak, M.Z., Wen, S.C., Zon, G., Gewirtz, A.M., Perussia, B., and Calabretta, B. (1995). Phosphatidylinositol-3 kinase activity is regulated by BCR/ABL and is required for the growth of Philadelphia chromosome-positive cells. Blood *86*, 726-736.

Slusarski, D.C., Yang-Snyder, J., Busa, W.B., and Moon, R.T. (1997). Modulation of Embryonic Intracellular Ca2+Signaling byWnt-5A. Developmental Biology *182*, 114-120.

Smith, K.A., Ayon, R.J., Tang, H., Makino, A., and Yuan, J.X. (2016). Calcium-Sensing Receptor Regulates Cytosolic [Ca (2+)] and Plays a Major Role in the Development of Pulmonary Hypertension. Front Physiol *7*, 517. 10.3389/fphys.2016.00517.

Soh, H., and Park, C.S. (2001). Inwardly rectifying current-voltage relationship of small-conductance Ca2+-activated K+ channels rendered by intracellular divalent cation blockade. Biophys J *80*, 2207-2215. 10.1016/s0006-3495(01)76193-0.

Soverini, S., De Santis, S., Monaldi, C., Bruno, S., and Mancini, M. (2021). Targeting Leukemic Stem Cells in Chronic Myeloid Leukemia: Is It Worth the Effort? Int J Mol Sci *22*. 10.3390/ijms22137093.

Spencer, J.A., Ferraro, F., Roussakis, E., Klein, A., Wu, J., Runnels, J.M., Zaher, W., Mortensen, L.J., Alt, C., Turcotte, R., et al. (2014). Direct measurement of local oxygen concentration in the bone marrow of live animals. Nature *508*, 269-273. 10.1038/nature13034.

Staal, F.J.T., Famili, F., Garcia Perez, L., and Pike-Overzet, K. (2016). Aberrant Wnt Signaling in Leukemia. Cancers (Basel) *8*, 78. 10.3390/cancers8090078.

Stossel, T.P., Condeelis, J., Cooley, L., Hartwig, J.H., Noegel, A., Schleicher, M., and Shapiro, S.S. (2001). Filamins as integrators of cell mechanics and signalling. Nat Rev Mol Cell Biol *2*, 138-145. 10.1038/35052082.

Sugimoto, T., Kanatani, M., Kano, J., Kaji, H., Tsukamoto, T., Yamaguchi, T., Fukase, M., and Chihara, K. (1993). Effects of high calcium concentration on the functions and interactions of osteoblastic cells and monocytes and on the formation of osteoclast-like cells. J Bone Miner Res *8*, 1445-1452. 10.1002/jbmr.5650081206.

Sun, Y.H., Liu, M.N., Li, H., Shi, S., Zhao, Y.J., Wang, R., and Xu, C.Q. (2006). Calcium-sensing receptor induces rat neonatal ventricular cardiomyocyte apoptosis. Biochem Biophys Res Commun *350*, 942-948. 10.1016/j.bbrc.2006.09.142.

Swerdlow, S.H., Campo, E., Pileri, S.A., Harris, N.L., Stein, H., Siebert, R., Advani, R., Ghielmini, M., Salles, G.A., Zelenetz, A.D., and Jaffe, E.S. (2016). The 2016 revision of the World Health Organization classification of lymphoid neoplasms. Blood *127*, 2375-2390. 10.1182/blood-2016-01-643569.

Takahashi, K., Umebayashi, C., Numata, T., Honda, A., Ichikawa, J., Hu, Y., Yamaura, K., and Inoue, R. (2018). TRPM7-mediated spontaneous Ca(2+) entry regulates the proliferation and differentiation of human leukemia cell line K562. Physiol Rep *6*, e13796. 10.14814/phy2.13796.

Tang, J., Yu, J., Cai, J., Zhang, L., Hu, S., Gao, J., Jiang, H., Fang, Y., Liang, C., Ju, X., et al. (2021). Prognostic factors for CNS control in children with acute lymphoblastic leukemia treated without cranial irradiation. Blood *138*, 331-343. 10.1182/blood.2020010438.

Tarlock, K., Alonzo, T.A., Wang, Y.C., Gerbing, R.B., Ries, R., Loken, M.R., Pardo, L., Hylkema, T., Joaquin, J., Sarukkai, L., et al. (2019). Functional Properties of KIT Mutations Are Associated with Differential Clinical Outcomes and Response to Targeted Therapeutics in CBF Acute Myeloid Leukemia. Clin Cancer Res *25*, 5038-5048. 10.1158/1078-0432.Ccr-18-1897.

Tavor, S., Eisenbach, M., Jacob-Hirsch, J., Golan, T., Petit, I., BenZion, K., Kay, S., Baron, S., Amariglio, N., Deutsch, V., et al. (2008). The CXCR4 antagonist AMD3100 impairs survival of human AML cells and induces their differentiation. Leukemia *22*, 2151-2158. 10.1038/leu.2008.238.

Taylor, J., and Lee, S.C. (2019). Mutations in spliceosome genes and therapeutic opportunities in myeloid malignancies. Genes Chromosomes Cancer *58*, 889-902. 10.1002/gcc.22784.

Tennakoon, S., Aggarwal, A., and Kállay, E. (2016). The calcium-sensing receptor and the hallmarks of cancer. Biochim Biophys Acta *1863*, 1398-1407. 10.1016/j.bbamcr.2015.11.017.

Terry, P., Vainio, H., Wolk, A., and Weiderpass, E. (2002). Dietary factors in relation to endometrial cancer: a nationwide case-control study in Sweden. Nutr Cancer *42*, 25-32. 10.1207/s15327914nc421_4.

Tfelt-Hansen, J., Schwarz, P., Terwilliger, E.F., Brown, E.M., and Chattopadhyay, N. (2003). Calcium-sensing receptor induces messenger ribonucleic acid of human securin, pituitary tumor transforming gene, in rat testicular cancer. Endocrinology *144*, 5188-5193. 10.1210/en.2003-0520.

Thakker, R.V. (2012). Calcium-sensing receptor: Role in health and disease. Indian J Endocrinol Metab *16*, S213-216. 10.4103/2230-8210.104041.

Thakker, R.V. (2015). The calcium-sensing receptor: And its involvement in parathyroid pathology. Ann Endocrinol (Paris) *76*, 81-83. 10.1016/j.ando.2015.03.013.

Tharmalingam, S., and Hampson, D.R. (2016). The Calcium-Sensing Receptor and Integrins in Cellular Differentiation and Migration. Front Physiol *7*, 190. 10.3389/fphys.2016.00190.

Thelin, W.R., Chen, Y., Gentzsch, M., Kreda, S.M., Sallee, J.L., Scarlett, C.O., Borchers, C.H., Jacobson, K., Stutts, M.J., and Milgram, S.L. (2007). Direct interaction with filamins modulates the stability and plasma membrane expression of CFTR. J Clin Invest *117*, 364-374. 10.1172/jci30376.

Thomsen, A.R., Hvidtfeldt, M., and Bräuner-Osborne, H. (2012). Biased agonism of the calcium-sensing receptor. Cell Calcium *51*, 107-116. 10.1016/j.ceca.2011.11.009.

Tian, H.M., Liu, X.H., Han, W., Zhao, L.L., Yuan, B., and Yuan, C.J. (2013). Differential expression of filamin A and its clinical significance in breast cancer. Oncol Lett *6*, 681-686. 10.3892/ol.2013.1454.

Tiscornia, G., Singer, O., and Verma, I.M. (2006). Production and purification of lentiviral vectors. Nature Protocols *1*, 241-245. 10.1038/nprot.2006.37.

Toka, H.R., Al-Romaih, K., Koshy, J.M., DiBartolo, S., 3rd, Kos, C.H., Quinn, S.J., Curhan, G.C., Mount, D.B., Brown, E.M., and Pollak, M.R. (2012). Deficiency of the calcium-sensing receptor in the kidney causes parathyroid hormone-independent hypocalciuria. J Am Soc Nephrol *23*, 1879-1890. 10.1681/asn.2012030323.

Topol, L., Jiang, X., Choi, H., Garrett-Beal, L., Carolan, P.J., and Yang, Y. (2003). Wnt-5a inhibits the canonical Wnt pathway by promoting GSK-3-independent beta-catenin degradation. J Cell Biol *162*, 899-908. 10.1083/jcb.200303158.

Torii, S., Yamamoto, T., Tsuchiya, Y., and Nishida, E. (2006). ERK MAP kinase in G cell cycle progression and cancer. Cancer Sci *97*, 697-702. 10.1111/j.1349-7006.2006.00244.x.

Travis, M.A., van der Flier, A., Kammerer, R.A., Mould, A.P., Sonnenberg, A., and Humphries, M.J. (2004). Interaction of filamin A with the integrin beta 7 cytoplasmic domain: role of alternative splicing and phosphorylation. FEBS Lett *569*, 185-190. 10.1016/j.febslet.2004.04.099.

Tu, C.L., Chang, W., Xie, Z., and Bikle, D.D. (2008). Inactivation of the calcium sensing receptor inhibits E-cadherin-mediated cell-cell adhesion and calcium-induced differentiation in human epidermal keratinocytes. J Biol Chem *283*, 3519-3528. 10.1074/jbc.M708318200.

Uckun, F.M., Sather, H., Reaman, G., Shuster, J., Land, V., Trigg, M., Gunther, R., Chelstrom, L., Bleyer, A., Gaynon, P., and et al. (1995). Leukemic cell growth in SCID mice as a predictor of relapse in high-risk B-lineage acute lymphoblastic leukemia. Blood *85*, 873-878.

Uramoto, H., Akyürek, L.M., and Hanagiri, T. (2010). A positive relationship between filamin and VEGF in patients with lung cancer. Anticancer Res *30*, 3939-3944.

van der Flier, A., and Sonnenberg, A. (2001). Structural and functional aspects of filamins. Biochim Biophys Acta *1538*, 99-117. 10.1016/s0167-4889(01)00072-6.

Vieira Torquato, H.F., Ribeiro-Filho, A.C., Buri, M.V., Araújo Júnior, R.T., Pimenta, R., de Oliveira, J.S., Filho, V.C., Macho, A., Paredes-Gamero, E.J., and de Oliveira Martins, D.T. (2017). Canthin-6-one induces cell death, cell cycle arrest and differentiation in human myeloid leukemia cells. Biochim Biophys Acta Gen Subj *1861*, 958-967. 10.1016/j.bbagen.2017.01.033.

Visnjic, D., Kalajzic, Z., Rowe, D.W., Katavic, V., Lorenzo, J., and Aguila, H.L. (2004). Hematopoiesis is severely altered in mice with an induced osteoblast deficiency. Blood *103*, 3258-3264. 10.1182/blood-2003-11-4011.

Walter, M.J., Shen, D., Ding, L., Shao, J., Koboldt, D.C., Chen, K., Larson, D.E., McLellan, M.D., Dooling, D., Abbott, R., et al. (2012). Clonal architecture of secondary acute myeloid leukemia. N Engl J Med *366*, 1090-1098. 10.1056/NEJMoa1106968.

Wang, R., Gao, X., and Yu, L. (2019). The prognostic impact of tet oncogene family member 2 mutations in patients with acute myeloid leukemia: a systematic-review and meta-analysis. BMC Cancer *19*, 389. 10.1186/s12885-019-5602-8.

Wang, S., Qiu, L., Song, H., and Dang, N. (2018). NPS-2143 (hydrochloride) inhibits melanoma cancer cell proliferation and induces autophagy and apoptosis. médecine/sciences *34*, 87-93.

Wang, Y., Krivtsov, A.V., Sinha, A.U., North, T.E., Goessling, W., Feng, Z., Zon, L.I., and Armstrong, S.A. (2010). The Wnt/beta-catenin pathway is required for the development of leukemia stem cells in AML. Science *327*, 1650-1653. 10.1126/science.1186624.

Warady, B.A., Ng, E., Bloss, L., Mo, M., Schaefer, F., and Bacchetta, J. (2020). Cinacalcet studies in pediatric subjects with secondary hyperparathyroidism receiving dialysis. Pediatr Nephrol *35*, 1679-1697. 10.1007/s00467-020-04516-4.

Washington, R.W., and Knecht, D.A. (2008). Actin binding domains direct actin-binding proteins to different cytoskeletal locations. BMC Cell Biology *9*, 10. 10.1186/1471-2121-9-10.

Weidle, U.H., Birzele, F., Kollmorgen, G., and Rüger, R. (2016). Molecular Mechanisms of Bone Metastasis. Cancer Genomics Proteomics *13*, 1-12.

Wesely, J., Kotini, A.G., Izzo, F., Luo, H., Yuan, H., Sun, J., Georgomanoli, M., Zviran, A., Deslauriers, A.G., Dusaj, N., et al. (2020). Acute Myeloid Leukemia iPSCs Reveal a Role for RUNX1 in the Maintenance of Human Leukemia Stem Cells. Cell Rep *31*, 107688. 10.1016/j.celrep.2020.107688.

White, B.S., and DiPersio, J.F. (2014). Genomic tools in acute myeloid leukemia: From the bench to the bedside. Cancer *120*, 1134-1144. 10.1002/cncr.28552.

Winters, A.C., and Bernt, K.M. (2017). MLL-Rearranged Leukemias-An Update on Science and Clinical Approaches. Front Pediatr *5*, 4-4. 10.3389/fped.2017.00004.

Wu, Q., Shao, H., Darwin, E.D., Li, J., Li, J., Yang, B., Webster, K.A., and Yu, H. (2009). Extracellular calcium increases CXCR4 expression on bone marrow-derived cells and enhances pro-angiogenesis therapy. J Cell Mol Med *13*, 3764-3773. 10.1111/j.1582-4934.2009.00691.x.

Xie, Y., Yin, T., Wiegraebe, W., He, X.C., Miller, D., Stark, D., Perko, K., Alexander, R., Schwartz, J., Grindley, J.C., et al. (2009). Detection of functional haematopoietic stem cell niche using real-time imaging. Nature *457*, 97-101. 10.1038/nature07639.

Yamaguchi, T., Chattopadhyay, N., Kifor, O., Butters, R.R., Jr., Sugimoto, T., and Brown, E.M. (1998a). Mouse osteoblastic cell line (MC3T3-E1) expresses extracellular calcium (Ca2+o)-sensing receptor and its agonists stimulate chemotaxis and proliferation of MC3T3-E1 cells. J Bone Miner Res *13*, 1530-1538. 10.1359/jbmr.1998.13.10.1530.

Yamaguchi, T., Olozak, I., Chattopadhyay, N., Butters, R.R., Kifor, O., Scadden, D.T., and Brown, E.M. (1998b). Expression of extracellular calcium (Ca2+o)-sensing receptor in human peripheral blood monocytes. Biochem Biophys Res Commun *246*, 501-506. 10.1006/bbrc.1998.8648.

Yamaguchi, T., Yamauchi, M., Sugimoto, T., Chauhan, D., Anderson, K.C., Brown, E.M., and Chihara, K. (2002). The extracellular calcium Ca2+o-sensing receptor is expressed in myeloma cells and modulates cell proliferation. Biochem Biophys Res Commun *299*, 532-538. 10.1016/s0006-291x(02)02690-6.

Yamamura, A., Guo, Q., Yamamura, H., Zimnicka, A.M., Pohl, N.M., Smith, K.A., Fernandez, R.A., Zeifman, A., Makino, A., Dong, H., and Yuan, J.X. (2012). Enhanced Ca(2+)-sensing receptor function in idiopathic pulmonary arterial hypertension. Circ Res *111*, 469-481. 10.1161/circresaha.112.266361.

Yamamura, A., Nayeem, M.J., and Sato, M. (2019). Calcilytics inhibit the proliferation and migration of human prostate cancer PC-3 cells. Journal of pharmacological sciences *139*, 254-257.

Yang, C.Y., Chiu, H.F., Cheng, M.F., Tsai, S.S., Hung, C.F., and Tseng, Y.T. (1999). Pancreatic cancer mortality and total hardness levels in Taiwan's drinking water. J Toxicol Environ Health A *56*, 361-369. 10.1080/009841099158051.

Yarova, P.L., Stewart, A.L., Sathish, V., Britt, R.D., Jr., Thompson, M.A., AP, P.L., Freeman, M., Aravamudan, B., Kita, H., Brennan, S.C., et al. (2015a). Calcium-sensing receptor antagonists abrogate airway hyperresponsiveness and inflammation in allergic asthma. Sci Transl Med *7*, 284ra260. 10.1126/scitranslmed.aaa0282.

Yarova, P.L., Stewart, A.L., Sathish, V., Britt, R.D., Thompson, M.A., Lowe, A.P., Freeman, M., Aravamudan, B., Kita, H., and Brennan, S.C. (2015b). Calcium-sensing receptor antagonists abrogate airway hyperresponsiveness and inflammation in allergic asthma. Science translational medicine *7*, 284ra260-284ra260.

Yeung, J., Esposito, M.T., Gandillet, A., Zeisig, B.B., Griessinger, E., Bonnet, D., and So, C.W. (2010). β-Catenin mediates the establishment and drug resistance of MLL leukemic stem cells. Cancer Cell *18*, 606-618. 10.1016/j.ccr.2010.10.032.

Zhang, C., Miller, C.L., Brown, E.M., and Yang, J.J. (2015). The calcium sensing receptor: from calcium sensing to signaling. Sci China Life Sci *58*, 14-27. 10.1007/s11427-014-4779-y.

Zhang, C., Zhang, T., Zou, J., Miller, C.L., Gorkhali, R., Yang, J.Y., Schilmiller, A., Wang, S., Huang, K., Brown, E.M., et al. (2016a). Structural basis for regulation of human calcium-sensing receptor by magnesium ions and an unexpected tryptophan derivative co-agonist. Sci Adv *2*, e1600241. 10.1126/sciadv.1600241.

Zhang, C.C., Kaba, M., Ge, G., Xie, K., Tong, W., Hug, C., and Lodish, H.F. (2006). Angiopoietin-like proteins stimulate ex vivo expansion of hematopoietic stem cells. Nat Med *12*, 240-245. 10.1038/nm1342.

Zhang, J., Niu, C., Ye, L., Huang, H., He, X., Tong, W.G., Ross, J., Haug, J., Johnson, T., Feng, J.Q., et al. (2003). Identification of the haematopoietic stem cell niche and control of the niche size. Nature *425*, 836-841. 10.1038/nature02041.

Zhang, K., Zhu, T., Gao, D., Zhang, Y., Zhao, Q., Liu, S., Su, T., Bernier, M., and Zhao, R. (2014). Filamin A expression correlates with proliferation and invasive properties of human metastatic melanoma tumors: implications for survival in patients. J Cancer Res Clin Oncol *140*, 1913-1926. 10.1007/s00432-014-1722-3.

Zhang, M., and Breitwieser, G.E. (2005). High affinity interaction with filamin A protects against calcium-sensing receptor degradation. J Biol Chem *280*, 11140-11146. 10.1074/jbc.M412242200.

Zhang, Y., Dépond, M., He, L., Foudi, A., Kwarteng, E.O., Lauret, E., Plo, I., Desterke, C., Dessen, P., Fujii, N., et al. (2016b). CXCR4/CXCL12 axis counteracts hematopoietic stem cell exhaustion through selective protection against oxidative stress. Scientific Reports *6*, 37827. 10.1038/srep37827.

Zhang, Y., Gao, S., Xia, J., and Liu, F. (2018). Hematopoietic Hierarchy – An Updated Roadmap. Trends in Cell Biology *28*, 976-986.

Zhang, Z.-L., Li, Z.-R., Li, J.-S., and Wang, S.-R. (2020). Calcium-sensing receptor antagonist NPS-2143 suppresses proliferation and invasion of gastric cancer cells. Cancer Gene Therapy *27*, 548-557. 10.1038/s41417-019-0128-4.

Zhu, Y.M., Foroni, L., McQuaker, I.G., Papaioannou, M., Haynes, A., and Russell, H.H. (1999). Mechanisms of relapse in acute leukaemia: involvement of p53 mutated subclones in disease progression in acute lymphoblastic leukaemia. Br J Cancer *79*, 1151-1157. 10.1038/sj.bjc.6690183.

Acknowledgements

Throughout my PhD, I had great help and support from a large number of people, without whom I would have not been able to complete my project and finish my thesis. First and foremost, I would like to express my gratitude to Prof. Dr. Daniela Krause, my supervisor, for her guidance during this study. This thesis would not have been completed without her assistance and dedicated involvement in this project. She provided me with the tools that I needed to sharpen my thinking and steered me in the right direction.

My sincere thanks also go to Prof. Dr. Rolf Marschalek, for his mentoring and productive meetings. All the insightful comments, questions and discussions contributed significantly to the project.

I would particularly like to single out my lab mate and dear friend Dr. Rahul Kumar. I want to thank him for his mentorship, his treasured support in the experiments, critical discussion of the results and for the unwavering enthusiasm throughout the research project.

From the bottom of my heart, I would like to acknowledge my lab mates for their help in the experiments and for all the discussions, meetings and conversations which undoubtedly constructively contributed to the project. Because getting through the thesis required more than academic support, I need to thank their friendship, energy, inspiration and memorable good moments. It truly has been a fantastic experience in the lab.

I would like to extend my sincere thanks to the brilliant students I had the pleasure of supervising, particularly to Alessia Cais, which worked on this project during her master's thesis. In addition to the contribution to the project, the teaching experience allowed me to grow as scientist and it was very gratifying to see them become independent researchers.

I would also like to thank the collaborators who were involved in this research project and contributed with their expertise. My gratitude extends to the Georg-Speyer-Haus, for the help provided by the flow cytometry, histology and animal facilities, as well as the technical and support staff of the institute.

Finally, I must express my very profound gratitude to my family which is extended to my new family from Germany, specially to Dennis, and my friends, who unconditionally encourage and support me.

Tendo consciência que sozinha nada disto teria sido possível, dirijo um especial agradecimento para a minha família mais próxima: aos meus pais César e Maria da Luz, ao meu irmão Tiago, à minha irmã Nídia e ao Jan, e aos meus sobrinhos Sloan e Mathis.

Raquel S. Pereira

Mobile:
+49 (0)172 9677162

E-Mail:
pereiraraquelsoares@gmail.com

Date of birth:
09.06.1992

Nationality:
Portuguese

Home address:
Kelsterbacher Str. 34
60528 Frankfurt am Main
Germany

Languages

Portuguese – native

English – fluent in written and spoken

German – A1

French – A1

Education

March 2017 - present

PhD in Bone Marrow Microenvironment and Leukemogenesis
Georg Speyer Haus (GSH), Institute for Tumor Biology and Experimental Therapy, Goethe University Frankfurt (Germany)
Prof. Dr. Daniela S. Krause lab

October 2014 - October 2016

Master in Molecular Genetics (M.Sc.)
University of Minho, Braga – School of Sciences (Portugal)
Master thesis at University of Groningen – European Research Institute for Biology of Ageing (ERIBA) (Netherlands)

October 2010 - December 2013

Bachelor in Biotechnology (B.Sc.)
Polytechnic Institute of Coimbra – High School of Agriculture (Portugal)
Bachelor thesis at Institute for Biomedical Imaging and Life Sciences (IBILI) – Faculty of medicine, University of Coimbra (Portugal)

Research Experience

PhD projects:

The role of calcium ions in the leukemic bone marrow microenvironment

- Led independent research project in the field of leukemia research
- Stablished several *in vivo* and *in vitro* models for the study of calcium sensing receptor (CaSR)
- Identified novel mechanism of CaSR in the development, progression and response to therapy in leukemia
- Supervised several bachelor and master students

Lipid raft-associated proteins on leukemia cells and their importance for interactions with the bone marrow microenvironment (BMM)

- Researched the function of lipid raft-associated proteins in leukemogenesis, with focus on their interaction with the BMM
- Studied the function of the protein flotillin 2 using various *in vivo* and *in vitro* approaches, classical molecular biology methods and diverse imaging techniques

Master thesis:

Studying genes implicated with aneuploidy

- Investigated the unknown function of two poorly notated proteins which are possibly involved in aneuploidy
- Independent research using classical molecular cloning techniques, fluorescent and epitope tagged proteins technology

Bachelor thesis:

The study of protein quality control during the aging process using a transgenic mouse model expressing carboxyl-terminus of Hsc70 interacting protein (CHIP) in the lens

- Trained in molecular and cell biology research, focused on the role of CHIP protein overexpression in lens of transgenic mice
- Performed independent research on the protein quality control machinery of epithelial cells

Publications

Kumar R*, **Pereira RS***, Niemann J, *et al.* The differential role of the lipid raft-associated protein flotillin 2 for progression of myeloid leukemia. *Under major revision in Blood advances*. **Both authors contributed equally.*

Kumar R, **Pereira RS**, Zanetti C, *et al.* Specific, targetable interactions with the microenvironment influence imatinib-resistant chronic myeloid leukemia. *Leukemia* 34, 2087-2101 (2020).

Godavarthy PS, Kumar R, Herkt SC, **Pereira RS**, *et al.* The vascular bone marrow niche influences outcome in chronic myeloid leukemia *via* the E-selectin - SCL/TAL1 - CD44 axis. *Haematologica* 105(1), 136-147 (2020).

Verma D, Kumar R*, **Pereira RS***, *et al.* Vitamin K antagonism impairs the bone marrow microenvironment and hematopoiesis. *Blood* 134(3), 227-238 (2019). **Both authors contributed equally.*

Selected oral Presentations and Awards

October 2021

Oral presentation

Pereira RS, Cais A, Kumar R, *et al.* Chemical factors and their signaling in the leukemic bone marrow microenvironment. 23rd Annual John Goldman E-Conference on Chronic Myeloid Leukemia: Biology and Therapy.

September 2019

Oral presentation & LEUKA / ESH Scholarship

Pereira RS, Kumar R, Azimpour A, *et al*. Lipid raft-associated proteins on leukaemia cells and their importance for interactions with the bone marrow microenvironment. 21st Annual John Goldman Conference on Chronic Myeloid Leukemia: Biology and Therapy. Bordeaux, France

February 2019

Poster presentation

Pereira RS, Kumar R, Azimpour A, *et al*. A role for lipid raft-associated proteins in hematopoiesis and leukemogenesis. European School of Haematology (ESH), 3rd Scientific Workshop: The Haematological Tumour Microenvironment and its Therapeutic Targeting. London, United Kingdom

Leadership Roles

March 2017 - present

Training and supervision of two bachelor's thesis student, two master's practicum students and two master's thesis students with excellent theses (1.0).

Relevant Courses

April 2017

Animal experimental license: FELASA A and D. Frankfurt, Germany

Personal Interests

Music: French horn & Orchestras

2017 – 2020: Sinfonieorchester Philharmonische Verein 1834
2018 – present: Frankfurter Bläserphilharmonie
2018 – present: Sinfonisches Blasorchester der Goethe-Universität Frankfurt am Main

Sports: Crossfit, hiking and surfing